THE ADSORPTION
OF
DEHYDROABIETYLAMINE ACETATE
ON
OXIDE MINERALS

by

Gordon Wainwright Smith

A thesis submitted to the Faculty of
Graduate Studies and Research in partial
fulfilment of the requirements for the
Degree of Doctor of Philosophy

McGill University
Montreal, Canada.

July, 1967

ACKNOWLEDGEMENTS

The author wishes to express his appreciation to Dr. T. Salman under whose direction and guidance this work was undertaken.

The financial assistance offered by the Government of Canada in the form of a National Research Council Fellowship for 1965-66 and 1966-67 has been appreciated greatly.

Acknowledgement is also due to Mr. M. D. Beals and Mr. W.J. Baldwin of National Lead Co.; Mr. W. T. Bishop of Hercules Powders Inc.; Quebec Cartier Mining Co.; and Dominion Silica for respectively supplying the high purity zirconia and rutile, dehydroabietylamine acetate, Canadian specular hematite, and silica used in this research.

Ph.D. ABSTRACT Metallurgical Engineering

Gordon Wainwright Smith

THE ADSORPTION OF DEHYDROABIETYLAMINE ACETATE ON OXIDE MINERALS

The adsorption and desorption of dehydroabietylamine acetate on quartz, hematite, rutile and baddeleyite were investigated in neutral solutions. The adsorption followed a Freundlich type equation, $\Gamma = kC^n$, where n ranged from 0.41 to 0.51. The effect of pH was found to be complicated but, in general, adsorption decreased with decreasing pH.

The ionization constant, K_b, and the solubility of dehydroabietylamine were determined. The variation of surface tension, resistivity, and equivalent conductance with concentration of dehydroabietylamine has been determined in neutral solutions.

The zero-points-of-charge of quartz, hematite, rutile, and baddeleyite were found to be 2.6, 8.68, 7.13, and 6.08, respectively. Surface charge density and differential capacity were calculated as a function of pH.

Contact angles and work of adhesion were determined for each oxide in neutral solutions. Floatability tests indicated that high recoveries were possible with poor selectivity. Changes in surface free energy were calculated as a function of pH and dehydroabietylamine concentration.

TABLE OF CONTENTS

LIST OF ILLUSTRATIONS

LIST OF ILLUSTRATIONS

LIST OF TABLES

INTRODUCTION

Until approximately twenty years ago, iron ore was considered suitable for blast furnace feed in the raw state. Today, in North America, only ten percent of the ore mined is directly fed to the blast furnace, the remainder is being beneficiated to improve its physical characteristics and to upgrade its iron content (1). This situation was caused by the large surplus capacity to produce iron ore and iron products which existed throughout the world after World War II. The lack of demand forced mining companies to improve their products to meet increasingly stringent specifications from the steelmakers. Although this situation has changed with the increased world demand (2), all iron ore presently used is marketed to rigid specifications. Seventy-eight percent of all iron ore shipped from U.S. mines in 1963 (73,500,000 long tons) was beneficiated in some way. This percentage is increasing yearly. From 1952 to 1964, the average iron content of ores and pellets shipped to blast furnaces in the U.S. increased from 50.4% to 57.2%. In Canada, the proportion of beneficiated iron ore has been steadily increasing since 1958. In 1964, seventy-three percent of 35,900,000 long tons mined was beneficiated, up five percent from the previous year (3). A further increase of 2.5 percent is indicated in 1965 (4) and an even greater increase in 1966 is forecast.

As the reserve of high-grade ore is gradually reduced, increasing importance is being attributed to various ore upgrading techniques. In the case of iron ore, these include heavy media separation, spiral concentration, tabling, magnetic and electrostatic separation and flotation.

Presently, flotation techniques play a minor role in benefication of iron ores due to non-selectivity of available collectors, and the lack of economic advantage over other methods of separation. Most of the ore processed in Canada is beneficiated by gravity concentration, mainly heavy media and spirals. Although relatively inexpensive, these methods are best suited to coarse ground material with a large specific gravity differential between desired minerals and gangue. With finely disseminated materials, such as taconites and specular hematites, these processes become non-selective and uneconomical.

Magnetic separation cannot be applied to hematite ores in which the magnetic portion of the iron content is low. High intensity dry magnetic and high tension electrostatic methods have proved useful for some specular hematite in the size range from 14 to 35 mesh (5) but were applicable to finer sizes only if multi-unit separators were used. At the present, they cannot compete with more conventional gravity separation methods of iron ore concentration.

In 1954, the first commercial flotation plant operated by Humbolt Mining Company to concentrate iron ore was opened in Marquette County, Michigan. The plant, with a capacity of 250,000 long tons per year, processed specular hematite ore averaging 34 percent iron which was upgraded to a concentrate containing 62.5 percent iron (6). The success of this plant prompted the opening of another in 1956. In 1960, the estimated iron ore flotation capacity was 2.1 million tons per year. By 1963, this capacity was estimated to have more than doubled to 4.6 million tons per year.

Gravity concentration has been used in all concentration plants in Canada. Work is now under way into the possibility of using flotation to remove silica from finely disseminated hematite ores (7-9).

Flotation

Flotation is a physico-chemical process for separating finely divided solids from one another in an aqueous suspension to produce a tailing which usually contains the gangue or waste, and one or more concentrates which contain the valuable ore minerals. The concentrates are further processed to recover metallic values.

Originally, the term flotation was used with descriptive adjectives to denote all processes of concentration in which the levitation in water of particles heavier than water was obtained. These included "Bulk-oil flotation", "Skin flotation", and "Froth flotation". Now, flotation is used universally to describe froth flotation.

The principle of froth flotation is that if finely divided particles come in contact with and stick to rising bubbles of gas in a liquid, the resultant density of the particle-bubble aggregate is less than the liquid, hence the bubble will carry the particle to the surface. If the particles do not stick to the bubbles, then the particles remain in the bulk liquid. For economic reasons, the liquid is almost universally water, and the gas is air. Minerals to be separated rarely have the suitable physico-chemical surface properties to render the valuable one floatable alone. Outside intervention is required in almost all cases to alter the natural surfaces of the mineral particles that

make up the flotation pulp. The mineral to be floated (by attachment to an air bubble) must have a hydrophobic surface and all other minerals in the pulp must have a hydrophilic or easily-wettable surface. The attachment of various heteropolar organic compounds to the mineral surface produces the required hydrophobicity.

The attachment of these organic compounds occurs by a process called adsorption. If a material is added to a solution containing a solid, a certain portion of it may be taken up by the solid, leaving less in the solution. If the molecules of the material added enter into the solid, the process is known as "absorption". If the material remains on the outside of the solid, the process is called "adsorption". These two processes often occur together, and the total uptake from solution is known as "sorption". Adsorption from the liquid phase is complex and most theoretical equations are based on extension of gas phase adsorption theory. Organic material may adsorb as ions, molecules, or as multi-molecular units.

The effect of adsorption of heteropolar compounds on minerals is of importance to the mineral industry. In fact, flotation has almost reached the point where improvements in the process can only come about through a better understanding of the mechanisms involved. The fundamental mechanisms are quite complex, involving surface adsorption and establishment of a stable three-phase interface.

THEORETICAL REVIEW

Adsorption

The process by which atoms or molecules of one material, called "adsorbate", becomes attached to the surface of another, called "adsorbent", is known as "adsorption". The adsorbate concentrates at the contiguous area between the two phases known as the interface.

The adsorption from solution is more complex due to the presence of a solvent which may also adsorb on the solid surface. In general, adsorption can be classified as chemisorption or physical adsorption. They in turn may be subdivided as follows (10):

a) Chemisorption:- characterized by high heats of adsorption (generally above 15 Kcal./mole) and by the complete or partial transfer of an electron or orbital overlap;adsorbate is reactive ion or molecule forming

   i) a true chemical compound capable of existing in the the bulk state.

   ii) a surface compound for which an analogous species is known to exist as a crystal, or in solution, with the same molecular configuration.

   iii) a surface compound in which no analogous compounds have been isolated.

b) Physical Adsorption:- characterized by low heats of adsorption (generally below 3 Kcal./mole), and having no true bond formation; adsorbate may be an ion or unionized molecule.

Cases include:-

i) Un-ionized molecule, held in vicinity of surface by dispersion forces.

ii) Ion held in outer surface of double layer by electrostatic forces.

iii) Ion held close to the surface by combination of electrostatic and dispersion forces.

iv) Molecule or ion retained by relatively weak bonding, e.g., hydrogen bonding, etc. (This type of adsorption could equally well be classified as a weak chemisorption)

In chemisorption, the adsorbate enters the crystal lattice through chemical reaction at the inner double layer. The extent of this depends on the dimensions of the ions being adsorbed and how closely they approximate the dimensions of the crystal lattice ions, the structure and composition of the mineral surface layer, and the solubility of the compounds formed. These factors, in general, lead to the high selectivity of chemisorption.

In physical adsorption, the adsorption takes place in the outer double layer. Any ions may be adsorbed, irrespective of their nature, dimensions or size of charge, since only the overall electrical balance is important. Consequently, physical adsorption cannot be selective in relation to the solid, thus accounting for the difficulty in the flotation of mineral oxides.

Adsorption Isotherms

An adsorption isotherm is a relationship between the amount of material adsorbed and one or more variables which affect the adsorption at constant temperature. The simplest adsorption equation is as follows(11):

$$\Gamma = \frac{NP}{2\pi MRT} \tau_o e^{Q/RT} \qquad (1)$$

where T is the absolute temperature, P is the pressure, Γ is the amount adsorbed, Q is the heat of adsorption, R is the gas constant, N is Avogadro's number, M is the molecular weight, τ_o is the oscillation time of adsorbed molecules, and π is 3.1416. From this equation, graphs at constant temperature, pressure, and amount adsorbed may be drawn. These are known as isotherms, isobars, and isoteres, respectively. In general, the equation expresses an oversimplification of the adsorption process.

Experimental adsorption isotherms have been the subject of many theoretical calculations in order to arrive at an adsorption theory. The three most important adsorption isotherms are discussed below:

Langmuir's Adsorption Isotherm

Langmuir's adsorption isotherm, based on the assumption that a monomolecular layer is the maximum adsorption possible, and on a balance of evaporation and condensation rates, is expressed by the following equation (12):-

$$v = v_m \frac{bP}{1 + bP} \qquad (2)$$

The adsorption equation may be rearranged in linear form as follows:-

$$\frac{P}{v} = \frac{1}{bv_m} + \frac{P}{v_m} \qquad (3)$$

where v is the volume of gas at S.T.P. adsorbed

v_m is the volume of gas at S.T.P. adsorbed for a monolayer coverage

P is the pressure of adsorbing gas

b is a constant.

If there are several competing adsorbates, a similar expression is derived

$$v_i = \frac{v_{m_i} \; b_i \; P_i}{1 + b_i \; P_i} \qquad (4)$$

where the subscripts "i" refer to the "i"th adsorbate, and each symbol has the same meaning as before. For adsorption from liquid solution, the equation may be written as follows:

$$\frac{x}{m} = \frac{abC}{1 + bC} \qquad (5)$$

and in linear form

$$\frac{C}{x/m} = \frac{1}{ab} + \frac{C}{a} \qquad (6)$$

where x/m denotes the amount of adsorbate per unit amount of solid (eg. millimoles/gm., etc.), C is the concentration of adsorbate in solution, a is a constant which corresponds to a monolayer on the adsorbent, and b is related to the heat of adsorption ,Q, by the equation:-

$$b = b' \exp(Q/RT) \qquad (7)$$

There are several assumptions involved in the derivation of Langmuir's Isotherm, the most important of which are:-

i) The energy of adsorption, Q, is a constant, independant of surface coverage (which implies uniform sites and no interaction between adsorbate molecules).

ii) The adsorption is on localized sites (which implies no translational motion of adsorbate molecules in the plane of the surface).

iii) The maximum adsorption corresponds to a complete monomolecular layer.

The Freundlich Isotherm

A very old equation attributed to Freundlich due to its repeated use in his book (13) is:

$$v = k\, p^{1/n} \tag{8}$$

The exponent n is generally greater than one. Unlike the Langmuir Isotherm, there is no low or high pressure region. Although the Freundlich equation is widely used in qualitative literature as an empirical equation, there does not seem to be any significant theoretical basis for it. However, it is possible to obtain the Freundlich equation as the net of superimposed Langmuir's equations (14).

For adsorption from solution, the Freundlich Isotherm is usually written in the form

$$x/m = a\, C^{1/n} \tag{9}$$

where a and n are constants. Constant a is a measure of the surface area of the solid and n is a measure of the intensity of adsorption. For plotting experimental data, the linear form of the equation is

$$\log(x/m) = \log a + 1/n \log C \qquad (10)$$

Thus, a plot of $\log(x/m)$ versus $\log C$ should give a straight line of slope $1/n$ and intercept $\log a$.

The B.E.T. Adsorption Isotherm

Brunauer, Emmett and Teller (15) showed how to extend Langmuir's approach to multilayer adsorption, and their equation has come to be known as the BET equation. The derivation is based on balancing the forward and reverse rates of adsorption. The equation, in linear form, may be written as

$$\frac{P}{(P_o - P)v} = \frac{1}{v_m c} + \frac{c-1}{v_m c} \cdot \frac{P}{P_o} \qquad (11)$$

where P_o is the saturation pressure of adsorbate, c is a constant, and P,v and v_m have the same significance as before. The value of c is given by

$$c = \exp((Q_1 - Q_v)/RT) \qquad (12)$$

where $Q_1 - Q_v$ is known as that net heat of adsorption. If it is assumed that multilayer adsorption is limited to n layers, the BET equation becomes (16)

$$v = \frac{[v_m cx/(1-x)][1 - (n+1)\ x^n + nx^{n+1}]}{[1 + (c-1)x - cx^{n+1}]} . \qquad (13)$$

Multilayer adsorption from solutions has been reported in the literature following sigmoidal or "S"-shaped isotherms. Hansen et al (17) found that, for a number of higher acids and alcohols (four or more carbon atoms) adsorbed on various carbons from aqueous solutions, the isotherms showed no saturation effect but rather the general sigmoidal shape of multilayer adsorption. The final marked increase in adsorption took place significantly as the saturation concentration was approached.

Since, in low temperature gas adsorption, the rapid increase in adsorption occurs as P approaches P_o, and the rational variable is P/P_o, the proper rational variable in the case of solution adsorption is C/C_o, where C_o is the solubility of the adsorbate in the solvent. Hansen and Craig (18) have found that the adsorption isotherms of members of a homologous series of fatty acids or alcohols on Graphon (carbon) and Speron (silica) were superimposable on each other if adsorption is plotted against reduced concentration C/C_o. At high C/C_o values for lower members of the series, deviations were due to the high concentrations (and solubilities) which caused a secondary effect due to the solvent.

Negative Adsorption in Binary Liquid Systems.

In general, adsorption equations, such as Langmuir and Freundlich which have been applied to gas adsorption, are useful in the case of adsorption from solution only if the adsorbate is present in dilute solution

and is strongly adsorbed. When adsorption takes place from binary mixtures where a complete range of concentrations from pure liquid A to pure liquid B are available, the above isotherms become ambiguous since the distinction between solvent and solute becomes arbitrary. Choosing B as the solute and therefore the adsorbate, the apparent adsorption is defined as

$$(x_2/m)_{app.} = M(C_2^o - C_2)/m \tag{14}$$

where M = initial mass (or volume) of solution

C_2^o = initial concentration of component B in solution (mass per unit volume)

C_2 = final concentration of component B in solution (mass per unit volume)

m = mass of adsorbent.

A more symmetrical definition of apparent adsorption is that used by Bartell et al (19)

$$(x_2/m)_{app.} = H\Delta N_2/m \tag{15}$$

where H = total moles of original solution

ΔN_2 = change in mole fraction of component B on adsorption.

This effect is due to co-adsorption of solvent and solute and to changes in volume with adsorption (20). Since negative adsorption occurs in concentrated solutions, it is not of particular interest in the field of mineral separation.

Electrical Double Layer

The surface of any solid or liquid phase differs from the interior in that there is not a complete balance of intermolecular forces at the surface. When a solid is immersed in water, the electrical balance at the surface is further disturbed by the passage of surface ions into solution. To restore the electrical neutrality there is a migration of counter ions to the surface. Finally, a state of equilibrium is established between the solid surface and the solution in which an excess of positive charges is produced on one side and an excess of negative charges on the other side of the boundary layer. This layer with its electrical charge distribution is known as an "electrical double layer".

According to the Helmholtz theory (10), the electrical double layer at a solid-liquid interface is analogous to the two plates of an electrical condenser, the potential of which is generally termed electrokinetic or zeta-potential. The theory assumes that the double layer is of atomic thickness, the inner layer being adjacent to the surface of the solid, evenly distributed, and fixed by surface forces to it. The single outer moveable layer consists of charges of the opposite sign contained in the liquid. Gouy (22) pointed out that the ions of the double layer could not be concentrated at a definite distance from the surface because there must be an equilibrium between the electrical forces that are responsible for the existence of the double layer and the thermal motion of the ions. Consequently, there can be no sudden change in the concentration of any kind of ions in the vicinity of the double layer,

but merely a gradual increase in concentration of ions of one sign and a decrease in concentration of ions of the opposite sign. The ionic distribution is very sensitive to the concentration and valency of electrolytes present. Chapman (23) developed Gouy's idea and derived an expression for the equilibrium distribution of ions in such a diffuse layer. The expression is similar to that derived by Debye and Hückel (24) to describe the distribution of ions in the ionic atmosphere around a given ion.

These theories all assumed that the ionic charges were concentrated point charges and gave theoretical capacity values of the double layer far higher than found in practice. In 1924, Stern (24) proposed an important correction to the double layer theory by considering the finite dimensions of the ions in the first ionic layer next to the particle. The possibility of specific adsorption of the ions was also considered. He assumed that these ions were located in a plane, known as the Stern layer at a distance from the wall. The Stern double layer at the absolute zero temperature is equivalent to the original Helmholtz double layer.

A further modification has been suggested by Grahame (25) to take account of ions held to the surface by covalent bonds or Van der Waals forces. These Grahame considered to be dehydrated, while ions of the opposite sign remain hydrated and are attracted to the surface by electrostatic forces. As a result of this, the locus of closest approach to the solid surface of hydrated ions is a plane, which he calls the outer Helmholtz plane. Dehydrated ions, on the other hand, can approach closer to the solid surface and are located at the inner Helmholtz plane. Grahame assumes the capacity of this inner layer is constant.

Figure 1 illustrates the distribution of charges surrounding a positively charged particle, which gives rise to an electrical double layer (26-28). The double layer consists essentially of three parts:-

1) Positive charges in the inner circle (a) of the illustration are potential-determining ions. These ions are evenly distributed over the surface and are usually considered as part of the surface crystal lattice.

2) Counter ions, held close to the solid surface, occupy the Stern layer (b) which is seldom more than one hydrated molecule thick. The Stern layer is often considered as a separate inner layer of dehydrated or desolvated, specifically adsorbed ions (inner Helmholtz plane) and a second layer of hydrated ions held close to the solid surface as a molecular condenser being separated from the solid surface by the strongly bound water molecules. The distance of closest approach of the ions of same sign as the surface ions is the outer edge of the Stern layer or the inside edge of the Gouy layer. For this reason, it is known as the "limiting Gouy plane " or "outer Helmholtz plane".

3) Counter ions form a diffuse, or Gouy layer (c). The counter ion density decreases exponentially and the similiion density increases exponentially until a point is reached where the number of positive and negative ions is equal and there is no further change in potential. When the solution moves relative to the solid, a portion of the electrical double layer is moved with it. It seems likely that the ions and surrounding medium in the Stern layer would be rather rigidly held to the solid and resist shear. There is no reason why the shear plane should coincide exactly

FIGURE 1

THE STRUCTURE AND POTENTIAL GRADIENT
OF AN ELECTRICAL DOUBLE LAYER

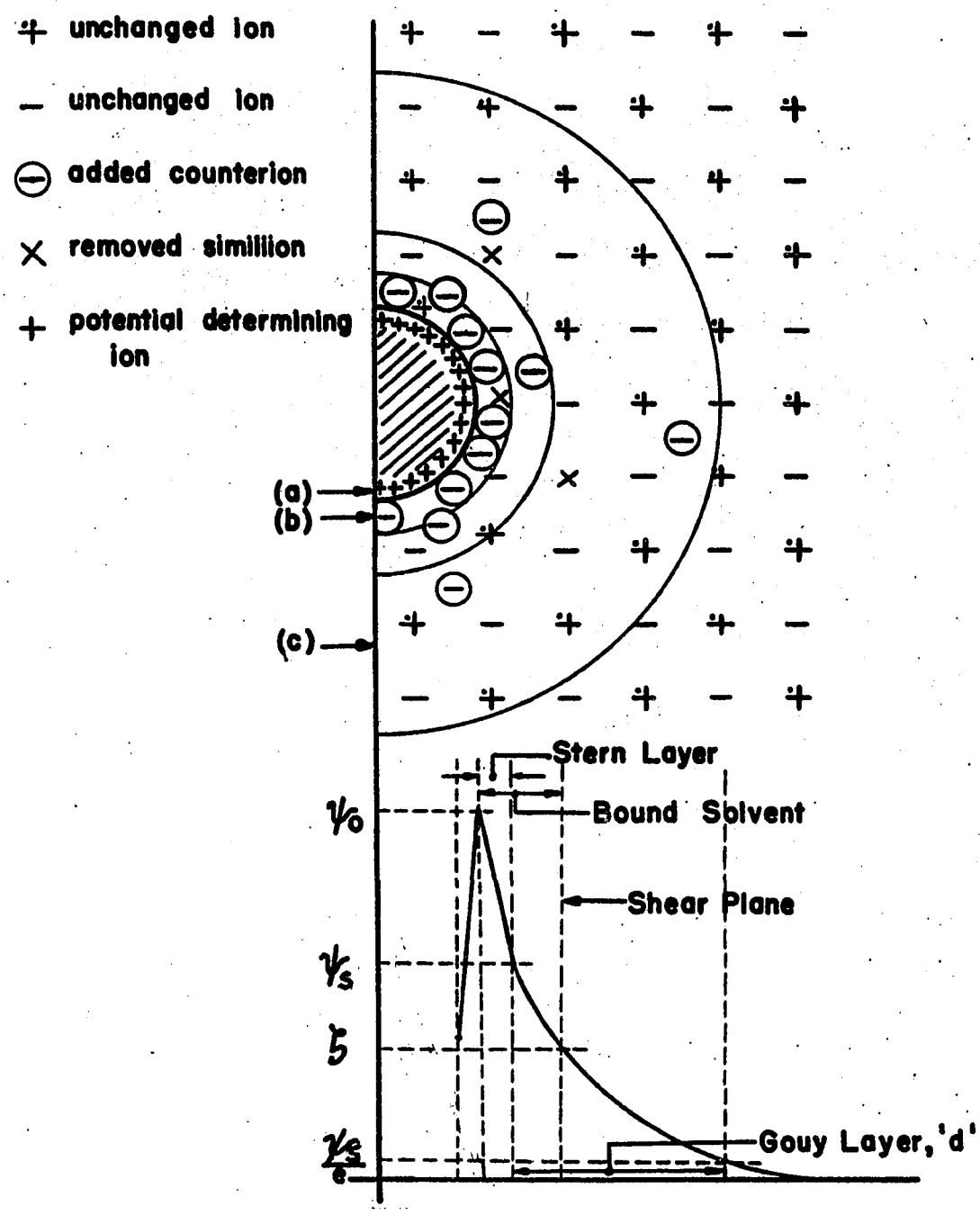
unchanged ion
unchanged ion
added counterion
removed similiion
potential determining ion
(a)
(b)
(c)
Stern Layer
Bound Solvent
Shear Plane
Gouy Layer, 'd'

with the Stern layer-Gouy layer interface as suggested by some authors (26,28,36) and may well be located further out. The potential at this shear plane is known as the zeta-potential. The thickness of this diffuse layer is said to be equal to $1/\kappa$ where κ is the Debye-Hückel function (29)

$$\kappa = \sqrt{\frac{4\pi e^2 \Sigma n_{i_o} z_i^2}{DkT}} \tag{16}$$

Where e is the charge on an electron, n_{i_o} is the concentration of the ith component in the bulk solution, z_i is the valence with sign of the ith component, D is the dielectric constant, k is the Boltzmann constant, and T is the absolute temperature. The thickness is approximately 1000 angstroms in 10^{-5} molar solutions of a uni-univalent electrolyte such as sodium chloride. Gaudin (30) shows that, in flotation systems, the Gouy layer has an approximate thickness of 97 angstroms.

According to the Gouy-Chapman treatment (29), the distribution of the ions in the diffuse layer surrounding a charged particle is governed by a Boltzmann relation

$$n_i = n_{i_o} e^{-ze\psi/kT} \tag{17}$$

where n_i is the concentration of ions of the ith kind at the point where the potential is ψ. The coulombic interaction between charges is expressed by Poisson's equation,

$$\nabla\psi = -4\pi\rho/D \tag{18}$$

where ψ is the potential which varies from ψ_o at the interface to zero in the bulk solution, ρ is the space charge density, and ∇ is the Laplace operator, defined as

$$\rho = \Sigma z_i \, en_i \tag{19}$$

$$\nabla = \partial^2/\partial x^2 + \partial^2/\partial y^2 + \partial^2/\partial z^2 \tag{20}$$

Combining the above equations, the following differential equation is obtained.

$$\nabla\psi = - \frac{4\pi}{D} \sum z_i e \, n_{i_o} e^{-z_i e\psi/kT} \tag{21}$$

This equation can only be solved with certain simplifying assumptions.

If one assumes an infinitely large plane surface and a single binary electrolyte of valency z in the solution, then the change of potential with distance from the surface is

$$\frac{d\psi}{dx} = -\sqrt{\frac{8\pi n_o kT}{D}} \left(e^{ze\psi/2kT} - e^{-ze\psi/2kT}\right) \tag{22}$$

and the surface charge density

$$\begin{aligned} \sigma &= \int_o^\infty \rho dx = \frac{D}{4\pi} \left(\frac{d\psi}{dx}\right)_{x=0} \\ &= \sqrt{\frac{Dn_o kT}{2\pi}} \left(e^{ze\psi_o/2kT} - e^{-ze\psi_o/2kT}\right) \\ &= \sqrt{2Dn_o kT/\pi} \, \sinh(ze\psi_o/2kT) \end{aligned} \tag{23}$$

For small values of $ze\psi_o/2kT$, the above equation reduces to

$$\sigma = \sqrt{2Dn_o kT/\pi}\,(ze\psi_o/2kT)$$

$$= D\kappa\psi_o/4\pi \qquad (24)$$

where κ is the Debye-Hückel function (Eq.16).

When Stern considered the two sections of the double layer (28), the surface charge relationships had to be modified. The potential gradient, $d\psi/dx$, of the compact layer (Stern Layer) whose thickness is δ, is approximated to be $(\psi_o-\psi_s)/\delta$, and hence

$$\sigma_1 = (D'/4\pi\delta)(\psi_o - \psi_s) \qquad (25)$$

where ψ_s is the potential at the Stern layer-Gouy layer interface and D' is the dielectric constant of the Stern layer (not usually equal to D).

The surface charge density of the diffuse layer (Gouy layer) is the same as Eq.(23), except ψ_o is replaced by ψ_s, hence the total surface charge density becomes

$$\sigma = \sigma_1 + \sigma_2$$

$$= (D'/4\pi\delta)(\psi_o-\psi_s) + \sqrt{2Dn_o kT/\pi}\,\sinh(ze\psi_s/2kT) \qquad (26)$$

Furthermore, the sinh term can be expanded to $\sinh\dfrac{(ze\psi_s + \phi)}{2kT}$ where ϕ accounts for any additional chemical adsorption potential. The total electrical capacity may be considered as two capacitors in series (28,31), thus

$$\frac{1}{C} = \frac{1}{C_1} + \frac{1}{C_2} \tag{27}$$

where

$$C_1 = \frac{d\sigma_1}{d\psi} = \frac{D'}{4\pi\delta} \tag{28}$$

and

$$C_2 = \frac{d\sigma_2}{d\psi} = \sqrt{\frac{Dz^2 e^2 n_o}{2\pi kT}} \cosh(ze\psi_s/2kT) \tag{29}$$

In concentrated solutions, C_1 becomes so large, that as an approximation, $C = C_2$. The crux of this treatment is the estimation of the extent to which ions enter the compact layer and the degree to which ψ is reduced by that factor. The only point at which ψ_s is known accurately is in a solution where the potential ψ_o is zero. Now,

$$\psi_o = \psi_s = \zeta = \sigma = 0 \tag{30}$$

This condition is known as the zero-point-of-charge.

In the case of simple oxides, the potential-determining ions are usually the hydrogen and hydroxyl ions (32). If the concentration of potential-determining ions is changed, then the changes in thermodynamic potential and surface potential are given by

$$\Delta\mu = kT\, \ell n(a/a_1) \tag{31}$$

$$\Delta\psi_o = \psi_o - (\psi_o)_1 = \frac{\Delta\mu}{ze} = \frac{kT}{ze}\, \ell n(a/a_1) \tag{32}$$

If a_o is the activity of the potential determining ion at the z.p.c., where $(\psi_o)_1 = 0$ and $a_1 = a_o$, then ψ_o becomes

$$\psi_o = \frac{kT}{ze} \ln (a/a_o)$$

$$= 2.3 \frac{kT}{ze}(pH_o - pH) \qquad (33)$$

where pH_o is the pH at the zero-point-of-charge and pH is the bulk solution pH.

The mechanism of surface charging has been discussed by Parks and de Bruyn (33) and others (32,34). The charging occurs in two stages as shown schematically in Figure 2. The first step is surface hydration which may be considered as an attempt by the exposed surface atoms to complete their co-ordination shell of nearest neighbours. Oxygen-metallic cation bonds are broken followed by migration of hydroxyl ions, thus forming a surface of hydroxyl ions with cations buried below the surface. To support this argument, Glemser and Rieck (35) have observed that part of the water vapour adsorbed by hematite appears as hydroxyl groups in the infrared spectra.

The second step is surface charging which is accomplished either by adsorption of hydrogen and hydroxyl ions or by dissociation of the surface sites which then assume a positive or negative charge. Since adding OH^- to the uncharged surface increases the Fe ion's co-ordination number to seven (unlikely to occur), the negative surface probably results from hydrogen ion desorption from the surface.

FIGURE 2

SCHEMATIC DIAGRAM OF THE MECHANISM

OF SURFACE CHARGING IN AQUEOUS SOLUTION

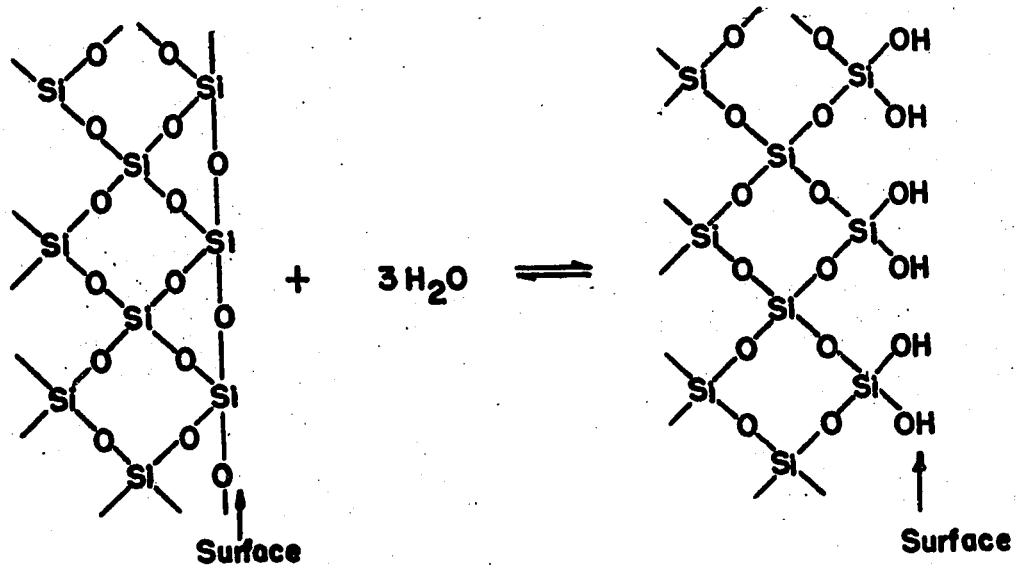

STEP 1 - HYDRATION

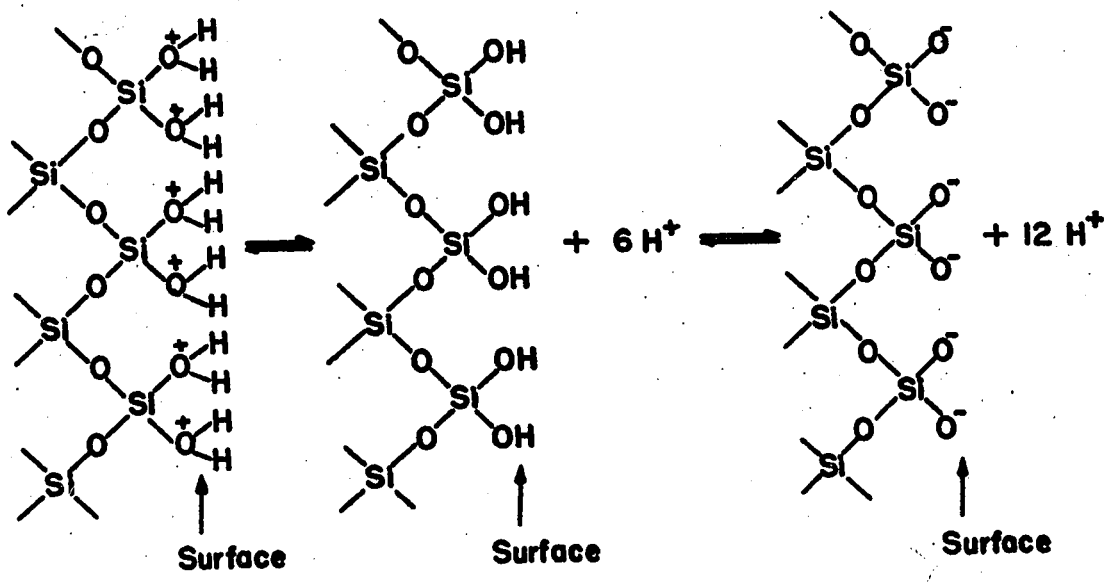

POSITIVE ZERO-POINT-OF-CHARGE NEGATIVE

STEP 2 - DISSOCIATION

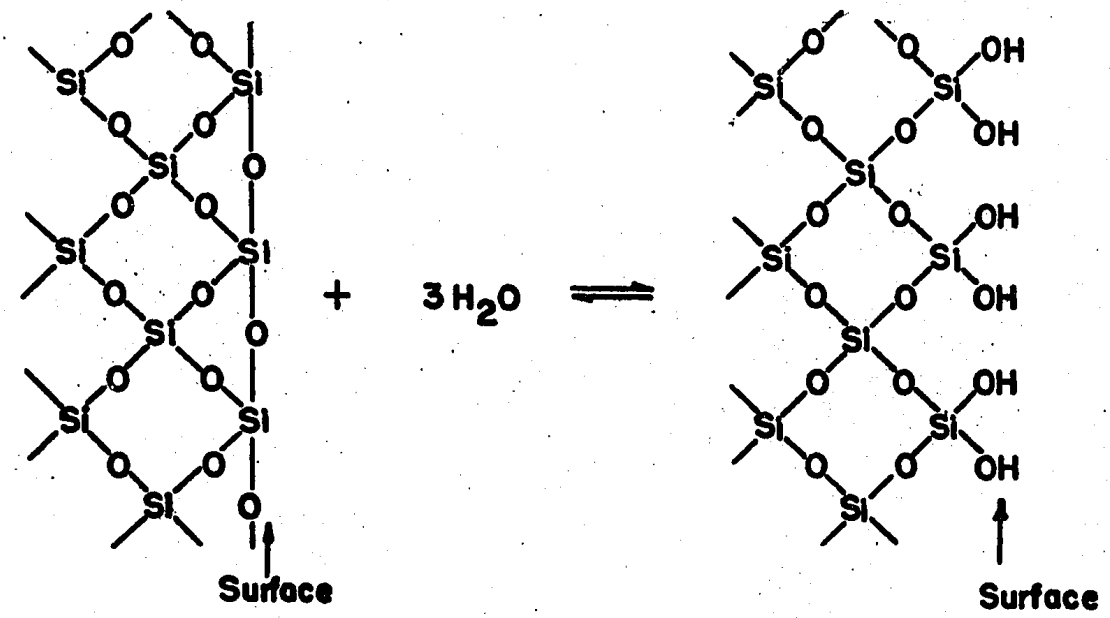

STEP 1 - HYDRATION

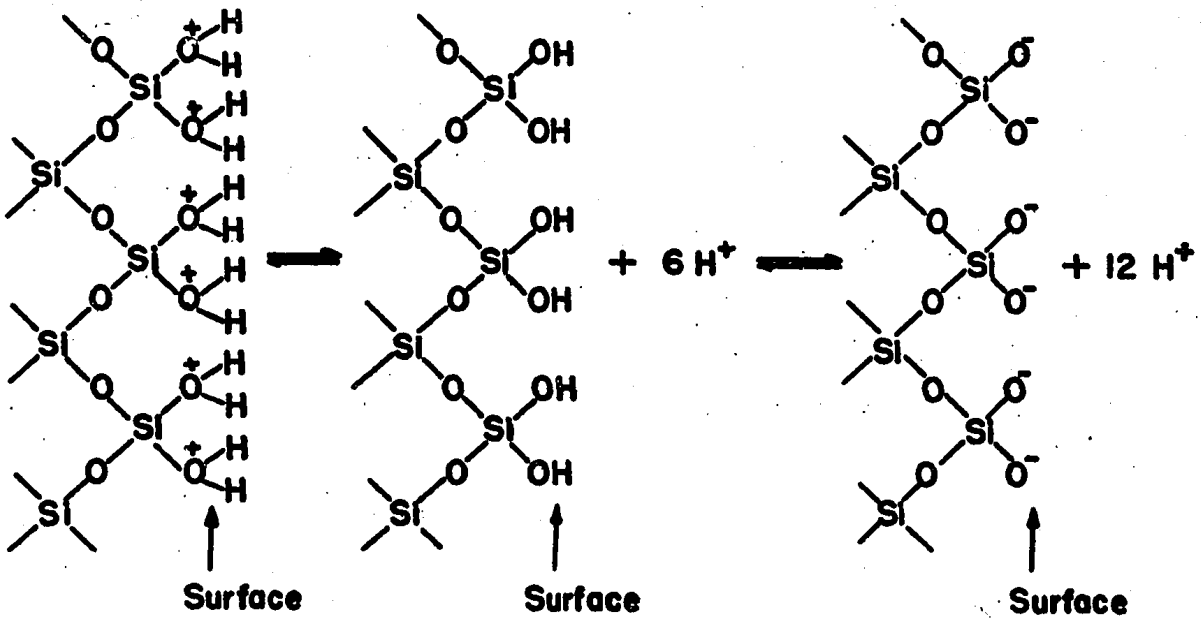

POSITIVE ZERO-POINT-OF-CHARGE NEGATIVE

STEP 2 - DISSOCIATION

The zero-point-of-charge may be related to the pH of the solution in which the adsorption densities of H^+ and OH^- ions are equal or when, by dissociation, an equal number of positively and negatively charged surface sites are exposed. Thus, the surface reactions for hematite may be written (33) as

$$Fe(OH)_2^+ \text{ (surface)} + 2\ H_2O \rightleftharpoons Fe(OH)_3 \text{ (surface)} + H_3O^+ \text{(aq.)} \quad (34)$$

$$Fe(OH)_3 \text{ (surface)} \rightleftharpoons FeO_2^- \text{ (surface)} + H_3O^+ \text{ (aq.)} \quad (35)$$

In these reactions, the $Fe(OH)_3$ (surface) represents an uncharged surface site which adsorbs a proton to become positively charged or desorbs a proton to become negatively charged. By addition of Eq. (34) and Eq. (35), we obtain

$$Fe(OH)_2^+ \text{ (surface)} \rightleftharpoons FeO_2^- \text{ (surface)} + 2\ H^+ \text{ (aq.)} \quad (36)$$

for which the equilibrium constant is

$$K_1 = \frac{[FeO_2^-]}{[Fe(OH)_2^+]} \times \left(\frac{\gamma_-}{\gamma_+}\right) \times a_{H^+}^2 \quad (37)$$

This constant measures the strength with which ferric oxide binds its protons. If the ratio of the activity coefficients of the surface sites is close to unity, then the magnitude of K_1 is determined by the pH of the z.p.c. Since the complex ferric ion concentrations are also equal at the z.p.c., K_1 may be written as:

$$K_1 = (a_{H^+})_o^2 \tag{38}$$

For many oxides and hydroxides, the existance of many positive and negative complexes has been established and their stability constants are known. The iso-electric-point is defined as the solution in which the number of positive and negative ions of a dissociating ampholyte are equal in solution (36), and ampholyte being an electrolyte which can dissociate either acidly or basicly. In this case, the ampholyte is usually the hydroxide of the oxide under examination. This point can be calculated from stability constants and other thermodynamic data, in which case, it is primarily a theoretical quantity. However, Parks (37) in a detailed review of iso-electric-point data, points out that there are several equilibrium points besides the i.e.p., such as $E(M(OH)^+,OH^-)$ and $E(M(OH)_3^-,H^+)$. The z.p.c., found experimentally, often is more closely related to one of these points. Thus, the dissociating ampholyte may be dissociating into ion pairs such as:-

$Pb(OH)^+ - Pb(OH)_3^-$ (iep.)

$Pb(OH)^+ - OH^-$

$H^+ - Pb(OH)_3^-$

$\frac{1}{2}(Pb^{++}) - Pb(OH)_3^-$

These various equivalence points may explain the wide variations in z.p.c. found experimentally especially with natural materials.

Contact Angle and Work of Adhesion

It is observed that in many instances a liquid placed on a solid will not wet it, but rather remains as a drop having a finite angle of contact between the liquid and solid phases. Similarly, in a liquid-solid system, a gas bubble may form a definite angle of attachment or contact angle between the liquid-solid interface and the gas-liquid interface as shown in Figure 3. A simple derivation leads to a useful relationship known as the Young and Dupre Equation (38,39). The change in surface free energy ΔF_s, produced by a change in area of solid covered, ΔA is

$$\Delta F_s = \Delta A(\gamma_{SL} - \gamma_{SV}) + \Delta A \gamma_{LV} \cos(\theta - \Delta\theta) \qquad (39)$$

where γ_{SL}, γ_{SV}, and γ_{LV} are the surface tensions of the solid-liquid, solid-vapour, and liquid-vapour surfaces respectively, θ is the angle of contact, and $\Delta\theta$ is the change in the angle of contact.

$$\lim_{\Delta A \to 0} \Delta F_s / \Delta A = 0 \qquad (40)$$

and

$$\gamma_{SL} - \gamma_{SV} + \gamma_{LV} \cos\theta = 0$$

or

$$\gamma_{SV} = \gamma_{SL} + \gamma_{LV} \cos\theta \qquad (41)$$

This equation, may also be derived from a simple balance of forces at point A of Figure 3(b).

FIGURE 3

(a) EQUILIBRIUM RELATIONSHIPS FOR A BUBBLE OF WATER IN CONTACT WITH A MINERAL SURFACE.

(b) EQUILIBRIUM RELATIONSHIPS FOR A BUBBLE OF AIR IN CONTACT WITH A MINERAL SURFACE UNDER WATER.

(c) EFFECT OF SURFACE ROUGHNESS ON THE CONTACT ANGLE.

γ_{LV} = air-water interfacial tension

γ_{SV} = air-mineral interfacial tension

γ_{SL} = mineral-water interfacial tension

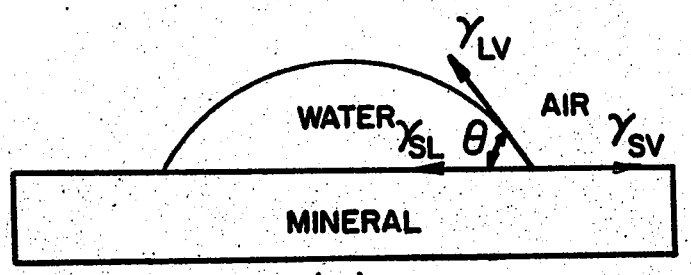
γ_{LV}
WATER
γ_{SL}
θ
AIR
γ_{SV}
MINERAL

(a)

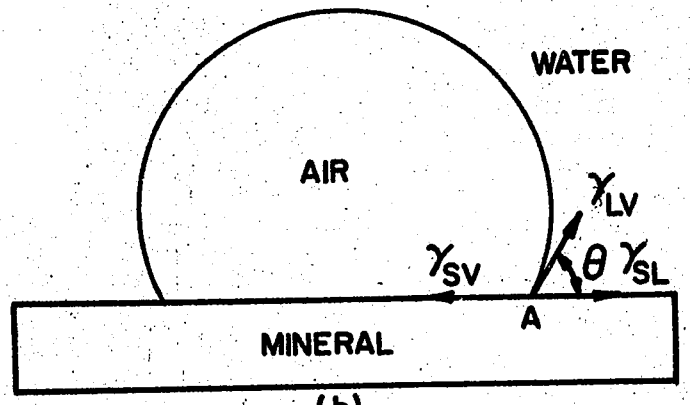
WATER
AIR
γ_{LV}
γ_{SV}
θ
γ_{SL}
A
MINERAL

(b)

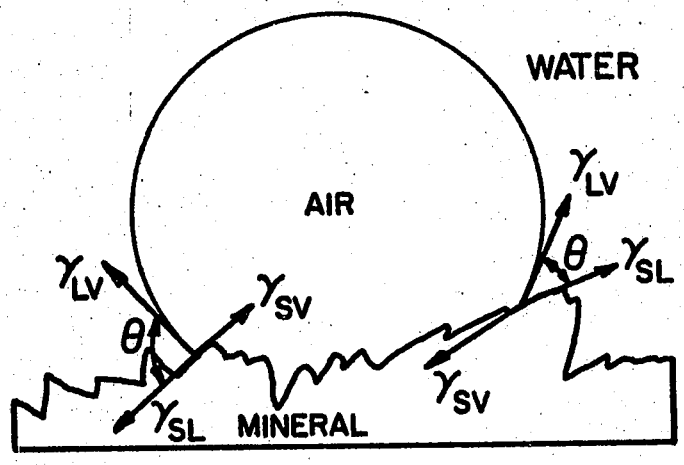
WATER
AIR
γ_{LV}
θ
γ_{SL}
γ_{LV}
γ_{SV}
θ
γ_{SV}
γ_{SL}
MINERAL

(c)

The work of adhesion is defined in two ways depending upon whether one is concerned with liquid drop or gas bubble attachment.

The work of adhesion of a drop of liquid to a solid surface is defined as the amount of work required to break the solid-liquid surface and form a solid-vapour and a liquid-vapour surface (40), and is given by

$$W_{A(SL)} = \gamma_{SV} + \gamma_{LV} - \gamma_{SL} \tag{42}$$

where $W_{A(SL)}$ is the work adhesion of a liquid drop to a solid surface.

Furthermore, the work of adhesion of a bubble of gas to a solid surface is defined as the amount of work required to break the solid-vapour surface and form a solid-liquid and a liquid-vapour surface, and is given by

$$W_{A(SL)} = \gamma_{SL} + \gamma_{LV} - \gamma_{SV} \tag{43}$$

where $W_{A(SL)}$ is the work of adhesion of a gas bubble to a solid surface.

By combining these equations with Young's equation, the work of adhesion is expressed as

$$W_{A(SL)} \text{ (liquid drop)} = \gamma_{LV}(1 + \cos \theta) \tag{44}$$

$$W_{A(SL)} \text{ (gas bubble)} = \gamma_{LV}(1 - \cos \theta) \tag{45}$$

The validity of these equations has been questioned on the grounds that the vertical component of γ_{LV} and the effect of the gravitational field have not been considered, and that the bubble is not necessarily spherical (41-44). Several papers (45,46) have been published in support of the

equation, and it is generally agreed that it may be applied to rigid solids (47), which is the case for mineral flotation (48-52).

Although, the contact angle is very important, it is most difficult to measure accurately. The mineral surface must be completely clean and perfectly flat. The former is impossible theoretically and the latter is impossible practically due to micro-crystalline cracks that will always be present no matter how carefully the polishing is carried out. This effect can be seen in Figure 3, where Figure 3(b) shows the equilibrium angle on a smooth surface and Figure 3(c) shows the variation found on a rough surface. Many attempts have been made to relate contact angle values to the floatability of minerals (53), but no definite relationship has been found. It is only possible to say that a finite angle of contact is a pre-requisite for flotation.

Amine Collectors

Organic derivatives of ammonia, in which some or all the hydrogen ions are replaced by aliphatic, aromatic, or heterocyclic radicals are known as amines. These compounds have been used as collectors in flotation, particularly in silica and silicate flotation. Representative cationic collectors include primary, secondary, and tertiary aliphatic amines and their salts, primary and secondary aromatic amines and their salts, and salts of the pyridine and quinoline families (54).

Ionization constants of amines in water indicate that primary amines ($K_B \simeq 4 \times 10^{-4}$) are more basic than ammonia, and that the length of the hydrocarbon chain does not affect its basicity. Secondary amines are more basic while tertiary amines are weaker. Aryl amines are about a million times weaker bases ($K_B \simeq 10^{-10}$) than primary amines.

Technical data on amines and amine salts is of prime importance and yet there is almost no data published on the subject.

Collecting Action of Amines on Sulphides and Oxides.

Amyl amines have been shown to be good collectors for chalcocite and sphalerite at pH 10 to 11 (55,56) in a range where undissociated amine and aminium ions are present in equal quantities. Furthermore, Kellogg and Vásquez-Rosas (57) have shown that n-dodecylamine acts as a good collector on quartz, sphalerite, and galena giving a maximum contact angle at a pH between 10 and 11. According to Gaudin(54), it appears that the same mechanism is involved in all cases. Careful calculation of the

concentrations of the various forms in which the amine is present in solution indicates that one half of the reagent is in the undissociated form and one half is dissociated at a pH of 10.6 (57-60). Kellogg et al. (57) conclude that it is the free amine molecule which is the effective agent causing the coating of the mineral surface.

The ratio of aminium ion concentration to hydrogen ion concentration is proportional to the concentration of molecularly dissolved amine. This is implied in the very concept of ionization constant; thus if

$$K_B = \frac{[RNH_3^+]\ [OH^-]}{[RNH_2]} \tag{46}$$

and

$$K_W = [OH^-]\ [H^+] = 10^{-14} \tag{47}$$

then

$$\frac{[RNH_3^+]}{[H^+]} = [RNH_2] \cdot \frac{K_B}{K_W} \tag{48}$$

A choice of three hypothesis is put forward (54) to explain the adsorption:-

1) Ion exchange between aminium and hydrogen ions.

2) Simultaneous adsorption of aminium and hydrogen ions.

3) Adsorption of molecularly undissociated amine.

Any one of these mechanisms could be favoured by the existance, in other circumstances, of zinc-amine complexes (61). However, the similarity between quartz, galena, and sphalerite indicate that complex-formation is not the principal factor.

DeBruyn has shown that the adsorption of dodecylamine on quartz follows a square root relationship (62).

$$\Gamma = K\sqrt{C} \tag{49}$$

up to 2×10^{-4} moles/1. Similarly, Morrow (63,64) has found that the adsorption on hematite follows the equation

$$\Gamma = K\,C^{0.6} \tag{50}$$

An increase in adsorption above that given by these relationships near the monolayer was attributed to the possibility of micelles or hemi-micelles in the double layer. The adsorption is strongly affected by pH but the effects are complex and imperfectly interpreted. Generally, adsorption is greater in alkaline media. Bloecher (65) found that, with 7% of the surface covered with dodecylamine, flotation recovery was 100%. DeBruyn (62) further indicated that the longer the hydrocarbon chain, the lower the concentration required for flotation. Above a pH of 12, flotation was impossible, regardless of chain length.

Dehydroabietylamine Acetate

Dehydroabietylamine is a member of a group of amines known as the abietylamines. The structure of this family is shown in Figure 4, and the members are known by the number of hydrogen atoms they are lacking or have in excess compared to abietylamine. This also is indicated by the number of double bonds as shown in the Table I.

TABLE I

Compound	Extra Hydrogen Atoms	Double Bonds
Abietylamine	0	2
Dehydroabietylamine	-2	3
Dihydroabietylamine	2	1
Tetrahydroabietylamine	4	0

These materials are derived from pine resin acids and are marketed by Hercules Powders Inc.under the trade names of Amine 750 and Amine D. They are sold for use in fungicides, bactericides, as surface-active agents, as corrosion inhibitors and as flotation reagents.

Amine D and Amine 750 differ only in the secondary amine content as indicated in Table II which tabulates some physical and chemical properties of these reagents (66,67).

FIGURE 4

STRUCTURE OF THE ABIETYLAMINE FAMILY

A - Dehydroabietylamine

B - Abietylamine

C - Dihydroabietylamine

D - Tetrahydroabietylamine

E - Dehydroabietylamine Acetate

TABLE II

	Amine D	Amine 750
Dehydroabietylamine	50-60%	50-60%
Dihydroabietylamine	20%	20%
Tetrahydroabietylamine	20%	20%
Secondary Amines	3%	1%
Total Amine Content	92%	95%
Physical State	Amber Viscous Liquid	Amber Viscous Liquid
Colour, (Gardner scale)	7	6
Specific Gravity at 25/15.6°C	1.000	1.000
Refractive Index at 20°C	1.5430	1.5447
Viscosity (poises) at 25°C	87	87

Dehydroabietylamine, Amine D, and Amine 750 are practically insoluble in water (less than 0.5 gm. in 100 gm. of water at 100°C.) but are readily soluble in alcohols, ether, hydrocarbons, or chlorinated solvents.

For use in water, the amines are reacted with acetic acid to form the acetate salt. (solubility-more than 1 gm. in 100 gm. water at 25°C.)

High-purity dehydroabietylamine acetate, supplied by Hercules Powders Inc., has the following composition:-

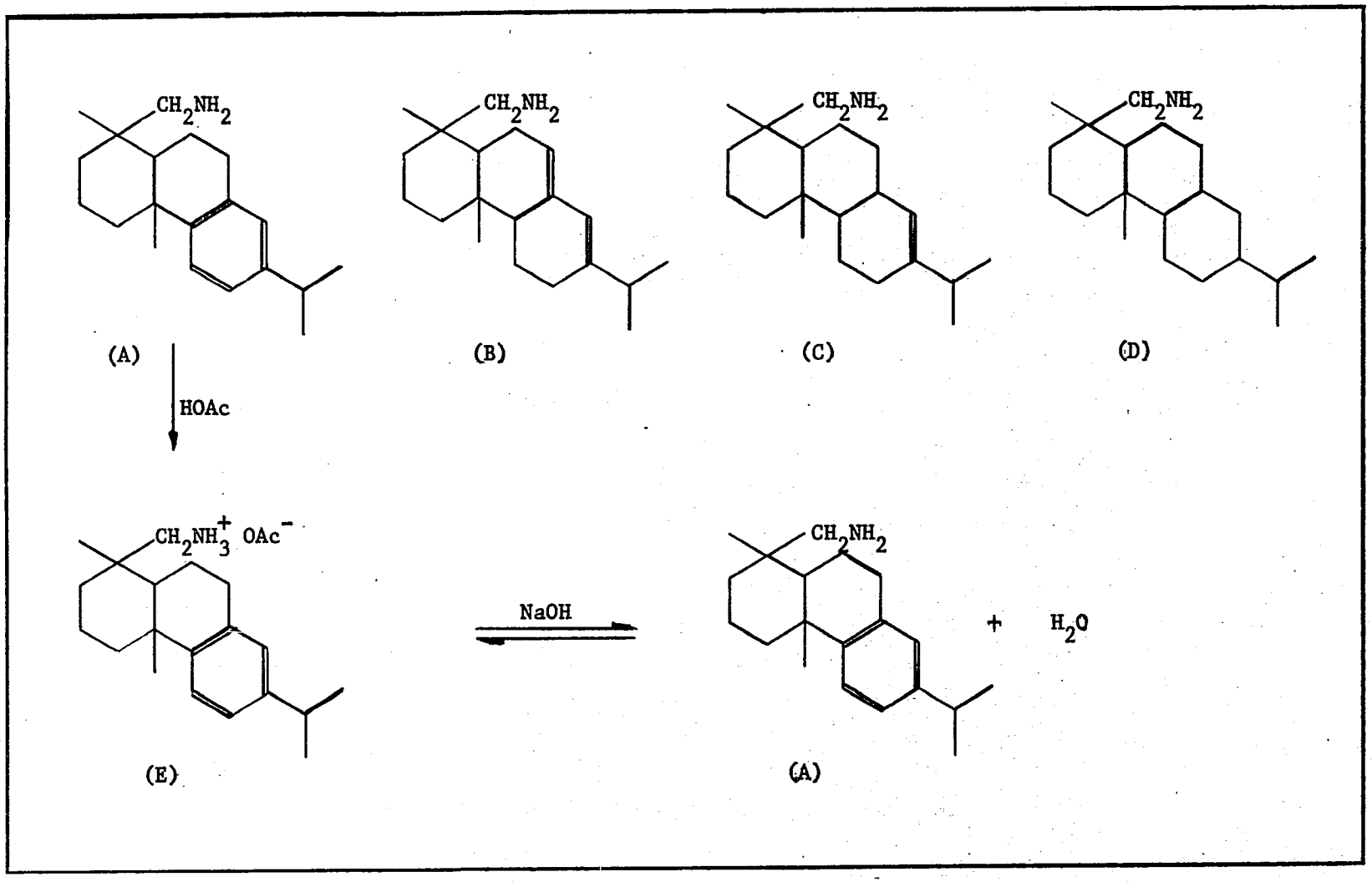
CH2NH2
(A)
(B)
(C)
(D)
HOAc
CH2NH3+ OAc−
(E)
NaOH
+ H2O
(A)

TABLE III

ANALYSIS OF DEHYDROABIETYLAMINE ACETATE

	Theoretical	Actual
Carbon	76.47	76.72
Hydrogen	10.21	10.44
Nitrogen	4.06	3.95
Oxygen	9.26	9.27
Total	100.00	100.38

Based on this analysis, the empirical formula was found to be $C_{22}H_{35}NO_2$, with a molecular weight of 345.51. The structural formula is as shown in Figure 4.

The molecular cross sectional area of the acid molecule is approximately 50 $Å^2$ and will be assumed to be the same for the amine (68,69).

Use of Dehydroabietylamine in Flotation

Steeprock Mines Ltd. (7) initiated an evaluation of various processes to handle their - 140 mesh crude ore. Of several processes, cationic flotation of the siliceous gangue was found to be the most economical and versatile. Several collectors out of twelve tried, (including Amine 750 and Rosin Amine D Acetate) were found suitable for further study but Rosin Amine D Acetate (70%) was found to be most economical. A pilot mill is presently confirming batch test results which indicate the production of hematite concentrates containing 3 to 6% SiO_2 from ore containing 36% SiO_2 is possible.

Maltby and Pickett (8) have produced concentrates with 0.12% SiO_2 and 51.1% recovery using 0.4 lb/Ton of Rosin Amine D Acetate. By suitable use of re-cleaners, a concentrate containing 0.06% SiO_2 and a recovery 70.7% of the original feed was found to be possible. It was found that cationic flotation will produce a higher grade of concentrate but was slightly more expensive than anionic flotation. (The major costs are grinding and collector consumption).

Major-Marothy (9) in a major research investigation at Schefferville tested more than a dozen cationic amine collectors. The results showed that good recoveries could be obtained with both ring and chain type amines but that, economically, ring types such as Amine D Acetate were best. For better recovery and grade, more sophisticated and more costly beta-amines could be used. These reagents offer better selectivity.

STATEMENT OF PROBLEM

The purpose of this investigation was to study the heteropolar organic compound, dehydroabietylamine acetate, as a collector in the flotation of mineral oxides. A comparison of the results with those using other amine collectors was desired.

The method of attack was first to determine adsorption, contact angle and floatability data for four amine-mineral oxide systems, namely dehydroabietylamine (DHAA.) and quartz, hematite, rutile and baddeleyite. Secondly, to supplement this work, data concerning concentration of ions in solution, surface tension and equivalent conductance of dehydroabietylamine solutions was obtained. Thirdly, in order to establish the effect of the double layer, the zero-points-of-charge of the oxides were determined. A comparison with dodecylamine acetate was made, as it was the only other amine acetate which has been studied in detail.

MATERIALS, EXPERIMENTAL EQUIPMENT AND PROCEDURES

Materials

1) Mineral Preparation

A. Hematite

The mineral used in this investigation was -10 mesh specular hematite spiral concentrate supplied by the Quebec Cartier Mining Company. This material had been previously crushed and ground by wet autogenous Cascade mills and up graded by spirals. The -325 + 400 mesh portion was used throughout the adsorption and flotation experiments as this is the finest portion which could be sized without the use of the infrasizer. The preparation of the sample consisted of size separation, the removal of silica and other low specific gravity minerals, the removal of magnetite, and the cleaning and washing of the hematite surface.

The concentrate was first roughly screened dry to remove all material that was - 400 mesh or + 270 mesh. The - 270 + 400 mesh material was then wet screened into 3 portions: - 270 + 325 mesh, - 325 + 400 mesh, and - 400 mesh. The latter was formed by small particles, which adhered to the larger particles when dry, but washed off the larger particles with the wet screening. Similarly, a portion of the + 325 mesh material passed through to the finer screen sizes. A final dry screening of the coarser fraction (- 270 + 325 mesh and - 325 + 400 mesh) produced a very uniform material of -325 + 400 mesh size.

The silica and other low specific gravity minerals were removed in a Richards Laboratory type free settling classifier (70), followed by superpanning in a Haultain Superpanner. The product was considered silica free when, on microscopic examination, no free silica particles could be observed.

The magnetic portion was removed using a Ding Laboratory magnetic separator, after which the non-magnetic portion was tested with a strong hand magnet to ensure complete removal of the magnetics.

Since surface impurities greatly affect the adsorption of organic collectors and the flotation characteristics of a mineral, the sample was washed twice with cold 10% hydrochloric acid solution. This treatmentwas similar to that used by Oko (71), and Iwasaki, Kim and Strathmore (72). The sample was then washed repeatedly with distilled water followed by conductivity water until no further change in pH or conductivity of the washings could be detected. The sample,now considered clean, was dried in a steam oven, thoroughly mixed and kept in a closed dessicator jar. The specific surface as determined by B.E.T. adsorption method using krypton gas was found to be 1372 $cm.^2/gm.$ (see Appendix III).

A second sample was prepared having as high a specific surface as possible. To obtain this sample, a portion of the spiral concentrate was recleaned on an air table (0.2 to 0.5% SiO_2) and reground in a pulverizer at the Department of Mines and Technical Surveys, Ottawa. It was finally ground for two hours in an Abbé ball mill.

The + 400 mesh portion was discarded. The sample was freed from magnetics and cleaned in the same manner as the coarse fraction. The specific surface as determined by the B.E.T. adsorption method using nitrogen gas was found to be 26.4 M^2./gm. (see Appendix III).

Semi-quantitative analysis of the hematite used in this investigation was as follows:

SiO_2	0.013%
MgO	< 0.03%
Al_2O_3	0.01 to 0.1%
Na_2O	0.01 to 0.1%
Fe_2O_3	99.7 to 99.96% by difference .

B. Quartz

The sample of quartz used in this investigation was supplied by Dominion Silica Co. Ltd., as Silex Flour. The sample was screened in the same manner as the hematite. Due to a small amount of kaolinite present, the sample was leached in a Soxhlet extractor with concentrated hydrochloric acid followed by washing with boiling distilled water, cold water, and finally with conductivity water. When cleaning was complete the silica sample was dried in a steam oven, mixed thoroughly, and stored in a dessicator. The specific surface of the silica was determined by krypton gas adsorption to be 1407 $cm.^2$/gm. (see Appendix III).

Semi-quantitative analysis of the silica sand used indicated the following impurities:

Fe_2O_3	0.01 to 0.1%
MgO	< 0.03%
Cu	0.01 to 0.05%
SiO_2	99.8 to 99.98% by difference .

C. Rutile

A sample of synthetic rutile was obtained from the National Lead Co. Ltd., (Titanium Division). This sample, was prepared by the crushing of larger crystals which were grown by the flame fusion technique, was screened to -325 mesh (73). Although there was considerable amount of - 400 mesh material, the sample was used as received without further sizing. The sample was cleaned with concentrated hydrochloric acid, washed with strong sodium hydroxide, and rinsed with distilled water followed by conductivity water as described previously. The surface area was determined by B.E.T. kryton gas adsorption method to be 3610 $cm.^2/gm.$ (see Appendix III). The chemical analysis, determined spectrographically, of the rutile sample was found to be as follows:

Impurity	Percentage
SiO_2	0.02
Fe_2O_3	0.0001
Al_2O_3	0.01
Sb_2O_3	0.01
SnO_2	0.002
Mg	0.0001
Cu	0.0001
Pb	0.0005
Mn	0.00005
Ni	0.001
V	0.0005
Cr	0.0001

By the difference, the TiO_2 content is 99.95%.

D. Baddeleyite

Unfortunately, a sample of high purity baddeleyite, or zirconia was not available in the size range - 325 + 400 mesh. A finely divided sample, prepared by precipitation of ZrO_2 from zirconium oxysulphate solution, was obtained from the National Lead Co. The sample as received was analysed as follows (74):-

	Impurity	Percentage
Chemical Analysis	SO_3	0.91
	Ign. Loss	1.16
Spectrographic Analysis	SiO_2	0.15
	P_2O_5	0.01
	HfO_2	0.005
	Al_2O_3	0.005
	Fe_2O_3	0.005
	MgO	0.02
	CaO	0.03

The sample, after washing and drying, would by difference analyse 99.77% ZrO_2, if all the SO_3 could be removed. The sample was washed with 10% hydrochloric acid, distilled water, and conductivity water as described previously. The filtrate was checked for chloride and sulphate ions. The sample was dried, mixed, and stored in the usual way. The surface area was determined by B.E.T. nitrogen gas adsorption to be 16.3 M^2./gm.

All minerals were identified by X-ray diffraction to determine if there was more than one compound present (e.g. FeOOH in Fe_2O_3). No compounds other than the minerals being examined were detected (see Appendix IV).

2) Chemical Reagents

A. Dehydroabietylamine Acetate

The dehydroabietylamine acetate used in this investigation was a specially prepared sample supplied by Hercules Powders Inc. For the present adsorption study, this high purity dehydroabietylamine acetate was used because it is easily soluble in water, whereas the amine is practically insoluble. The composition of the acetate was checked and the results are reported in Table III (68).

Stock solution containing 0.2 gram of dehydroabietylamine acetate per 100 ml. of solution was prepared as follows:- To a tared beaker, exactly 0.2000 grams of dehydroabietylamine acetate was added followed by 20 ml. of conductivity water. When dissolution was complete, the solution was transferred to a volumetric flask and the required volume of water added to make exactly 100 ml. of solution. The above procedure was necessary due to the sticky nature of dehydroabietylamine acetate (similar to pine pitch). The stock solution had a concentration of 2,000 mg./l. dehydroabietylamine acetate. From the stock solution, other solutions of varying concentrations were made for the adsorption tests by simple dilution.

B. Conductivity Water

Conductivity water for these experiments was prepared from water distilled in a Barnstead Water Still, Type SL-1. This water was redistilled in an all-pyrex Yoe-type still(Corning Glass Water Distillation

Apparatus, Model AG-2). Purified nitrogen was allowed to bubble through it for not less than two hours to give a solution with a conductivity varying from 2.6 to 5.0 $X10^{-7}$ mhos/cm. The pH of these solutions varied from 7.0 to 7.3 indicating the presence of slight amount of basic impurity.

C. Purified Nitrogen

Water-pumped commercial nitrogen was purified by bubbling through a strong potassium hydroxide solution to remove carbon dioxide, then through a 15 inch column of a 0.1 N solution of vanadyl sulphate to remove oxygen, and finally through a column of distilled water to remove any traces of vanadium salts or acid that might have been carried over. The vanadium solution was prepared by the method suggested by Meites (75). Lightly amalgamated zinc was added to 0.1 N solution of vanadyl sulphate. A small amount of concentrated sulphuric acid was added to liberate hydrogen, which reduced the vanadium to a lower oxidation state. The vanadyl sulphate solution was thus regenerated at the expense of the zinc.

D. Hydrochloric Acid.

Concentrated hydrochloric acid(A.C.S. Spec.) was diluted to approximately 1 N acid solution with conductivity water. This hydrochloric acid was standardized against sodium carbonate (A.C.S. Spec.). The acid was found to be exactly 1.000 N HCl. (see Appendix II).

E. Sodium Hydroxide

Eighty grams of sodium hydroxide pellets(A.C.S. Spec.) were dissolved in 80 ml. of conductivity water in a glass stoppered separatory funnel. The solution was allowed to stand for ten days after which the precipitated sodium carbonate had settled to the bottom. Twenty ml. of the clear solution was diluted to 400 ml. with conductivity water to give a solution of approximately 1 N. This base solution was standardized against the above hydrochloric acid and found to be 1.181 N NaOH. (see Appendix II).

F. Other Reagents.

All other chemicals used in this investigation were commercially available. Only the purest grades were purchased and used. These include:-

Glacial Acetic Acid	Merck Co. (A.C.S.)	99.8% Min.Assay
Chloroform	Fisher Certified (A.C.S.)	Largest Impurity Acetone 0.005%
Bromophenol Blue (Na-salt)	Fisher Certified (A.C.S.)	- -

Experimental Equipment and Procedures

1 (a) Agitation Adsorption Tests

Two gram samples of the cleaned and sized oxides were used in all adsorption tests. Adsorption tests were carried out in 50 ml. glass vials, which had an average capacity of 48.0 ml. when empty. If the vials were filled with two grams of hematite, zirconia, or rutile, the liquid volume was 47.5 ml. If the vials contained two grams of silica, the solution volume was 47.2 ml. These vials were completely filled with amine solution to minimize the formation of bubbles. The vials were stoppered with rubber serum caps and the last air bubble was removed with a hypodermic needle. Agitation was provided by packing fourteen vials in a metal container and turning the vials on their longitudinal axis at 86 r.p.m. This was similar to that of Lapointe (76).

The initial and final amine concentrations were determined using a Beckman DU Spectrophotometer (see Appendix I), and the difference taken as the amount adsorbed.

Equilibrium times were determined for various amine concentrations (Table IV , and Figure 5) and a contact time of eighteen hours was taken to be sufficient for equilibration. Above 30 mg./l., the equilibrium time appeared to be less than one hour, but, in order to make all the tests uniform, a period of eighteen hours was used for each test. All tests were conducted at room temperature (23 ± 2 deg. C.).

TABLE IV

ADSORPTION TESTS TO DETERMINE THE EQUILIBRIUM CONTACT TIME

Time of Contact (hours)	Initial Concentration (mg./l.)	Final Concentration (mg./l.)	Amount Adsorbed (μmoles/cm.^{2})
0	5.0	5.0	0.0
1/12	5.0	3.1	9.50×10^{-5}
1/4	5.0	3.0	1.00×10^{-4}
1/2	5.0	2.8	1.10×10^{-4}
1	5.0	2.6	1.20×10^{-4}
18	5.0	1.8	1.60×10^{-4}
0	50	50	0.0
1/12	50	33.5	8.25×10^{-4}
1/4	50	34.2	7.90×10^{-4}
1/2	50	33.0	8.50×10^{-4}
1	50	35.5	7.25×10^{-4}
18	50	34.5	7.75×10^{-4}
0	500	500	0.0
1/12	500	465	1.75×10^{-3}
1/4	500	460	2.00×10^{-3}
1/2	500	450	2.50×10^{-3}
1	500	455	2.25×10^{-3}
10	500	465	1.75×10^{-3}

FIGURE 5

THE ADSORPTION OF DEHYDROABIETYLAMINE
ACETATE ON HEMATITE AS A FUNCTION OF CONTACT TIME

□ - 500 mg./1.

○ - 50 mg./1.

△ - 5 mg./1.

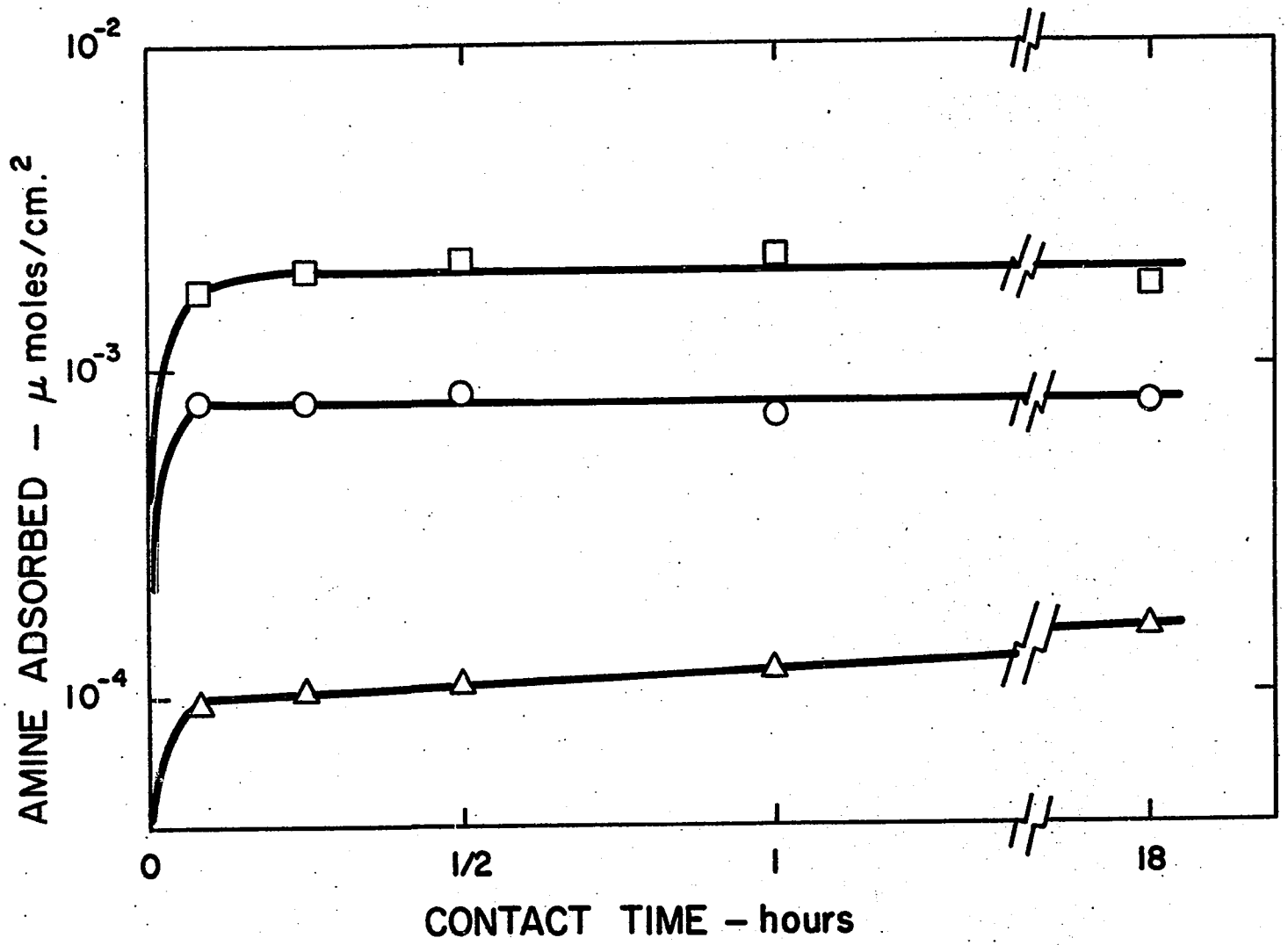
AMINE ADSORBED – μ moles/cm.²
10⁻²
10⁻³
10⁻⁴
0
1/2
1
18
CONTACT TIME – hours

1 (b) Desorption Tests

Amine ions or molecules adsorbed to the surface of the solid minerals were desorbed in an apparatus similar to the one used by Gaudin and Bloecher (78). The apparatus consisted of a 250 ml. filter flask on which a 20 mm. coarse fritted glass filter was mounted. The mineral sample was placed in the fritted glass filter and well mixed with a small portion of the amine stock solution. When wetting was assured, a funnel was attached to the filter with a rubber stopper as shown in Figure 6. The remaining solution was added to the funnel, thus maintaining a constant solution coverage over the bed of mineral. The same solution (100 ml. total) was passed through the bed three times to assure equilibration of the solid and solution. After analysis, a portion was removed and replaced with conductivity water. The dilute solution was then passed through the bed to desorb amine until equilibrium was again established. This procedure was continued until the concentration fell to the lowest possible level. Calculations were made to determine the amount of amine adsorbed at each concentration. To establish the error due to adsorption on the fritted glass filter, a check was made between the amount adsorbed in these tests and in the agitation adsorption tests. Adsorption on the filter was found to be negligible.

2. Surface Tension Determination

The surface tension of the organic amine solutions were determined at a natural pH of 5.4 to 6.6 using a modification of the glass capillary method described by Harkins and Brown (80). The surface

FIGURE 6

DESORPTION APPARATUS

M - Mineral Bed

S - Solution

R - Rubber Stoppers

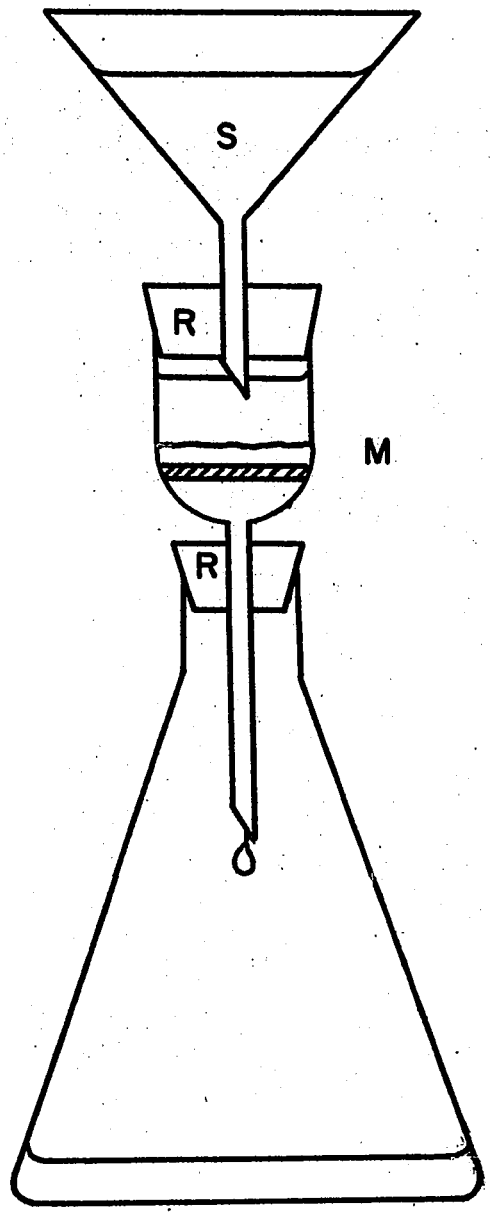
S
R
M
R

tension was measured by determining the equilibrium height of amine solution in two vertical capillary glass tubes of different internal radii (81) as shown in Figure 7. If the meniscus in each capillary is falling to the equilibrium position, then the formula for the surface tension,

$$\gamma = 1/2\ \rho g h\ r \cos \theta \tag{51}$$

becomes

$$\gamma = 1/2\ \rho g h\ r \tag{52}$$

since $\cos \theta \simeq 1$ when θ, the angle between the meniscus and the glass wall, approximates zero. Due to experimental difficulties in measuring the height of the liquid in the container, two capillary tubes of different diameter were used. Only the difference in height of the two menisci was required as the surface tension is expressed as:

$$\gamma = \frac{1}{2} \rho g \frac{r_1 \cdot r_2}{r_2 - r_1} \Delta h \tag{53}$$

where γ is the surface tension in dynes/cm.

ρ is the density difference between the amine solutions and the air above it (Assumed to be 1.00 gm./cm.^{3})

g is the acceleration of gravity (980.6 cm./sec.^{2})

r_1, r_2 are the radii of the two capillary tubes in cm.

Δh is the difference in height of the menisci in each tube in cm.

The glass capillaries were cut into ten inch long sections. The radius of the bore of each was determined by filling the capillary with triple distilled mercury and measuring the length and weight of mercury

FIGURE 7

DOUBLE GLASS CAPILLARY APPARATUS FOR
SURFACE TENSION DETERMINATION

A - Fine Capillary Tube

B - Coarse Capillary Tube

C - Pressurizing Tube

D - Solution

E - Rubber Stopper

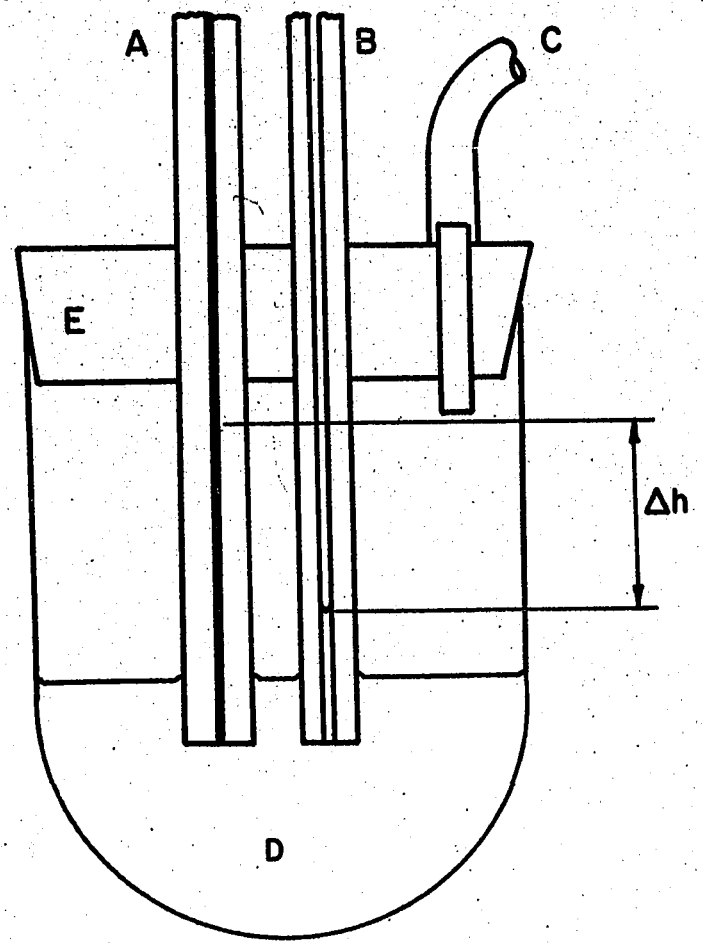
A
B
C
E
Δh
D

RESULTS

Adsorption and Desorption Tests

The amount of dehydroabietylamine acetate adsorbed on quartz, hematite, rutile, and baddeleyite (Γ_R) has been determined as a function of the equilibrium concentration of amine acetate in solution (C_R). The adsorption isotherms, shown in Figures 10 to 13 for each mineral respectively, were drawn using logarithmic scales for specific adsorption and equilibrium concentration. The concentration was varied from 0.3 to 5600 micromoles per litre while the specific adsorption varied from 0.2 to 49.0 micromoles per square meter (or Gibbs). The results are detailed in Tables XLIV to XLVII, Appendix VII. As a comparison, the adsorption of dodecylamine acetate on quartz and hematite are shown in Figure 10 and Figure 11.

The four isotherms indicate that the adsorption is related to the concentration in the bulk solution by the following equation.

$$\Gamma_R = k\,(C_R)^n \qquad (54)$$

where k and n are constants. This equation is similar to the Freundlich equation, except that the volume adsorbed per unit weight of adsorbent, v, is replaced by the specific adsorption, Γ_R, and the exponent $\frac{1}{n}$ is replaced by n. The values of k and n are recorded in Table V, when Γ_R is expressed in Gibbs and C_R in micromoles per litre.

used . Prior to surface tension measurements, the two capillaries and the solution container were thoroughly cleaned with glass cleaning solution followed by rinsing with distilled water, conductivity water and a small portion of the solution to be measured.

3. Contact Angle Determination

The construction of the contact angle apparatus was based on the one designed by Taggart, Taylor and Rice (79). It consisted of a microscope with its stage and objective horizontally mounted. A transparent plastic container, in which the solution and the specimen were placed, was set on the stage. The bubble holder consisted of a glass capillary tube mounted on an independant mechanical stage positioned on top of the microscope stage. The mineral specimen with a horizontal surface was placed in the flotation solution in the plastic container on the microscope stage and an air bubble was introduced onto its horizontal surface through the capillary tube. The angle of contact of the gas-liquid-solid interfaces was observed as a magnified image through the microscope's eyepiece, which was provided with graduations allowing direct reading of the angle to the nearest degree.

The samples were polished under water prior to each test to ensure a fresh surface. A contact time of one hour was taken as sufficient for equilibrium to be established between the amine and the mineral. An air bubble was then brought into contact with the mineral surface and an additional time of one-half hour was found sufficient for the contact angle to reach equilibrium.

4. Floatability Tests

One gram samples of each mineral were used for the flotation tests using a modified Hallimond tube (82,83). The samples were conditioned with amine in exactly the same manner as for the adsorption tests. A flotation time of one minute, with an air flow rate of 250 ml./min.(measured by an RGI spherical float meter) were arbitrarily chosen for the tests. Cell agitation was provided by a magnetic stirrer. The flotation tests were conducted at room temperature and at the natural pH. Tests were conducted in acid and base solution to determine the effect of pH.

5. Zero-Point-of-Charge Determination

The zero-points-of-charge of specular hematite, rutile and baddeleyite (zirconia) were determined using the adsorption of potential-determining ions technique (34).

The apparatus used to determine the zero-point-of-charge consisted of a 600-millilitre beaker with pouring lip removed, fitted with a rubber stopper with holes through which a calomel electrode and glass electrode for pH measurements, a thermometer, two burette tips, and inlet and outlet tubes for purified nitrogen were inserted (Figure 8). The beaker was placed in a 5 x 5 x 8 inch battery jar on top of a magnetic stirrer. Thermostated water was passed through the battery jar ($25.00 \pm 0.05^{\circ}C$). To prevent bicarbonate formation and dehydration, purified nitrogen was passed through the cell. The pH was read

FIGURE 8

APPARATUS USED FOR ZERO-POINT-OF-CHARGE DETERMINATION

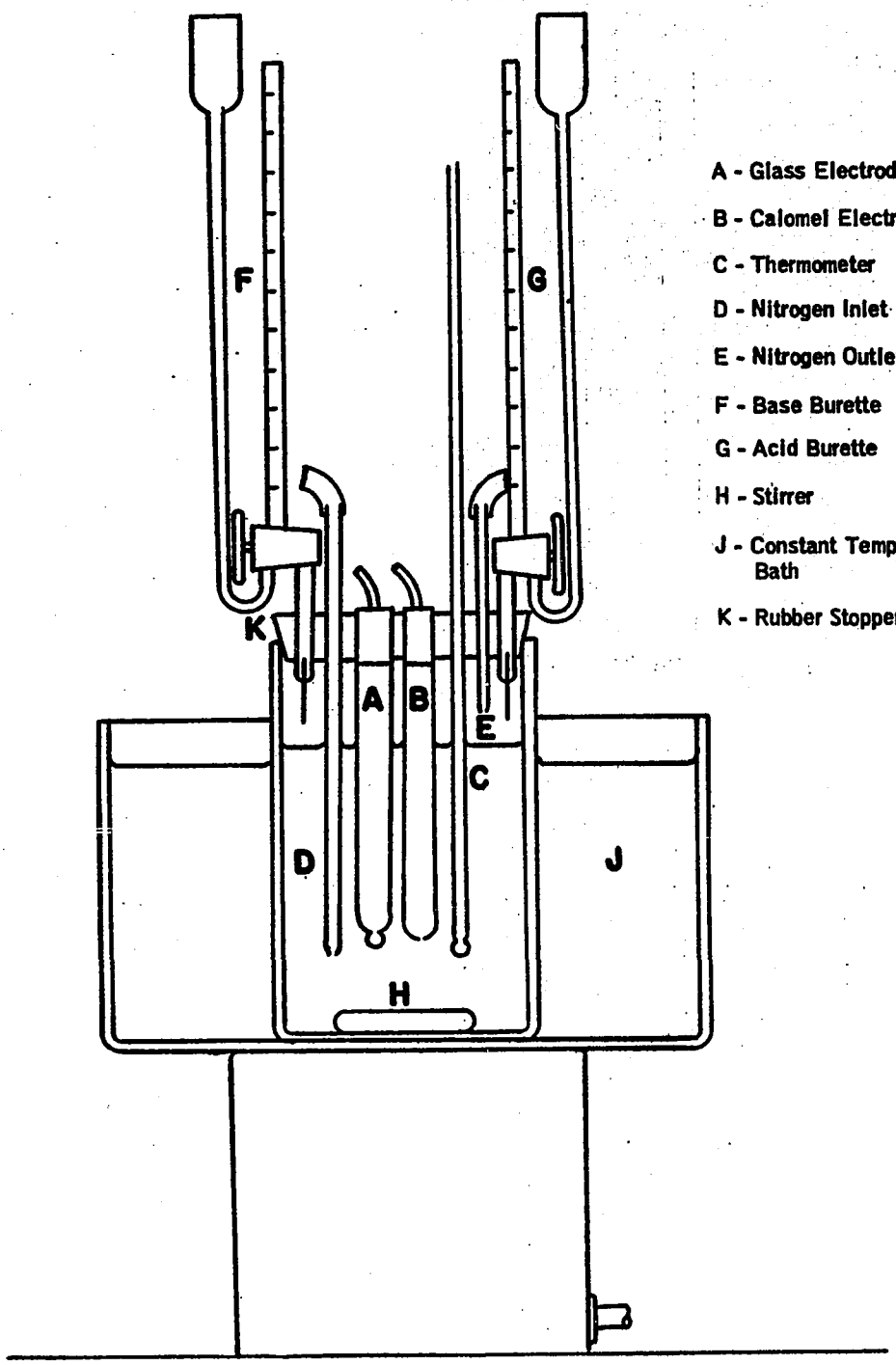

A - Glass Electrode

B - Calomel Electrode

C - Thermometer

D - Nitrogen Inlet

E - Nitrogen Outlet

F - Base Burette

G - Acid Burette

H - Stirrer

J - Constant Temperature Bath

K - Rubber Stopper

(± 0.005) with a Model 12 Corning pH meter with Corning electrodes, Type E-1.

Two titration curves were established for each concentration of supporting electrolyte, one with no solids present and the other with 4.000 gm. of hematite in 400 ml. of solution. The curves were both started with 1.000 ml. of 1.181 N NaOH and back-titrated with small amounts of 1.000 N HCl. Conversely, for rutile and zirconia, tests were started with 1.000 ml. of 1.000 N HCl and back-titrated with small amounts of 1.181 N NaOH. The pH was recorded when there was no change for one hour (usually one-half to eight hours).

In order to determine the zero-point-of-charge of quartz, the streaming potential method was used. The apparatus used is similar to that used by Purcell (27), Fuerstenau (84), and Buchanan (85) and is shown in Figure 9. Modifications included the insertion of the conductivity cell above the streaming cell and the use of nitrogen gas purification of the solution within the apparatus.

The solution under consideration was made up of acid or base additions made through a burette (B) and conductivity water which had been flushed with purified nitrogen in burette (I0). It was mixed in bulb A_1, and streamed back and forth through the mineral plug C into bulb A_2 until the conductivity was constant as measured by the conductivity cell immediately below A_1. The streaming cell was made up of two bright platinum electrodes in ground glass joints as shown in Figure 9.

FIGURE 9

STREAMING POTENTIAL APPARATUS

A_1, A_2 - Solution Bulbs
B - Burette
C - Manometer
D - Manifold
E - Streaming Cell
F - Conductivity Cell
G - pH Cell
H - Pressure Release
J - Ballast Tank
K - CO_2 Scrubber
L - Conductivity Cell

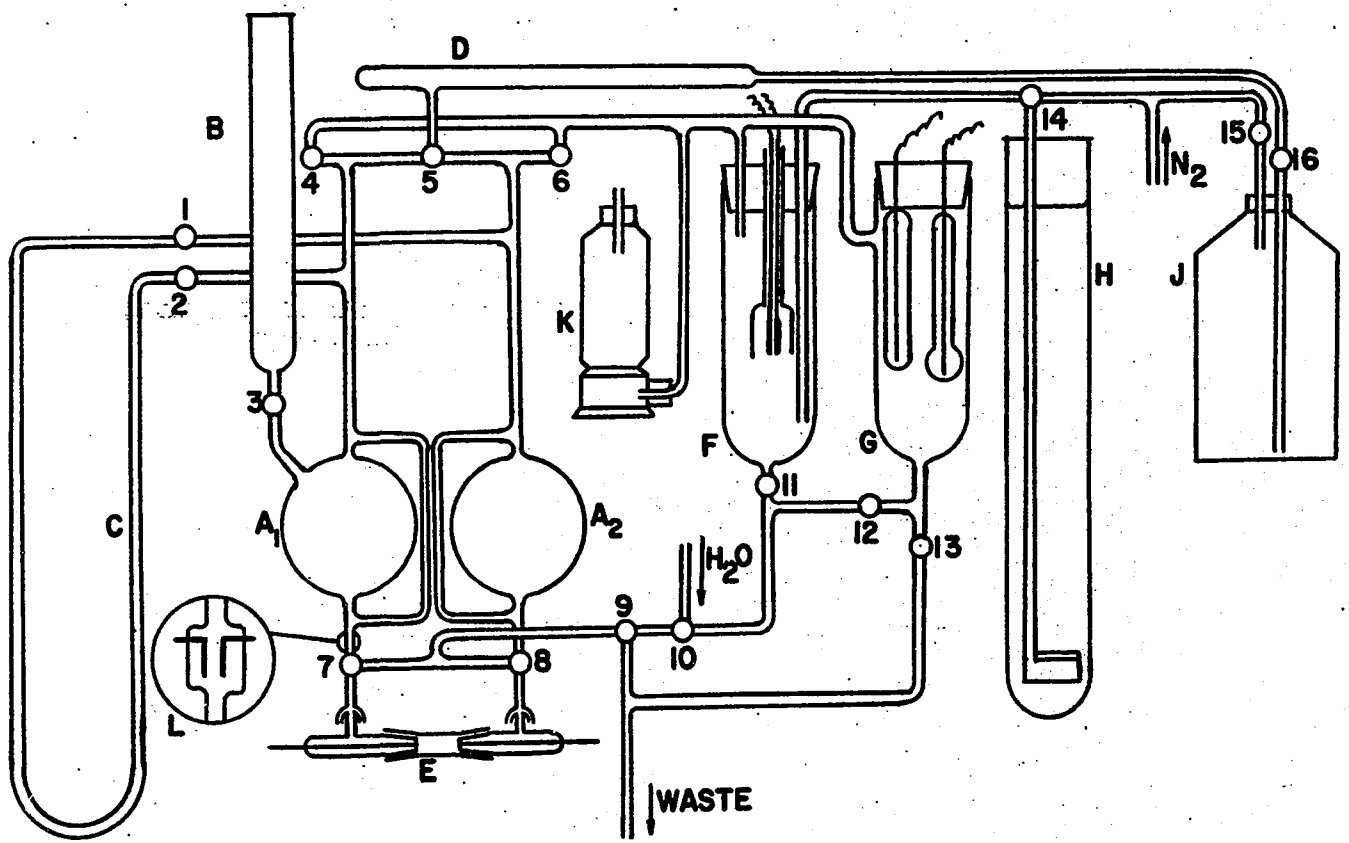
D
B
1
2
3
4
5
6
K
F
G
11
12
13
14
15
16
N_2
H
J
C
A_1
A_2
H_2O
9
10
7
8
L
E
WASTE

FIGURE 10

ADSORPTION OF DEHYDROABIETYLAMINE

ACETATE ON QUARTZ

A - ○ Adsorption Isotherm

□ Desorption Isotherm

B - Adsorption of Dodecylamine Acetate (deBruyn)

C - Adsorption of Dodecylamine Acetate (Bloecher)

M - Monolayer

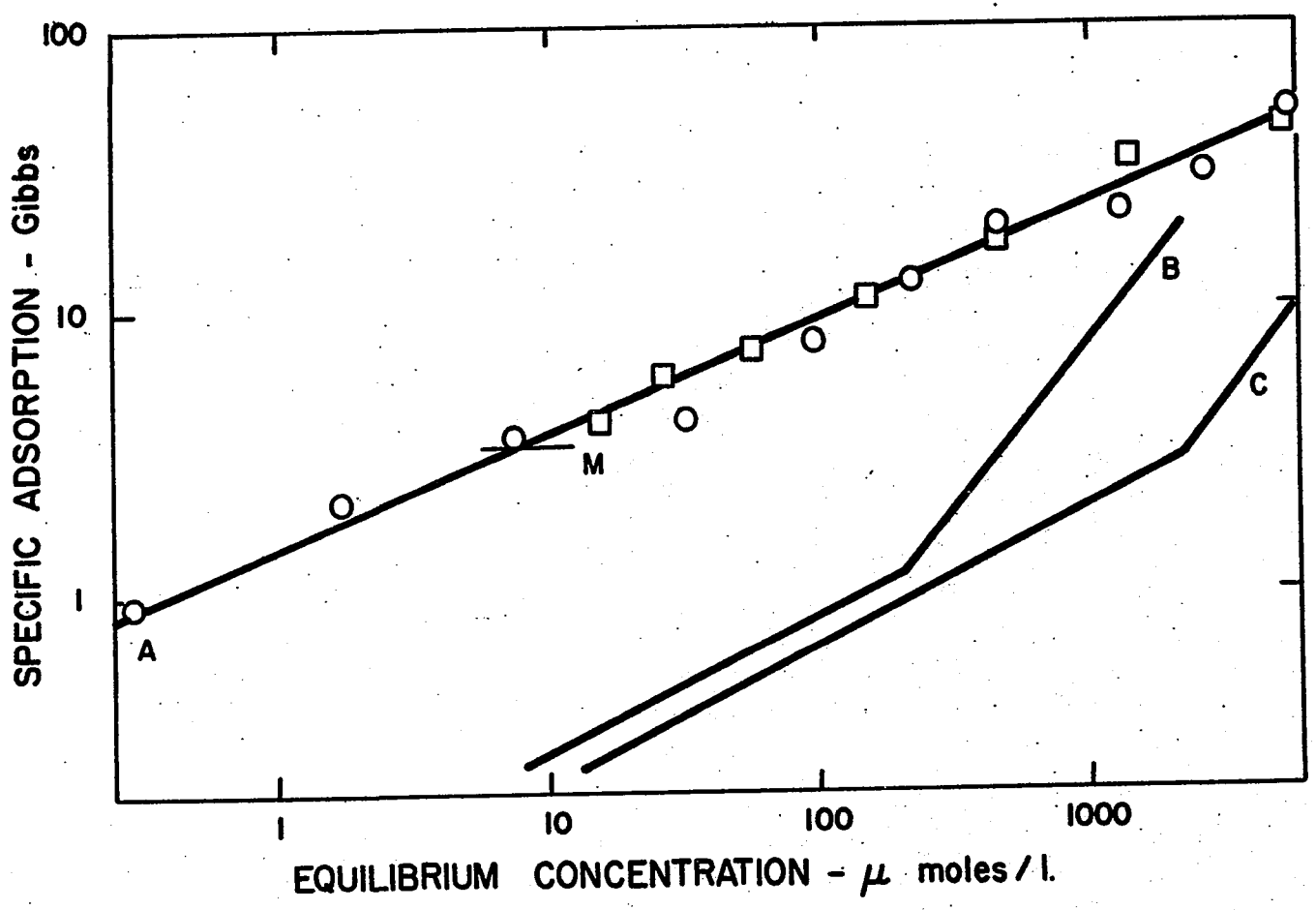
100
10
1
SPECIFIC ADSORPTION - Gibbs
A
M
B
C
1
10
100
1000
EQUILIBRIUM CONCENTRATION - μ moles / l.

FIGURE 11

ADSORPTION OF DEHYDROABIETYLAMINE

ACETATE ON HEMATITE

A - ○ Adsorption Isotherm

□ Desorption Isotherm

B - Adsorption of Dodecylamine Acetate (Morrow)

M - Monolayer

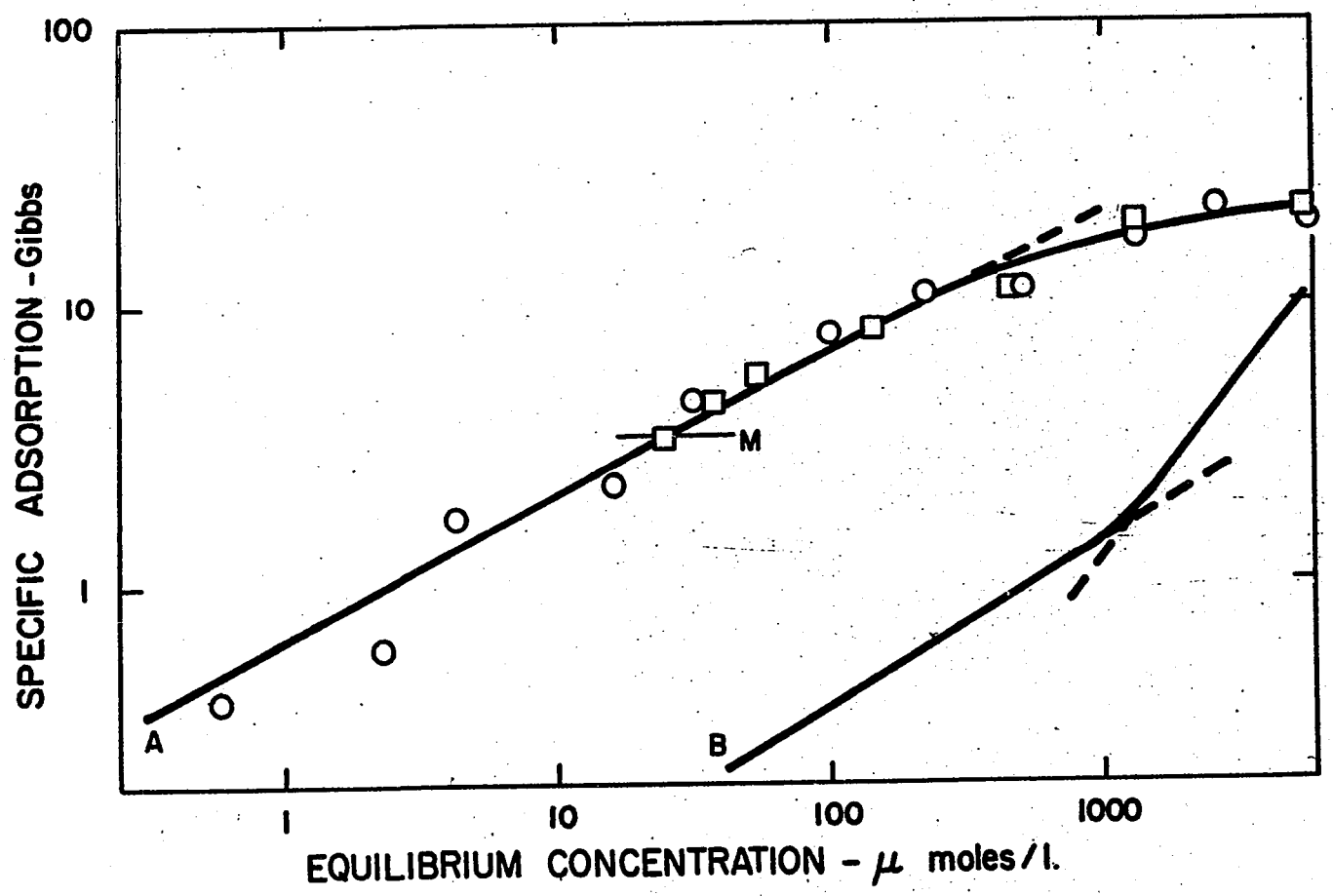
100
10
1
SPECIFIC ADSORPTION - Gibbs
A
B
M
1
10
100
1000
EQUILIBRIUM CONCENTRATION - μ moles/l.

FIGURE 12

ADSORPTION OF DEHYDROABIETYLAMINE

ACETATE ON RUTILE

○ - Adsorption Isotherm

□ - Desorption Isotherm

M - Monolayer

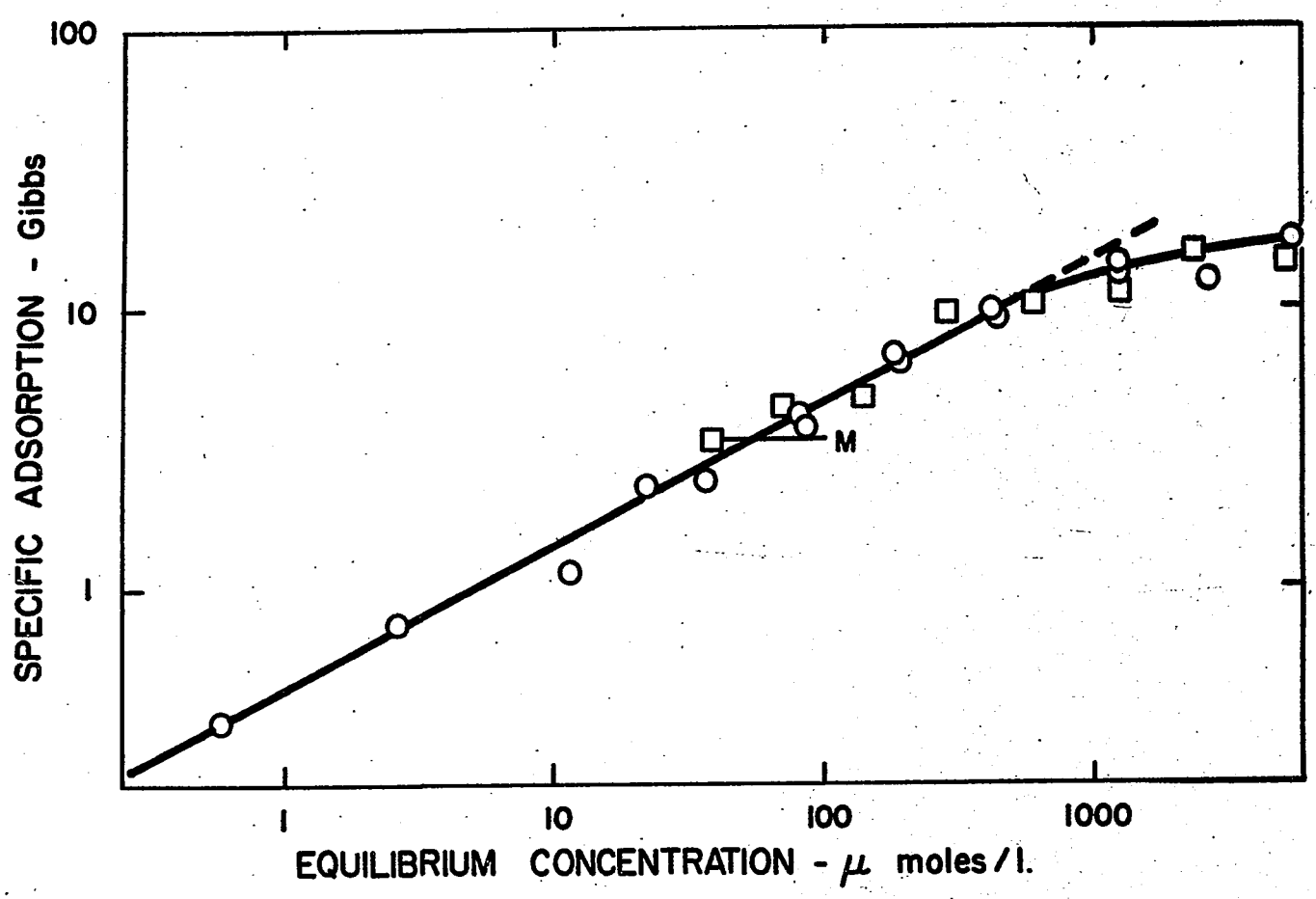
100
10
1
SPECIFIC ADSORPTION - Gibbs
M
1
10
100
1000
EQUILIBRIUM CONCENTRATION - μ moles / l.

FIGURE 13

ADSORPTION OF DEHYDROABIETYLAMINE

ACETATE ON BADDELEYITE
(Precipitated Zirconia)

○ - Adsorption Isotherm

M - Monolayer

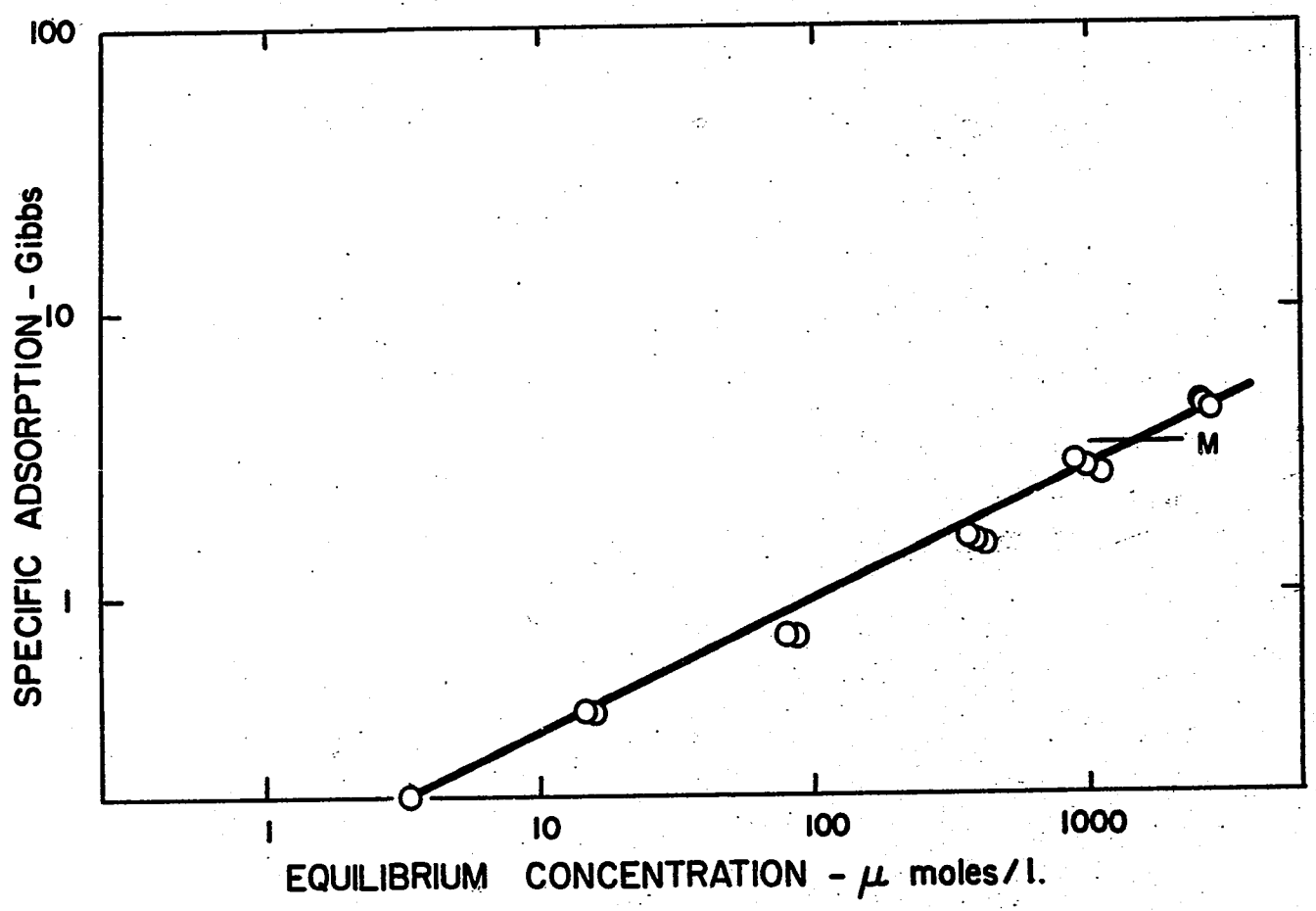
100
10
1
SPECIFIC ADSORPTION - Gibbs
M
1
10
100
1000
EQUILIBRIUM CONCENTRATION - μ moles/l.

TABLE V

k AND n VALUES FOR THE FREUNDLICH EQUATION

MINERAL	k	n
Quartz	1.41	0.41
Hematite	0.645	0.51
Rutile	0.440	0.50
Baddeleyite	0.106	0.49

The adsorption isotherms for rutile and hematite reach a saturation point at high concentrations. In this concentration range, the adsorption follows a modified Langmuir isotherm which may be expressed as follows:

$$\Gamma_R = \frac{(\Gamma_R)_o \, bC_R}{1 + bC_R} \qquad (55)$$

where $(\Gamma_R)_o$ is the maximum adsorption under existing solution conditions, and b is a constant which determines the concentration above which the adsorption approaches saturation. From the slope and intercept of the graph of C_R/Γ_R vs. C_R shown in Figure 14 for rutile and hematite, the constants $(\Gamma_R)_o$ and b are determined and are reported in Table XLVIII , Appendix VII.

No attempt was made to control the temperature of the adsorption system, but the small variations in room temperature did not have any systematic effect on the adsorption results.

FIGURE 14

DETERMINATION OF LANGMUIR ISOTHERM

CONSTANTS

△ - Rutile

□ - Hematite

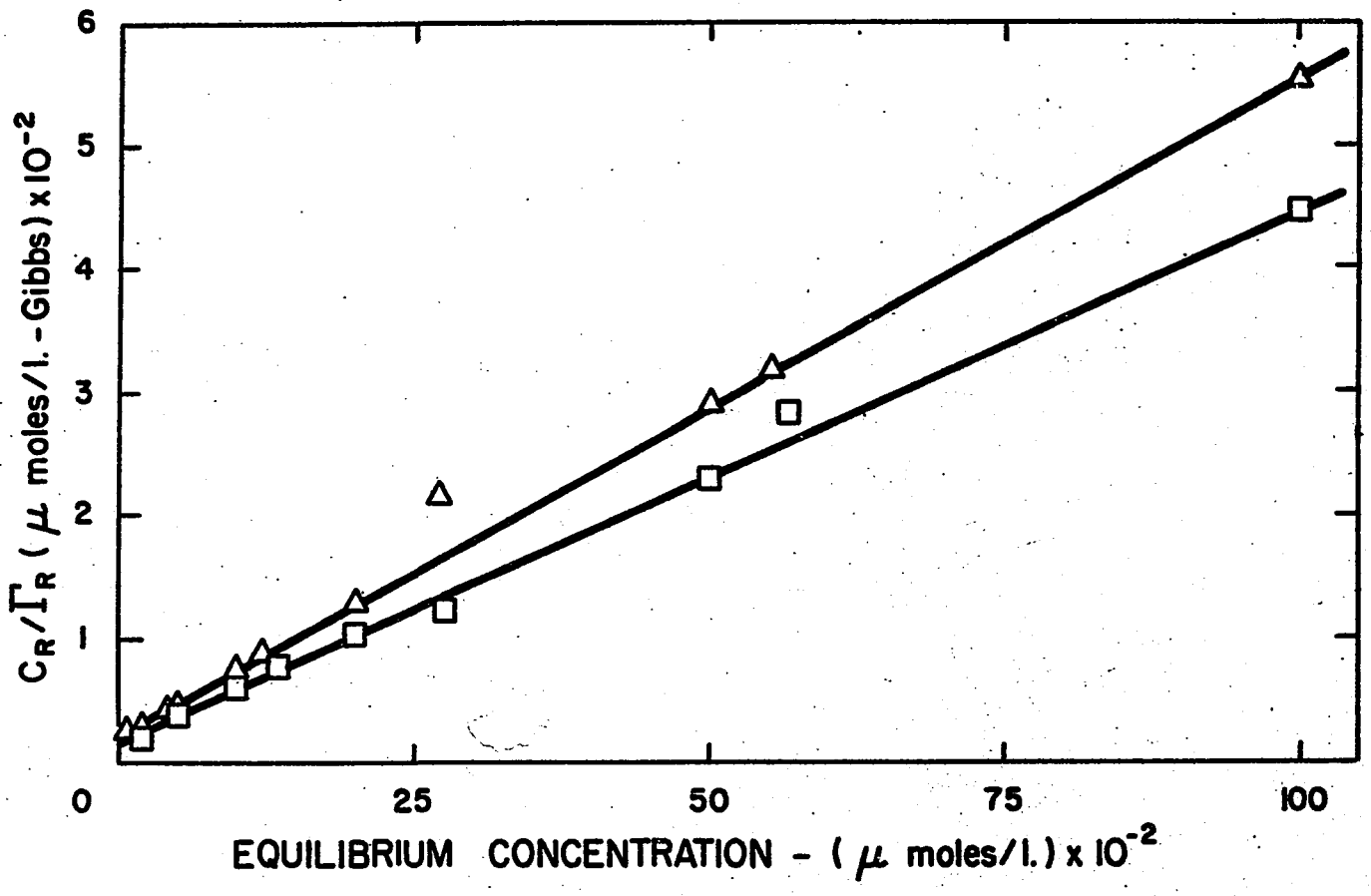
6
5
4
3
2
1
0
25
50
75
100
C_R/Γ_R (μ moles/l. - Gibbs) x 10^{-2}
EQUILIBRIUM CONCENTRATION - (μ moles/l.) x 10^{-2}

The solutions used were found to be slightly acid (pH of 5 to 6), even though no acid was added to the system. Since amine acetate solutions should be slightly basic due to the hydrolysis of the amine (approximately 0.4 pH units maximum in this case), the observed acidity must be due either to dissolved carbon dioxide or traces of acetic acid (from the amine acetate) in the unbuffered solutions. Even though a variation in pH of about one unit has been noted, no consistent change in the adsorption with respect to pH was observed. Absolute pH measurements around neutrality are unreliable in unbuffered solutions and not too much value should be attached to the magnitude of the experimental pH readings.

Attempts to calculate the weight of surfactant required to complete an adsorbed monolayer have been made by considering the location of oxygen atoms on cleaved mineral surfaces and determining the number of available sites (62,63). Using this technique and the cross-sectional area of dehydroabietylamine molecules of approximately 50 $Å^2$ (68,77), the area of quartz and hematite occupied by one dehydroabietylamine molecule is 46.8$Å^2$ and 48.1$Å^2$ respectively. However, since surface coverage is not uniform and since high and low specific adsorption regions are present (87), the calculated monolayer can be considered only as an approximate guide to determine the average number of adsorbed layers present. Thus, considering only the cross-sectional area of the amine molecule and the specific surface of each mineral, the weight of amine required to cover one square centimeter of surface

is 0.1146 microgram. The weight of amine required for an adsorbed monolayer on one gram of quartz, hematite, rutile and baddeleyite is 150, 146, 425, and 18,700 micrograms respectively. The accuracy of this determination is ± 10% due to uncertainty in the cross-sectional area of the dehydroabietylamine molecule.

Effect of pH

A series of tests was conducted to investigate the effect of pH on the adsorption of dehydroabietylamine acetate on the four minerals under study. The initial adsorbate concentration was 50 mg./l. in all tests. The pH was varied from 2.50 to 10.68 using acetic acid and sodium hydroxide. The results are shown in Figures 15 to 18 and are tabulated in Tables L to LIII in Appendix VII. The specific adsorption was corrected for differences in equilibrium concentration to correspond to a constant equilibrium concentration of 34.5 mg./l.(100 μmoles/l). The correction was made by applying equation (54) using the experimental values of n. In order to check the validity of this correction, the specific adsorption on rutile as a function of concentration at five different pH values was determined. Results are shown in Figure 19 and recorded in Table XLIX, Appendix VII. With the exception of the lowest points on curve E (at much higher pH than the rest of curve E), the specific adsorption is proportional to the square root of the equilibrium concentration at constant pH over the pH range 2.50 to 6.6.

The largest variation in specific adsorption occurs in the slightly acid region (pH of 3 to 7) regardless of the mineral on which

FIGURE 15

EFFECT OF pH ON SPECIFIC ADSORPTION
OF DEHYDROABIETYLAMINE ACETATE
ON QUARTZ

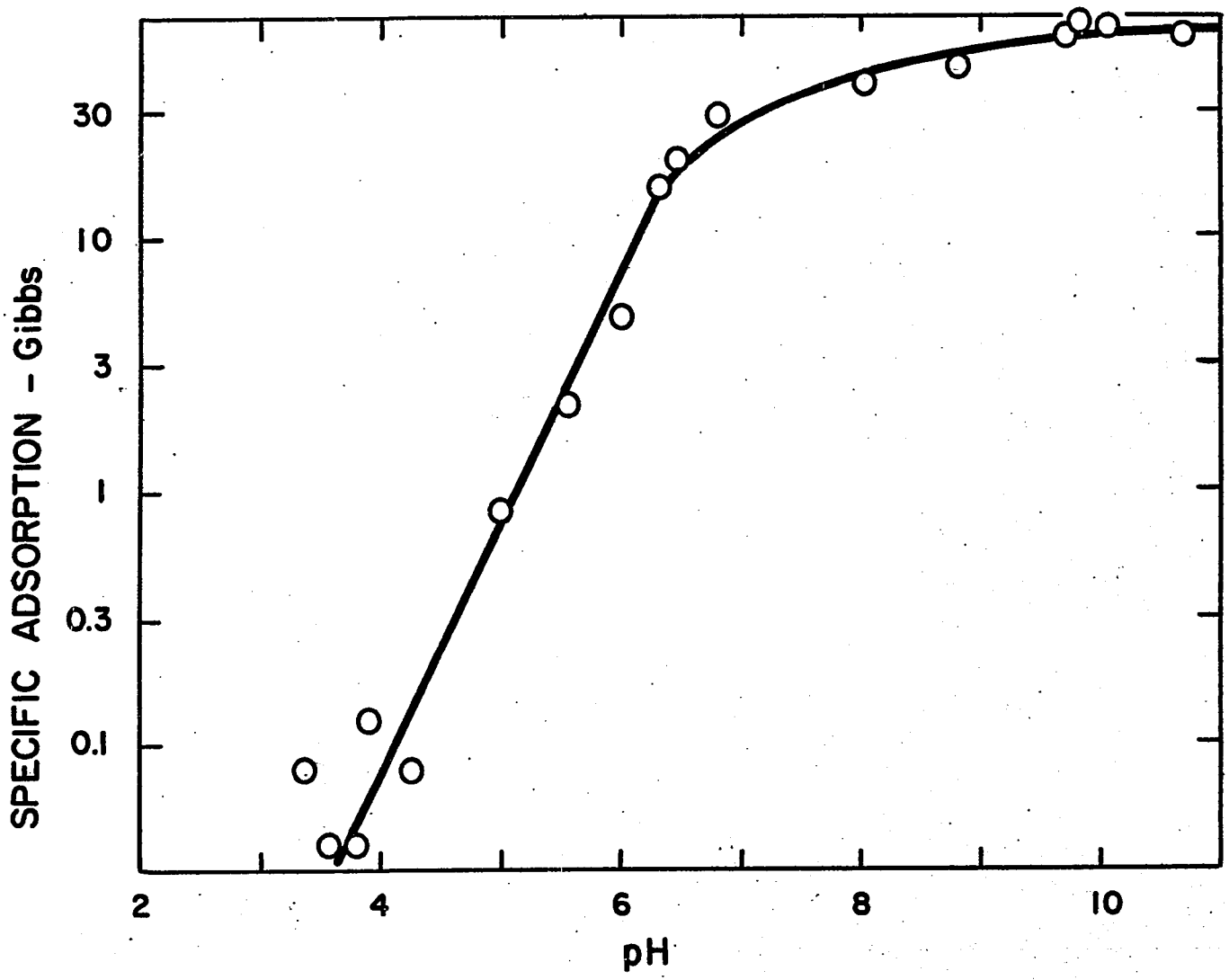
SPECIFIC ADSORPTION - Gibbs
30
10
3
1
0.3
0.1
2
4
6
8
10
pH

FIGURE 16

EFFECT OF pH ON SPECIFIC ADSORPTION

OF DEHYDROABIETYLAMINE ACETATE

ON HEMATITE

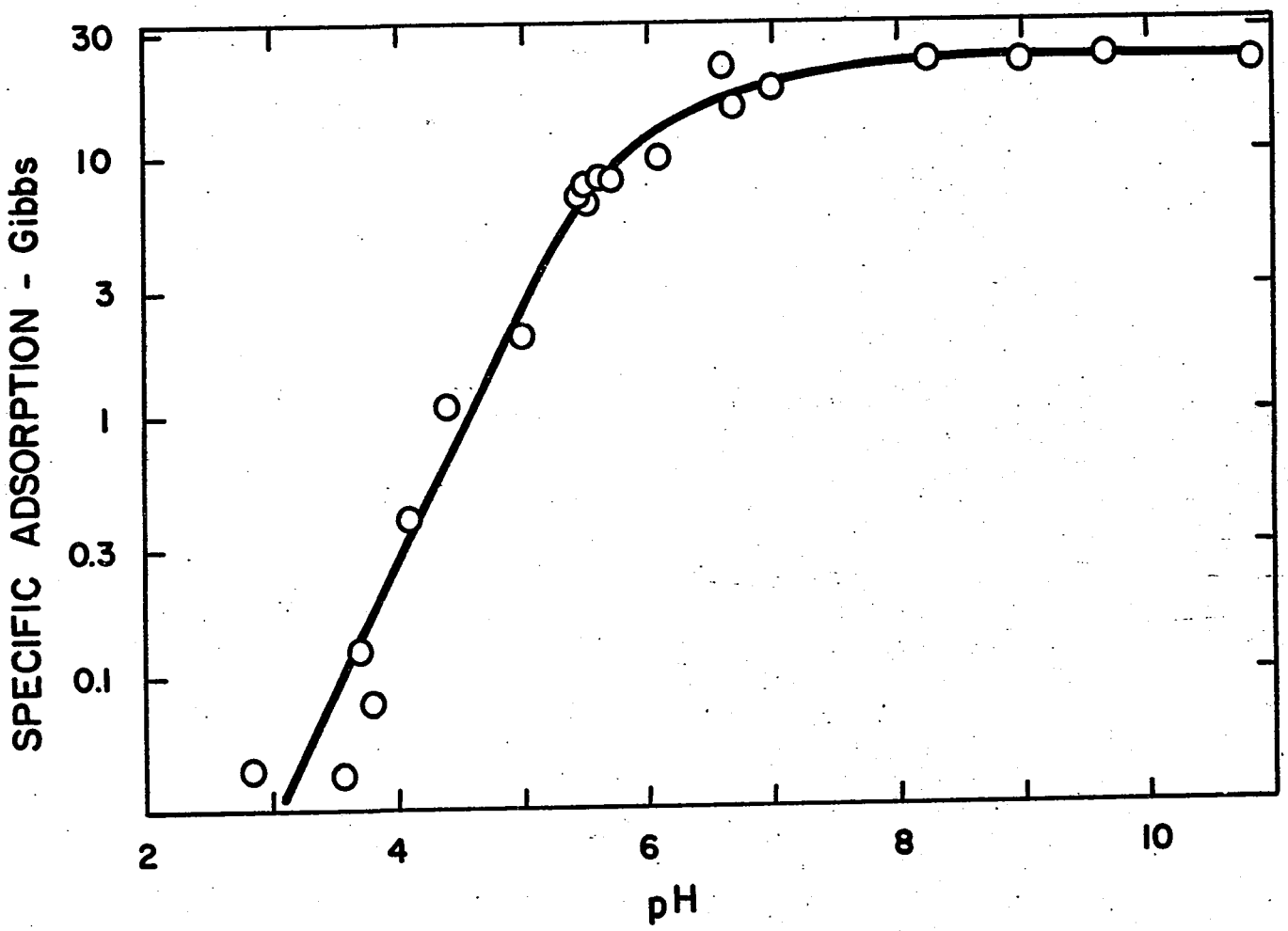
SPECIFIC ADSORPTION - Gibbs
30
10
3
1
0.3
0.1
2
4
6
8
10
pH

FIGURE 17

EFFECT OF pH ON SPECIFIC ADSORPTION

OF DEHYDROABIETYLAMINE ACETATE

ON RUTILE

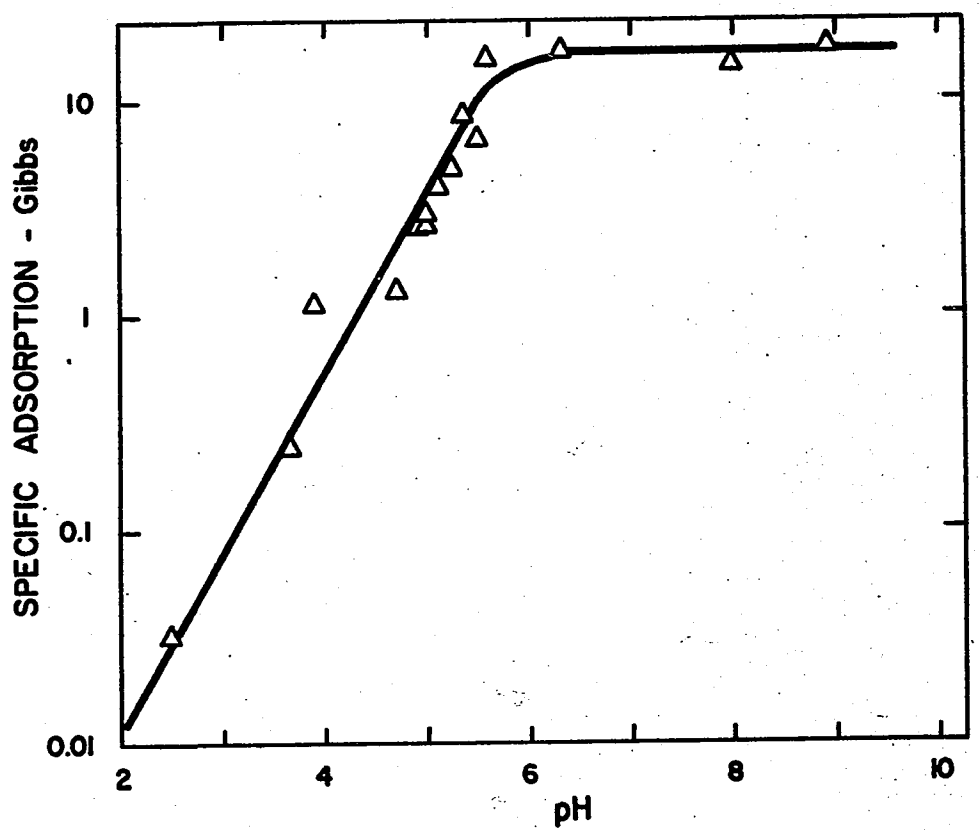
SPECIFIC ADSORPTION - Gibbs
10
1
0.1
0.01
2
4
6
8
10
pH

FIGURE 18

EFFECT OF pH ON SPECIFIC ADSORPTION

OF DEHYDROABIETYLAMINE ACETATE

ON BADDELEYITE

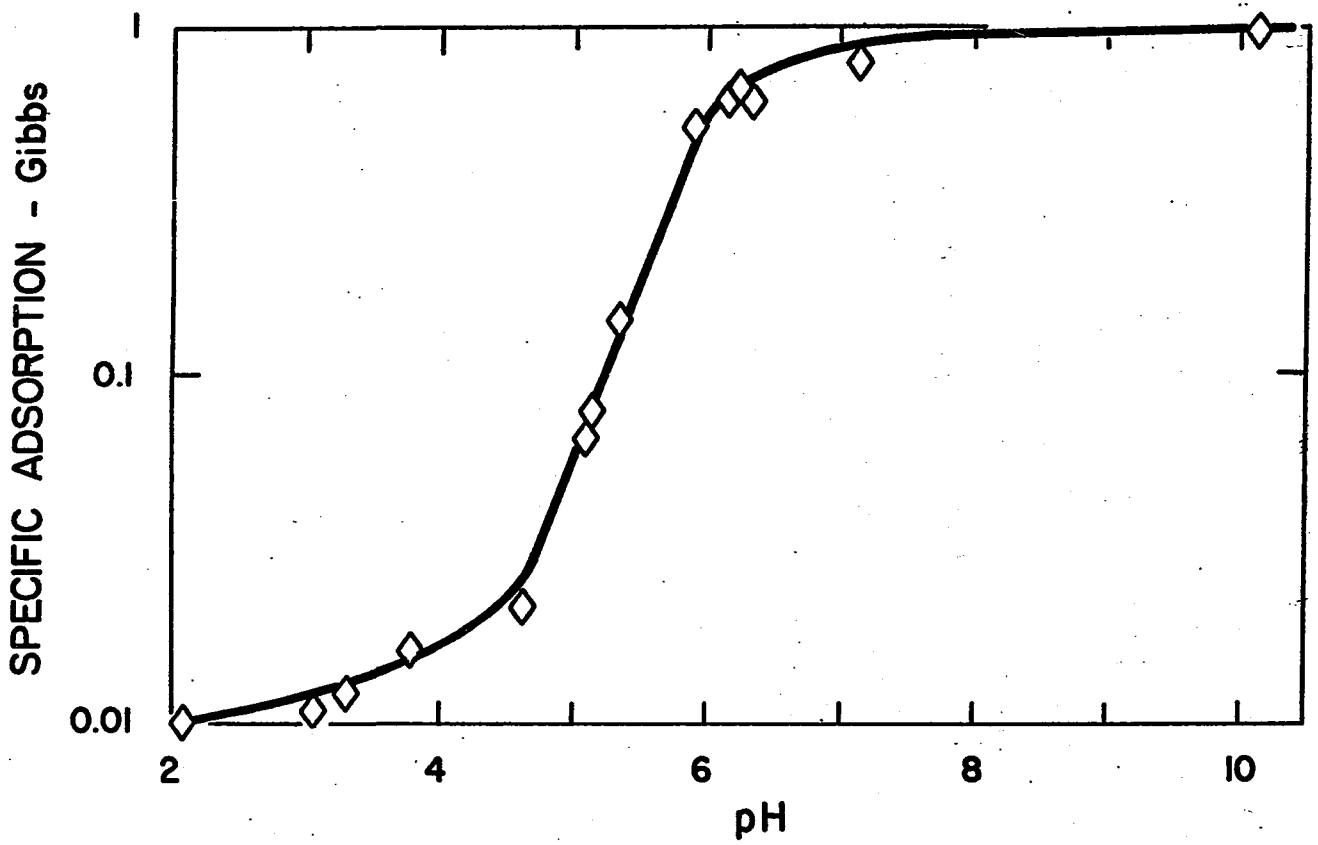
SPECIFIC ADSORPTION - Gibbs
1
0.1
0.01
2
4
6
8
10
pH

FIGURE 19

ADSORPTION OF DEHYDROABIETYLAMINE

ACETATE ON RUTILE AT

VARIOUS pH VALUES

A - pH = 2.50

B - pH = 3.98

C - pH = 4.99

D - pH = 6.30 to 6.55

E - pH = 6.80 to 9.70

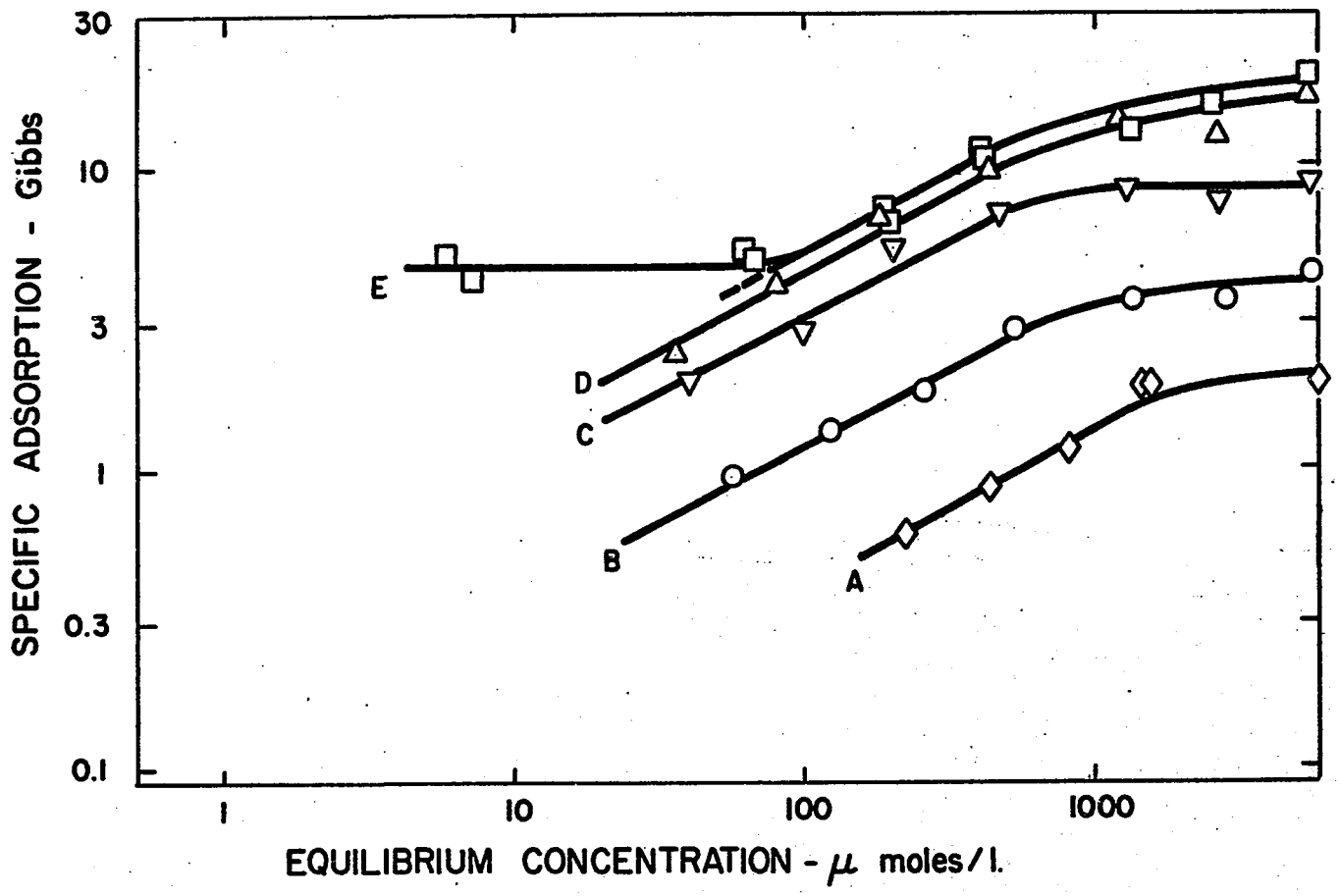
SPECIFIC ADSORPTION - Gibbs
30
10
3
1
0.3
0.1
1
10
100
1000
EQUILIBRIUM CONCENTRATION - μ moles/l.
E
D
C
B
A

the adsorption takes place. Below a pH of approximately three, the amount adsorbed is negligible and above a pH of seven the adsorption is nearly complete and constant, depending on the capacity of the mineral surface to adsorb the amine. The straight line portion of each curve may be represented by the following equation:

$$\Gamma_R = k(C_{H^+})^{-1} \tag{56}$$

where C_{H^+} is the concentration of the hydrogen ions and k is a constant.

Adsorption tests in the pH range of 8.80 to 10.68 were turbid initially due to partial hydrolysis of the amine. At the completion of the adsorption test, the solutions were clear due to the reduction in amine concentration. Thus, these results are included but must be considered doubtful due to uncertainty in the mechanism of the amine removal from the bulk solution.

Tables VI, VII and VIII summarize the results of tests to determine the desorption of dehydroabietylamine acetate from quartz, hematite and rutile, using water as the solvent. The tests indicate that most of the amine was desorbed readily, but that a small amount remained which could consequently be removed into acidic solutions. This quantity probably could be removed by continuous dilution with water, but, at low concentrations, the analysis became inaccurate. It was easier to remove the remainder with acid which accounts for the high concentration and low adsorption in the last desorption test on quartz and hematite.

TABLE VI

DESORPTION OF DEHYDROABIETYLAMINE ACETATE
FROM QUARTZ (wt. = 4.5628 gm.)

Equilibrium Test No.	Equilibrium Concentration	Amine in Solution	Amine Adsorbed	Amine Total	Amine Removed From Solution
	mg./l.	mg.	mg.	mg.	mg.
1 before	1905	190.50	9.50	200.00	143.00
after	1905	47.50	9.50	57.00	
2 before	496	49.60	7.40	57.00	37.20
after	496	29.80	7.40	19.80	
3 before	160	16.00	3.80	19.80	12.00
after	160	4.00	3.80	7.80	
4 before	54.8	5.48	2.32	7.80	4.11
after	54.8	1.37	2.32	3.69	
5 before	21.5	2.15	1.54	3.69	1.54
after	21.5	0.61	1.54	2.15	
6 before	9.5	0.95	1.20	2.15	0.71
after	9.5	0.24	1.20	1.44	
7 before	5.5	0.55	0.89	1.44	0.41
after	5.5	0.14	0.89	1.03	
8	9.6	0.96	0.07	1.03	(Acid)

TABLE VII

DESORPTION OF DEHYDROABIETYLAMINE ACETATE
FROM HEMATITE (wt. = 8.6872 gm.)

Equilibrium Test No.	Equilibrium Concentration	Amine in Solution	Amine Adsorbed	Amine Total	Amine Removed from Solution
	mg./ℓ.	mg.	mg.	mg.	mg.
1 before	1910	191.00	9.00	200.00	143.20
after	1910	47.80	9.00	56.80	
2 before	481	48.10	8.70	56.80	36.07
after	481	12.03	8.70	20.73	
3 before	160.3	16.03	4.70	20.73	12.01
after	160.3	4.02	4.70	8.72	
4 before	52.2	5.22	3.50	8.72	3.90
after	52.2	1.32	3.50	4.82	
5 before	22.4	2.24	2.58	4.82	1.68
after	22.4	0.56	2.58	3.12	
6 before	13.4	1.34	1.80	3.14	1.00
after	13.4	0.34	1.80	2.14	
7 before	8.5	0.85	1.29	2.14	0.64
after	8.5	0.21	1.29	1.50	
8	14.5	1.45	0.05	1.50	(Acid)

TABLE VIII

DESORPTION OF DEHYDROABIETYLAMINE ACETATE
FROM RUTILE (wt. = 9.6137 gm.)

Equilibrium Test No.	Equilibrium Concentration	Amine in Solution	Amine Adsorbed	Amine Total	Amine Removed From Solution
	mg./ℓ.	mg.	mg.	mg.	mg.
1 before	1834	174.24	16.90	191.14	9.18
after	1834	165.06	16.90	181.96	
2 before	860	163.50	18.46	181.96	86.00
after	860	77.50	18.46	95.96	
3 before	438	83.10	12.86	95.96	43.80
after	438	39.10	12.86	52.16	
4 before	214	40.60	11.56	52.16	21.40
after	214	19.20	11.56	30.76	
5 before	102.6	19.20	11.26	30.76	15.40
after	102.6	4.10	11.26	15.36	
6 before	50.5	9.60	5.76	15.36	5.05
after	50.5	4.55	5.76	10.31	
7 before	24.5	4.65	5.60	10.31	3.68
after	24.5	1.03	5.60	6.63	
8	13.6	2.58	4.05	6.63	-

Surface Tension, Conductance and Ion Concentration.

1) Surface Tension Measurements

The effect of amine concentration on the surface tension of aqueous solutions is shown in Figure 20. The results are tabulated in Appendix VI. With increasing amine concentration, the surface tension dropped rapidly at low concentrations followed by a more gradual decrease at higher concentrations. The effect is similar to that obtained by adding ethyl alcohol to aqueous solutions (88). When the surface tension is plotted as a function of the logarithm of the equilibrium concentration, the result, shown in Figure 21, indicates that there was no effect up to 5 mg./l. dehydroabietylamine acetate. Above 30 mg./l., the surface tension was a function of the logarithm of the concentration according to

$$\gamma = 91.1 - 16.7 \log_{10}(C_R) \qquad (57)$$

where γ is the surface tension in dynes/cm. and C_R is the amine acetate concentration in mg./l. In the concentration range of 5 to 30 mg./l., there is a transition zone where the change in surface tension increases with concentration until the above equation is satisfied. There is no indication of an abrupt change in the decrease in surface tension with increasing concentration that would mark the onset of micelle formation. Therefore, the critical micelle concentration has not been reached in the concentration range below 2 gm./l. Since dodecylamine acetate has a critical micelle concentration of 0.013 molar (3.18 gm./l.)

FIGURE 20

SURFACE TENSION OF DEHYDROABIETYLAMINE

ACETATE SOLUTIONS

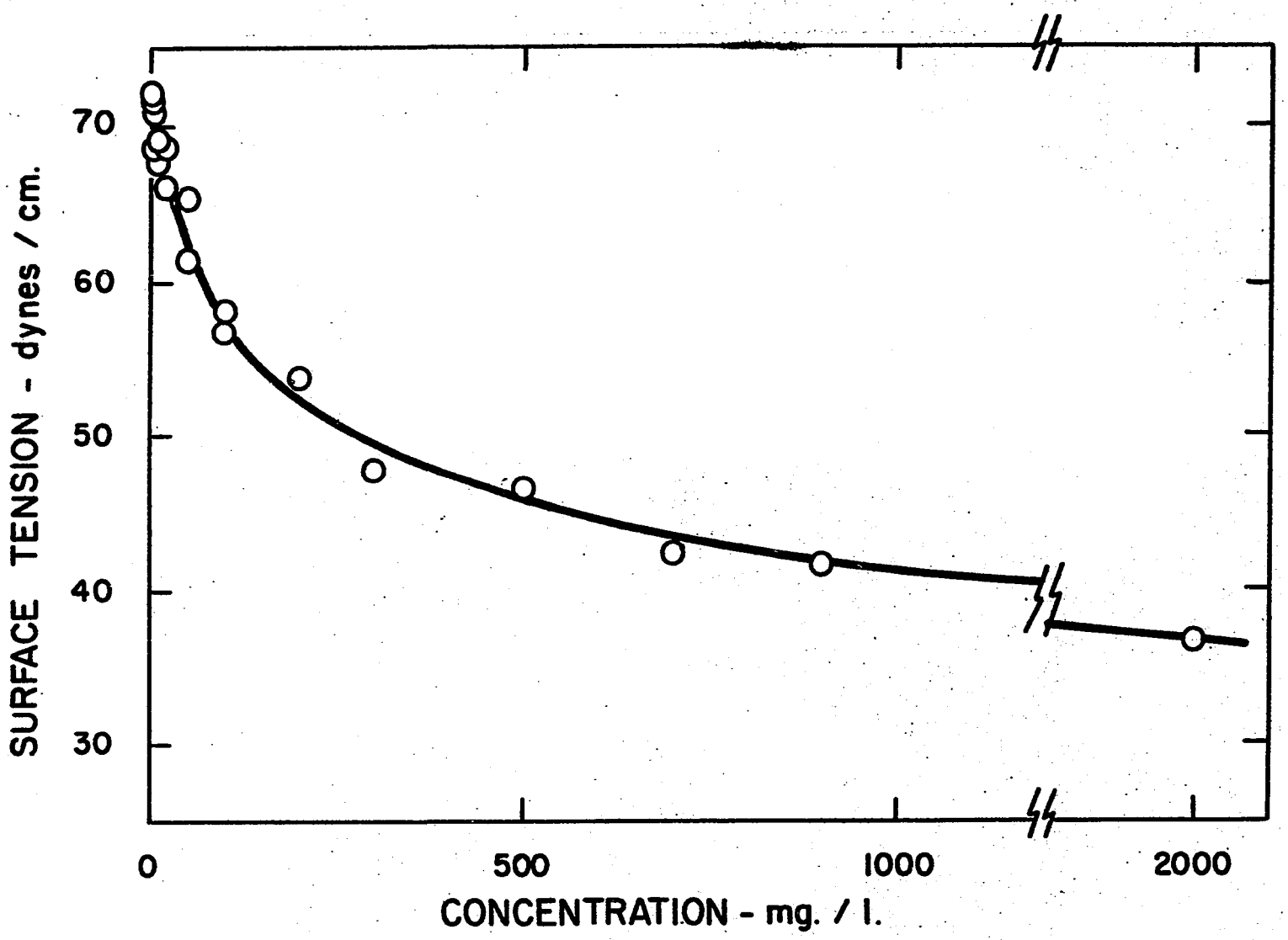
SURFACE TENSION - dynes / cm.
70
60
50
40
30
0
500
1000
2000
CONCENTRATION - mg. / l.

FIGURE 21

SURFACE TENSION OF DEHYDROABIETYLAMINE ACETATE SOLUTIONS AS A FUNCTION OF THE LOGARITHM OF THE CONCENTRATION

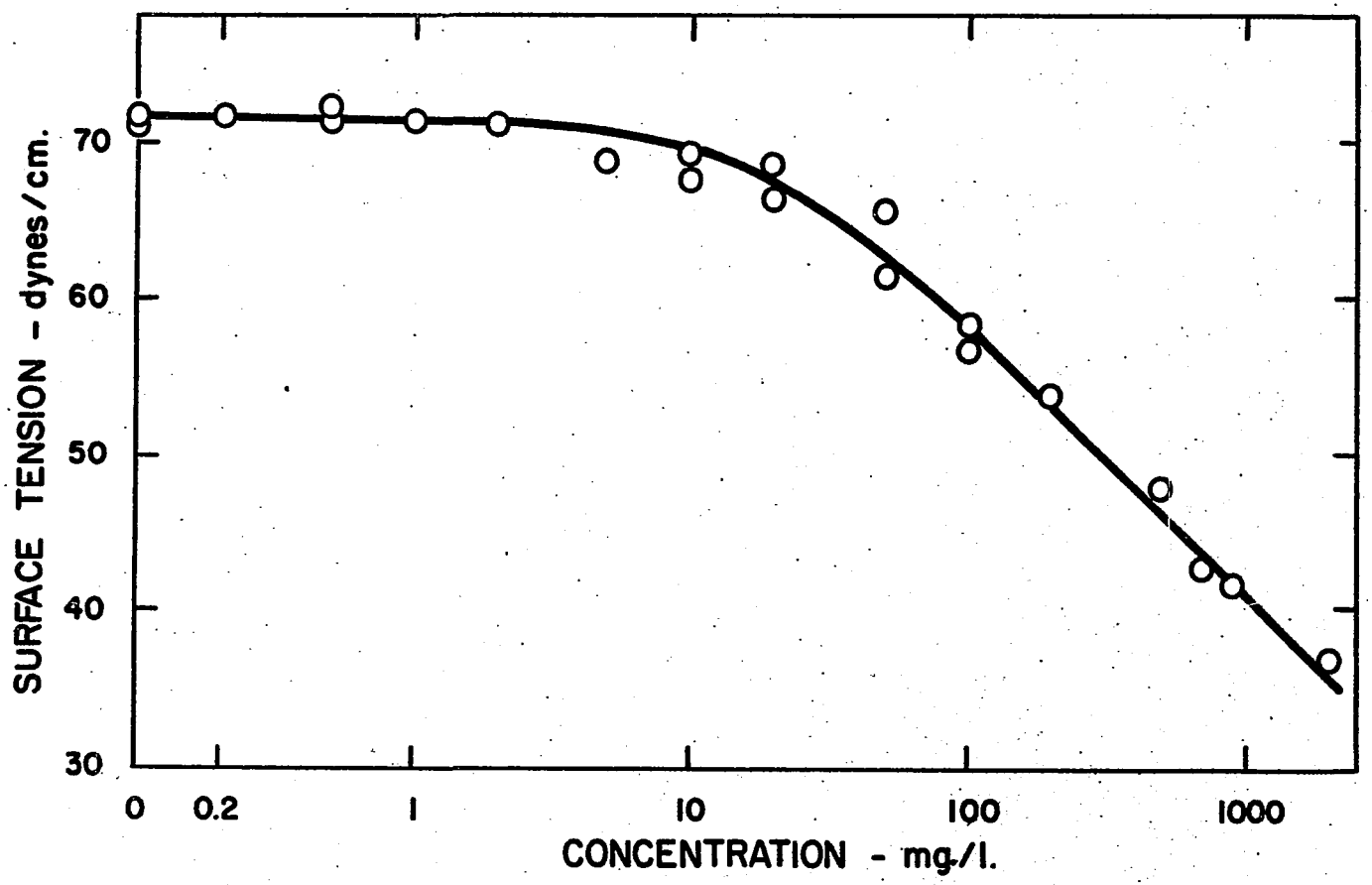
SURFACE TENSION - dynes/cm.
70
60
50
40
30
0
0.2
1
10
100
1000
CONCENTRATION - mg./l.

(89), it can be estimated that the critical micelle formation for dehydroabietylamine acetate is in the order of $4\frac{1}{2}$ gm./l. (0.013 Molar), well above the concentration range covered in this investigation.

2) Equivalent Conductance Measurements

In order to check the conclusion from surface tension measurements that the critical micelle concentration had not been reached at 2000 mg./l., the equivalent conductance of dehydroabietylamine acetate solutions was determined. The equipment used was identical to that used for the zero-points-of-charge (see Figure 8) except that the pH electrodes were replaced by a dip-type conductivity cell(cell constant 0.1003). The results are tabulated in Table XLI, Appendix VI and the specific conductance is shown as a function of concentration in Figure 22.

To test the applicability of Onsager's Equation,

$$\Lambda = \Lambda_o - (\Theta \Lambda_o + \sigma)\sqrt{C} \qquad (58)$$

the equivalent conductance, Λ, is plotted as a function of the square root of the concentration in Figure 23. The calculations are shown in Table XLII, Appendix VI. Since this amine has not been the subject of many investigations, no comparable conductance data were available. As a comparison, work by Ralston et al (89) on dodecylamine acetate is included in Figure 23.

FIGURE 22

SPECIFIC CONDUCTANCE OF DEHYDROABIETYLAMINE

ACETATE SOLUTIONS

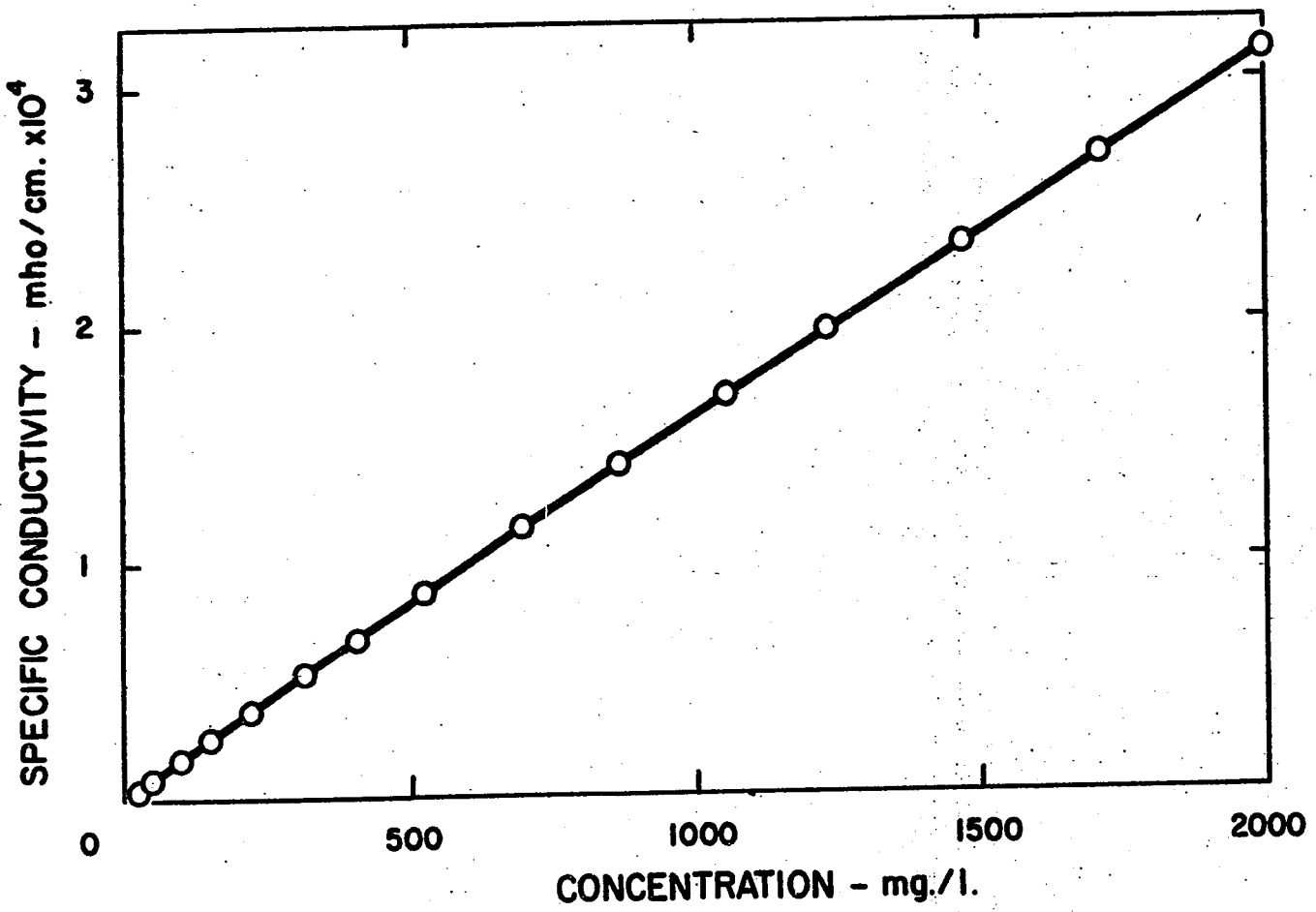
SPECIFIC CONDUCTIVITY - mho/cm. x10^4
3
2
1
0
500
1000
1500
2000
CONCENTRATION - mg./l.

FIGURE 23

EQUIVALENT CONDUCTANCE OF DEHYDROABIETYLAMINE

ACETATE SOLUTIONS

□ - Dehydroabietylamine Acetate

○ - Dodecylamine Acetate

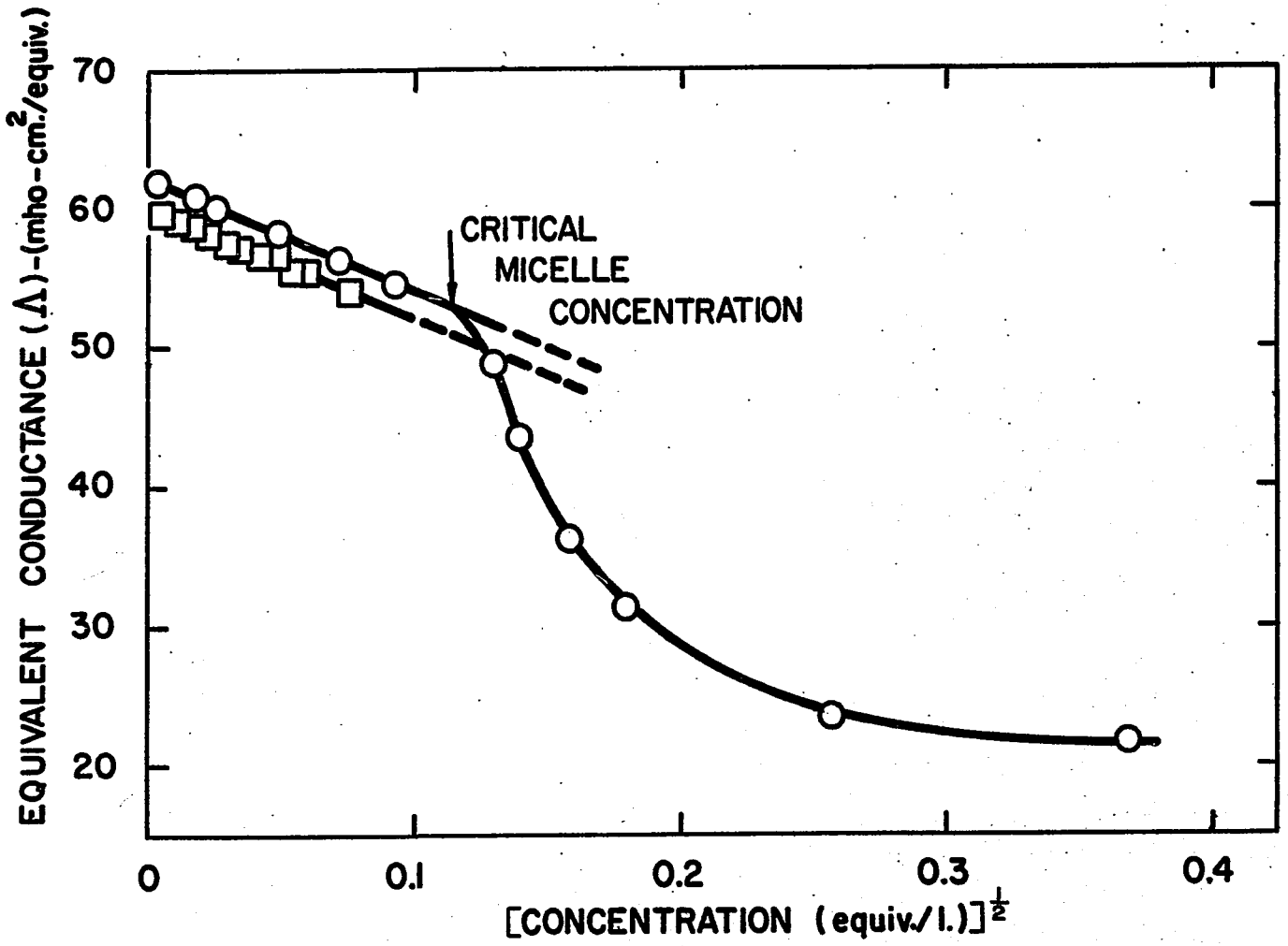
EQUIVALENT CONDUCTANCE (Λ)-(mho-cm.²/equiv.)
70
60
50
40
30
20
0
0.1
0.2
0.3
0.4
[CONCENTRATION (equiv./l.)]½
CRITICAL
MICELLE
CONCENTRATION

It may be concluded that the critical micelle concentration has not been reached at 2000 mg./l. dehydroabietylamine acetate. Further, at 25°C., the values for Λ_o and l_c have been determined to be :

$$\Lambda_o = 60.1 \text{ mho - cm.}^2\text{/equiv.}$$
$$l_c = 23.3 \text{ mho - cm.}^2\text{/equiv.}$$

The slope of the straight line in Figure 23 is 80.6 which is not in good agreement with the calculated slope of 73.5. The calculated slope is based on theoretical values of θ (0.2273) and σ (59.78) given in the literature (90) for Onsager's Equation. However, in Ralston's work (89), the experimental slope (84.0) is higher than the theoretical slope (74.0) calculated from the same constants.

3) Calculation of Concentration of Amine Ions and Free Amine.

The ionization constant for dehydroabietylamine has been determined experimentally to be approximately 4.2×10^{-5}. The solubility of free dehydroabietylamine was found to be 4.0 mg./l. (expressed as dehydroabietylamine acetate) or 1.16×10^{-5} moles per litre. The concentration of the dehydroabietylamine ion (RNH_3^+), the concentration of the free dehydroabietylamine (RNH_2), and the equivalent concentration of precipitated dehydroabietylamine (RNH_2(precipitated)) have been calculated in Tables IX to XI. The graph in Figure 24 shows the variation of these quantities with pH.

TABLE IX

CONCENTRATION OF AMINIUM IONS AS A FUNCTION OF pH AND TOTAL AMINE CONCENTRATION

Total Concentration mg./l.	pH 6	pH 7	pH 8	pH 9	pH 9.62	pH 10	pH 11
1	1.00	0.99	0.98	0.81	0.50	0.29	0.04
2	2.00	1.99	1.95	1.62	1.00	0.59	0.08
4	4.00	3.98	3.90	3.23	2.00	1.18	0.16
8	8.00	7.97	7.80	6.46	4.00	1.72	0.17
20	20.00	19.93	19.52	16.17	4.00	1.72	0.17
50	50.00	49.8	48.8	17.2	4.0	1.7	0.17
100	100	99.6	97.6	17.2	4.0	1.7	0.17
200	200	199	172	17.2	4.0	1.7	0.17
500	500	498	172	17.2	4.0	1.7	0.17
1000	1000	996	172	17.2	4.0	1.7	0.17
2000	2000	1720	172	17.2	4.0	1.7	0.17

TABLE X

CONCENTRATION OF UNIONIZED AMINE (SOLUBLE) AS A FUNCTION OF pH AND TOTAL AMINE CONCENTRATION.

Total Concentration mg./l.	pH 6	pH 7	pH 8	pH 9	pH 9.62	pH 10	pH 11
1	-	-	0.03	0.19	0.50	0.71	0.96
2	-	0.01	0.05	0.39	1.00	1.41	1.92
4	-	0.02	0.10	0.77	2.00	2.82	3.84
8	-	0.03	0.20	1.54	4.00	4.00	4.00
20	-	0.07	0.48	3.83	4.00	4.00	4.00
50	0.01	0.12	1.2	4.0	4.0	4.0	4.0
100	0.02	0.24	2.4	4.0	4.0	4.0	4.0
200	0.05	0.5	4.0	4.0	4.0	4.0	4.0
500	0.12	1.2	4.0	4.0	4.0	4.0	4.0
1000	0.24	2.4	4.0	4.0	4.0	4.0	4.0
2000	0.48	4.0	4.0	4.0	4.0	4.0	4.0

TABLE XI

CONCENTRATION OF PRECIPITATED UNIONIZED AMINE AS FUNCTION OF pH AND TOTAL AMINE CONCENTRATION

Total Concentration mg./l.	pH 6	pH 7	pH 8	pH 9	pH 9.62	pH 10	pH 11
1	-	-	-	-	-	-	-
2	-	-	-	-	-	-	-
4	-	-	-	-	-	-	-
8	-	-	-	-	-	2.28	3.83
20	-	-	-	-	12.00	14.28	15.83
50	-	-	-	28.8	42.0	44.3	45.8
100	-	-	-	78.2	92.0	94.3	95.8
200	-	-	24	178	192	194	196
500	-	-	324	478	492	494	496
1000	-	-	824	978	992	994	996
2000	-	76.0	1824	1978	1992	1994	1996

Furthermore, the total solubility, drawn as a function of pH, agrees well with experimental points. Some supersaturation occurs at low concentrations. Similar calculations have been reported by Smith (60) for dodecylamine acetate with similar results.

Qualitatively, dehydroabietylamine acetate is found to react with mineral acids (H_2SO_4, HCl, HNO_3) to form a white gelatinous precipitate. The ultra violet absorption spectrum of this amine in solution was examined to locate a suitable analysis wavelength. The spectrum in Figure 25, (see Table XLIII, Appendix VI), was determined but the regions of high absorption are unsuitable for analysis due to interference from metallic ions and inaccuracy at low concentrations.

FIGURE 24

ION CONCENTRATIONS IN DEHYDROABIETYLAMINE

ACETATE SOLUTIONS

□ - Experimental Solubility Points

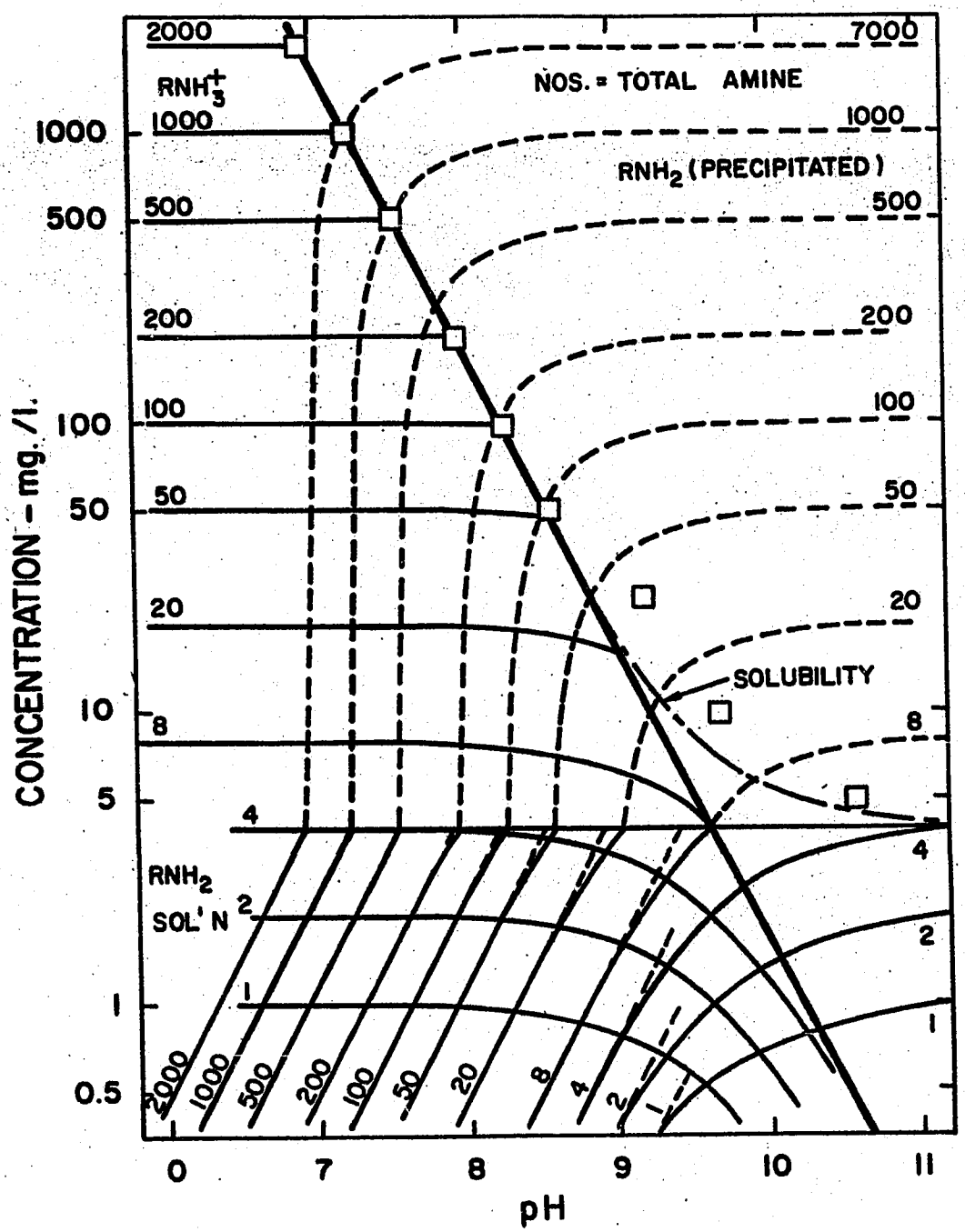
NOS. = TOTAL AMINE
RNH_3^+
RNH_2 (PRECIPITATED)
SOLUBILITY
RNH_2 SOL'N
CONCENTRATION - mg./l.
pH
2000
1000
500
200
100
50
20
10
8
5
4
2
1
0.5
7000
0
7
8
9
10
11

FIGURE 25

ABSORPTION SPECTRUM OF DEHYDROABIETYLAMINE

ACETATE SOLUTIONS

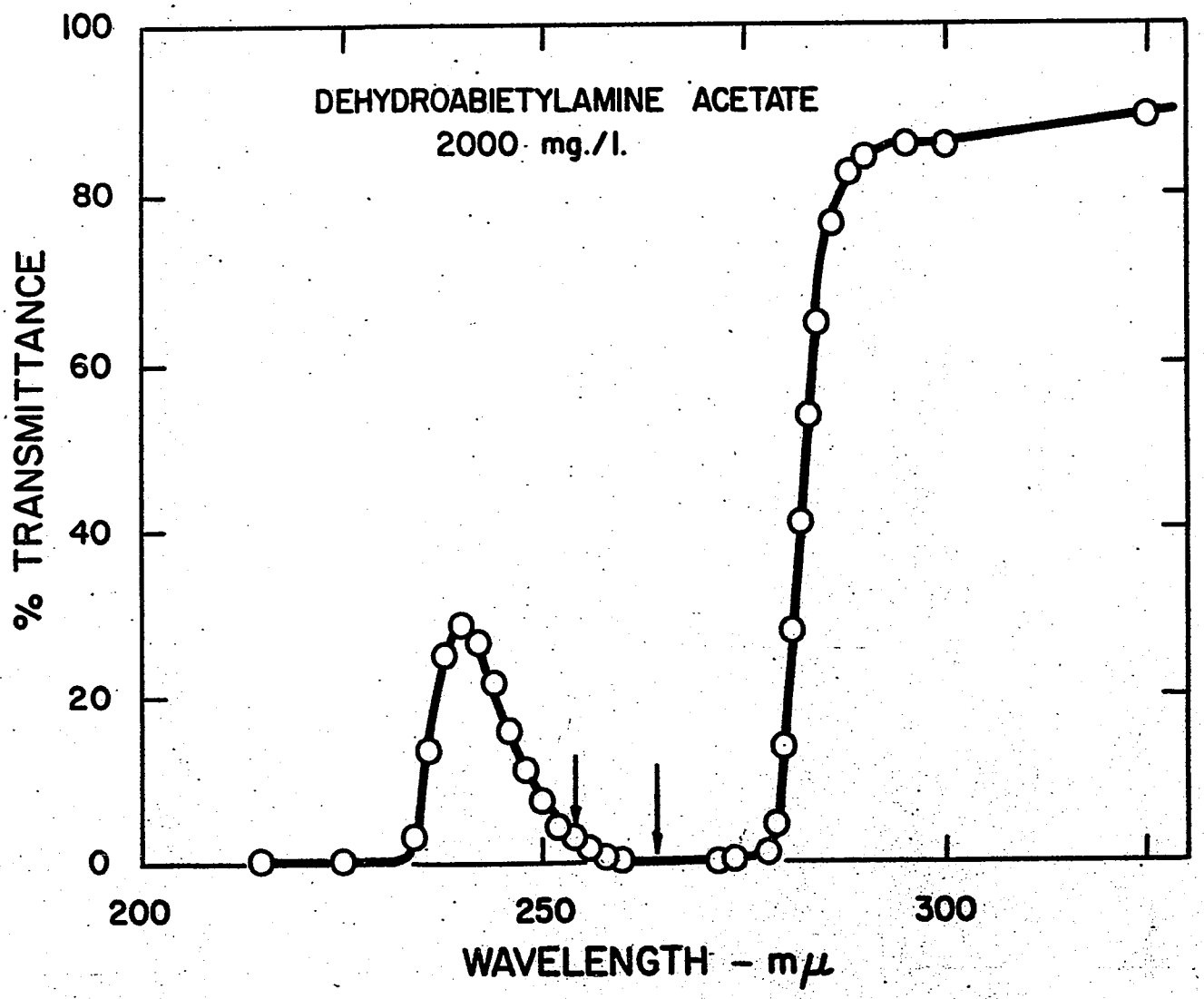
DEHYDROABIETYLAMINE ACETATE
2000 mg./l.
% TRANSMITTANCE
100
80
60
40
20
0
200
250
300
WAVELENGTH – mμ

Contact Angle Measurements and Work of Adhesion

Contact angle measurements were made on polished surfaces of quartz, hematite, and rutile immersed in aqueous solutions of dehydroabietylamine acetate. Conditions of essentially constant pH (6 to 7) and temperature were maintained. The results are shown in Figure 26 as a function of concentration. All the oxides exhibited a zero contact angle in water. Measurable contact angles were obtained at concentrations of 0.5 mg./l., or more, after measurable amounts of adsorption had occurred.

The contact angle reached a maximum of 51° for hematite at a concentration of 500 mg./l., after which it decreased to 44° at a concentration of two grams of dehydroabietylamine acetate per litre. The contact angle of quartz increased more rapidly with concentration than the corresponding values for hematite. From a concentration of 2 to 10 mg./l., where the surface coverage was approximately a monolayer, the contact angle on quartz remained constant at 38°. Above 10 mg./l., the contact angle on quartz increased to a maximum of 53° at 500 mg./l.and then decreased to 48° at 2 gm./l. The angles on quartz were comparable to those on hematite except that they were slightly higher on quartz.

On rutile, the contact angles increased much more rapidly, reaching a maximum angle of 64° at 2 mg./l., dehydroabietylamine acetate. This maximum angle was maintained until a concentration of 60 mg./l., was reached. Above 60 mg./l., the contact angle decreased steadily

FIGURE 26

EFFECT OF DEHYDROABIETYLAMINE ACETATE
CONCENTRATION ON THE CONTACT ANGLE

○ - Quartz

□ - Hematite

△ - Rutile

▽ - Baddeleyite

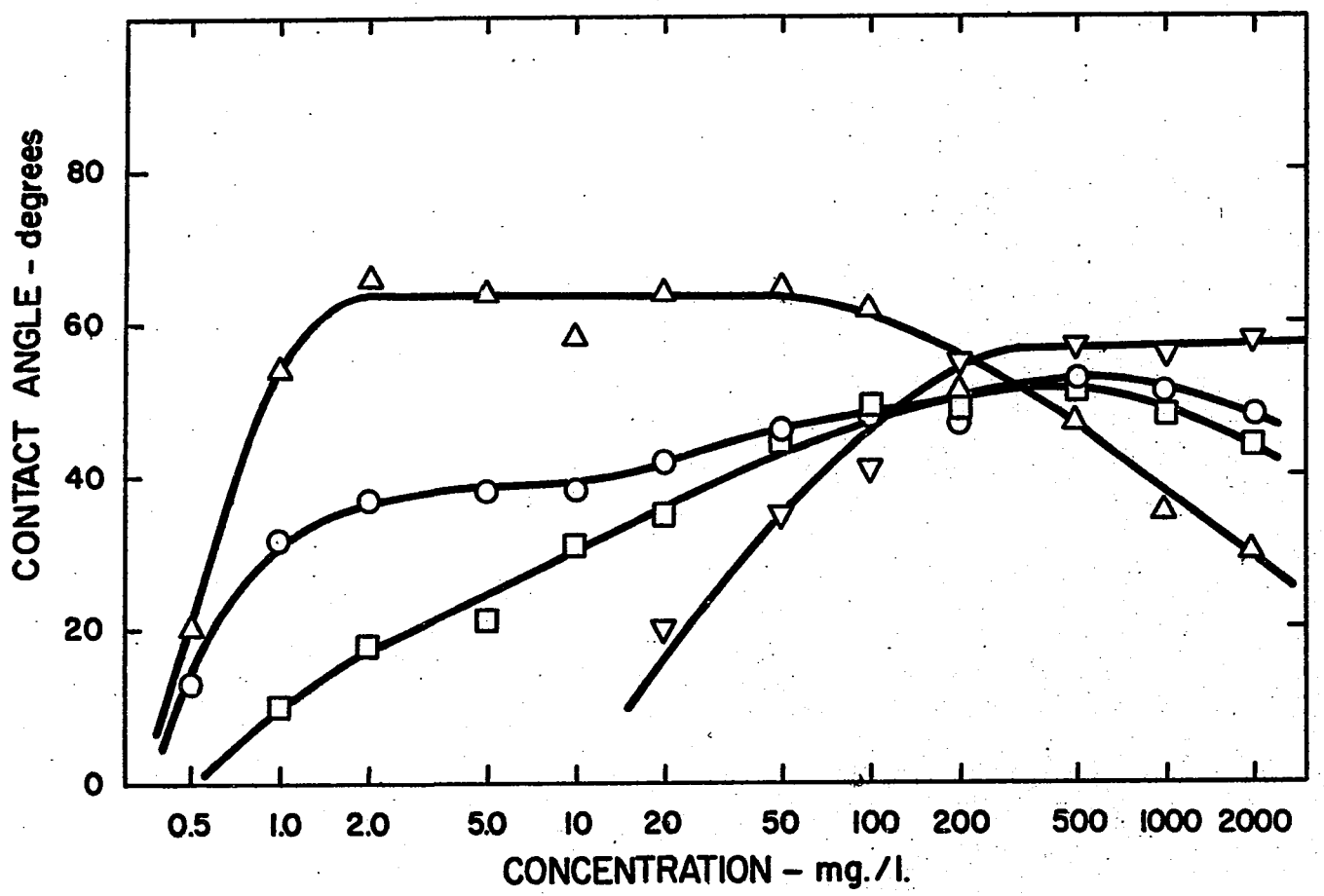
CONTACT ANGLE - degrees
0
20
40
60
80
0.5
1.0
2.0
5.0
10
20
50
100
200
500
1000
2000
CONCENTRATION – mg./l.

to 30° at 2 gm./l. The contact angle on rutile was greater than the corresponding angle on quartz and hematite for all concentrations below 300 mg./l. Above 300 mg./l., the angles on rutile were less than those on the other minerals. The maximum contact angle on rutile occurred at lower concentrations than those for the other oxides.

An attempt was made to measure the contact angle on baddeleyite but the results are somewhat questionable. The only pure mineral available was the powder with a specific surface of 16.3 M^2./gm. A portion was mounted on top of that section of "quickmount", taking care that no "quickmount" covered the mineral. The surface, being flat, was comparable to a piece of bulk mineral except that it was porous and could adsorb considerable weight of amine due to its large surface. As seen in Figure 26, no contact was observed until a concentration of 20 mg./l., was reached. The contact angle increased to a maximum of 57° at 300 mg./l., above which it remained constant. The adsorption on baddeleyite may have been considerable, whereas the adsorption on the other oxides was negligible.

The work of adhesion of an air bubble to the surface of each of the four oxides was determined. Calculations are contained in Tables LIV to LVII, Appendix VII and the results are shown as a function of concentration (Figure 27).

The work of adhesion increased smoothly with concentration of amine for α-quartz, rutile, hematite and baddeleyite. At a certain concentration in the case of quartz, the maximum work of adhesion was

FIGURE 27

EFFECT OF DEHYDROABIETYLAMINE ACETATE

CONCENTRATION ON THE WORK OF ADHESION

○ - Quartz

□ - Hematite

△ - Rutile

▽ - Baddeleyite

\+ - Monolayer

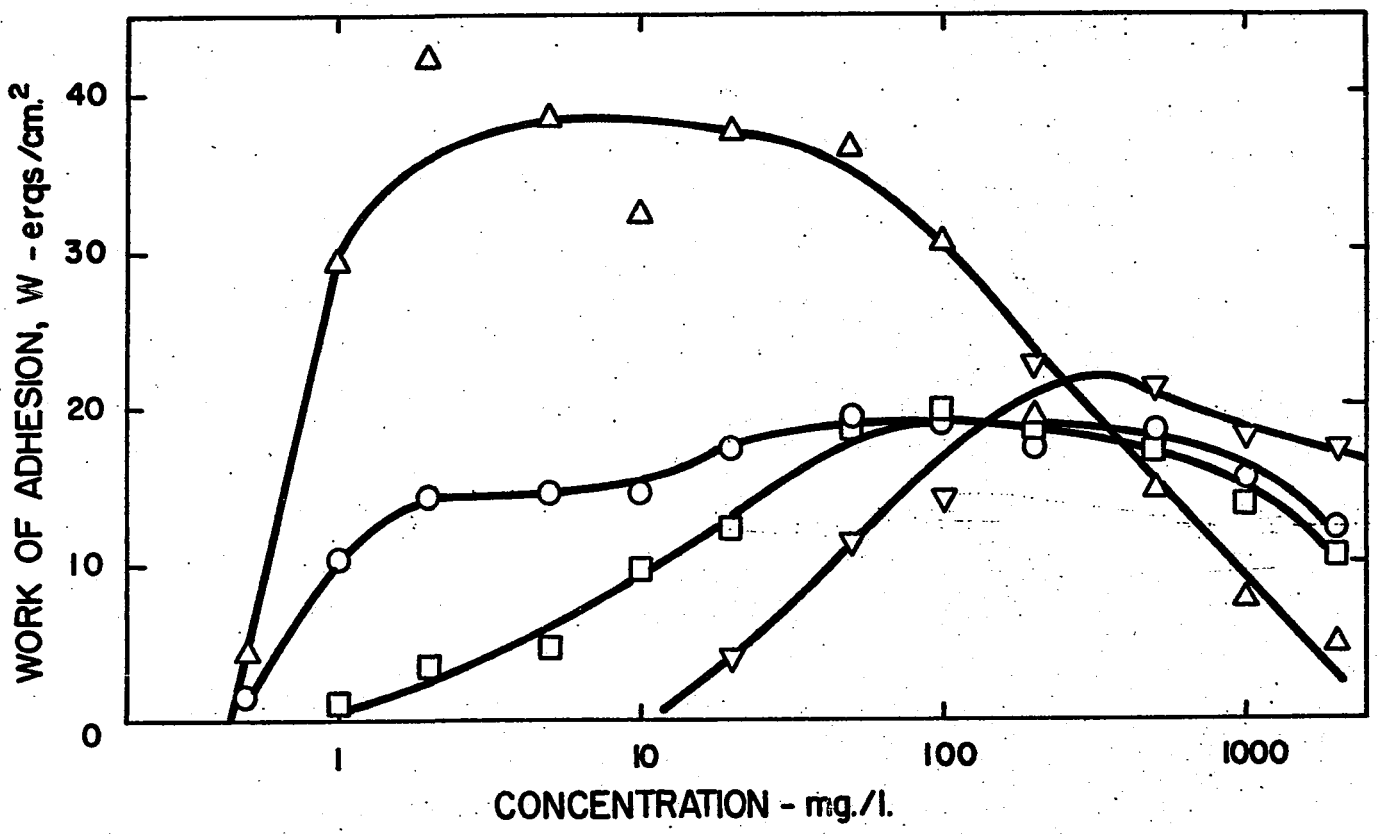
WORK OF ADHESION, W - ergs/cm.²
40
30
20
10
0
1
10
100
1000
CONCENTRATION - mg./l.

attained after which it decreased rapidly. This decrease was caused by the decrease in contact angle as well as the decrease in surface tension of the solutions.

The work of adhesion on hematite decreased rapidly above a specific adsorption of 20 Gibbs as shown in Figure 28. This was due to the continuous decrease in the work of adhesion at high amine concentrations, while the increase in specific adsorption became very small.

The work of adhesion on rutile was almost twice that for the other minerals, a phenomena which may be significant. The high purity rutile samples used in this investigation were unlike those found in nature which contain various dissolved impurities such as iron. The sharp decrease in the work of adhesion as the specific adsorption increased above 6 Gibbs was due to the decrease in contact angle, to the decrease in surface tension, and to the slow increase in specific adsorption above 15 Gibbs.

FIGURE 28

EFFECT OF SPECIFIC ADSORPTION OF DEHYDROABIETYLAMINE ACETATE ON THE WORK OF ADHESION

○ - Quartz

□ - Hematite

△ - Rutile

▽ - Baddelyite

\+ - Monolayer

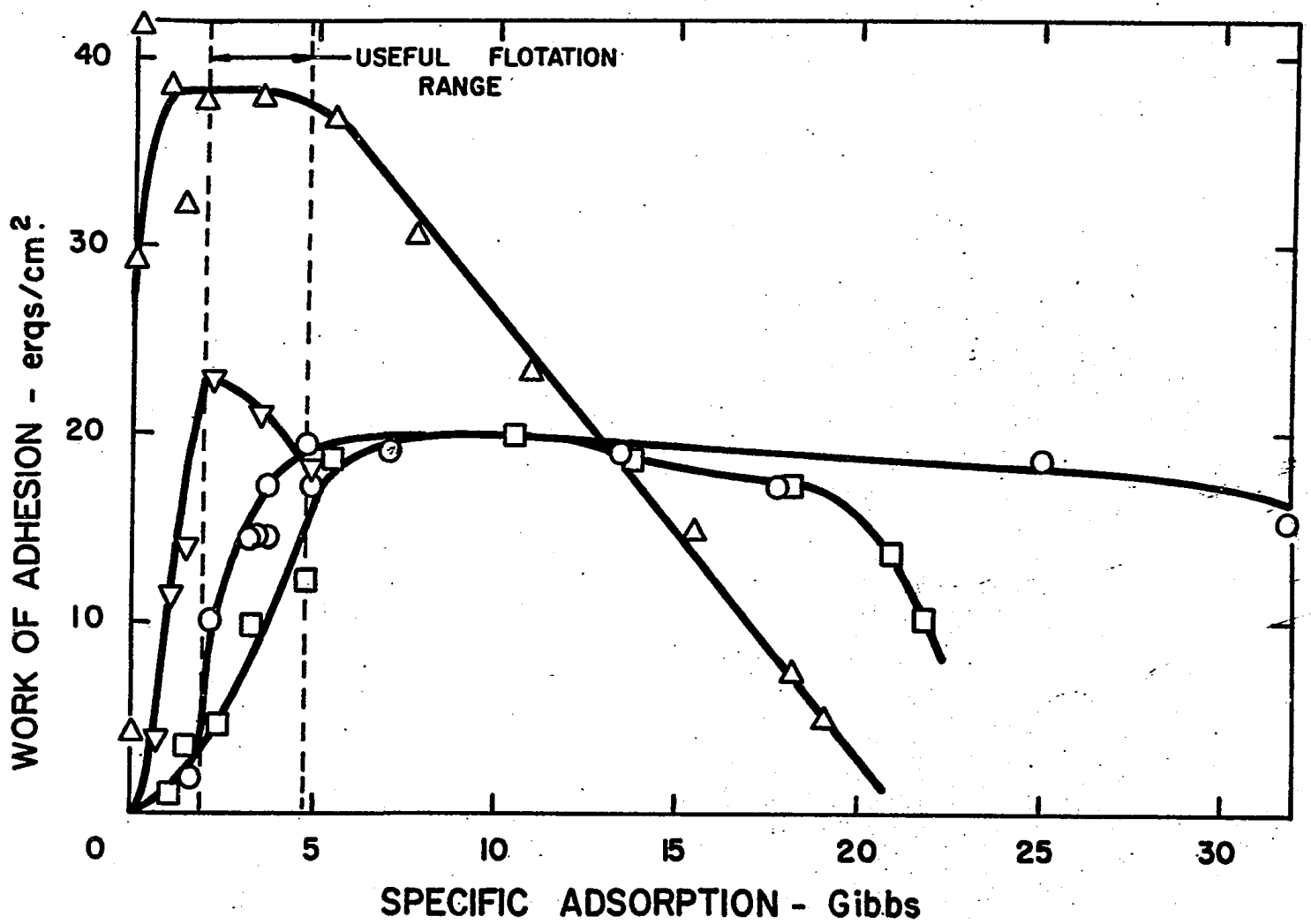
USEFUL FLOTATION RANGE
WORK OF ADHESION - ergs/cm.²
SPECIFIC ADSORPTION - Gibbs
0
5
10
15
20
25
30
10
20
30
40

Zero-Point-of-Charge and Streaming Potentials

1) Zero-Point-of-Charge of Oxides

The results of the titration tests to determine the zero-point-of-charge of hematite, zirconia and rutile are contained in Tables XII to XIV. Titration curves are shown in Figures 29,30 and 31 for hematite, zirconia and rutile respectively.

The relationship between the ionic strength and the potassium chloride ion content, considering the acid and base added, is as follows:

Normality of KCl Solution	Ionic Strength of Solution
10^{-4}	2.6×10^{-3}
10^{-3}	3.5×10^{-3}
10^{-2}	1.25×10^{-2}
10^{-1}	1.025×10^{-1}

The titration curves in the absence of any solid material for each of the four tests in Figure 29, when superimposed on each other, show very small variations at the same pH. It was decided, therefore, to run only one blank curve for zirconia and rutile and to assume that it was constant over the ionic strength range considered. The difference between each curve with solids and without solids is, in general, as expected from the double layer theory. At the cross-over point of each set of curves, the adsorption of hydrogen and hydroxyl ions was equal, resulting in a surface charge of zero. Toward higher pH values, there

TABLE XII

RESULTS OF TITRATION TESTS USING HEMATITE

Test No.14-10^{-4}N KCl(Blank)		Test No.16-10^{-4}N KCl		Test No.17-10^{-3}N KCl(Blank)		Test No.18-10^{-3}N KCl	
Acid Added	pH	Acid Added	pH	Acid Added	pH	Acid Added	pH
mℓ.		mℓ.		mℓ.		mℓ.	
0.000	11.250	0.000	11.180	0.000	11.354	0.000	11.170
0.770	10.795	0.651	10.720	0.650	10.970	0.532	10.858
0.992	10.375	0.873	10.290	0.971	10.465	0.849	10.312
1.080	9.935	0.998	9.765	1.090	9.835	1.000	9.640
1.118	9.555	1.081	9.210	1.145	8.475	1.090	8.955
1.140	9.038	1.151	8.600	1.163	4.690	1.155	8.400
1.155	8.410	1.222	8.100	1.265	3.660	1.201	7.975
1.166	8.260	1.271	7.320	1.600	3.060	1.295	6.675
1.198	4.587	1.334	6.327	2.000	2.800	1.360	5.588
1.240	4.028	1.429	5.015	2.760	2.530	1.500	4.280
1.347	3.602	1.484	4.629			1.500	4.280
1.601	3.198	1.563	4.090				
2.295	2.785	1.783	3.525				

TABLE XII (cont'd)

Test No.20-10^{-2}N KCl(Blank)		Test No.21-10^{-2}N KCl		Test No.23-10^{-1}N KCl(Blank)		Test No.24-10^{-1}N KCl	
Acid Added	pH	Acid Added	pH	Acid Added	pH	Acid Adde	pH
mℓ.		mℓ.		mℓ.		mℓ.	
0.000	11.300	0.000	11.200	0.000	11.280	0.000	11.121
0.687	10.905	0.700	10.675	0.672	10.882	0.611	10.624
1.010	10.300	0.978	10.020	1.005	10.155	0.815	10.232
1.098	9.788	1.115	9.350	1.085	9.340	0.975	9.641
1.140	8.920	1.214	8.565	1.184	4.305	1.053	9.150
1.180	8.245	1.420	7.435	1.300	3.510	1.165	8.400
1.210	4.351	1.560	6.875	1.655	2.986	1.340	8.025
1.296	3.696	1.700	6.631	2.490	2.564	1.630	7.526
1.600	3.125						
2.955	2.495						

TABLE XIII

RESULTS OF TITRATION TESTS USING BADDELEYITE

Test 30a Control		Test No.30b 0.1 N KCl		Test No.31 0.01 N KCl		Test No.32 0.001 N KCl	
Base Added	pH	Base Added	pH	Base Added	pH	Base Added	pH
mℓ.		mℓ.		mℓ.		mℓ.	
0.000	2.654	0.000	2.840	0.000	2.785	0.000	2.735
0.422	2.948	0.386	3.129	0.400	3.083	0.386	3.058
0.644	3.259	0.610	3.519	0.616	3.440	0.604	3.420
0.735	3.516	0.710	3.920	0.703	3.750	0.715	3.780
0.794	3.835	0.749	4.240	0.766	4.216	0.770	4.370
0.842	4.300	0.771	4.580	0.795	4.753	0.799	4.850
0.852	8.730	0.806	5.275	0.825	5.628	0.853	6.300
0.869	9.431	0.841	5.981	0.868	6.642	0.917	7.580
0.897	9.825	0.866	6.480	0.935	7.890	0.987	9.025
0.943	10.140	0.897	7.165	0.998	9.241		
1.044	10.448	0.940	7.850				
1.195	10.702	0.978	8.396				
1.429	10.880	1.020	9.115				
		1.069	9.694				

TABLE XIV

RESULTS OF TITRATION TESTS USING RUTILE

Test No.34 Control		Test No.35 0.1N KCl		Test No.33 0.01N KCl		Test No.36 0.001N KCl	
Base Added	pH	Base Added	pH	Base Added	pH	Base Added	pH
mℓ.		mℓ.		mℓ.		mℓ.	
0.000	2.640	0.000	2.770	0.000	2.757	0.000	2.689
0.418	2.915	0.358	3.015	0.401	3.030	0.370	2.911
0.598	3.140	0.645	3.455	0.657	3.405	0.662	3.335
0.717	3.436	0.735	3.799	0.759	3.777	0.767	3.766
0.802	3.915	0.792	4.243	0.809	4.219	0.834	4.883
0.841	5.080	0.811	4.625	0.841	6.043	0.854	8.805
0.850	8.870	0.826	5.300	0.862	9.178	0.889	0.685
0.894	9.990	0.868	9.180	0.900	9.702	0.957	10.140
0.989	10.490	0.910	9.642	0.966	10.133	1.041	10.490
1.094	10.734	0.993	10.145	1.030	10.398	1.256	10.900
1.238	10.920	1.097	10.540	1.135	10.720		
		1.266	10.830	1,225	10.865		

FIGURE 29

TITRATION CURVES FOR HEMATITE

○ - No Solids

□ - Solids

No. - Normality of KCl Solution

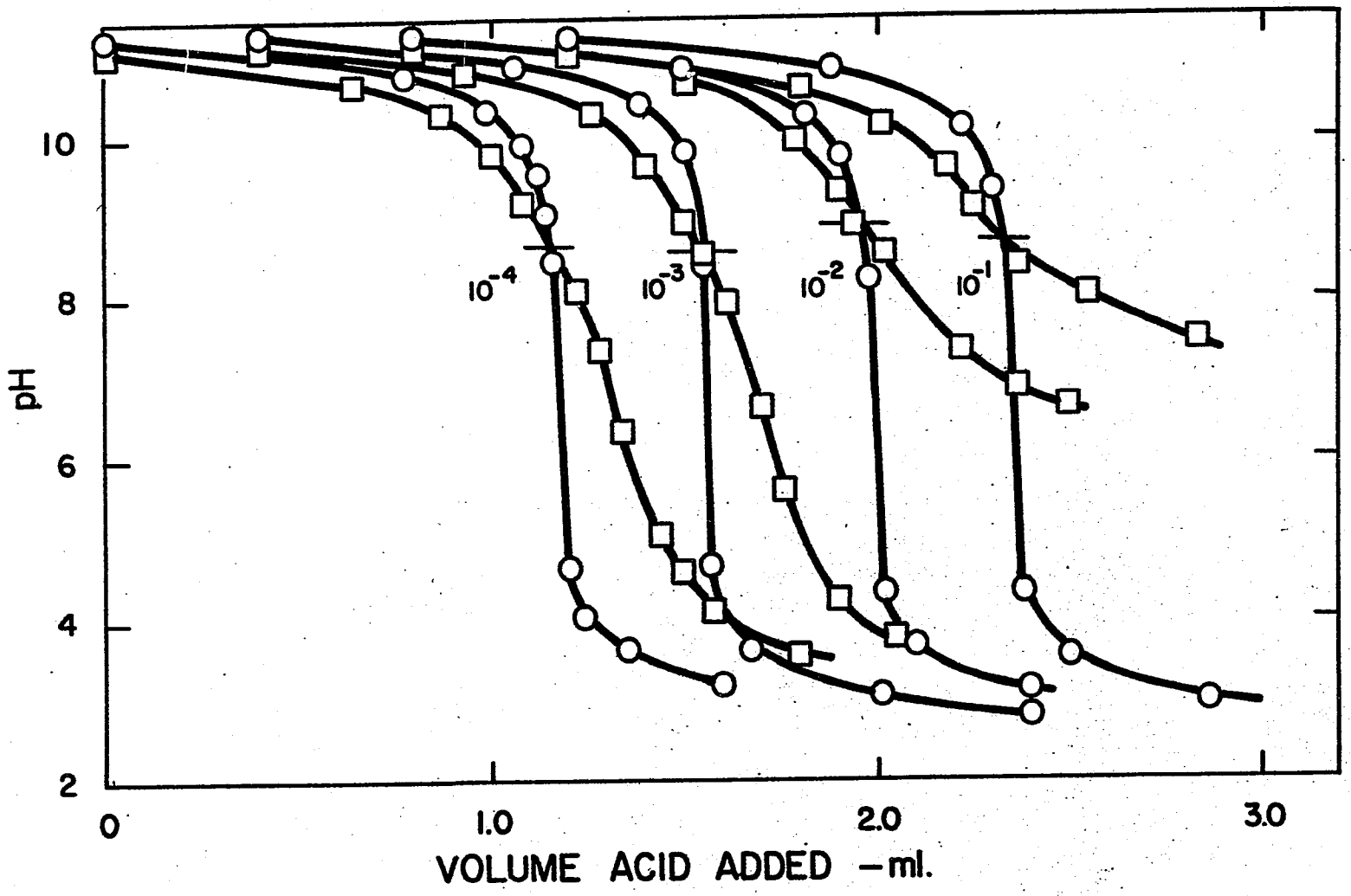
pH
10
8
6
4
2
0
1.0
2.0
3.0
VOLUME ACID ADDED —ml.
10^{-4}
10^{-3}
10^{-2}
10^{-1}

FIGURE 30

TITRATION CURVES FOR BADDELEYITE

○ - No Solids

□ - Solids

No. - Normality of KCl Solution

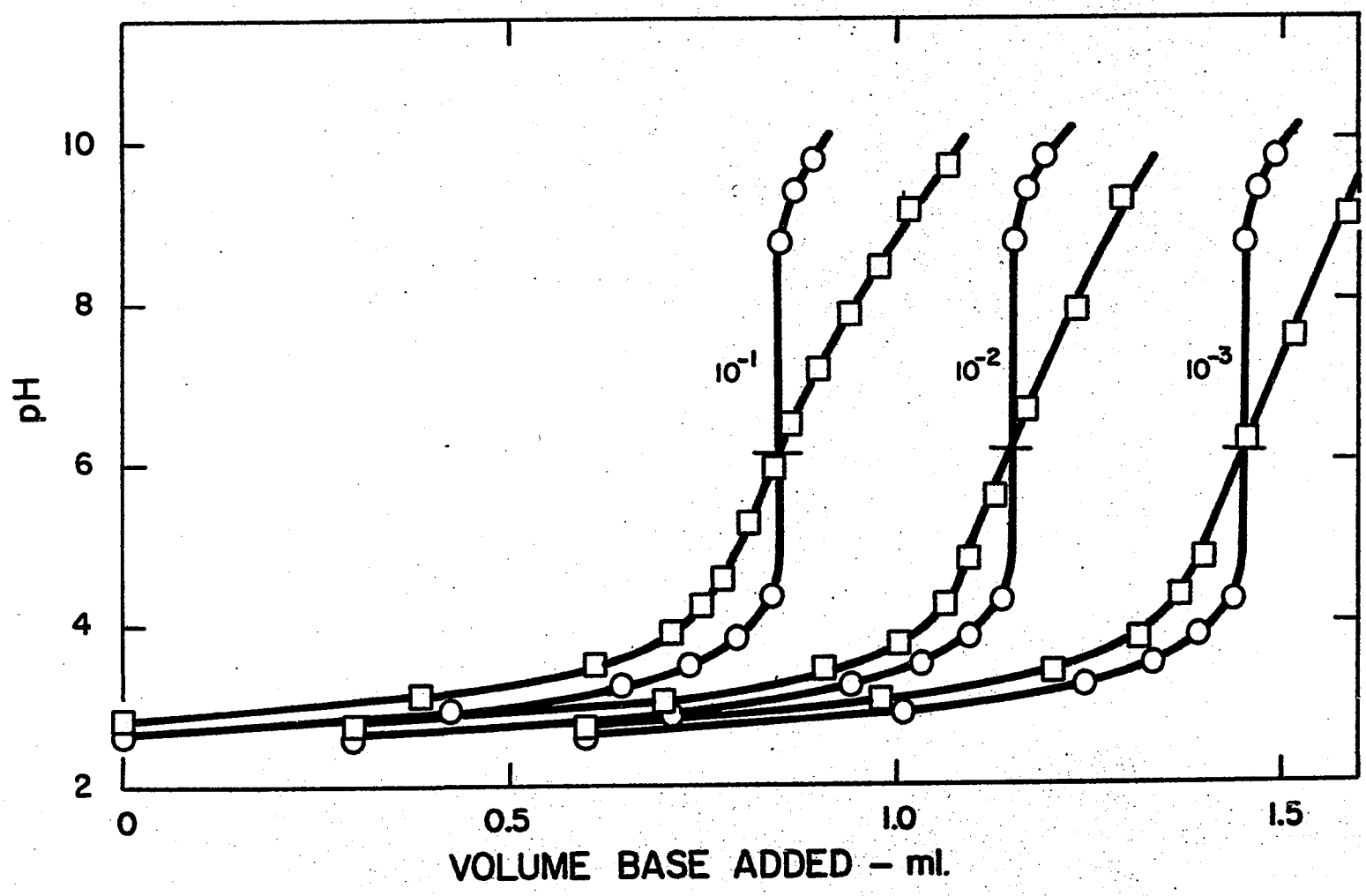
pH
10
8
6
4
2
0
0.5
1.0
1.5
VOLUME BASE ADDED – ml.
10^{-1}
10^{-2}
10^{-3}

FIGURE 31

TITRATION CURVES FOR RUTILE

○ - No Solids

□ - Solids

No. - Normality of KCl Solutions

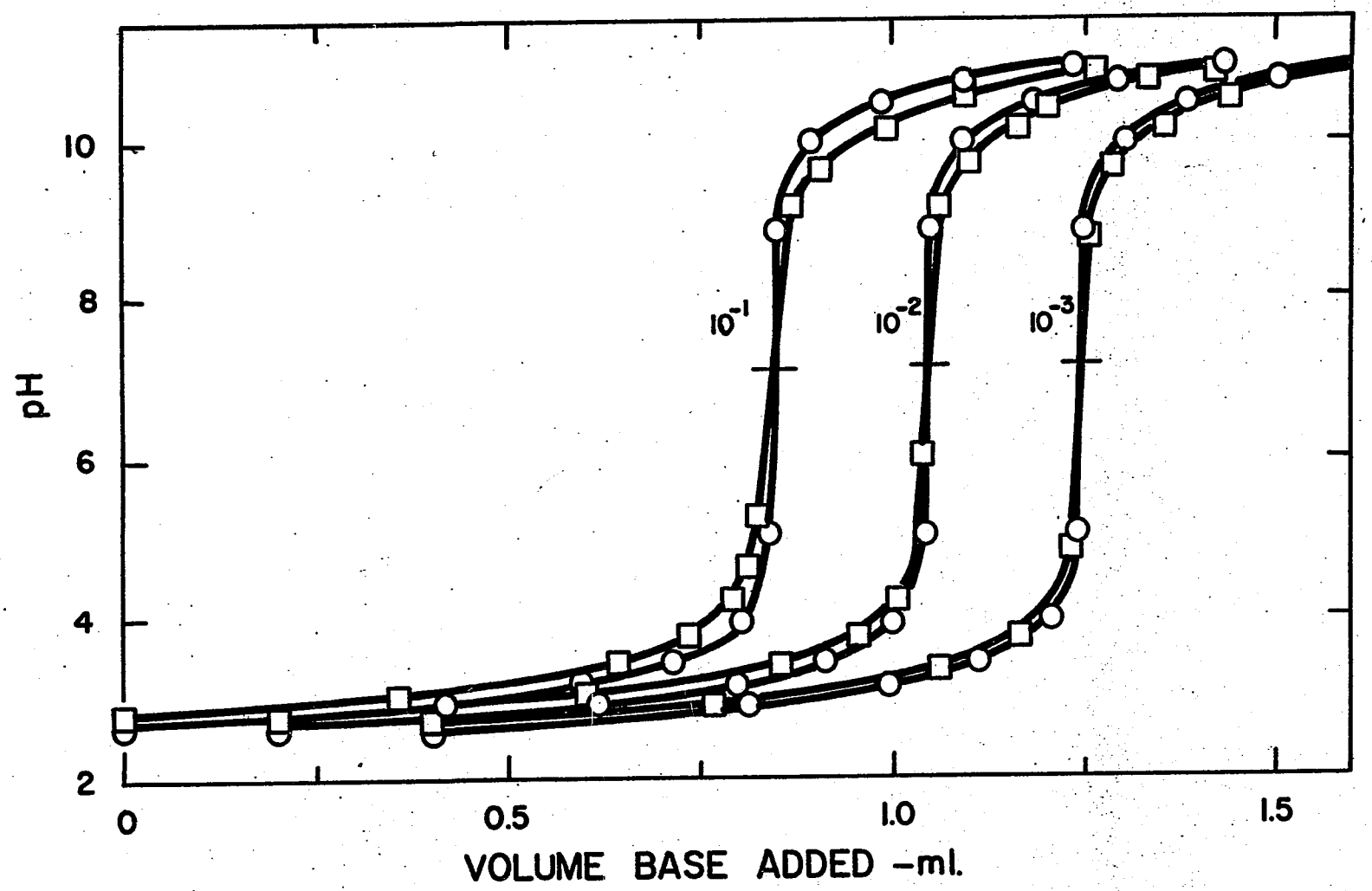
pH
10
8
6
4
2
0
0.5
1.0
1.5
VOLUME BASE ADDED –ml.
10^{-1}
10^{-2}
10^{-3}

was an increase in the hydroxyl ion adsorption and a decrease in hydrogen ion adsorption as shown by the decrease in pH at constant titrant addition, (or by the decrease in acid required to obtain a specific solution pH). Conversely, at lower pH values, there was an increase in hydrogen ion adsorption and a decrease in hydroxyl ion adsorption as shown by the increase in pH at constant titrant addition. An increase in ionic strength increased the net adsorption of hydrogen and hydroxyl ions, as shown by the increasing deviations of the titration curves with solids from the blank curves.

Calculations required to determine the adsorption density, the surface charge density and the differential capacity are tabulated in Appendix IV with sample calculations preceding the tables. Figures 32,33 and 34 show the adsorption density in micromoles per gram as a function of pH. The adsorption density is defined as the excess of hydrogen ion adsorbed (Γ_{H^+}) over the hydroxyl ion adsorbed (Γ_{OH^-}). In mathematical form, the net adsorption is written

$$A.D. = \Gamma_{H^+} - \Gamma_{OH^-} \tag{59}$$

Thus a negative adsorption density indicates that the hydroxyl ion adsorption is in excess of the hydrogen ion adsorption.

For hematite, the curves for all ionic strengths show a characteristic S-shaped curve, the S being more pronounced as the ionic strength decreases. The zero-point-of-charge was found to be at a pH of 8.68 $\pm$ 0.20. At higher pH values, the excess hydroxyl ion adsorption

FIGURE 32

EFFECT OF pH ON ADSORPTION DENSITY ON HEMATITE

No.- Normality of KCl Solutions

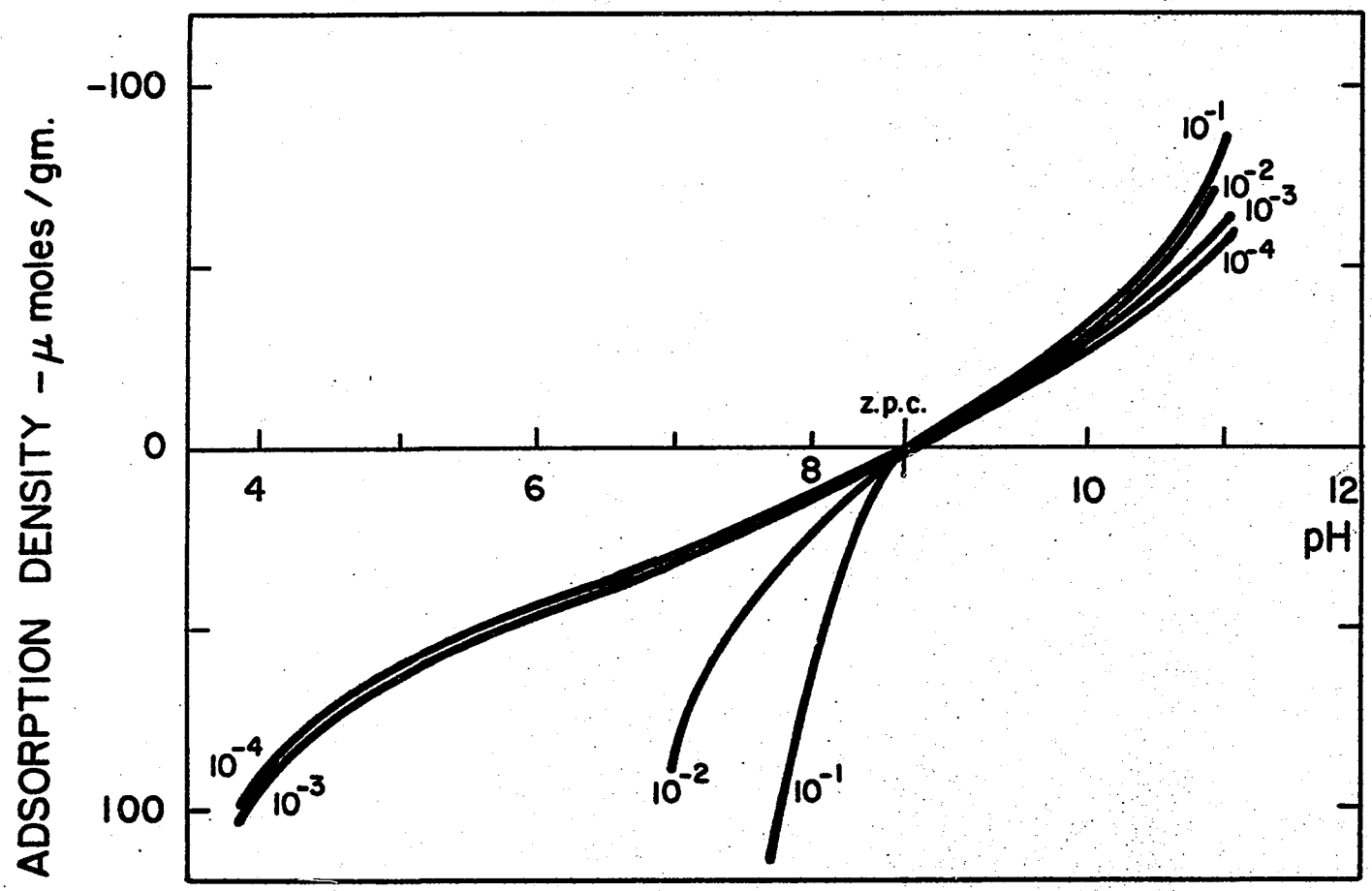
ADSORPTION DENSITY - μ moles / gm.
-100
0
100
4
6
8
10
12
pH
z.p.c.
10^-1
10^-2
10^-3
10^-4
10^-4
10^-3
10^-2
10^-1

FIGURE 33

EFFECT OF pH ON ADSORPTION DENSITY ON BADDELEYITE

No.- Normality of KCl Solutions

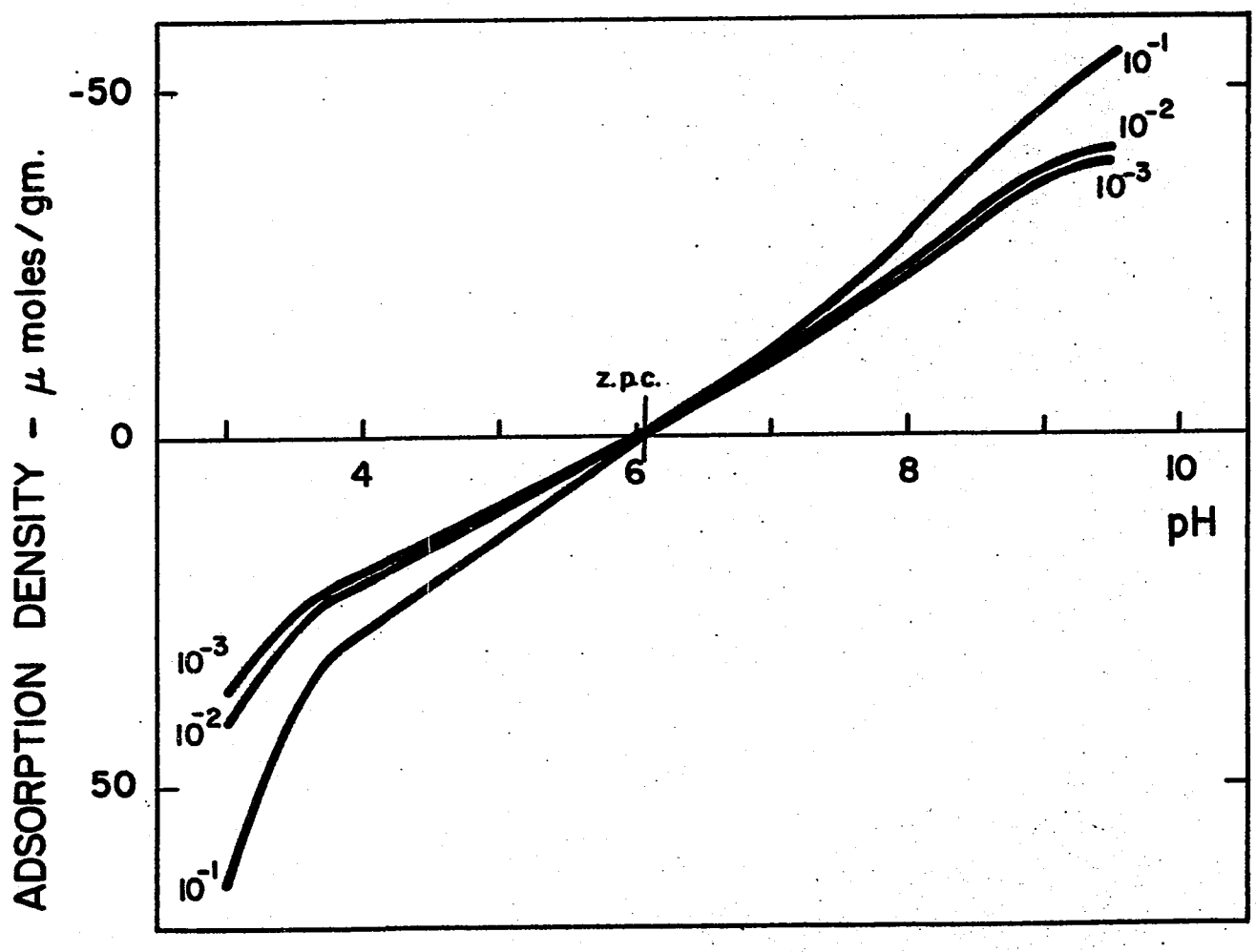
ADSORPTION DENSITY - μ moles/gm.
-50
0
50
4
6
8
10
pH
z.p.c.
10^-1
10^-2
10^-3
10^-3
10^-2
10^-1

FIGURE 34

EFFECT OF pH ON ADSORPTION DENSITY ON RUTILE

No. - Normality of KCl Solutions

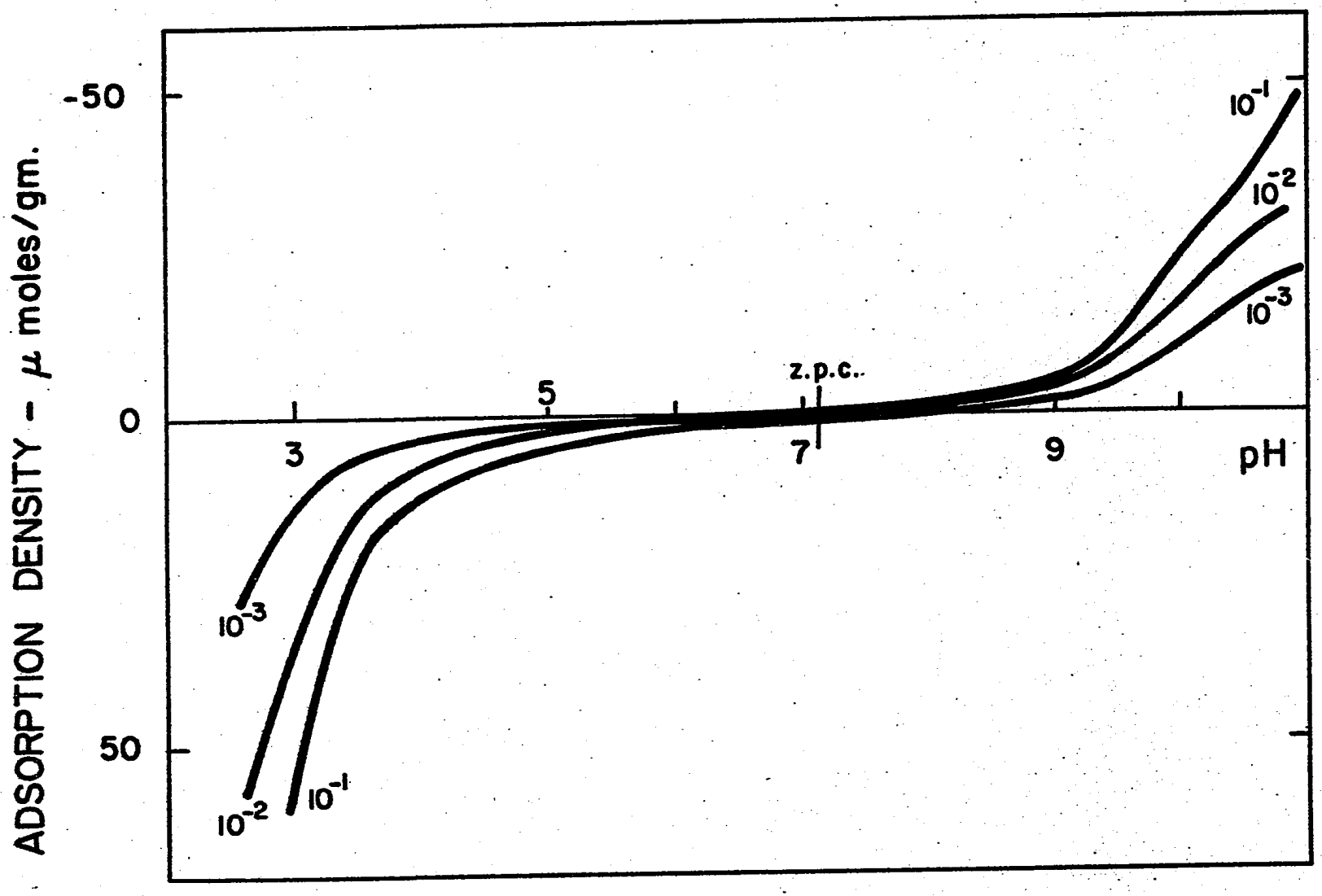
ADSORPTION DENSITY - μ moles/gm.
-50
0
50
3
5
7
9
pH
z.p.c.
10⁻¹
10⁻²
10⁻³
10⁻³
10⁻²
10⁻¹

was increasing slowly close to the zero-point-of-charge and more rapidly as the pH increases. The four curves are quite close together with a uniform increase of adsorption with ionic strength. At pH values less than the zero-point-of-charge, the hydrogen ion adsorption followed the same general pattern. However, there was a marked increase in the net hydrogen ion adsorption when ionic strength was increased above 10^{-3} N KCl. Also there was a portion of the adsorption curve around a pH of 6, where the rate of increase in adsorption decreased slightly followed by a continued increase.

For baddeleyite in Figure 33, the adsorption was lower than the equivalent hematite samples. This was to be expected as the specific surface area of zirconia was less than it was for hematite. The curves are smooth and almost straight between pH values of 4 to 8, indicating a direct proportionality between adsorption and pH. Below a pH of 4, the adsorption increased more rapidly than above a pH of 4. Above a pH of 8, the rate of increase in adsorption decreased to a low value. The zero-point-of-charge was found to be at a pH of 6.08 ± 0.05.

The net adsorption of hydrogen ions on rutile was similar to the adsorption on baddeleyite as shown by the smooth S-shaped curves in Figure 34. However, above a pH of 10, the increase in net adsorption of hydroxyl ion decreases in all cases. At a pH of 10.5, the rate of increase in net adsorption increases again in the case of 10^{-1} N KCl solution only.

The zero-point-of-charge has been found to be at a pH of 7.13 ± .05. A summary of the results of the zero-point-of-charge is shown in Table XV .

The surface charge density has been calculated in Appendix V and is reported in micro-coulombs per gram and in micro-coulombs per cm^2. The latter is more useful for the comparison of the behaviour of different oxides. Similarly, the differential capacity is reported as micro-farads per gram and micro-farads per cm^2. The results of these calculations are shown graphically in Figures 35 to 40. The first three graphs show the differential capacity for each oxide as a function of pH and the last three show the differential capacity as a function of the surface charge density. The inset in Figure 40 is an enlargement of the region A near the zero-point-of-charge. All the graphs indicate a minimum in differential capacity in the vicinity of the zero-point-of-charge. The minimum covers 3 to 4pH units which is quite a wide range.

TABLE XV

pH AT THE ZERO-POINT-OF-CHARGE

KCl Conc'n.	10^{-4}N	10^{-3}N	10^{-2}N	10^{-1}N	Average
Hematite	8.60	8.55	8.90	8.63	8.68
Zirconia	-	6.07	6.09	6.08	6.08
Rutile	-	7.17	7.13	7.10	7.13

FIGURE 35

EFFECT OF pH ON THE DIFFERENTIAL CAPACITY

OF HEMATITE

○ - 10^{-1} N KCl

□ - 10^{-2} N KCl

△ - 10^{-3} N KCl

▽ - 10^{-4} N KCl

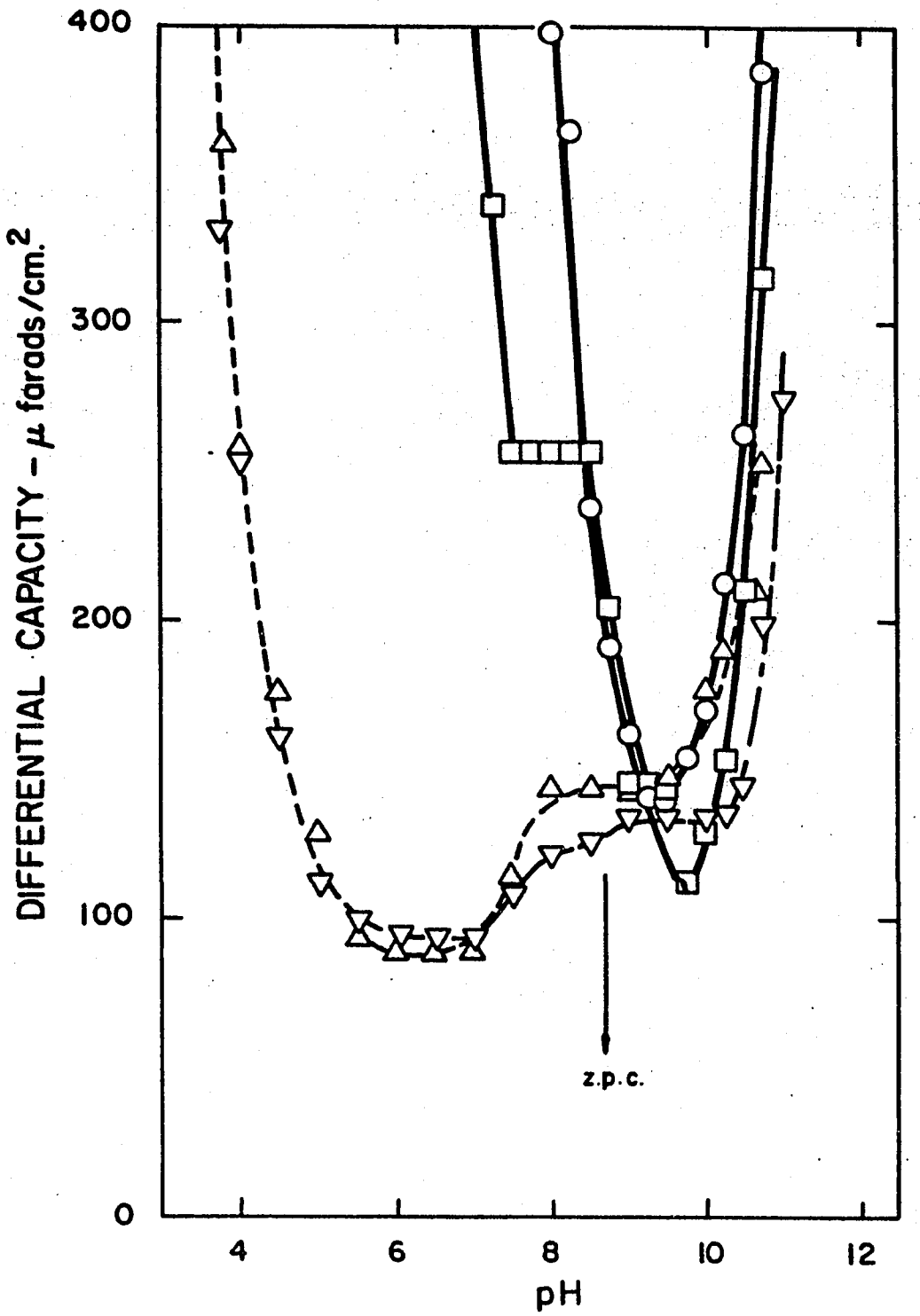
400
300
200
100
0
DIFFERENTIAL CAPACITY – μ farads/cm.²
4
6
8
10
12
pH
z.p.c.

FIGURE 36

EFFECT OF pH ON THE DIFFERENTIAL CAPACITY

OF BADDELEYITE

○ - 10^{-1} N KCl

□ - 10^{-2} N KCl

△ - 10^{-3} N KCl

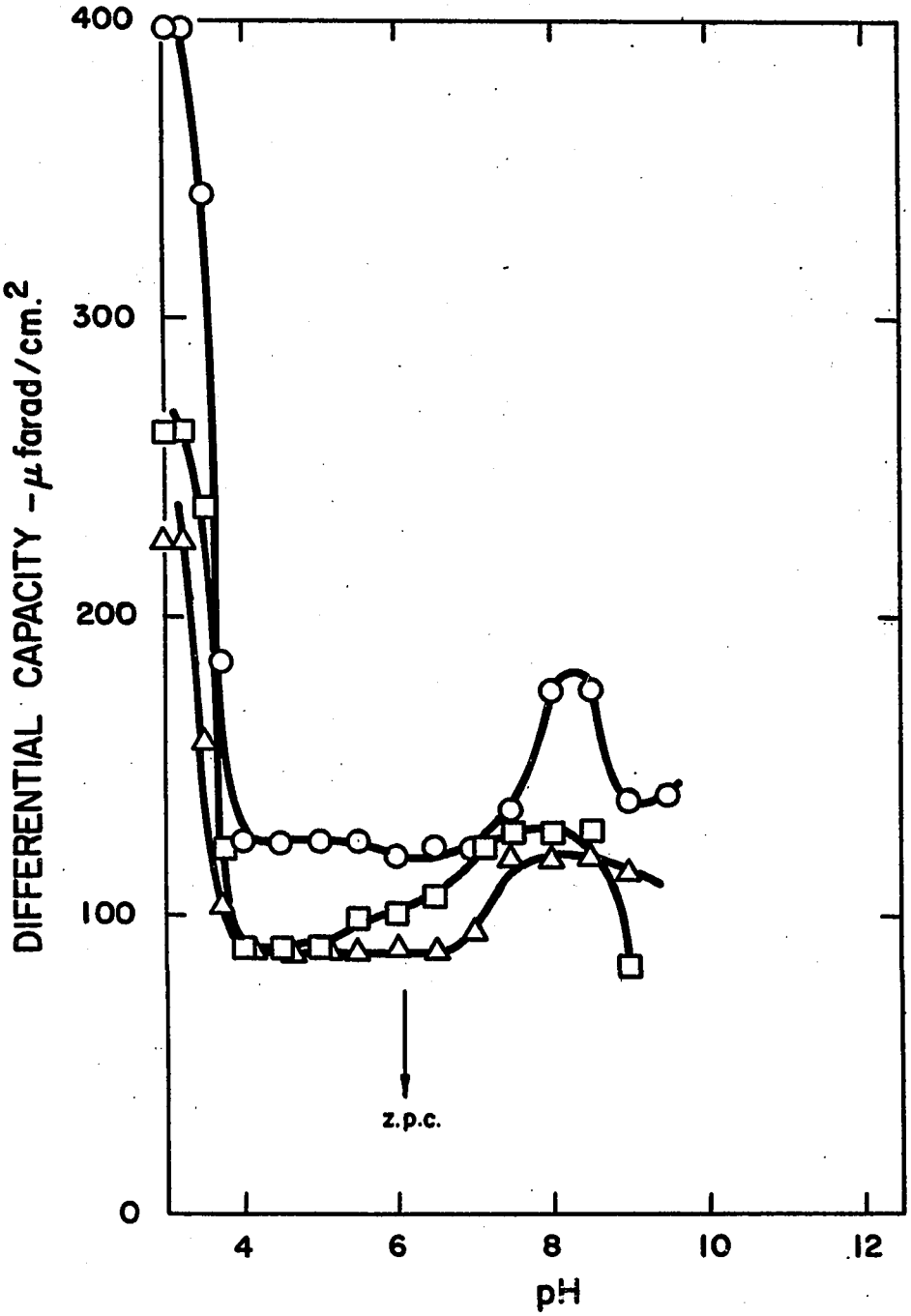
400
300
200
100
0
DIFFERENTIAL CAPACITY – μ farad/cm.²
z.p.c.
4
6
8
10
12
pH

FIGURE 37

EFFECT OF pH ON THE DIFFERENTIAL CAPACITY

OF RUTILE

○ - 10^{-1} N KCl

□ - 10^{-2} N KCl

△ - 10^{-3} N KCl

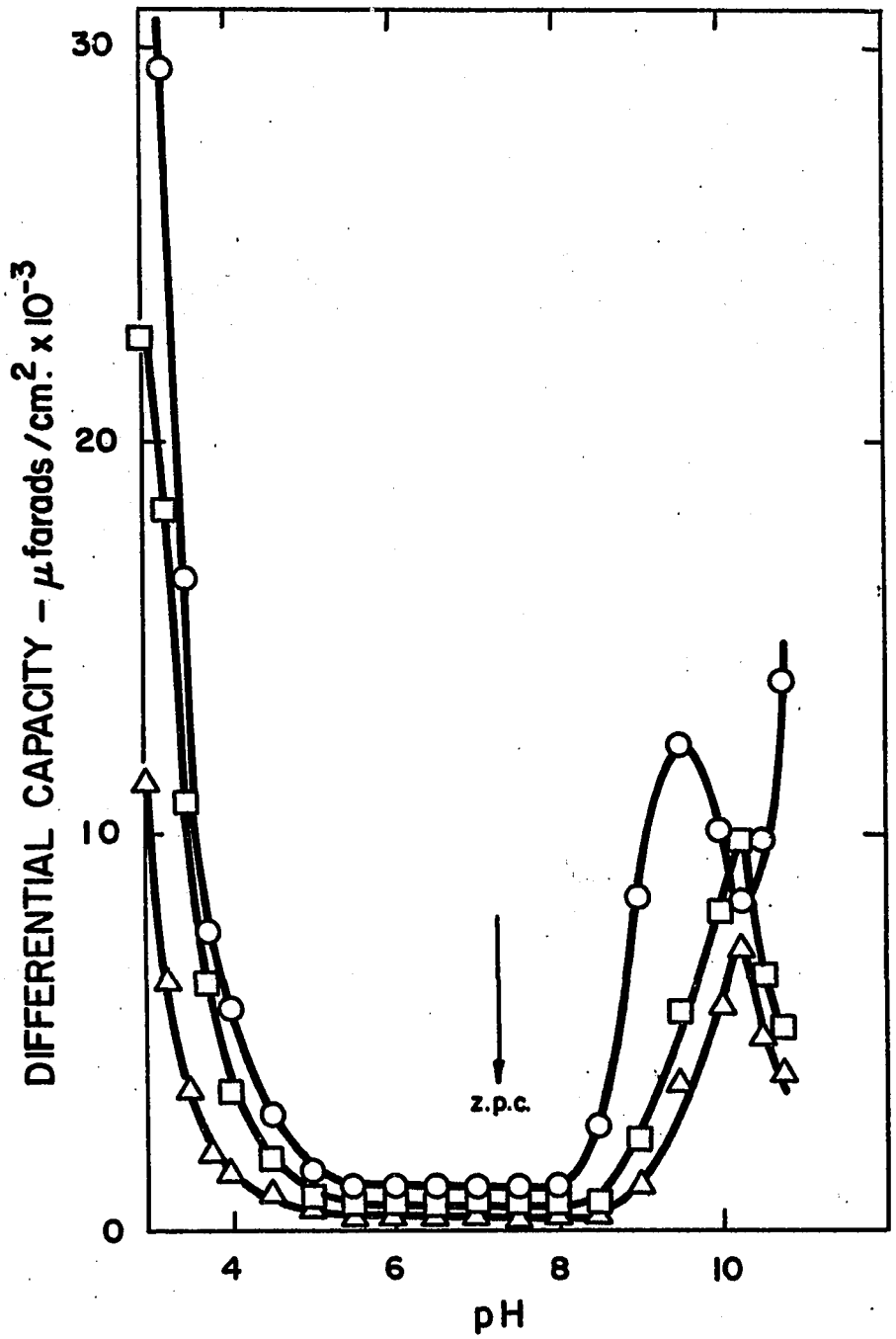
DIFFERENTIAL CAPACITY – μfarads/cm.^{2} x 10^{-3}
30
20
10
0
4
6
8
10
pH
z.p.c.

FIGURE 38

DIFFERENTIAL CAPACITY VS. SURFACE CHARGE DENSITY

OF HEMATITE

○ - 10^{-1} N KCl

□ - 10^{-2} N KCl

◇ - 10^{-3} N KCl

△ - 10^{-4} N KCl

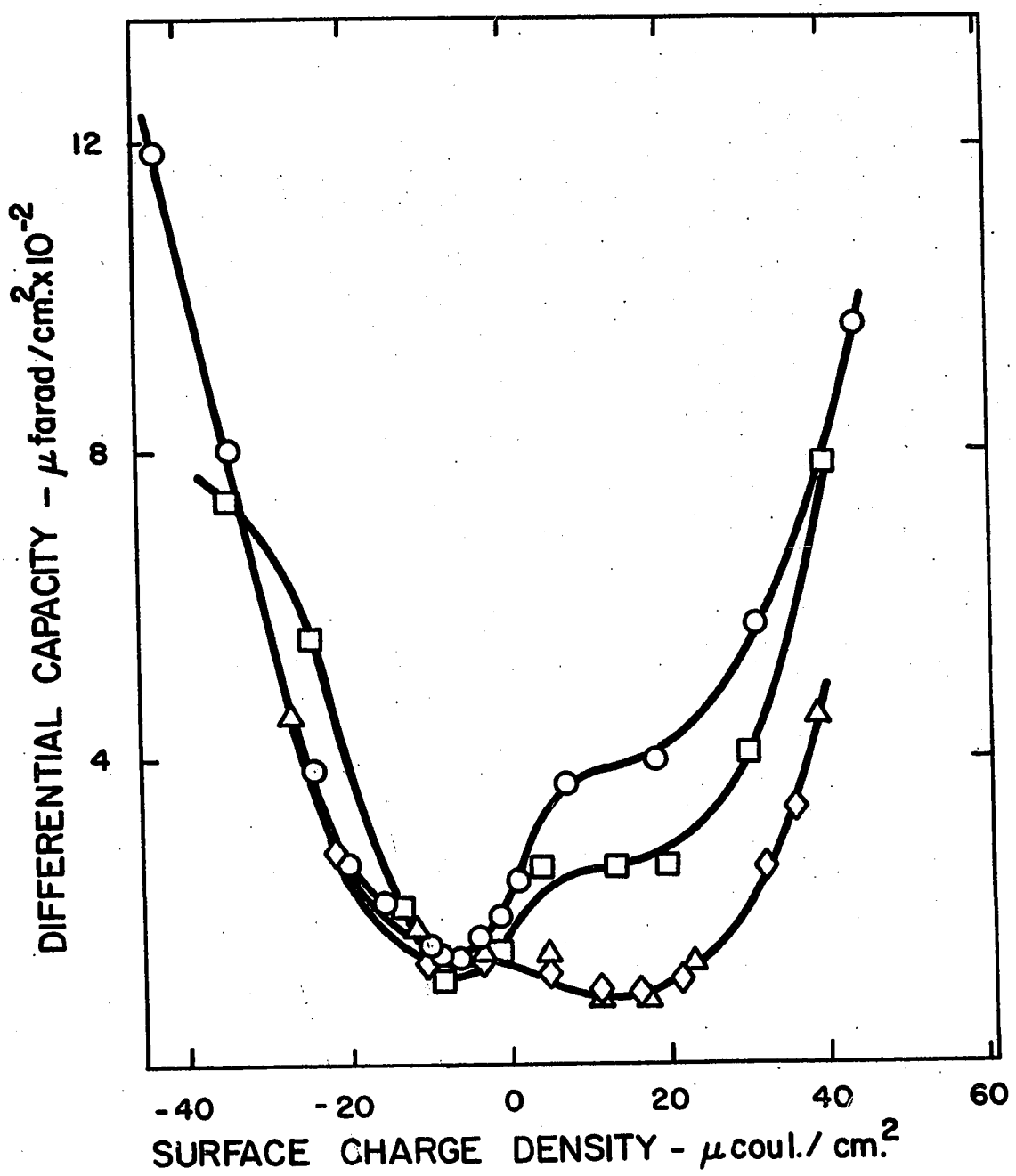
12
8
4
DIFFERENTIAL CAPACITY - μ farad/cm.² x 10⁻²
-40
-20
0
20
40
60
SURFACE CHARGE DENSITY - μ coul./ cm.²

FIGURE 39

DIFFERENTIAL CAPACITY VS. SURFACE CHARGE DENSITY

OF BADDELEYITE

○ - 10^{-1} N KCl

□ - 10^{-2} N KCl

◇ - 10^{-3} N KCl

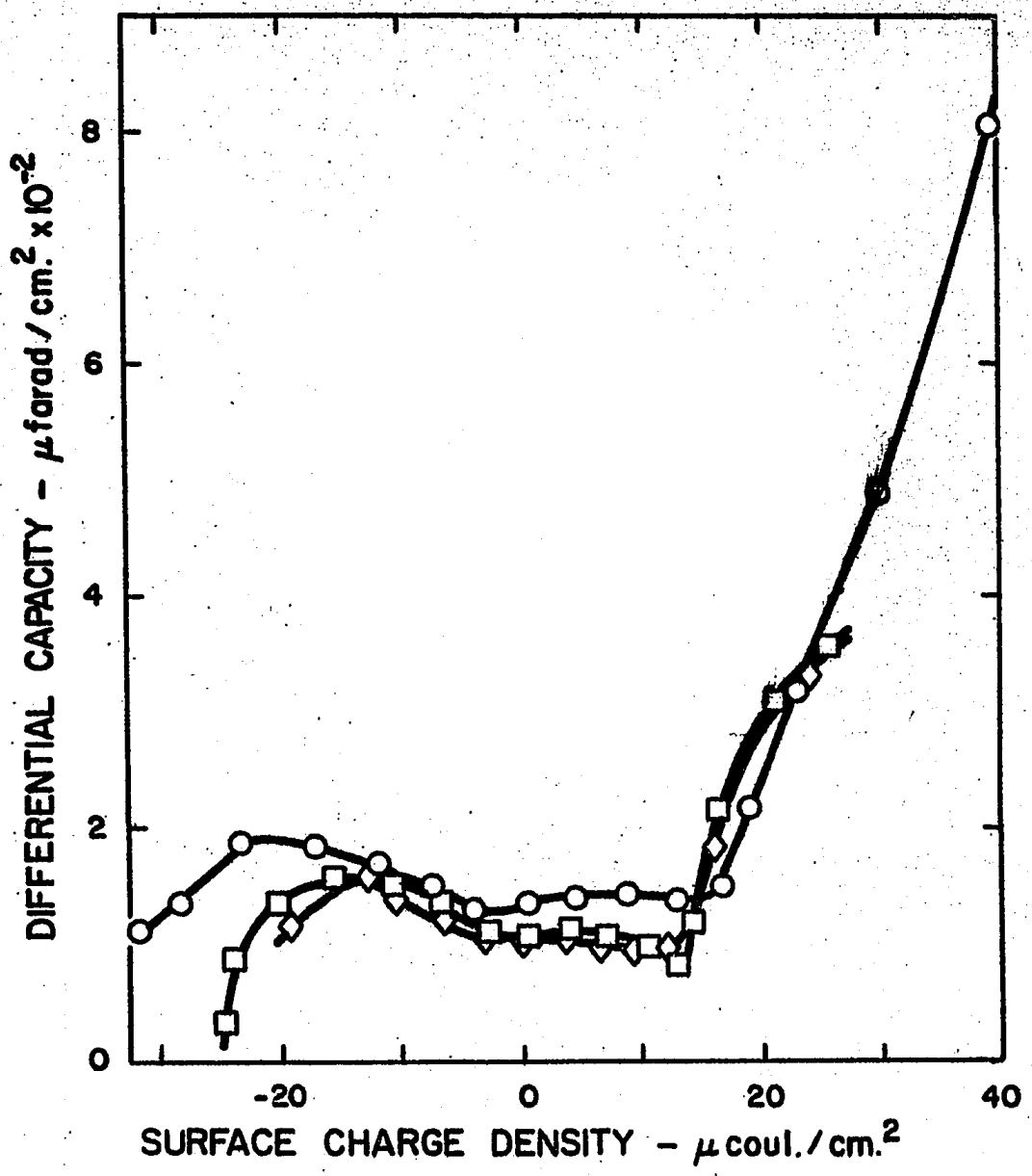
DIFFERENTIAL CAPACITY - μfarad/cm.² x 10⁻²
0
2
4
6
8
-20
0
20
40
SURFACE CHARGE DENSITY - μcoul./cm.²

FIGURE 40

DIFFERENTIAL CAPACITY VS. SURFACE CHARGE DENSITY

OF RUTILE

◇ - 10^{-1} N KCl

□ - 10^{-2} N KCl

○ - 10^{-3} N KCl

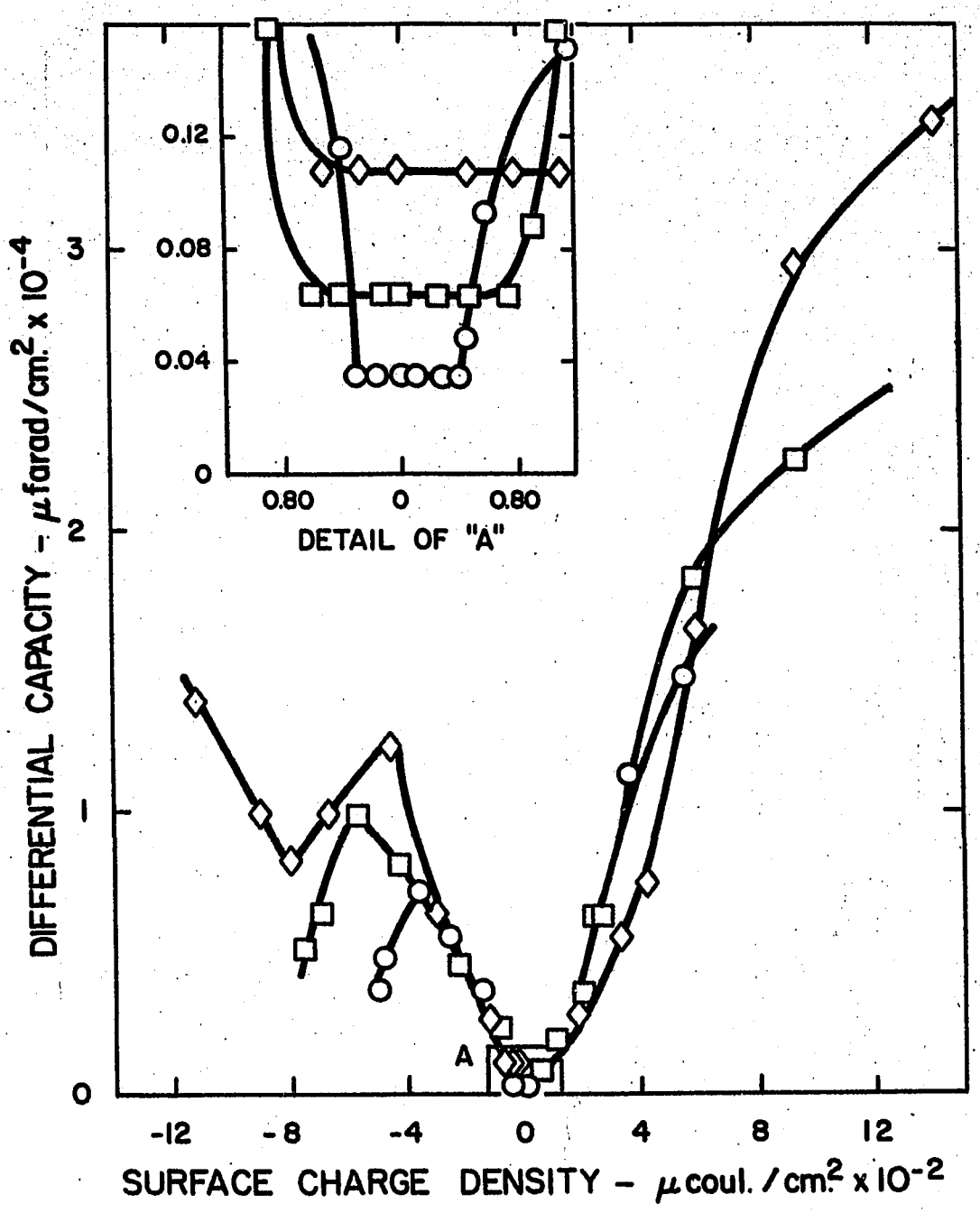
DIFFERENTIAL CAPACITY - μfarad/cm.² x 10⁻⁴
SURFACE CHARGE DENSITY - μcoul./cm.² x 10⁻²
0
1
2
3
-12
-8
-4
0
4
8
12
A
0.12
0.08
0.04
0
0.80
0
0.80
DETAIL OF "A"

2) Streaming Potential of Quartz.

At very low or very high pH values for the zero-point-of-charge of solids, the adsorption of potential determining ions technique cannot be used due to the difficulty in measuring the adsorption of small quantities of hydrogen or hydroxyl ion by the shift in pH. The method is most useful when the zero-point-of-charge is at a pH between 4 and 10. Therefore, the streaming potential of quartz was used to locate the zero-point-of-charge of the quartz used in this investigation. The results are tabulated in Table XVI and are shown in Figure 41 as a function of pH.

For these calculations, the Helmholtz-Smoluchowski equation was used. The conductivity used was that of the bulk solution, rather than the plug, which introduces some errors in the magnitude of the zeta potential due to surface conductance. The quartz exhibited a hystersis loop and an aging effect. The freshly prepared quartz had a maximum zeta-potential of about 12 mV greater than after it was aged for a week or more. After one week there was no further change in the potentials. The zero-point-of-charge was located at a pH of 2.6 $\pm$ 0.2.

$$\frac{E}{P} = \frac{V}{I} = \frac{D\zeta}{4\pi\eta k} \qquad (60)$$

where
- E = streaming potential
- P = streaming pressure
- I = streaming current
- V = volume flow rate
- η = viscosity
- k = specific conductivity
- D = dielectric constant
- ζ = zeta-potential

TABLE XVI

ZETA POTENTIALS OF QUARTZ

Test No.	pH	Zeta-Potential mV.	Conductivity mhos/cm.	Age days
25	7.37	-48.0	0.28	2
26	6.83	-50.7	0.61	3
27	5.95	-53.7	0.99	3
28	5.69	-51.6	1.70	6
29	5.16	-48.0	4.64	6
30	4.62	-40.4	13.6	6
31	4.23	-35.3	30.5	6
32	3.73	-18.2	94.8	7
33	3.45	-12.5	181	7
34	3.13	- 4.7	368	7
35	2.89	- 2.3	649	7
36	2.55	0.0	1420	7
37	2.90	- 2.1	620	7
38	3.20	- 6.3	304	7
39	3.53	-11.3	146	8
40	3.85	-17.6	72.1	8
41	4.18	-25.6	33.0	8
42	4.51	-32.2	16.6	8
44	4.83	-38.2	8.22	9
45	5.17	-40.9	3.96	9
46	5.60	-41.3	1.87	12
47	6.41	-37.4	0.57	12
48	6.93	-32.8	0.44	13
49	4.95	-39.1	6.81	13
50	4.02	-28.3	50.6	13
51	3.38	-10.0	211	14
52	3.76	-17.9	89.0	14
53	4.25	-29.0	29.6	14
53a	4.75	-36.5	10.0	15

FIGURE 41

ZETA POTENTIAL OF QUARTZ
AS A FUNCTION OF pH

Size - -35 + 48 mesh

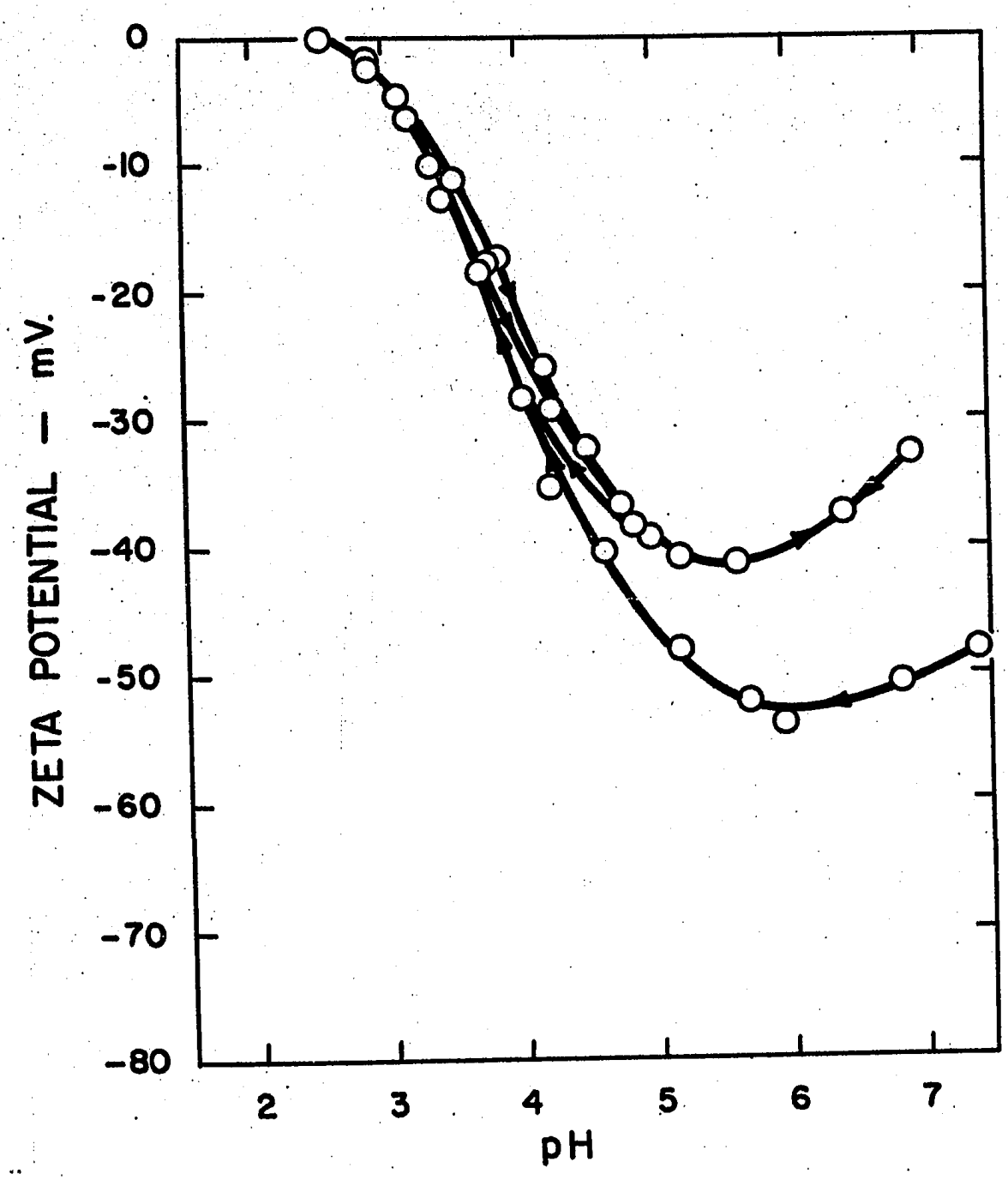
ZETA POTENTIAL — mV.
0
-10
-20
-30
-40
-50
-60
-70
-80
2
3
4
5
6
7
pH

Floatability

The flotation tests carried out in a Hallimond tube showed that maximum recoveries were obtained at amine concentrations between 100 and 200 micromoles per litre in the case of quartz, hematite and rutile. The flotation of baddeleyite, due to its fine size, was low and did not reach a maximum. The results are tabulated in Table LVIII, Appendix VII and are shown graphically as a function of concentration in Figure 42. At concentrations in excess of 200 micromoles of amine per litre, the floatability decreased continuously which corresponded to the decrease in contact angle noted in the results concerning contact angle. Several tests were conducted using quartz-hematite mixtures to determine whether or not separation could be obtained. The results, shown in Figure 43, indicated that no effective separation could be accomplished in the absence of modifiers, although good recovery of both minerals in the froth together could be obtained (74.3% Fe_2O_3 and 84.5% SiO_2 at 20 mg. amine /1.).

In the presence of 25 mg./1. of soluble starch, and at a pH of 9.6 to 9.9, better recoveries and grades were obtained under otherwise similar flotation conditions. A grade of 76% Fe_2O_3 and a recovery of 75% in one minute could be obtained under these conditions. If the solids were conditioned with starch and potassium hydroxide prior to the addition of the amine the results could be further improved to 86.5% Fe_2O_3 grade and 85.0% recovery in one minute using 20 mg./1. as the initial collector concentration.

FIGURE 42

THE EFFECT OF DEHYDROABIETYLAMINE CONCENTRATION

ON THE FLOTATION OF MINERAL OXIDES

○ - Quartz

□ - Hematite

△ - Rutile

▽ - Baddeleyite

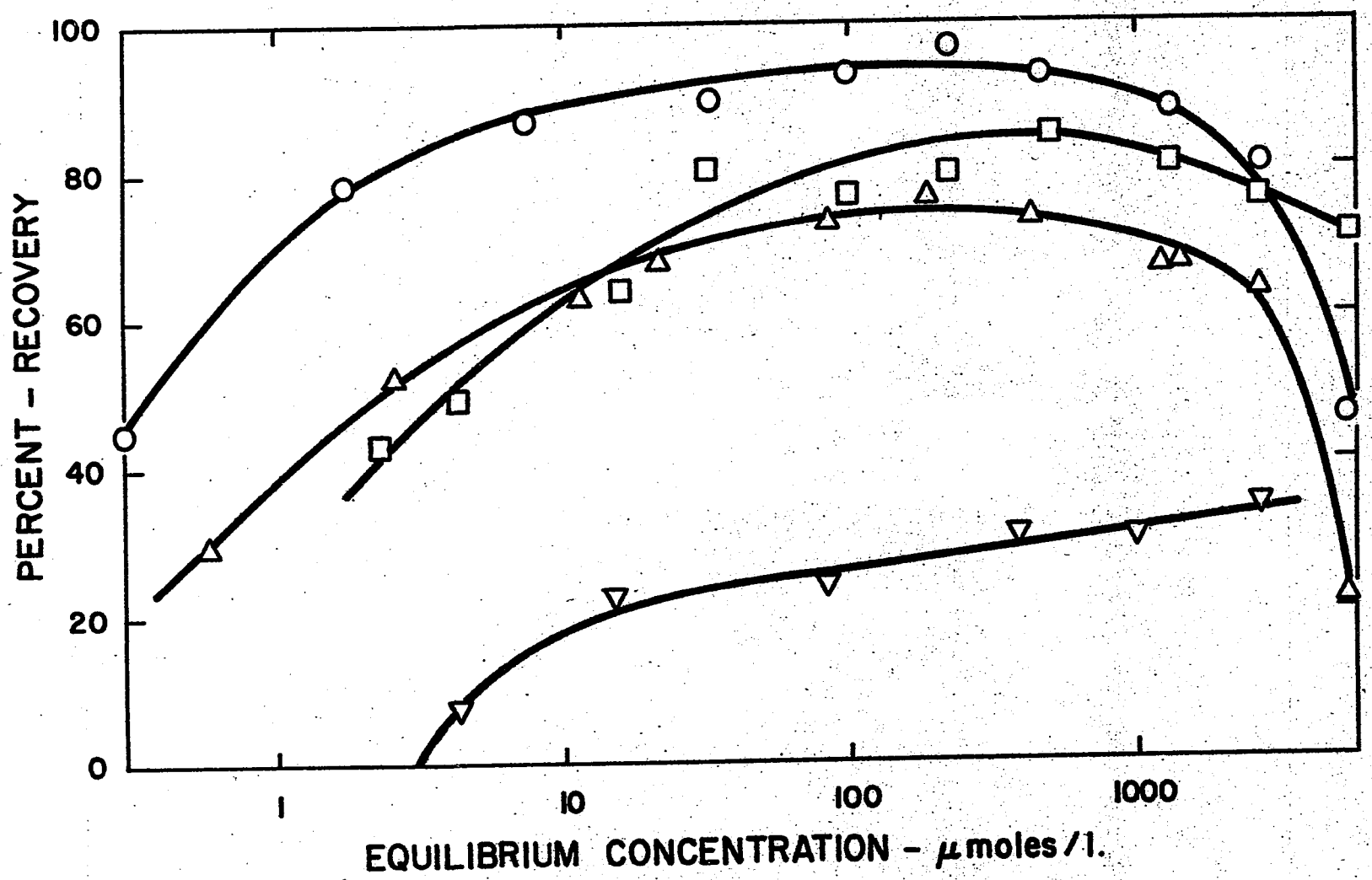
100
80
60
40
20
0
PERCENT - RECOVERY
1
10
100
1000
EQUILIBRIUM CONCENTRATION - μmoles/l.

FIGURE 43

THE EFFECT OF DEHYDROABIETYLAMINE CONCENTRATION
ON THE FLOTATION OF A 50-50 MIXTURE
OF QUARTZ AND HEMATITE

○ - Neutral, No starch

△ - pH = 9.6 to 9.9; 25 mg./l. starch

□ - pH = 9.6 to 9.9; 25 mg./l. starch (conditioned without amine)

——— - Percent Fe_2O_3 in Concentrate

- - - - Percent Recovery of Fe_2O_3

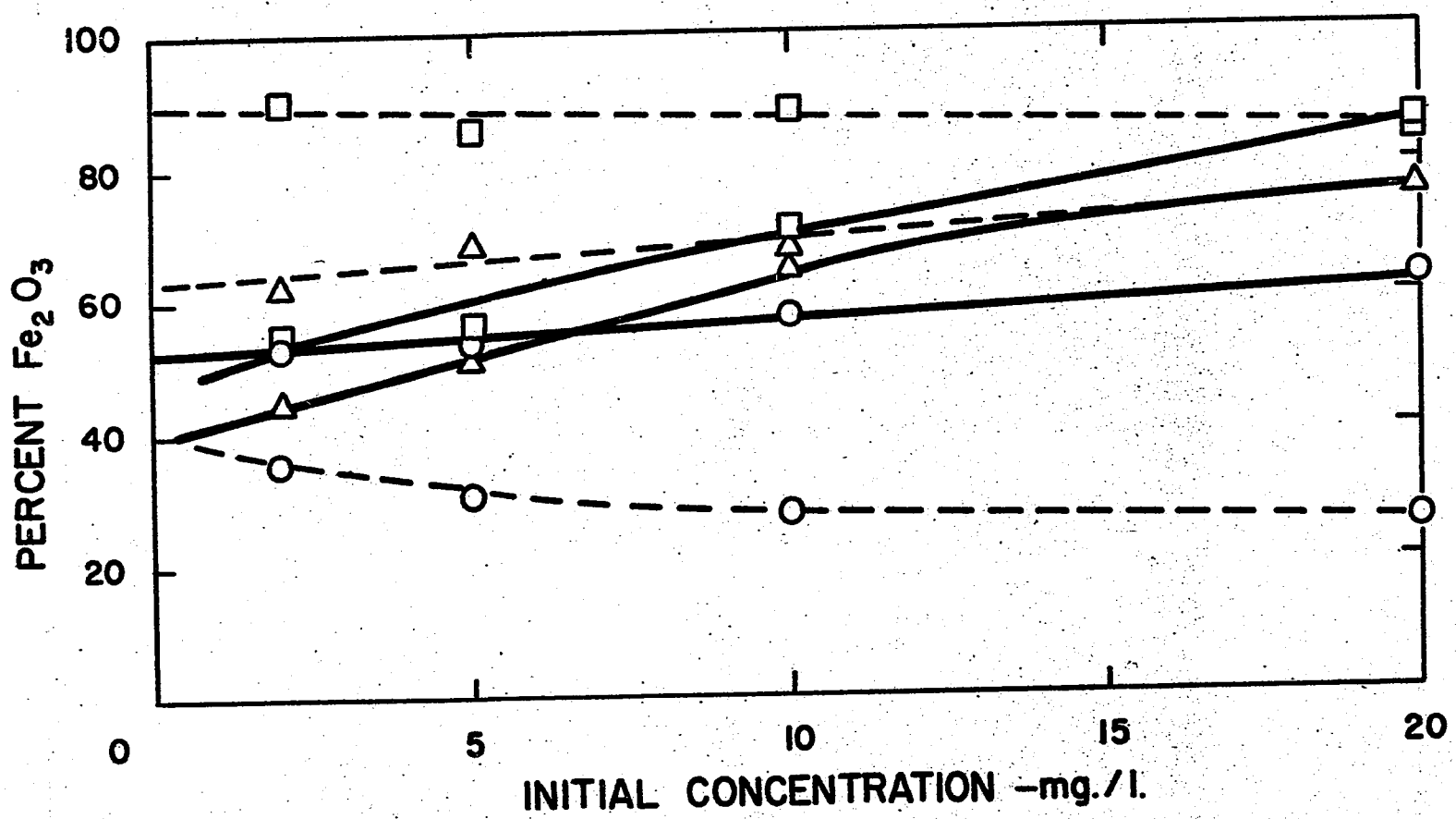
100
80
60
40
20
0
5
10
15
20
PERCENT Fe_2O_3
INITIAL CONCENTRATION –mg./l.

DISCUSSION OF RESULTS

Adsorption and Desorption Test

The adsorption isotherms of hematite, quartz, rutile, and baddeleyite presented in this thesis are similar to each other in shape. The adsorption density (Γ_R) increases regularly with increasing concentration (C_R) at low amine concentrations. At high concentrations of amine, the adsorption on hematite and rutile levels off at adsorption densities equivalent to 5 to 8 monolayers. The adsorption on baddeleyite may also level off at higher concentrations where the adsorption density is equivalent to several monolayers. The adsorption on quartz gives no indication of levelling off even at high concentrations. This may be due to the fact that quartz has a much more negative surface than the other minerals in neutral solution and that its capacity to hold positive ions physically in the double layer is much greater.

At low amine concentrations, the adsorption on quartz up to monolayer is greater than the other minerals at the same reagent concentration. It is suggested that, due to the highly negative surface, quartz will adsorb the first layer easily but will require a greater driving force (increased reagent concentration) to adsorb additional layers. The concentration required to adsorb these additional layers is similar to that required by the other minerals.

The adsorption on baddeleyite is from three to four times less than on the other minerals and may be due to the large surface area. The sample of pure baddeleyite used was a precipitated product and it is conceivable that up to 75% of its surface area is either not available to the dehydroabietylamine ions or molecules (small capillaries) or blocked by previously adsorbed material. For example, if the dehydroabietylamine molecule may be considered as a cylinder with a cross-sectional area of 50 $Å^2$ and a length of 16 $Å^2$ (length to diameter ratio of 2) and it just fits into a pore of this size, then the occupied area becomes 453 $Å^2$ instead of 50 $Å^2$. Therefore, the available surface area may be as low as 4 M^2./gm. and the adsorption density becomes similar to that on the other minerals.

The slopes of linear portion of the log-log graph of specific adsorption vs. concentration are all 0.50 with the exception of quartz. The curve for quartz has a slope of 0.41.

This marked similarity suggests the same mechanism or mechanisms may be involved in the adsorption process. Furthermore, work using dodecylamine (62,63) has indicated that the same slopes (0.50 to 0.60) have been found on quartz, hematite, and sphalerite, although the quantity adsorbed is much less. Since the aminium ion RNH_3^+ is ten thousand times more abundant than the undissociated amine (RNH_2) at pH of 5.8 (the pH at which the adsorption tests were made), the ion should be considered as the important surface-active species. At higher pH values or at high concentrations, the free amine may be present in significant

amounts. The free amine could be the active species which is adsorbed from solution. The amine would be replaced in the bulk solution by the rapid conversion of the aminium ions by the reaction

$$RNH_3^+(\text{Sol'n}) + OH^-(\text{Sol'n or Adsorbed}) \rightleftharpoons RNH_2(\text{Sol'n}) + H_2O \qquad (61)$$

The effect of pH on the adsorption of dehydroabietylamine acetate on mineral oxides is complex due to changes in other variables which change with pH. The experimental curves of adsorption vs. pH exhibit two distinct regions. In the pH range of 3 to 6, the curves are linear. For quartz and hematite, the slope of this portion of the curve is unity; while for rutile, the slope is 0.8 and, for baddeleyite, it is 0.98. Above a pH of approximately 8, the adsorption has reached a maximum and the curves become horizontal.

Due to experimental limitations in the analysis, specific adsorption results at lower pH values were impossible to obtain. If these results were to show that the curves are sigmoidal in shape on a log-log scale, this would indicate a complex dependance of adsorption of pH that could not be explained simply. However, if the results were to indicate that the straight lines continued, the explanations are simpler.

Nemeth (77) has found a sigmoid shape curve on a semi-log graph (using pH as the logarithmic scale) in his investigation. If his data is replotted on the same scale as this work, the results are

similar. Nemeth did not investigate the adsorption properties below a pH of 6 and, hence, did not have any problem with low adsorptions.

A change in the pH of the adsorbing solutions will cause a change in the surface charge on the oxides due to a change in the surface potential, ψ_o , and in the total ion concentration, n. Regardless of the value of the zero-point-of-charge, a decrease in pH will cause a decrease in the ability of the double layer to contain positively charged ions such as the aminium ions. It is clearly shown in Figure 19, that the maximum adsorption decreases with decreasing pH. The zero-points-of-charge of these oxides (range 2.6 to 8.7) appear to have little effect on the pH below which the adsorption rapidly decreases. Therefore, the chemistry of the amine solutions appears to be of greater importance to the adsorption process than the state of the mineral surface.

In amine solutions, an increase in hydrogen ion concentration will increase the ratio of aminium ion to free amine proportionally provided that precipitation of the amine does not occur. At a constant total amine concentration below a pH of 8, the aminium ion concentration is constant and approximately equal to the total amine present. The free amine concentration decreases with decrease in pH and may be expressed as

$$C_{RNH_2} = \frac{K_W}{K_B} \cdot \frac{C_{RNH_3^+}}{C_{H^+}}$$

$$\simeq \frac{K_W}{K_B} \cdot \frac{C_{(TOTAL)}}{C_{H^+}}$$

or $$\log (C_{RNH_2}) \simeq K_1 \cdot pH \qquad (62)$$

where $K_1 = \log K_W + \log C_{(TOTAL)} - \log K_B$

Therefore, the adsorption may be governed either by the concentration of free amine or the ratio of aminium ion to hydrogen ion concentration. It is not possible to separate these two cases.

If the free amine is the determining species and its concentration varies inversely as the hydrogen ion concentration, the adsorption should be proportional to these concentrations according to:-

$$\Gamma_R = k_1 C_{RNH_2} = k_2 \frac{C_{RNH_3^+}}{C_{H^+}}$$

$$\simeq k_3/C_{H^+} \qquad (63)$$

However, the adsorption should vary directly with concentration at constant pH according to

$$\Gamma_R = k_4 \cdot C_{RNH_3^+}$$

$$\simeq k_4 \cdot C_{(TOTAL)} \qquad (64)$$

But the adsorption at constant pH is found to be proportional to the square root of the total concentration. Therefore, the free amine concentration alone is not the determining factor.

If the aminium ion is the adsorbing species, an increase in hydrogen ion concentration increases the competition between hydrogen and aminium ions for available adsorption sites in the double layer. Thus, a decrease in the adsorption of amine over the entire concentration range is expected with a decrease in pH. This appears to be substantiated in the results (Figure 19). A simple stoichiometric ion exchange mechanism between the hydrogen ion and the aminium ion has been considered by deBruyn (62). It was rejected since it did not explain all the experimental results. The fraction of aminium ions which may adsorb on positive adsorption sites in the presence of hydrogen ions may be written as

$$\frac{C_{RNH_3^+}}{C_{RNH_3^+} + C_{H^+}}$$

The adsorption should be related to the total amine concentration by

$$\Gamma_R = k_5 \cdot \frac{C_{(TOTAL)}}{C_{(TOTAL)} + C_{H^+}} \qquad (65)$$

According to this equation, at low pH values, Γ_R should be proportional to $C_{(TOTAL)}$, whereas, at high pH values Γ_R should be constant.

This relationship does not apply to the experimental results of this system, since it does not provide for the square root relationship between adsorption and concentration.

The competition between positive ions is qualitatively supported by the results in three ways. At all amine concentrations, the specific adsorption decreases with decreasing pH. The maximum capacity to adsorb amine decreases with decreasing pH, due to increasing amounts of hydrogen ions in the double layer. The square root relationship favours the adsorption of aminium ions in the double layer.

In general, the effect of pH is more complex than the straight line relationships indicate. The effect of the zero-point-of-charge and its shift with amine content (if any) cannot be completely neglected. However, the sharp changes that have been reported (90) in adsorption and flotation characteristics at the zero-point-of-charge may be due not so much to the zero-point-of-charge but to changes in ion concentrations of the adsorbing species with pH. In this work, it is noted that, regardless of the surface charge and sign, the adsorption is in the same order of magnitude in all cases(or may be explained by other factors such as available area).

The desorption of this amine from mineral surfaces appears to be similar to that of other amines. At room temperature, the desorption isotherm follows the adsorption isotherm, indicating that the process is reversible in nature. This suggests that the adsorption takes place in the electrical double layer and that the amine does

not interact chemically with the mineral surface. Similar conclusions have been reached by Danilova (91) using laurylamine on quartz, and by Zagirova (92) using IM-11 and octadecylamine on quartz, fluorite, scheelite, cassiterite, and hematite.

Contact Angle

The results of the present investigation indicate that no simple relationship exists between specific adsorption and contact angle. In general, with increasing specific adsorption, the angle increases until several monolayers have been formed. The maximum angle varies from 51° to 64° depending on the mineral. The maximum angle is not maintained at higher amine concentrations as in other amine-oxide systems investigated by Bloecher (65), Morrow (63), and deBruyn (62). A general decrease is observed at high concentrations, indicating a decrease in the effectiveness of the amine already adsorbed.

Figure 26 suggests that a definite surface concentration is required before a finite contact angle is obtained. This might be interpreted to mean that the adhesion between a clean mineral surface and the surrounding liquid is greater than required to bring the contact angle to the value of zero. Thus, the usage of the phrase "no contact angle" rather than "zero contact angle" is suggested. This is in agreement with the proposals of Morrow (63).

The contact angle decrease above a certain concentration may be due to the adsorption of many layers of amine. When several layers of amine are adsorbed, the forces of attraction between the mineral surface and the outermost layer of amine becomes very weak. The air bubble may attach itself to the outermost layer of amine and, since the

forces of attraction are weak, exhibit a small contact angle. In the extreme case, zero contact angle is a possibility when the attractive force of the layer of amine (with bubble attached) for the mineral surface becomes equal to that for the surrounding liquid. In the case of hematite and rutile, the decrease in contact angle is accompanied by a decrease in the rate of adsorption of amine (i.e. the adsorption starts to follow Langmuir's isotherm.). It is apparent from contact angle measurements, that the quartz surface is almost completely covered with adsorbate at 2 gm./l. The quartz surface may follow a Langmuir type isotherm at concentrations slightly in excess of 2 gm./l., similar to those followed by the hematite and rutile surfaces.

There is no indication that micelle formation has occurred on the surfaces. This is usually noted by increased adsorption with little change in contact angle. The problem of relating contact angle to adsorption density is most complex. The exact structure and distribution of amine ions and/or molecules in the double layer is not known. In fact, the double layer in the absence of specific adsorbates is still under study. At the present time, one can say only that a finite angle of contact is required for flotation.

At high collector concentrations in neutral solutions, hematite and quartz exhibit non-flotation, yet the adsorption is higher than at lower concentrations where flotation is possible. This effect has been noted by Joy and Watson (93), and by Sutherland and Wark (94) in various systems. Unfortunately, these authors do not explain their results except to say that the condition exists.

Zero-Point-of-Charge

The determination of the zero-point-of-charge of oxides under consideration in this study yielded results which were in accord with those of other authors.

The zero-point-of-charge of specular hematite, found to be 8.68, is close to that found for synthetic alpha hematite (range 8.0 to 9.0) but is somewhat higher than that found for other natural hematites (range 5.4 to 6.9)(37). Among the natural hematites, only one is specified as Labrador specular hematite, (z.p.c. of 6.6) but the details are not reported in literature (95). This may suggest that the impurity level in the present case is lower than that in other samples, but this is not easily confirmed. A common explanation for the lowering of the zero-points-of-charge of natural oxides is the presence of impurities such as quartz.

The sample of zirconia used, with a zero-point-of-charge of 6.08, is not similar to any zirconia examined to date. Two other precipitated products have been tested:- one precipitated from $ZrO(NO_3)_2$ solution with NaOH (96) and the other from $Zr(NO_3)_4$ solution with NaOH (97). These oxides had zero-points-of-charge of 10-11 and 6.7 respectively. A natural zirconia sample was examined and found to have zero-point-of-charge of 4 (98). The purity of this mineral is not reported. The present sample, whose structure is that of the mineral baddeleyite (confirmed by X-rays), is precipitated from $ZrO(SO_4)$ solution by dilution. Therefore, the present sample is similar to the first two reported samples in that it is a

precipitated product and to the last reported sample in that it has a natural mineral structure. The zero-point-of-charge found in the present study is similar to that of hydrous ZrO_2 reported by Mattson and Pugh (97) which was precipitated from $Zr(NO_3)_4$ solution.

The difficulties encountered with the exchange of SO_4^{-2} with OH^- ions in the zirconia sample has been reported by others. Parks (99) has noted this phenomena with hematite and Thomas (100) and Rollinson (101) have reported similar results with alumina. Sufficient washing will remove the sulphate, at least from the surface where it interferes with zero-point-of-charge measurements.

The rutile under investigation exhibited a zero-point-of-charge of 7.13 which is slightly higher than that of 6.7 reported by Purcell and Sun (102). Other reports of the zero-point-of-charge of this oxide include values of 6.0 and 4.7 by Johnansen and Buchanan (85), 6.0 by Feeney and Holmes (95), and from 3.5 to 5.5 for natural rutile (85,95,103,104).

The sample of quartz was found to have a zero-point-of-charge of 2.6 which is about the average of the reported values. Other values include 3.7 by Gaudin and Fuerstenau (105), 1.3 by Sen and Ghosh (106), 2.8-3.0 by Hückel (107), 1.5-1.8 by Bhappu (108), and 2.5 by Purcell (27). From this data, the quartz sample used appears to be a typical alpha quartz specimen.

The object of locating the zero-point-of-charge was to establish that the decrease in adsorption of amine with decreasing pH

(discussed previously) is not related to the zero-point-of-charge of the mineral involved but rather to the chemistry of the solution in contact with the mineral. It is obvious in this work that the decrease in adsorption of amine in all cases occurs in the pH range of 4.5 to 6.0 whereas the zero-point-of-charge of the oxides range from a pH of 2.6 to 8.7.

The most striking feature of the differential capacity curves are the differences between them and those of other systems. In 10^{-3} M potassium chloride solution, the minimum differential capacity for hematite, baddeleyite, and rutile is 143, 88, and 350 μfd./cm.^{2} respectively. These are much higher than for silver sulphide (AgS) and silver iodide (AgI) (roughly 5 μfd./cm.^{2}) and for hematite (38.6 μfd./cm.^{2}) (99). The minimum differential capacity predicted by the double layer theory on the assumption that the identity of the solid plays no role, is 7.2 μfd./cm.^{2} (99) which is also much smaller than obtained in the present work.

As the differential capacity curves were obtained by graphical differentiation of the smoothened charge density curves (which were obtained from smoothened titration curves), no quantitative precision either in the upper range of values or in the shape of the curve can be expected. Qualitatively, it may be concluded that there is some specific adsorption of Na^+ and K^+ at high pH values (negative surface) and of Cl^- ions at low pH values(positive surface). Similar conditions have been reported on ThO_2, ZrO_2, and SiO_2 (109).

It has been reported (110) that on removing the oxide film from metals (such as Pt), the clean metals behave like mercury in their differential capacity curves. In the present case of oxides, specific adsorption of cations may be said to occur on the metal through chemisorbed O^{-2} ions (111).

Calculation of the Iso-Electric-Point of Oxides

If a group of positive and negative complexes of the same central ion is considered independently of any other ionic species in solution, this group will be electroneutral when

$$\Sigma z_+ c_+ = \Sigma z_- c_- \qquad (66)$$

where z_+,(z_-) is the net charge of a positive (negative) complex (33). The ligand activity (or concentration in dilute solution) at which this condition is satisfied determines the iso-electric-point of the complex solution (112,113). When the complex system includes a solid phase, the iso-electric-point corresponds to the point of minimum solubility of the solid. Proof is given by Beck (113) and Johnston (114). Figure 44 shows that the iso-electric-point and the minimum solubility of silver oxide (99) do, in fact, coincide. It should be noted that the concentration of the undissociated hydroxide is in excess of the ionic species over less than one pH unit near the iso-electric-point, thus its effect on the solubility is minimal.

The determination of the iso-electric-point for other materials and particularly for other oxides by minimum solubility determination has been seriously hampered by two factors:- (1) the accurate location of the minimum solubility is difficult due to a relatively high concentration of the undissociated hydroxide, and (2) accurate analytical methods for determination of low metallic ion concentrations in solution are not known. The concentration of undissociated hydroxide may be far

FIGURE 44

ISO-ELECTRIC-POINT OF SILVER OXIDE

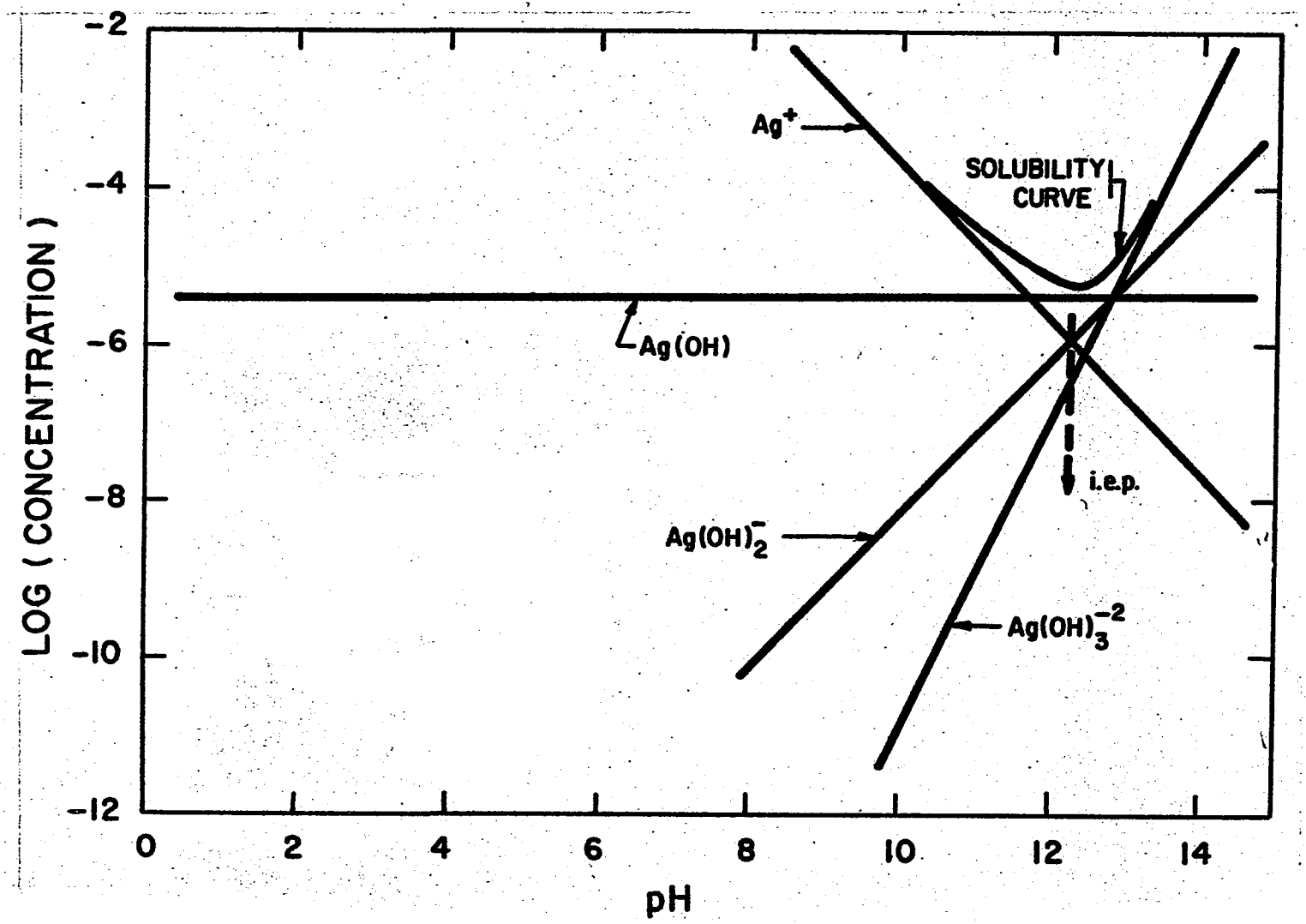
LOG (CONCENTRATION)
-2
-4
-6
-8
-10
-12
0
2
4
6
8
10
12
14
pH
Ag+
SOLUBILITY CURVE
Ag(OH)
i.e.p.
Ag(OH)2-
Ag(OH)3-2

in excess of that of the charged ions over a pH range as large as 12 to 14 pH units (e.g. $Fe(OH)_3$). Radiotracer techniques may solve the analysis problem but the other problem is not easily surmountable.

1) Rutile

Table XVII tabulates the equilibrium constants used in the calculation of the concentration of the ions in equilibrium with the solid oxide. The concentration of ions as a function of pH are listed in Table XVIII. The equilibria between positive ion complexes and the hydroxide have been determined by Liberti et al (115). The negative ion concentration has been calculated by Schmets and Pourbaix (116). The solubility data of Brown et al (117) has been used to determine the actual concentrations of the ions. As can be seen in Figure 45, the calculated solubility and the experimental points agree well and the iso-electric-point is found to be at a pH of 6.9 $\pm$ 0.1. The concentrations of each ion are recorded in Table XIX.

TABLE XVII

EQUILIBRIUM CONSTANTS USED TO CALCULATE THE ISO-ELECTRIC-POINTS

Element Oxide	$^*K_1$	$^*K_2$	$^*K_3$	$^*K_4$	$^*K_{inst(5)}$	$^*K_{inst(6)}$	Ref. No.
Rutile (TiO_2)	-	-1.80	-4.20	-6.30	-	-	(115)
Zirconia (ZrO_2)	-0.22	-0.62	-1.05	-1.17	-4.72	+1.79	(118,119)
Hematite (Fe_2O_3)	-2.17	-4.70	-	-	-5.15	-	(33,122, 123,124)
Quartz	-9.66	-11.7	-12.0	-12.0	-	-	(128)

where

$$^*K_1 = \frac{[M(OH)^{x-1}][H^+]}{[M^{+x}]} \qquad ^*K_4 = \frac{[M(OH)_4^{x-4}][H^+]}{[M(OH)_3^{x-3}]}$$

$$^*K_2 = \frac{[M(OH)_2^{x-2}][H^+]}{[M(OH)^{x-1}]} \qquad ^*K_{inst(5)} = \frac{[M(OH)_x][OH^-]}{[M(OH)^-_{x+1}]}$$

$$^*K_3 = \frac{[M(OH)_3^{x-3}][H^+]}{[M(OH)_2^{x-2}]} \qquad ^*K_{inst(6)} = \frac{[M(OH)^-_{x+1}][OH^-]}{[M(OH)^{-2}_{x+2}]}$$

TABLE XVIII

CONCENTRATION OF IONS IN SOLUTION

Ion	Concentration log(moles/l.)	Ion	Concentration log(moles/l.)
Rutile		**Hematite**	
Ti^{+4}	no evidence of existance	$Fe_2(OH)_2^{+4}$	-4.31 - 4 pH
$Ti(OH)^{+3}$	0.0 - 3 pH	Fe^{+3}	-0.73 - 3 pH
$Ti(OH)_2^{+2}$	-1.8 - 2 pH	$Fe(OH)^{+2}$	-2.90 - 2 pH
$Ti(OH)_3^{+}$	-4.2 - pH	$Fe(OH)_2^{-}$	-7.60 - pH
$Ti(OH)_4$	-6.3	$Fe(OH)_3$	-6.54
$HTiO_3^{-}$	-18.0 + pH	$Fe(OH)_4^{-}$, FeO_2^{-}	-24.6 + pH
Zirconia		**Quartz**	
Zr^{+4}	-5.65 - 4 pH	$Si(OH)_4$	-2.60
$Zr(OH)^{+3}$	-5.87 - 3 pH	$H_3SiO_4^{-}$	-12.26 + pH
$Zr(OH)_2^{+2}$	-6.49 - 2 pH	$H_2SiO_4^{-2}$	-23.96 + 2 pH
$Zr(OH)_3^{+}$	-7.54 - pH	$HSiO_4^{-3}$	-35.96 + 3 pH
$Zr(OH)_4$	-8.71	SiO_4^{-4}	-47.96 + 4 pH
$Zr(OH)_5^{-}$	-17.99 + pH		
$Zr(OH)_6^{-2}$	-32.78 + 2 pH		

FIGURE 45

ISO-ELECTRIC-POINT OF RUTILE

☐ - Experimental Solubility Points

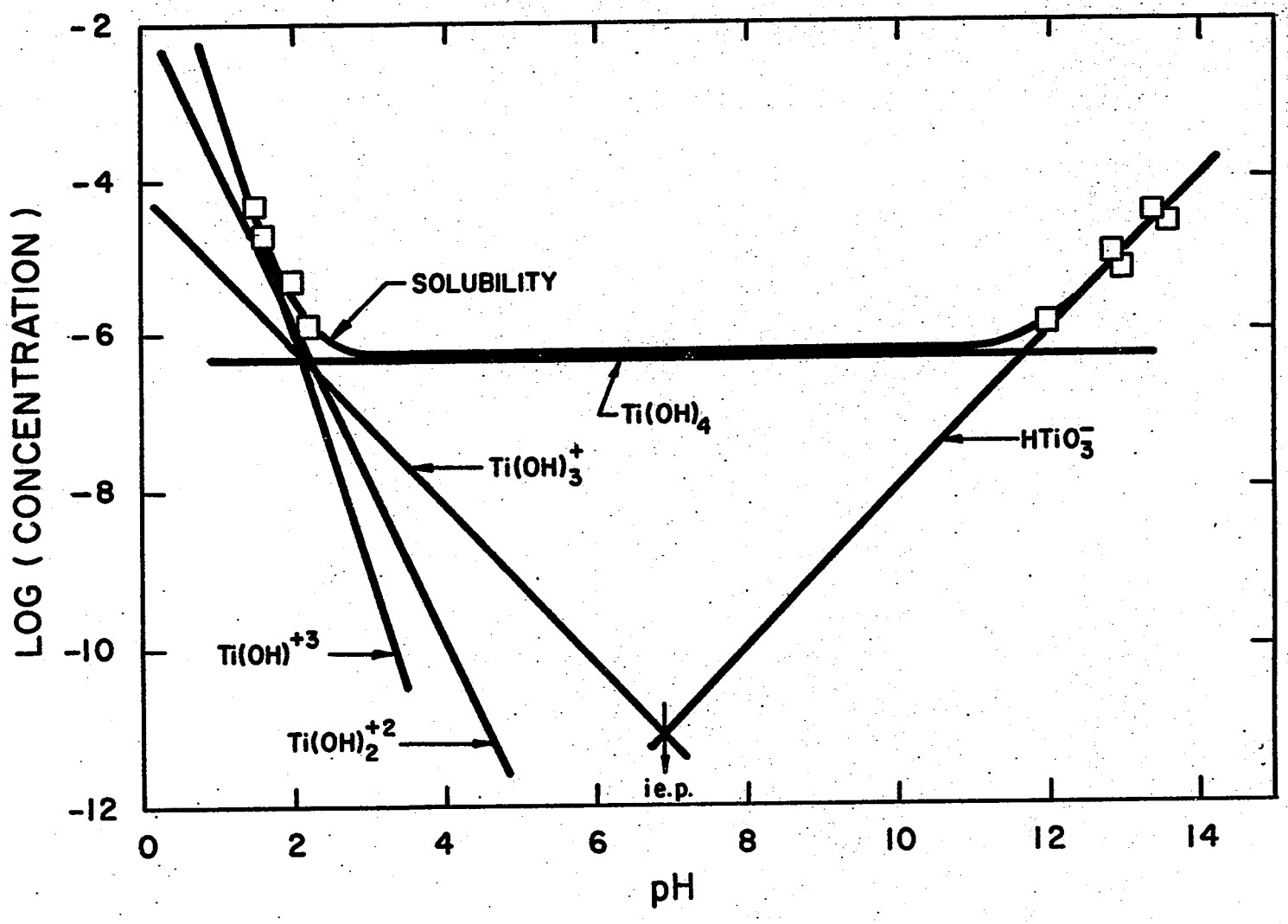
LOG (CONCENTRATION)
-2
-4
-6
-8
-10
-12
0
2
4
6
8
10
12
14
pH
SOLUBILITY
Ti(OH)4
Ti(OH)3+
HTiO3-
Ti(OH)+3
Ti(OH)2+2
i.e.p.

TABLE XIX

CONCENTRATION OF COMPLEX TITANIUM IONS IN SOLUTION

pH	0	2	4	6	12	14	16
Ti^{+4}	-	-	-	-	-	-	-
$Ti(OH)^{+3}$	0.0	-6.0	-12.0	-18.0	-	-	-
$Ti(OH)_2^{+2}$	-1.8	-5.8	-9.8	-13.8	-	-	-
$Ti(OH)_3^{+}$	-4.8	-6.2	-8.2	-10.2	-16.3	-18.3	-
$Ti(OH)_4$	-6.3	-6.3	-6.3	-6.3	-6.3	-6.3	-6.3
$HTiO_3^{-}$	-18.0	-16.0	-14.0	-12.0	-6.0	-4.0	-2.0

Concentrations are expressed in $\log_{10}$(moles/l.)

2) Baddeleyite.

No solubility data are available concerning the metallic cation zirconium. The following free energy data together with the equilibrium constants listed in Table XVII are used to calculate the ionic concentrations in Table VIII.

Concentration of $Zr(OH)_4$ (aq.) = 1.95×10^{-9} moles/l. (119)

ΔG_f^o $(Zr(OH)_4)$ = -370 kcal./gm.mole (120)

ΔG_f^o (ZrO_2) = -247.7 kcal./gm.mole (121)

ΔG_f^o (Zr^{+4}) = -141.0 kcal./gm.mole (120)

ΔG_f^o (H_2O) = -56.72kcal./gm.mole (121)

From this data, it is established that the zirconia surface is completely hydrated and the stable solid phase in solution is zirconium hydroxide. The maximum activity of zirconium dioxide in this phase is 3.5×10^{-7} . A sample calculation of the ionic concentration is given below:-

$$[Zr(OH)_3^+] = \frac{[Zr(OH)_4][H^+]}{{}^*K_4}$$

$$= \frac{1.95 \times 10^{-9}}{10^{-1.17}} [H^+]$$

$$= 10^{-7.54} \times (-\text{antilog}(pH))$$

$$\log [Zr(OH)_3^+] = -7.54 - pH$$

Table XX shows the actual concentrations at each pH. The diagram for the iso-electric-point determination is drawn in Figure 46. The iso-electric-point is found to be at a pH of 5.27 ± 0.1.

TABLE XX

CONCENTRATION OF COMPLEX ZIRCONIUM IONS IN SOLUTION

pH	0	2	4	6	12	14	16
Zr^{+4}	-5.65	-13.65	-	-	-	-	-
$Zr(OH)^{+3}$	-5.87	-11.87	-17.87	-	-	-	-
$Zr(OH)_2^{+2}$	-6.49	-10.49	-14.49	-18.49	-	-	-
$Zr(OH)_3^{+}$	-7.54	-9.54	-11.54	-13.54	-	-	-
$Zr(OH)_4$	-8.71	-8.71	-8.71	-8.71	-8.71	-8.71	-8.71
$Zr(OH)_5^{-}$	-17.99	-15.99	-13.99	-11.99	-5.99	-3.99	-1.99
$Zr(OH)_6^{-2}$	-	-	-	-	-8.78	-4.78	-0.78

Concentrations are expressed in $\log_{10}$(moles/l.)

3) Hematite

Of the oxides and hydroxides of ferric iron, α-hematite is the most stable in dry systems and goethite, α-FeOOH, is the most stable in aqueous systems at temperatures less than 100 deg.C. Ferric oxide is amphoteric (120). Equilibrium constants for the formation of positive hydroxo complexes have been given by Latimer (120), Gayer and Woontner (122), Hedstrom (123), Biederman and Schindler (124),

FIGURE 46

ISO-ELECTRIC-POINT OF BADDELEYITE

☐ - Experimental Solubility Points

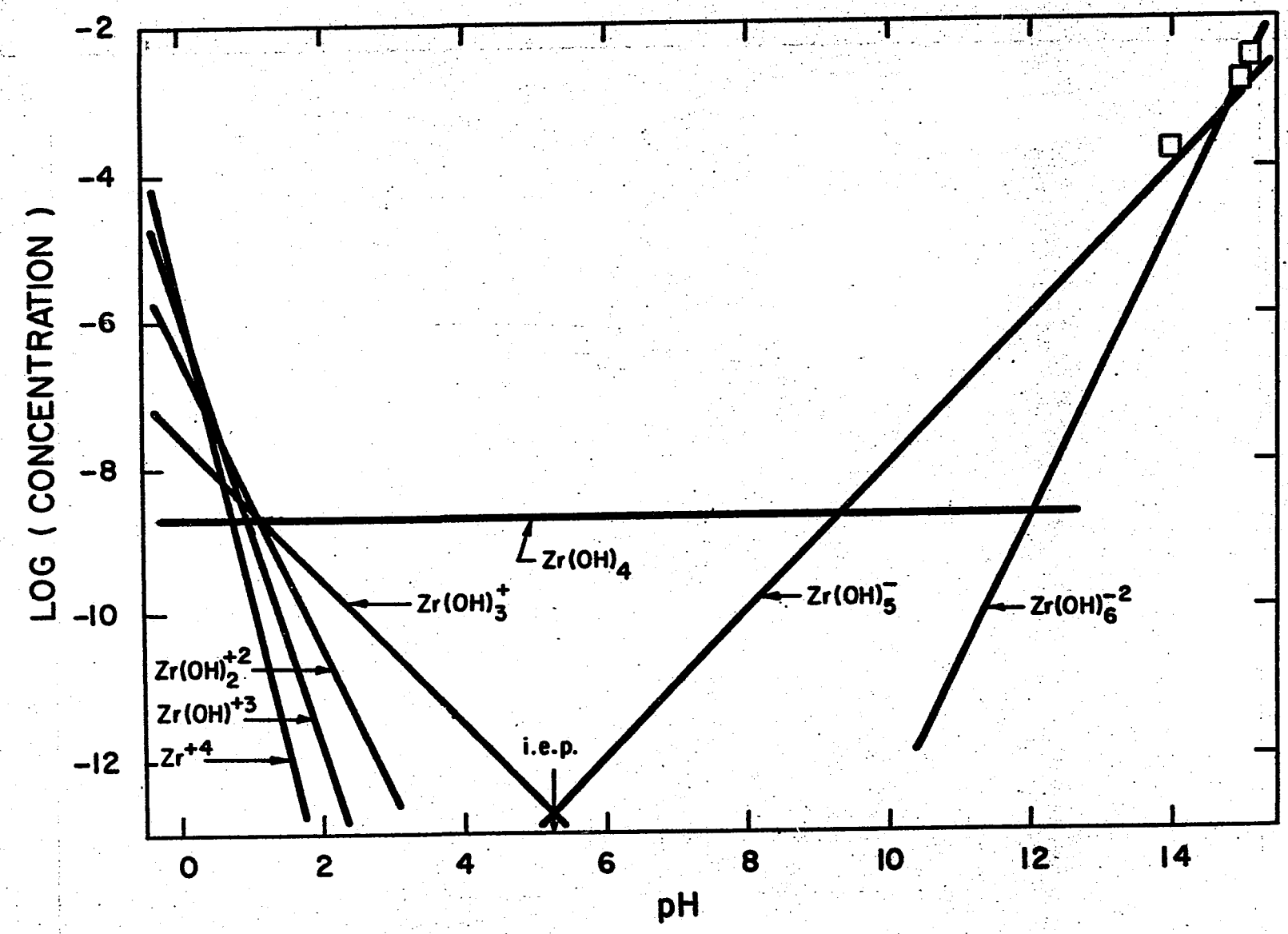
LOG (CONCENTRATION)
-2
-4
-6
-8
-10
-12
0
2
4
6
8
10
12
14
pH
$Zr(OH)_4$
$Zr(OH)_3^+$
$Zr(OH)_5^-$
$Zr(OH)_6^{-2}$
$Zr(OH)_2^{+2}$
$Zr(OH)^{+3}$
Zr^{+4}
i.e.p.

Milburn (125), and Lamb and Jacques (126). Constants for the negative hydroxo complexes have been determined by Lengweiler, Buser, and Feitnecht (127) using radioactive iron (Fe^{59}). This data has been combined by Parks (33,99), but his two diagrams do not agree with each other. The data considered correct by this author, reproduced in Table XXI and in Figure 47, is similar to that of Parks (33). The iso-electric-point is found to be at a pH of 8.5 ± 0.1. Table XXI indicates the equilibrium concentration in contact with solid hematite (α-Fe_2O_3).

TABLE XXI

CONCENTRATION OF COMPLEX FERRIC IONS IN SOLUTION

pH	0	2	4	6	12	14	16
$Fe_2(OH)_2^{+4}$	-4.31	-12.31	-	-	-	-	-
Fe^{+3}	-0.73	-6.73	-12.73	-18.73	-	-	-
$Fe(OH)^{+2}$	-2.90	-6.90	-10.90	-14.90	-	-	-
$Fe(OH)_2^{+}$	-7.60	-9.60	-11.60	-13.60	-	-	-
$Fe(OH)_3$	-6.54	-6.54	-6.54	-6.54	-6.54	-6.54	-6.54
$Fe(OH)_4^{-}$ or FeO_2^{-}	-	-	-	-18.6	-12.6	-10.6	-8.6

Concentrations are expressed in $\log_{10}$(moles/1.)

FIGURE 47

ISO-ELECTRIC-POINT OF HEMATITE

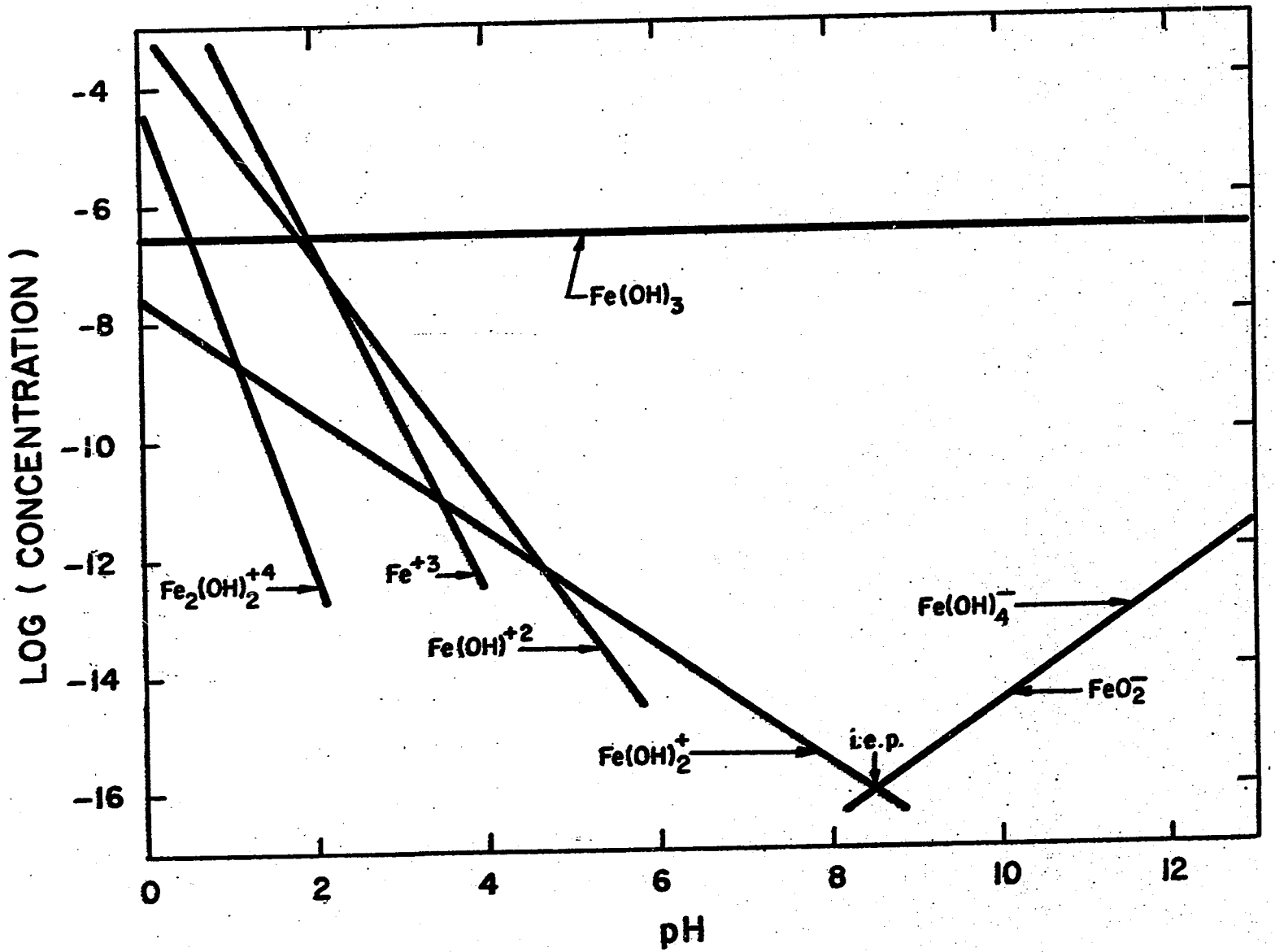
LOG (CONCENTRATION)
-4
-6
-8
-10
-12
-14
-16
0
2
4
6
8
10
12
pH
$Fe(OH)_3$
$Fe_2(OH)_2^{+4}$
Fe^{+3}
$Fe(OH)^{+2}$
$Fe(OH)_2^{+}$
i.e.p.
$Fe(OH)_4^{-}$
FeO_2^{-}

4) Quartz

The iso-electric-point of quartz is not determinable by this method, due to the lack of data for the positive complexes. It appears that data will not be forthcoming in the near future since, even in concentrated acid, the solubility will be far less than for undissociated $Si(OH)_4$ (aq.). A partial table of concentrations (Table XXII) and diagram (Figure 48) illustrate this point. The dotted line is a probable location of the concentration of $Si(OH)_3^+$ line.

The solubility of amorphous silica in water has been determined by Alexander, Heston, and Iler (129) as indicated in Figure 48 by the □ symbols. The solubility of silica dust in water by Brown et al (117) does not agree with the above data. The data indicate a sharp solubility minimum in the range of pH of 2.2 to 3.0 (as indicated by the ◯ symbols) suggesting that the iso-electric-point is in this range. Brown et al state that the high solubility of quartz is due to a highly soluble disturbed surface layer. In concluding, it may be said that the thermodynamic data for quartz-silica-water system is not complete and that the iso-electric-point can only be determined experimentally in each case.

FIGURE 48

ISO-ELECTRIC-POINT OF QUARTZ

○ - Solubility (117)

□ - Solubility (129)

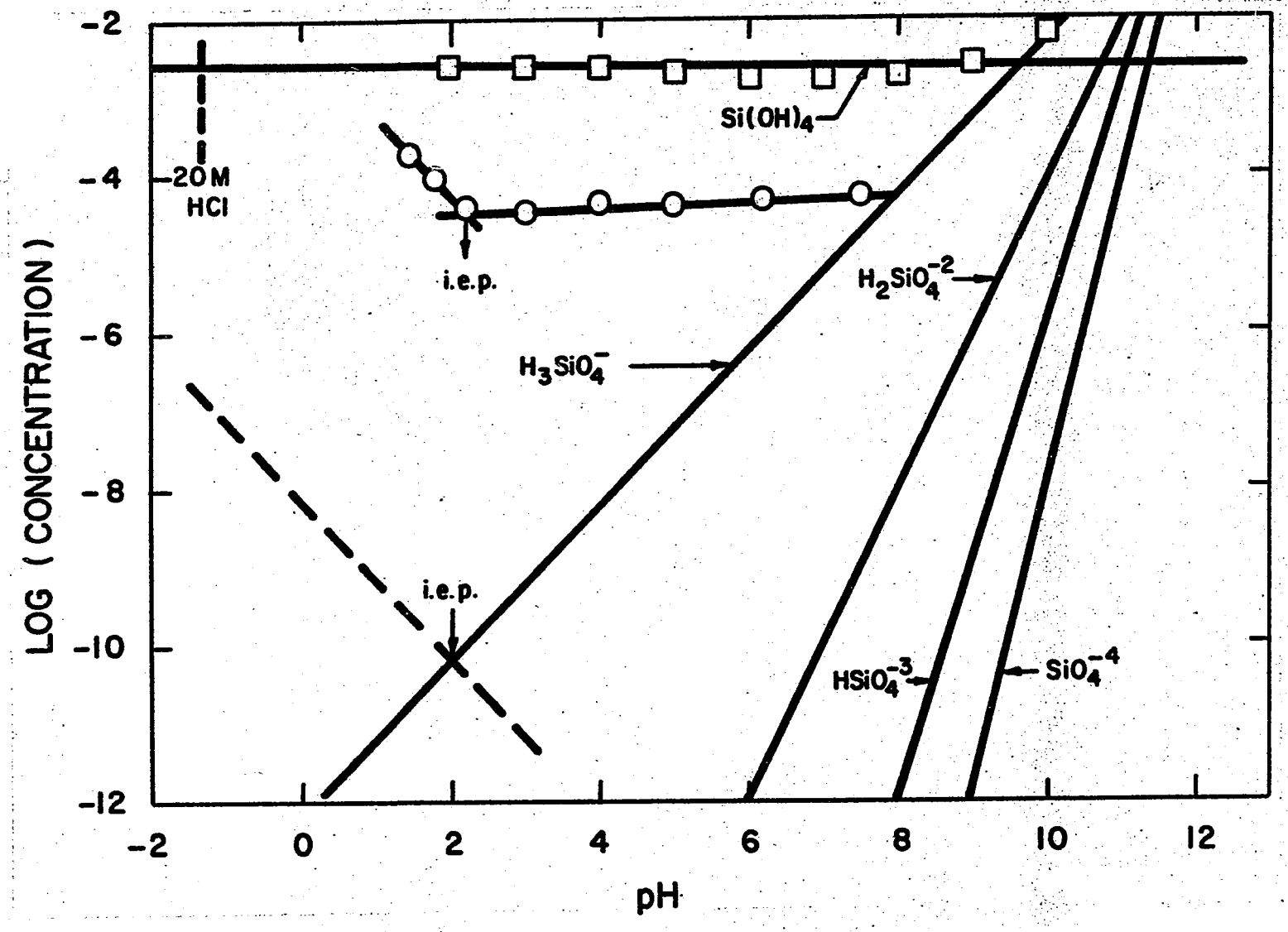
LOG (CONCENTRATION)
pH
-2
-4
-6
-8
-10
-12
-2
0
2
4
6
8
10
12
20 M
HCl
i.e.p.
i.e.p.
Si(OH)4
H3SiO4-
H2SiO4-2
HSiO4-3
SiO4-4

TABLE XXII

CONCENTRATION OF COMPLEX SILICON IONS IN SOLUTION

pH	0	2	4	6	10	12	14
$Si(OH)_4$	-2.60	-2.60	-2.60	-2.60	-2.60	-2.60	-2.60
$H_3SiO_4^-$	-12.26	-10.26	-8.26	-6.26	-2.26	-0.26	+1.74
$H_2SiO_4^{-2}$	-	-	-15.96	-11.96	-3.96	+0.04	+4.04
$HSiO_4^{-3}$	-	-	-	-17.96	-5.96	+0.04	+6.04
SiO_4^{-4}	-	-	-	-	-7.96	+0.04	+8.04

Concentrations are expressed in $\log_{10}$(moles/l.)

The most important feature of these calculations for rutile, baddeleyite, and hematite is the fact that the iso-electric-point of the complex solutions agree so well with the measured zero-point-of-charge. (Rutile -0.3 pH units, baddeleyite -0.8 pH units, hematite -0.2 pH units).

Floatability

In the concentration range 10 to 1000 μmoles/l., a maximum recovery is reached. At higher concentrations, the recovery decreases. Qualitatively, the decrease in recovery coincides with a decrease in the work of adhesion and with the completion of adsorption on the surface. The tests in acidic and basic media confirm the predictions of the adsorption data which indicate a sharp decrease in floatability in acidic media and a slight increase in basic solutions.

Tests on quartz-hematite mixtures indicate that, although floatability is high, the selectivity is poor in neutral solutions. The use of modifiers is required as indicated by the last series of tests. The use of a pH modifier (1 N potassium hydroxide) and a hematite depresent (starch) changes the flotation results considerably. The soluble starch, probably in straight chains (amylose), was of the following structure:-

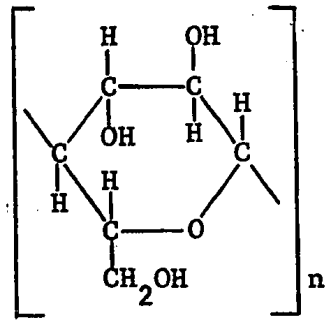

It is suggested that the hydrogen ions of many of the acetal ends are easily removed thus the hydrocarbon radical tends to be negatively charged in solution. The radical would be attracted to the less negatively

charged surface of hematite in preference to the highly charged negative surface of quartz. The large number of OH^- groups in the starch would tend to render the surface hydrophilic even in the presence of amines. Further work is necessary to clarify this point.

Surface Free Energy

Applying Gibb's adsorption equation to systemsat constant temperature, pressure, and ionic strength, it can be shown that

$$d\gamma = - \sum_i \Gamma_i \, d\mu_i$$

$$= - F(\Gamma_{H^+} - \Gamma_{OH^-})\mu_{K^+},\mu_{Cl^-} \, dE \qquad (67)$$

where $\mu_i = 2.3RT \log a_i$

By combining these equations,

$$d\gamma = - 2.3RT(\Gamma_{H^+} - \Gamma_{OH^-}) \, d(\log a_{H^+})$$

$$= 2.3RT \, (\Gamma_{H^+} - \Gamma_{OH^-}) \, d(pH) \qquad (68)$$

where γ is the surface free energy (or interfacial energy) of the solid-liquid interface in ergs/cm.^{2}

By integration of the above equation, the change in surface free energy from that at the zero-point-of-charge may be expressed as

$$\gamma - \gamma_o = 2.3RT \int_{pH=zpc}^{pH} (\Gamma_{H^+} - \Gamma_{OH^-}) d(pH) \qquad (69)$$

where γ_o is the surface free energy at the zero-point-of-charge in ergs/cm.^{2} The graphical integration of the adsorption density vs. pH curves (Figures 32 to 34) will yield the decrease in surface free energy as a function of pH. Since there is no direct or indirect method for the determination of the surface free energy of solid surfaces,

only the change in surface free energy may be calculated as shown in Figures 49 to 51 for hematite, rutile, and baddeleyite. These results are tabulated in Table LX of Appendix VIII.

Applying Gibbs-Duhem and Gibb's adsorption equations to the results obtained with dehydroabietylamine acetate at constant temperature and pressure, the change in surface free energy may be expressed by the relation :-

$$d\gamma = -\Gamma_{RNH_3^+}\, d\mu_{RNH_3^+} - \Gamma_{OAc^-}\, d\mu_{OAc^-} - \Gamma_{H_2O}\, d\mu_{H_2O}$$

But $$n_{RNH_3^+}\, d\mu_{RNH_3^+} + n_{OAc^-}\, d\mu_{OAc} + n_{H_2O}\, d\mu_{H_2O} = 0$$

and $$n_{RNH_3^+} = n_{OAc^-} \; ; \quad d\mu_{RNH_3^+} = d\mu_{OAc^-}$$

therefore $$d\gamma = -\{\Gamma_{RNH_3^+} + \Gamma_{OAc^-} - \Gamma_{H_2O}\left(\frac{2n_{RNH_3^+}}{n_{H_2O}}\right)\}\, d\mu_{RNH_3^+}$$

where $\Gamma_{RNH_3^+}$, Γ_{OAc^-}, Γ_{H_2O} refer to the adsorption density of dehydroabietylaminium ion, acetate ion, and water respectively at the solid-liquid interface, and $n_{RNH_3^+}$, n_{OAc^-}, and n_{H_2O} are the number of moles of dehydroabietylaminium ions, acetate ions and water molecules in a unit of solution. Adopting the Gibb's convention of defining adsorption density by writing

$$\Gamma_{H_2O} = 0$$

and, by assuming that the adsorption density of acetate ion is negligible (99),

$$\Gamma_{OAc^-} \simeq 0$$

FIGURE 49

DECREASE IN SURFACE FREE ENERGY OF HEMATITE VS. pH

○ - 10^{-4} N KCl

□ - 10^{-3} N KCl

△ - 10^{-2} N KCl

▽ - 10^{-1} N KCl

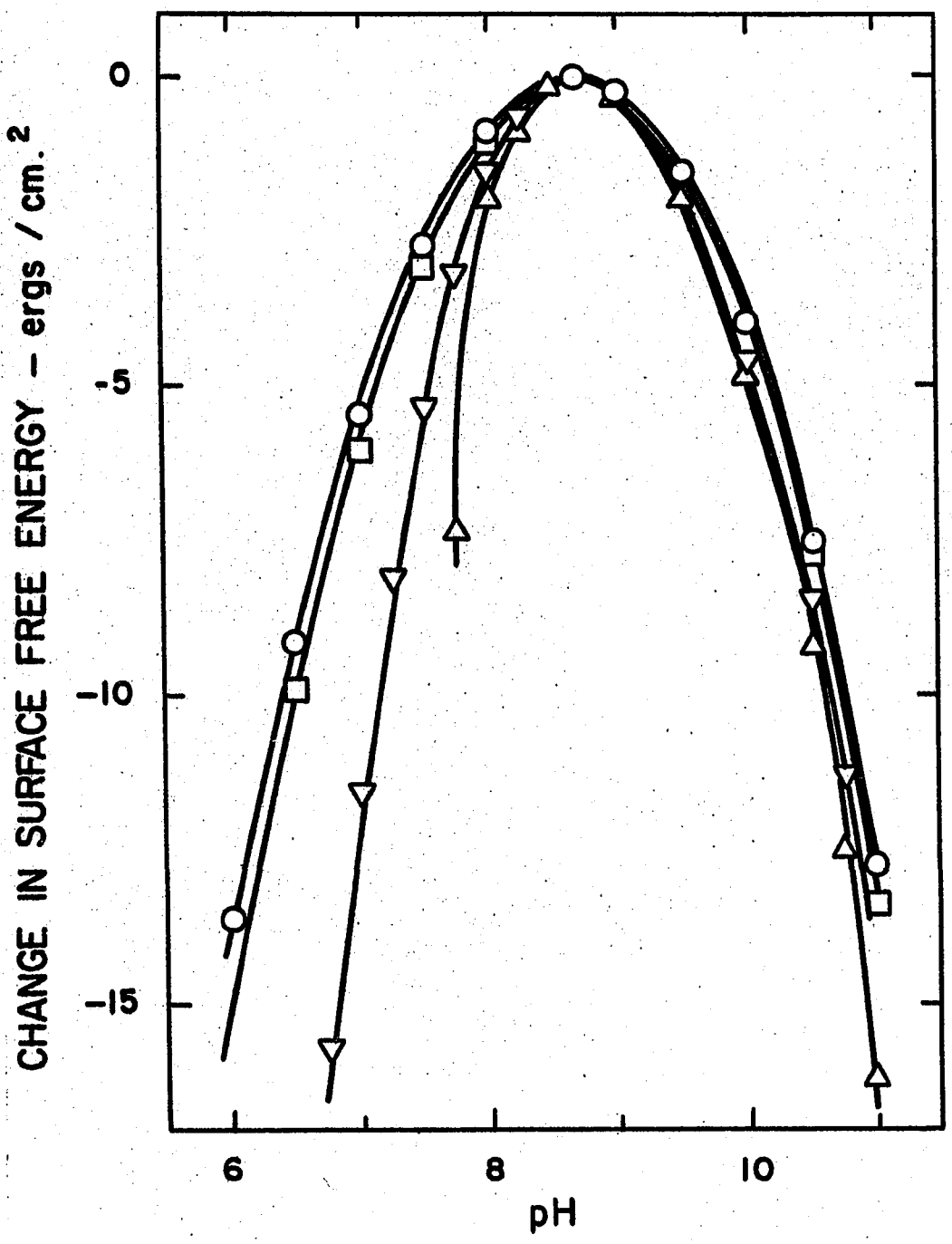
CHANGE IN SURFACE FREE ENERGY – ergs / cm.²
0
-5
-10
-15
6
8
10
pH

FIGURE 50

DECREASE IN SURFACE FREE ENERGY OF RUTILE VS. pH

□ - 10^{-3} N KCl

△ - 10^{-2} N KCl

▽ - 10^{-1} N KCl

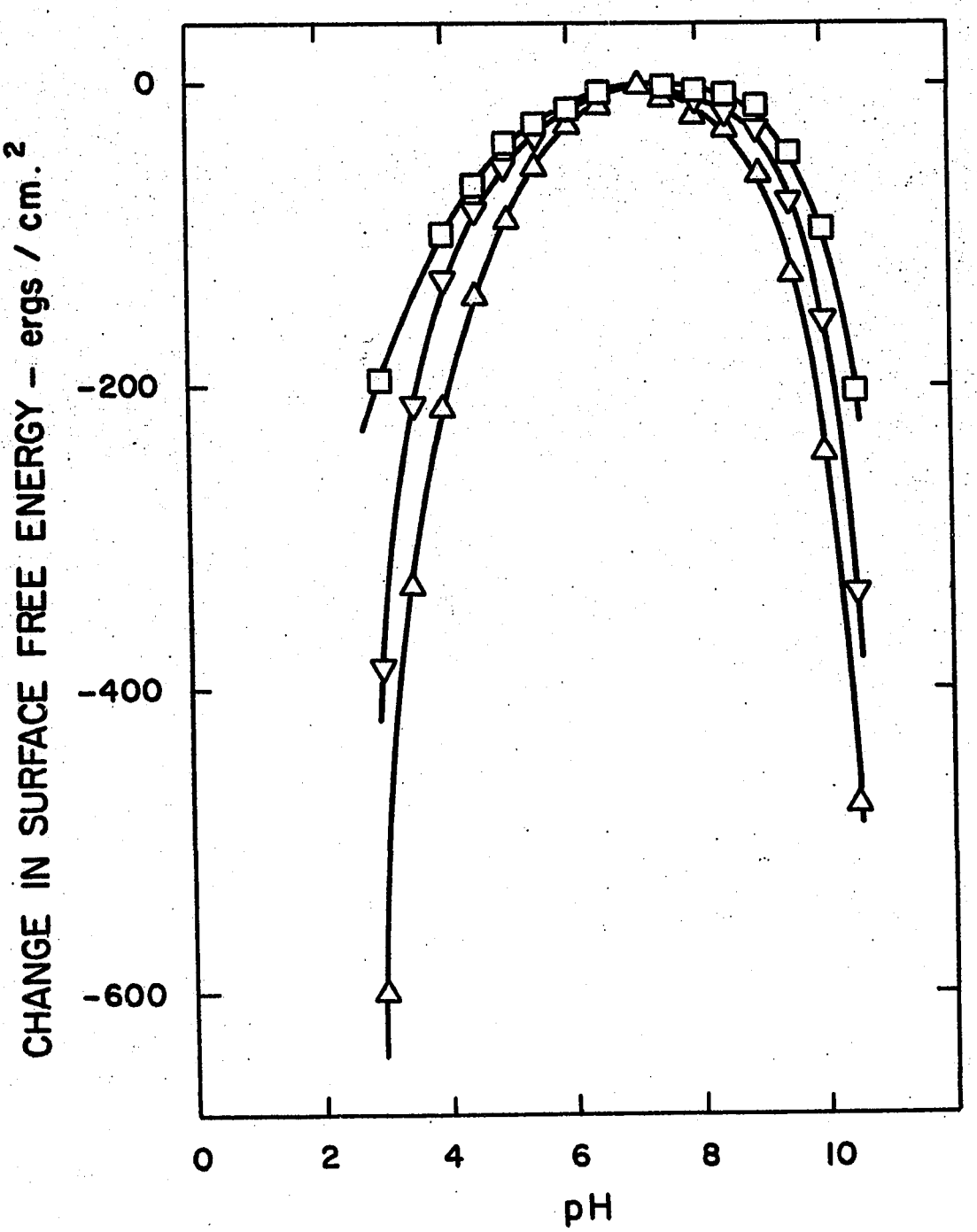
CHANGE IN SURFACE FREE ENERGY – ergs / cm.²
0
-200
-400
-600
0
2
4
6
8
10
pH

FIGURE 51

DECREASE IN SURFACE FREE ENERGY OF BADDELEYITE VS. pH

□ - 10^{-3} N KCl

△ - 10^{-2} N KCl

▽ - 10^{-1} N KCl

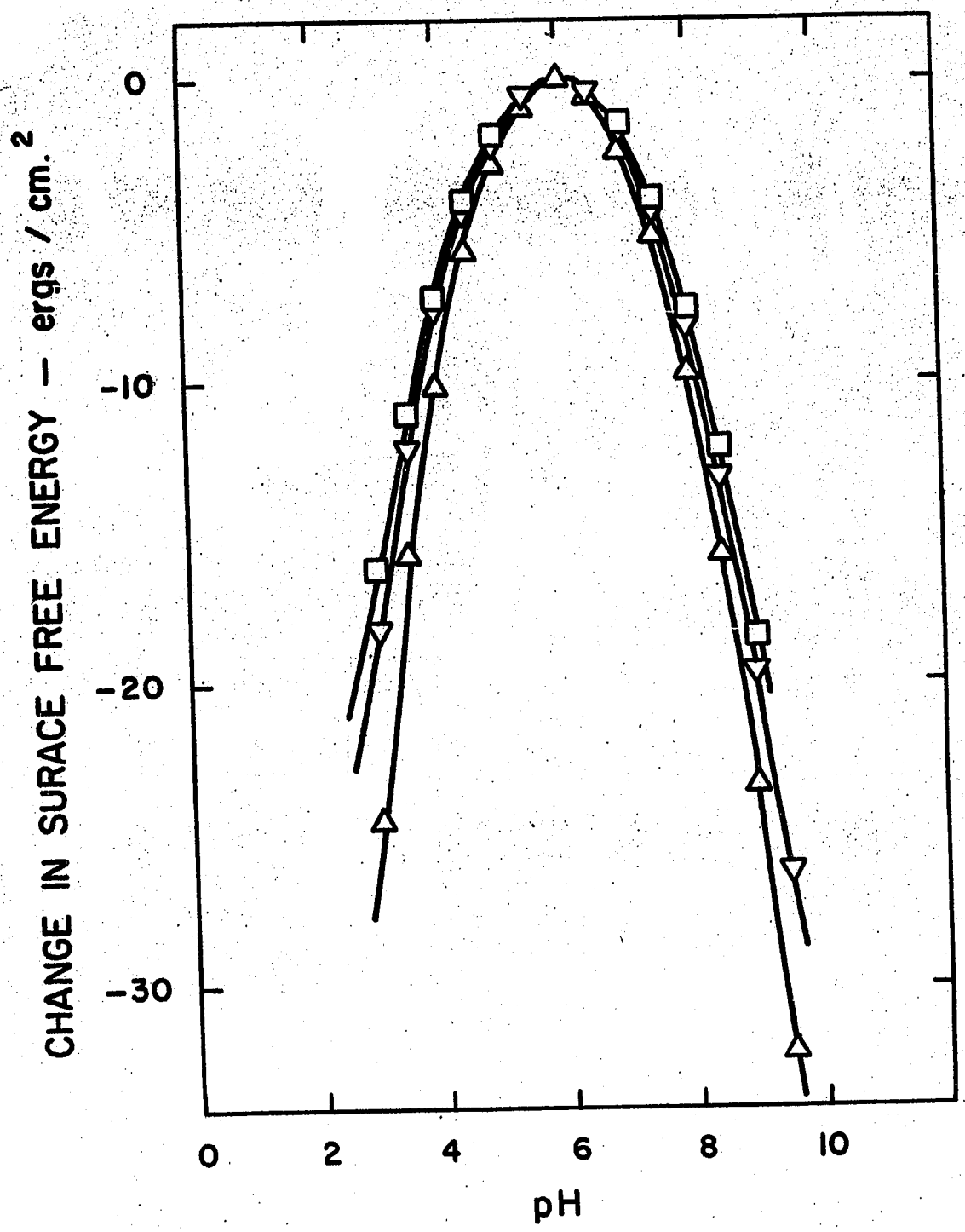
CHANGE IN SURACE FREE ENERGY — ergs / cm.²
0
-10
-20
-30
0
2
4
6
8
10
pH

the equation reduces to the simple expression

$$d\gamma = -\Gamma_{RNH_3^+} d\mu_{RNH_3^+} \tag{70}$$

where $\Gamma_{RNH_3^+}$ now refers to the adsorption density of the aminium ion relative to that of water which by convention is assumed zero. Since the concentrations used in this investigation are low, the activity $(a_{RNH_3^+})$ in solution may be replaced by the concentration $(C_{RNH_3^+})$. Integrating equation (70):-

$$\gamma - \gamma_o = -\int_o^a (2.3RT\,\Gamma_{RNH_3^+})d(\log a_{RNH_3^+})$$

$$= -2.3RT\int_o^C (\Gamma_{RNH_3^+})d(\log C_{RNH_3^+}) \tag{71}$$

where γ_o is the surface free energy of the solid-liquid interface in the absence of the collector (aminium ions). $\Gamma_{RNH_3^+}$ may be related to the concentration by the adsorption equation

$$\Gamma_{RNH_3^+} = kC^n_{RNH_3^+} \quad .$$

The decrease in surface free energy is simplified and integrated as follows:-

$$\gamma - \gamma_o = -2.3RT\int_o^C kC^n_{RNH_3^+}\left(\frac{d(C_{RNH_3^+})}{2.3C_{RNH_3^+}}\right)$$

$$= -\frac{RTk}{n}\,C^n_{RNH_3^+} \tag{72}$$

The decrease in surface free energy as a function of concentration of amine for hematite, rutile, quartz, and baddeleyite is shown in Figure 52. Results are tabulated in Table LXI of Appendix VIII. The change in surface free energy as a function of the adsorption density is recorded in Figure 53.

The change in surface free energy of the hematite-liquid surface per unit pH is between 1.5 and 6.0 ergs/cm.^{2} near the zero-point-of-charge, depending on the ionic strength, which is similar to the range of 1.0 to 2.5 ergs/cm.^{2} reported by Parks (99). These results also compare favourably with those using a silver sulphide-liquid surface (i.e. 0.5 to 1.5 ergs/cm.^{2} (133,134)).

FIGURE 52

DECREASE IN SURFACE FREE ENERGY AS A

FUNCTION OF AMINE CONCENTRATION

○ - Quartz

□ - Hematite

△ - Rutile

▽ - Baddeleyite

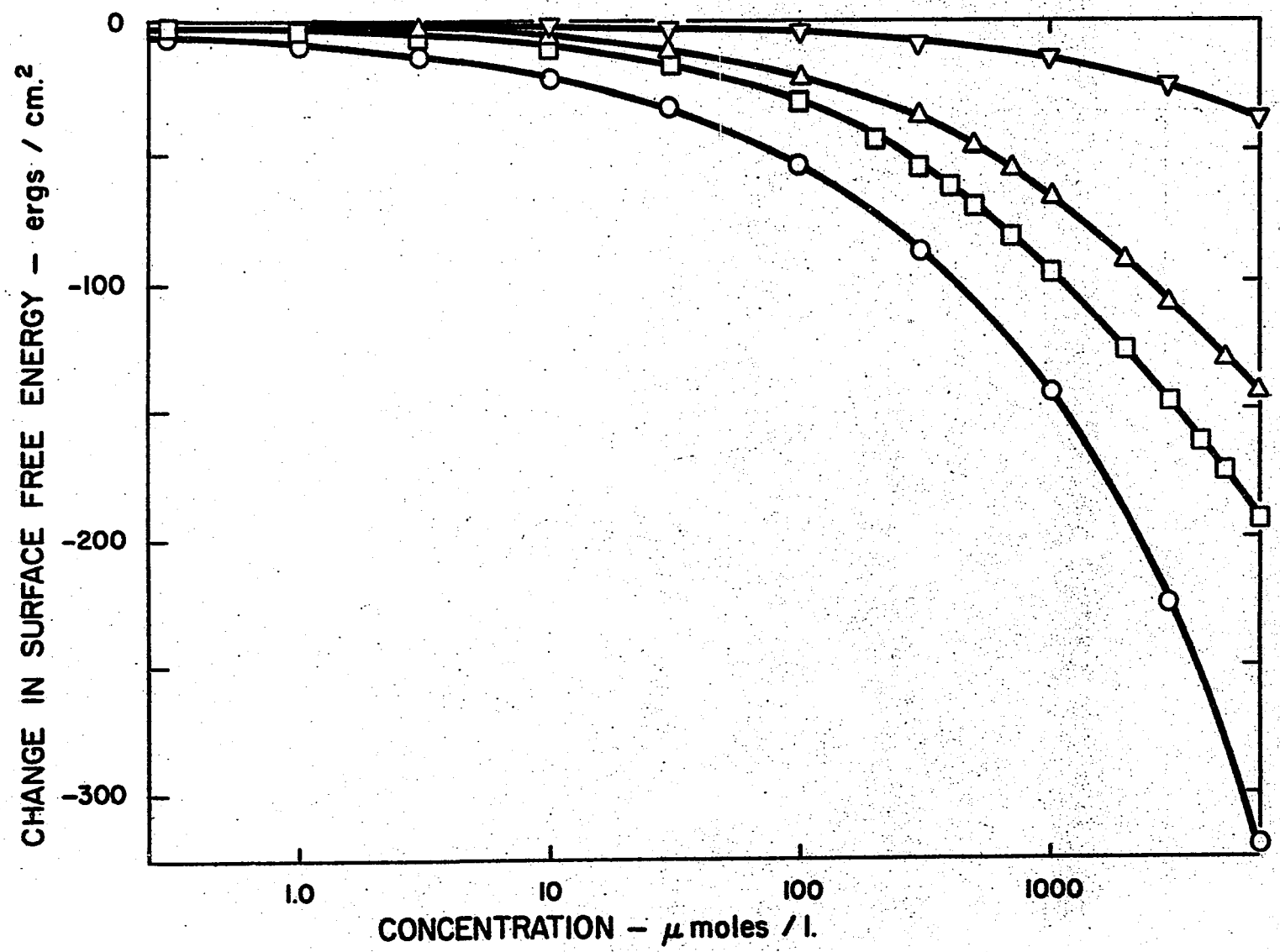
0
-100
-200
-300
CHANGE IN SURFACE FREE ENERGY – ergs / cm.²
1.0
10
100
1000
CONCENTRATION – μ moles / l.

FIGURE 53

DECREASE IN SURFACE FREE ENERGY AS A FUNCTION OF SPECIFIC ADSORPTION

○ - Quartz

□ - Hematite

△ - Rutile

▽ - Baddeleyite

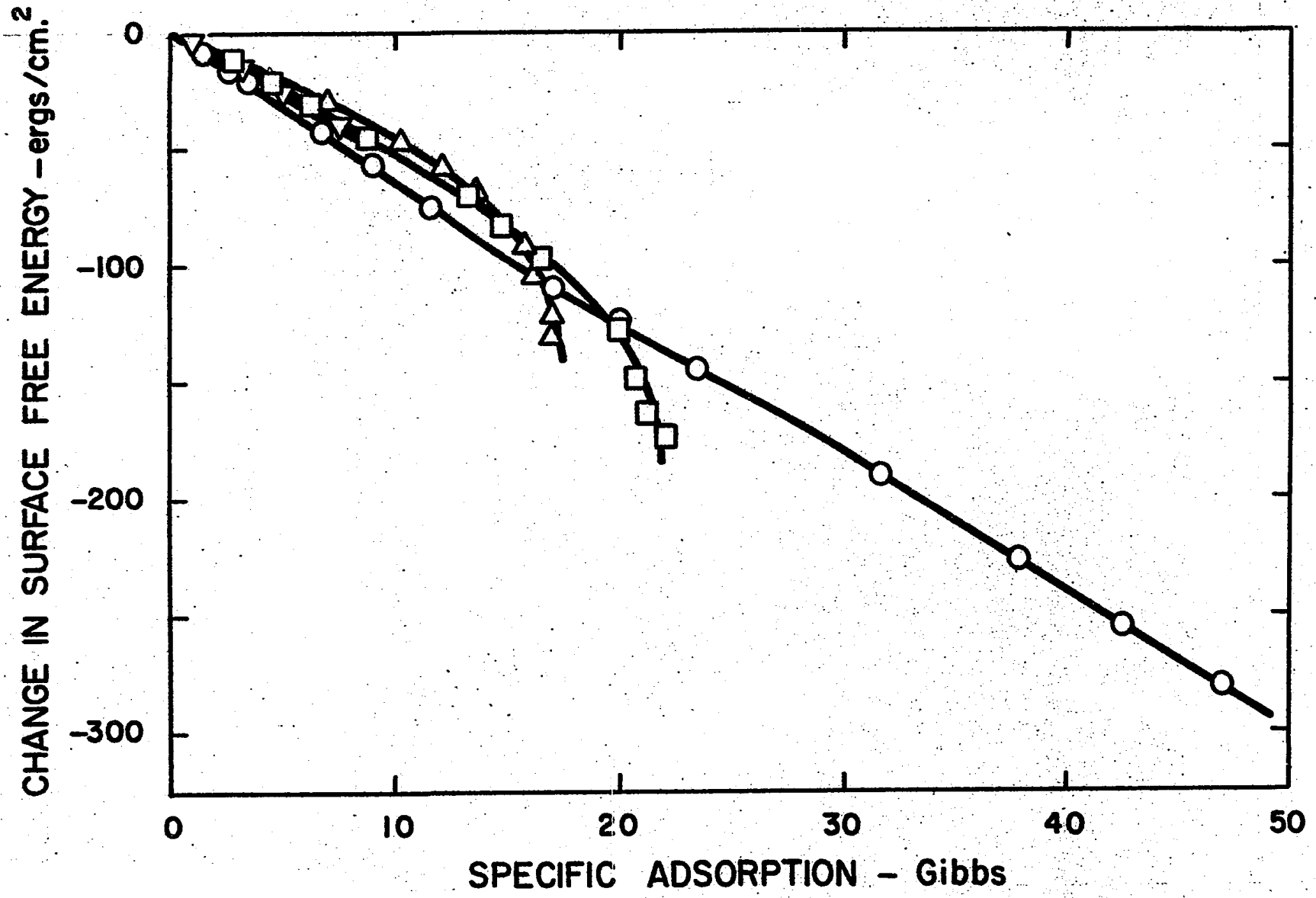
CHANGE IN SURFACE FREE ENERGY – ergs/cm.²
0
-100
-200
-300
0
10
20
30
40
50
SPECIFIC ADSORPTION – Gibbs

Proposed Mechanism and Discussion

The adsorption isotherms obtained in this investigation indicate that the weight of dehydroabietylamine adsorbed per unit surface of mineral is proportional to the square root of the concentration of dehydroabietylamine in solution. In the case of oxide minerals, it is accepted that the hydrogen and hydroxyl ions are the potential determining ions (31,32,33,63). At constant pH, ψ_o is constant, and the charge density in the diffuse layer may be written as

$$\sigma_d = A\sqrt{n}$$

where

$$A = \sqrt{\frac{2DkT}{\pi}} \sinh\left(\frac{ze\psi_o}{akT}\right) \tag{73}$$

Since the amine salt is the only electrolyte added to the solution and is almost completely ionized in the vicinity of pH = 6, Eq. (73) can be replaced by Eq. (74) which relates the charge per unit area of the diffuse layer, σ_d, to the concentration of amine salt, C

$$\Gamma_{RNH_3^+} = \sigma_d = A\sqrt{C} \tag{74}$$

When the minerals are placed in solution, the double layer is developed by hydrolysis and dissociation (32,34). The mineral surface may be considered as being made up of three groups of atoms and ions in varying proportions. The three groups may be schematically represented by

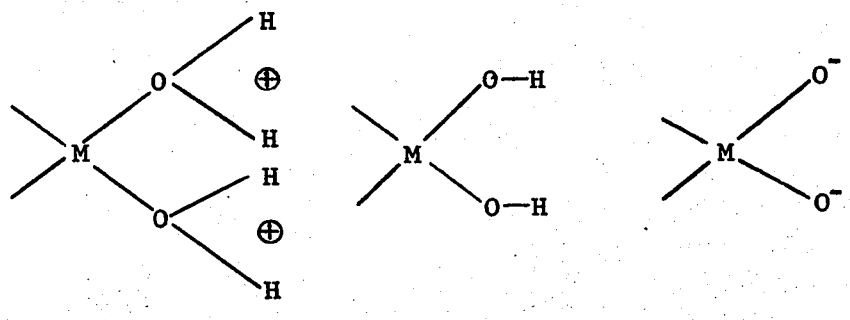

The adsorption of the heteropolar organic compound on the mineral surface occurs by a reaction involving the double layer. Since the adsorption may be expressed in terms of the charge of the diffuse layer, the dehydroabietylamine ions may be said to be adsorbing in the diffuse double layer.

The effect of the zero-point-of-charge on the quantity of amine adsorbed appears to be minimal. The quartz specimens adsorb the largest amount of amine and have the most negative surface. However, hematite has a strongly positive surface and adsorbs the second largest amount of amine. This may be explained by assuming that the aminium ion may replace hydrogen ions in the diffuse double layer, or replace the hydrogen ion of the hydroxyl group in either the diffuse or the Stern layer as suggested by Gaudin (54). Thus, the quantity of amine adsorbed depends more on the nature of the mineral and the chemistry of the solutions than it does on the charge of the surface. The neutral oxides have the least charge and the least adsorption on their surfaces.

At the zero-point-of-charge of each mineral with the exception of quartz, there is considerable adsorption on the mineral surface. This may be explained by the interaction of the aminium ions with hydrogen ions of the hydrated surface layer in the absence of a double layer. Thus, the interaction may be written as

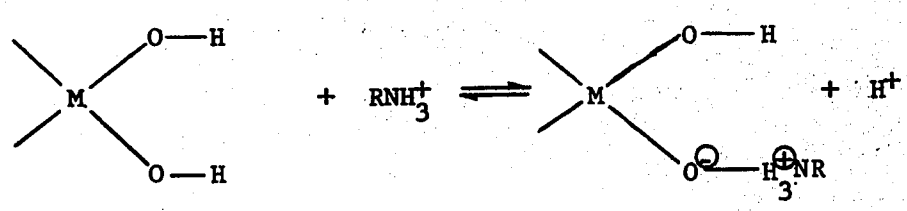

It is also possible that metal-amine complexes are formed similar to those suggested by Arbiter, Kellogg, and Taggart (130). However, since no evidence of the existance of oxide-amine compounds has been reported, it is not likely that these compounds are involved. The possibility of the adsorption of undissociated amine such as that favoured by Cook (131) is feasible but does not satisfactorily explain the dependance of adsorption on the square root of the bulk concentration.

If the surface is positively charged, such as the hematite surface in this investigation, there are several possible methods by which adsorption may take place.

1. Aminium ions may specifically adsorb on the hydrated inner layer (Stern layer) in exchange for hydrogen ions, shown schematically as

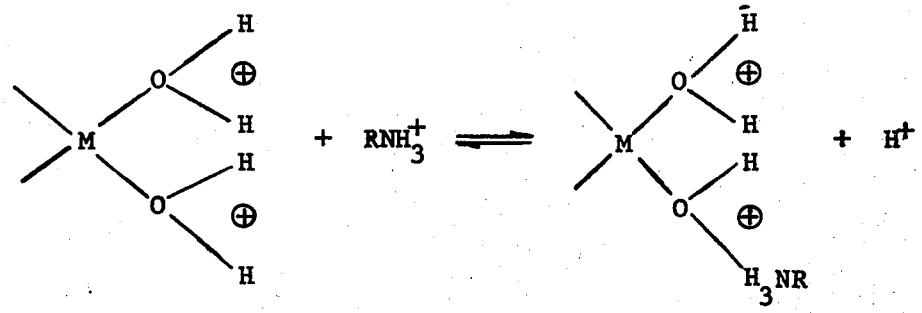

2. Aminium ions may react with hydroxyl ions in the diffuse double layer to form oxyamine compounds such as:

$$OH^- + RNH_3^+ \rightleftharpoons OH_3NR^- + H^+$$

3. Aminium ions may exchange with the remaining hydrogen ions (concentration of hydrogen ions is less than that of hydroxyl ions) in the diffuse double layer, which may be represented as

$$H^+ \text{ (diffuse layer)} + RNH_3^+\text{(bulk)} \rightleftharpoons RNH_3^+\text{(diffuse layer)} + H^+\text{(bulk)}$$

4. Undissociated amine molecules may adsorb specifically in the Stern layer.

When the surface is negatively charged, such as the quartz surface in this study, the same reactions may be used to explain the adsorption.

1. Aminium ions may adsorb on the negative surface thus reducing the net negative charge

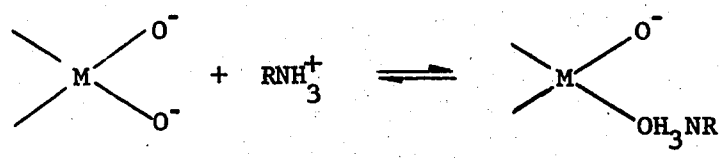

2. Aminium ions may exchange with the hydrogen ions in the diffuse layer which are present in excess of hydroxyl ions.

3. Aminium ions may react with hydroxyl ions of the diffuse layer even though the concentration is less than the hydrogen ion concentration.

4. Undissociated amine may adsorb specifically in the Stern layer.

All the methods are equivalent in that they represent merely different paths to the same end product:- the adsorption of the amine group without the desorption of metallic ions into the solution. The first three represent a release of hydrogen ions into the bulk solution from the interface whereas the fourth one involves no hydrogen ions. Qualitatively, a small pH decrease was noticed during the adsorption tests.

DeBruyn has discussed the effect of amine concentration on pH of a solution (62) and has derived the following expression:-

$$\frac{m}{1 + \frac{K_w}{K_b[H^+]}} + [H^+] - \frac{K_w}{[H^+]} - \frac{m}{1 + \frac{[H^+]}{K_a}} = 0 \qquad (75)$$

where m is the total amine concentration, K_w is the ionization constant for water, K_b is the basic dissociation constant of the amine, and K_a is the acidic dissociation constant of acetic acid. The curve is sigmoidal in shape starting at pH = 7 for zero amine concentration, turning to higher pH values, and assymptotically approaching a pH of about 7.4 at high amine concentrations. In the present study, a qualitatively similar relationship was found in the pH range of 5.3 to 6.0. If the effect of other variables is the same on all samples a pH shift of this type is expected.

Adsorption according to the third mechanism is not likely to occur in practice, since the concentrations of hydroxyl and hydrogen ions in the double layer are not in excess of those in the bulk solution. The adsorption is most likely to occur by interaction with surface hydroxyl groups near the zero-point-of-charge; by interaction with the surface $-OH_2^+$ groups or OH^- ions in the diffuse double layer when the surface is positively charged; and by interaction with surface $-O^-$ groups or H^+ ions in the diffuse double layer when the surface is negatively charged.

The deviation from the straight line relationship between adsorption and concentration at high total amine concentration may be explained in terms of Langmuir's concept of adsorption. When the first layer of ions adsorb on the surface by attraction to a negative site (i.e. an $-O^-$ surface site or space left vacant by a hydrogen ion), the tail of the hydrocarbon chain or group becomes

slightly electronegative and the amine head slightly more electropositive than the simple positive ion. Thus, by induction, more than one layer of amine ions may adsorb, especially if there is a large number of unsatisfied adsorption sites on the surface. Layers of ions continue to build up but the attractive forces become successively weaker as the number of layers increase and the adsorbed material becomes more loosely bound. Eventually, the capacity of the surface to hold amine ions is reached and further increases in concentration have no effect. As shown in the results, the deviation may be considered as a form of Langmuir's equation if the maximum adsorption, Γ_o, is considered not as a monolayer but as the maximum weight of amine that the surface can adsorb. The maximum coverage is in the order of 5 to 8 monolayers. If the length of the amine molecule is about 16 Å., the thickness of 5 to 8 monolayers is 80 to 128 Å., which is comparable to 77 Å. (99) and 97 Å. (30) found in similar systems.

CLAIMS TO ORIGINAL RESEARCH

1. Adsorption isotherms in natural solutions have been determined for dehydroabietylamine acetate on quartz, hematite, rutile, and baddeleyite.
2. The effect of pH on the adsorption of dehydroabietylamine acetate on quartz, hematite, rutile, and baddeleyite has been determined.
3. The surface tension and equivalent conductance of dehydroabietylamine acetate solutions have been determined in the range 0 to 2000 mg./l. Λ_o and l_c for dehydroabietylamine ion have been calculated. The ionization constant, K_b, has been determined to be 4.2×10^{-5} moles/l. The solubility of dehydroabietylamine (undissociated) has been found to be 4.0 mg. of amine acetate/l. or 1.16 μmoles/l.
4. The ion concentrations as a function of pH have been calculated for RNH_3^+, RNH_2(solution), and RNH_2(precipitated) where R is the dehydroabietyl radical.
5. The contact angles of the air-dehydroabietylamine solution-mineral oxide system for each of the four oxides studied have been determined as a function of amine concentration.
6. The work of adhesion for each of the above systems has been calculated.
7. The zero-point-of-charge of each of the four oxides under study has been determined. It is necessary to establish this point as there are wide variations in reported values in the literature.

8. Surface charge densities and differential capacities have been calculated for hematite, rutile, and baddeleyite as a function of hydrogen and hydroxyl ion adsorption.
9. Changes in surface free energy have been calculated for hydrogen and hydroxyl ion adsorption and for amine adsorption according to Gibb's equation.
10. Floatability tests in a Hallimond tube were conducted to correlate practical and theoretical aspects of flotation with dehydroabietylamine as a collector.

SUGGESTIONS FOR FUTURE WORK

1. In most mineral separation investigations associated with adsorption processes, information is lacking concerning the heats of adsorption. A better understanding of the mechanism involved might be obtained from heat of adsorption studies.
2. In the work reported in this thesis, the cross-sectional area of the amine molecule or ion was assumed to be 50 $Å^2$. Accurate determination of this value could be made from a study of the uni-molecular film behaviour on a surface balance. The effect of pH on the size of the ion or molecule (if any) should also be determined.
3. The accuracy of adsorption studies is dependant on the specific surface determinations. For any study of this type, B.E.T. surfaces should be compared with the results of liquid phase surface areas obtained by radiotracer or negative ion adsorption techniques.
4. To shorten the time of analysis and to measure small specific adsorptions (such as at low pH values), procedures to use radiotracers to determine quantities of collectors adsorbed should be established.
5. A scientific study of the effect of various starches used as a depressant for hematite on collector adsorption, contact angle, and floatability should be conducted. Also, adsorption isotherms for starches should be determined.

6. The critical micelle concentration of dehydroabietylamine should be determined. The effect of micelles on the adsorption and flotation characteristics should be investigated.
7. The effect of temperature is an important variable in adsorption processes. Due to its effect on many other variables, little work has been done to investigate the complex effect of this variable on collector adsorption.
8. More information concerning the attachment of ions to surfaces, the distribution and nature of adsorbing species is required.
9. Co-adsorption studies using cationic collectors and other inorganic cations should be undertaken to determine the effect of the other ions present in solution.

APPENDIX I

ANALYTICAL METHOD FOR THE DETERMINATION OF DEHYDROABIETYLAMINE ACETATE

In order to determine the adsorption of dehydroabietylamine acetate, a rapid and accurate method was required. Colorimetric determination, developed by Hercules Powders Inc., and used by Nemeth, was adopted with modifications as a suitable method for aqueous systems, containing from one to fifteen mg./l. of dehydroabietylamine acetate.

Chemistry of the Determination

The method is based on the formation of a yellow coloured salt in acidic aqueous solutions resulting from the reaction of the amine group of dehydroabietylamine or its salts with the acidic form of bromophenol blue. However, since bromophenol blue is an aqueous pH indicator, it forms a yellow complex with hydrogen ions below a pH of 3.8 which interferes with the determination. A portion of the amine complex, relatively insoluble in water, is extracted into chloroform from the mixture of complexes. It is recommended by the author that the sodium salt of bromophenol blue be used in place of bromophenol blue since the former is more soluble in water. Bromophenol blue solutions (0.04%) are supersaturated and the use of them may cause erratic results. Excess bromophenol blue is not soluble in chloroform and does not interfere with the analysis. The colour density of the chloroform extract is proportional to the amount of amine group present and can be measured visually, with photoelectric colormeters, or with spectrophotometers. Appropriate adjustment of sample

concentrations enables application of this determination to a wide range of amine concentrations. However, large dilution factors tend to decrease accuracy.

Procedure

Range	0 - 15 mg./l
Accuracy	± 0.03 mg./l.

Into a 125 ml. separatory funnel, pipet exactly 25 ml. of sample solution, 5 ml. of glacial acetic acid and 8 ml. of bromophenol blue solution (0.04% sodium salt of bromophenol blue). After mixing, allow solution to stand ten minutes. Pipet exactly 25 ml. of chemically pure chloroform into solution, mix gently for two minutes, and allow to stand for ten minutes (for equilibration between phases). Withdraw sufficient chloroform into 1-cm. spectrophotometer cells (3 ml.) and measure the absorbance immediately against distilled water using 0.11 mm. slit opening at a wavelength of 410mμ. For an accuracy of 3 per cent, all readings must be within 0.010 absorbance units and duplicate tests must be within 0.030 absorbance units.

A calibration curve is constructed from carefully prepared standards of 5,10,15 and 20 mg./l. dehydroabietylamine acetate. It was found that the 20 mg./l. standard did not obey Beer's law, hence the method is recommended up to 15 mg./l. only. The calibration curve is shown in Figure 54.

The bromophenol blue solution has a tendancy to vary its effectiveness. It has been reported by Nemeth (77) that fresh solutions must be made up daily as it decreases its effectiveness approximately ten percent per day. Experience in this investigation with the sodium salt of bromophenol blue has indicated a scatter rather than a decrease in its effectiveness. Temperature of the solutions is probably more important than time, but the effect can be corrected for when a standard and a blank are analysed with each lot of samples.

FIGURE 54

CALIBRATION CURVE FOR THE ANALYSIS OF

DEHYDROABIETYLAMINE ACETATE BY

SPECTROPHOTOMETRY

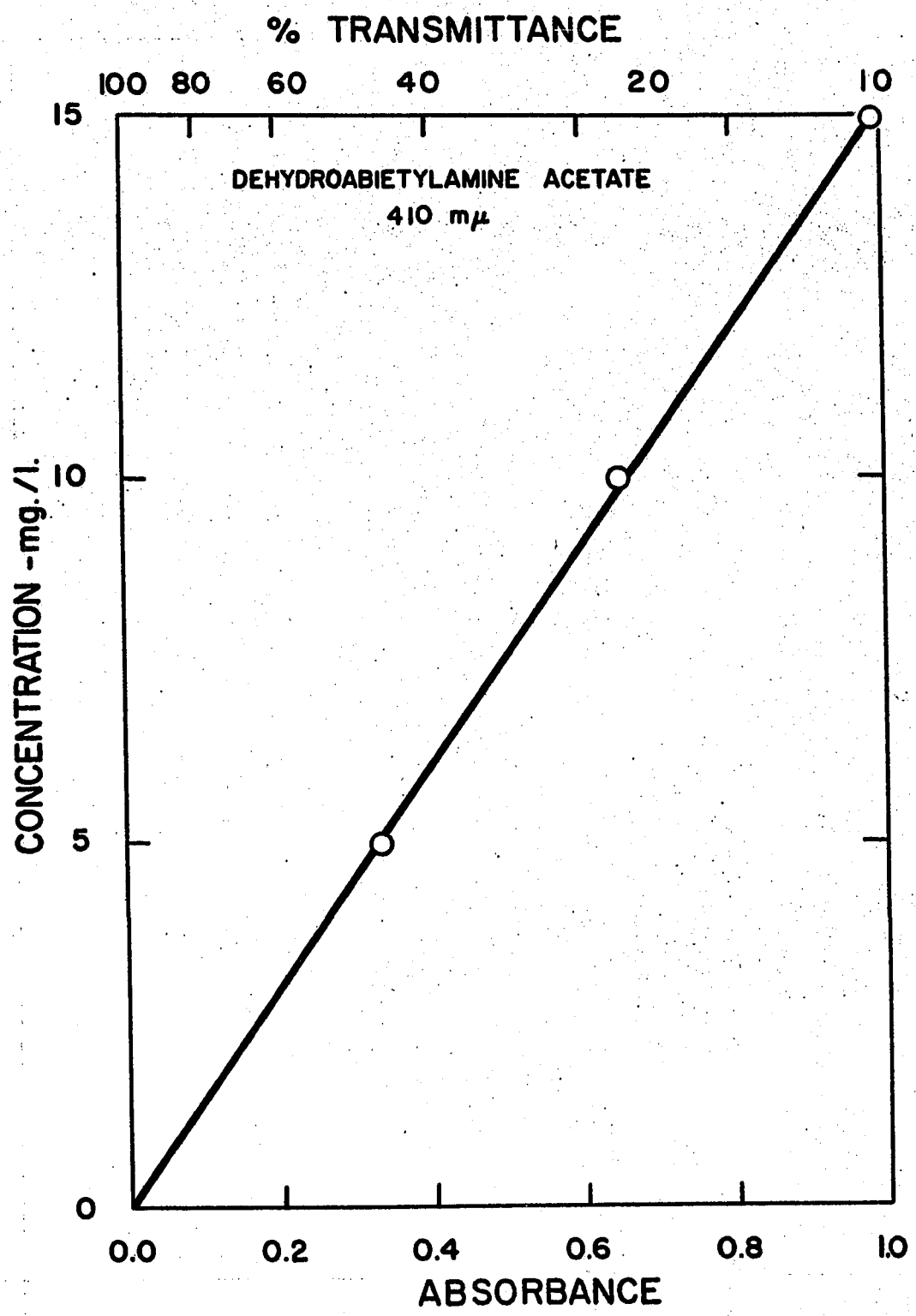
% TRANSMITTANCE
100
80
60
40
20
10
DEHYDROABIETYLAMINE ACETATE
410 mμ
CONCENTRATION - mg./l.
15
10
5
0
0.0
0.2
0.4
0.6
0.8
1.0
ABSORBANCE

APPENDIX II

STANDARDIZATION OF HYDROCHLORIC ACID AND SODIUM HYDROXIDE

Standardization of Hydrochloric Acid

Three accurately weighed dry samples (approx. 2 gm.) of sodium carbonate (Baker Analysed, A.C.S. grade) were dissolved in 25 ml. of conductivity water. Three drops of 0.1% phenophthalein solution (in alcohol) were added. Titration was continued until no pink colour returned after one minute boiling to remove carbonic acid. Results are tabulated below:-

Sample No.	Weight of Na_2CO_3(gm.)	Volume of HCl(ml.)	Normality
A	2.0042	37.85	0.999
B	2.0081	37.80	1.002
C	2.0046	37.82	1.000
Average			1.000

Standardization of Sodium Hydroxide

Twenty five ml. aliquots of standardized hydrochloric acid were titrated with the unknown solution of sodium hydroxide using phenophthalein as the indicator. Results are tabulated below:-

Sample No.	Volume of HCl(ml.)	Volume of NaOH(ml.)	Normality NaOH
A	25.00	21.10	1.184
B	25.00	21.20	1.179
C	25.00	21.20	1.179
Average			1.181

APPENDIX III

SURFACE AREA DETERMINATION

The surface area of each sample was determined using the Brunauer, Emmett and Teller method of gaseous adsorption, described previously (15).

If a plot of $\frac{P}{v(P_o-P)}$ against $\frac{P}{P_o}$ is drawn, a straight line should be obtained having a slope of $\frac{c-1}{v_m c}$ and an intercept of $1/v_m c$. Linearity is generally obtained in the relative pressure range of 0.05 to 0.35. The linear portion depends on the value c, for example, when $c = 100$, the monolayer point occurs at a relative pressure of about 0.1 and, when $c = 1$, the monolayer is reached at a relative pressure of 0.5.

In the present investigation, the surface area was determined by krypton and nitrogen adsorption at liquid nitrogen temperatures using the apparatus described by Salman (132). The surface area covered by one cubic centimeter of krypton gas at S.T.P. is taken as 5.24 M^2. Similarly, one cubic centimeter of nitrogen at S.T.P. covers 4.36 M^2 of adsorbent.

As shown in the following B.E.T. plots, straight lines were obtained in all cases. The following tables contain all the calculations required to determine the specific surface of each sample.

TABLE XXIII

KRYPTON ADSORPTION DATA FOR SURFACE AREA DETERMINATION

Test No.	Total Volume cc.STP.	McLeod Volume cc.STP.	Sample Tube Volume cc.STP.	Adsorbed Volume cc.STP.	Krypton P_o mm. Hg.	McLeod Pressure mm. Hg.	$\frac{P}{P_o}$	$\frac{P}{(P_o-P)v}$
			Coarse Hematite(A)					
1	0.061203	0.023367	0.002106	0.035730	2.570	0.22	0.086	2.620
2	0.088280	0.042644	0.003829	0.041807	2.570	0.40	0.156	4.409
3	0.113954	0.060953	0.005457	0.047544	2.590	0.57	0.220	5.935
4	0.138713	0.077719	0.006987	0.054007	2.590	0.73	0.282	7.267
			Coarse Hematite(B)					
1	0.071115	0.025508	0.002227	0.043380	2.605	0.24	0.092	2.339
2	0.100845	0.043695	0.003805	0.053345	2.637	0.41	0.155	3.451
3	0.129444	0.064899	0.005662	0.058883	2.625	0.61	0.232	5.141
4	0.157027	0.084135	0.007332	0.065560	2.625	0.79	0.301	6.567
			Silica(A)					
1	0.060595	0.037250	0.003078	0.020267	2.493	0.35	0.140	8.059
2	0.081987	0.054352	0.004486	0.023149	2.488	0.51	0.205	11.138
3	0.102584	0.071404	0.005892	0.025288	2.488	0.67	0.269	14.574
4	0.122498	0.086324	0.007924	0.029050	2.465	0.81	0.329	16.848
			Silica(B)					
1	0.043940	0.021221	0.001685	0.021034	2.465	0.20	0.081	4.198
2	0.086324	0.053106	0.004212	0.029006	2.458	0.50	0.203	8.804
3	0.105583	0.065896	0.005223	0.034464	2.465	0.62	0.252	9.804
4	0.124262	0.080640	0.006403	0.037219	2.468	0.76	0.308	11.955

continued...

TABLE XXIII(continued)

Test No.	Total Volume cc.STP.	McLeod Volume cc.STP.	Sample Tube Volume cc.STP.	Adsorbed Volume cc.STP.	Krypton P_o mm. Hg.	McLeod Pressure mm. Hg.	$\frac{P}{P_o}$	$\frac{P}{(P_o - P)v}$
			Silica(C)					
1	0.054612	0.021030	0.002908	0.030674	2.532	0.20	0.079	2.796
2	0.082510	0.038881	0.005522	0.038107	2.532	0.38	0.150	4.634
3	0.136550	0.075690	0.010753	0.050107	2.550	0.74	0.290	8.159
4	0.155989	0.090070	0.012788	0.053131	2.550	0.88	0.345	9.918
			Rutile(A)					
1	0.064434	0.005725	0.000836	0.057873	2.570	0.055	0.021	0.378
2	0.126537	0.019758	0.002885	0.103894	2.550	0.19	0.075	0.775
3	0.186426	0.041637	0.006074	0.138715	2.550	0.40	0.157	1.341
4	0.244474	0.067660	0.009870	0.166944	2.560	0.65	0.254	2.039
			Rutile(B)					
1	0.066987	0.004206	0.000462	0.062319	2.505	0.040	0.016	0.260
2	0.131237	0.016857	0.001849	0.112531	2.505	0.16	0.064	0.601
3	0.193285	0.036900	0.004045	0.152340	2.505	0.35	0.140	1.066
4	0.253132	0.061170	0.006703	0.185259	2.504	0.58	0.232	1.627
5	0.310747	0.084372	0.009245	0.217130	2.504	0.80	0.319	2.162

FIGURE 55

B.E.T. PLOTS FOR KRYPTON GAS ADSORPTION

□ - Silica (A)
○ - Silica (B)
△ - Silica (C)
◇ - Hematite (A)
▽ - Hematite (B)
▷ - Rutile (A)
⬠ - Rutile (B)

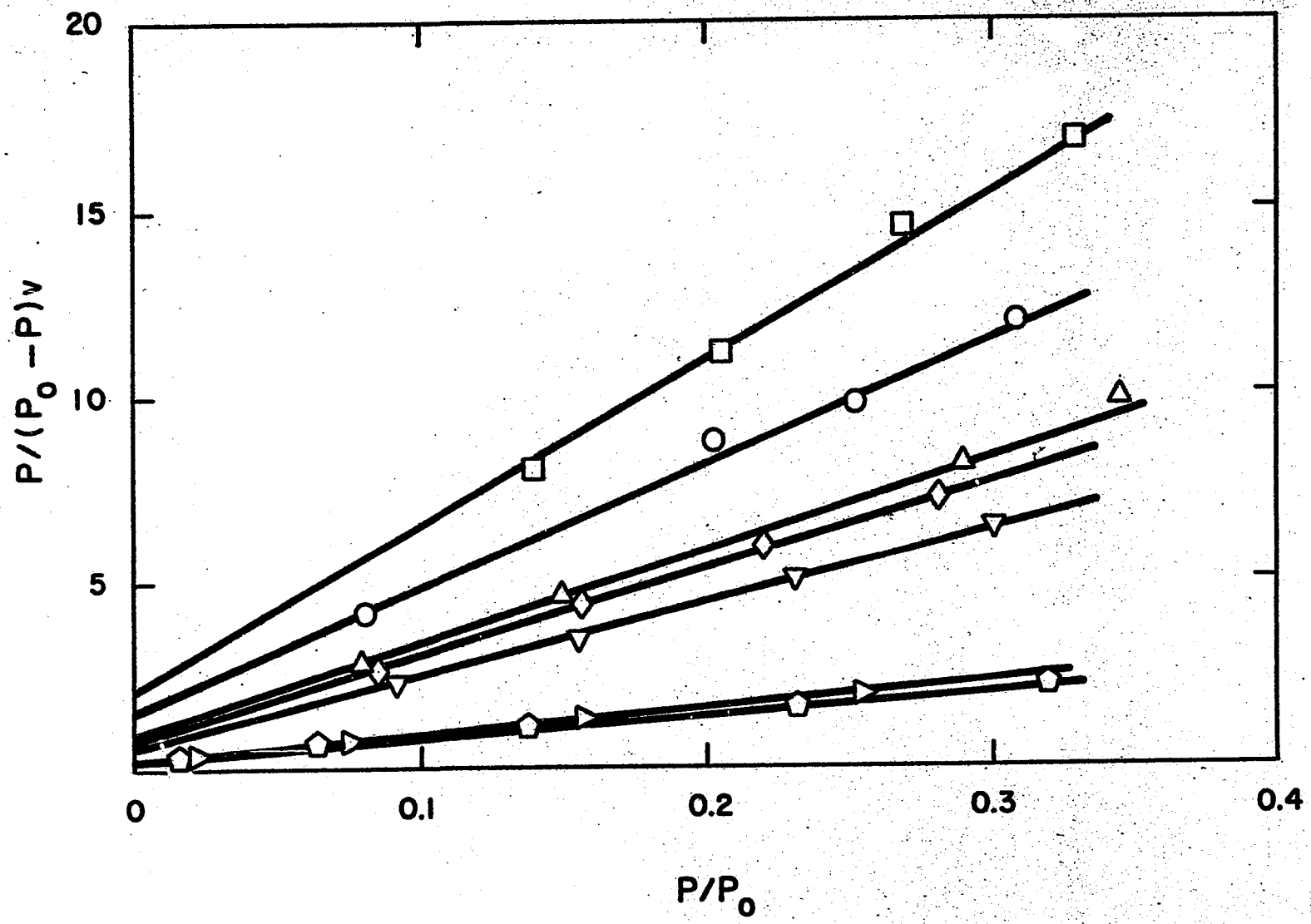
20
15
10
5
0
0.1
0.2
0.3
0.4
P/(P$_o$ − P)v
P/P$_o$

TABLE XXIV

NITROGEN ADSORPTION DATA FOR SURFACE AREA DETERMINATION

Test No.	Total Volume cc.STP.	Bulb Volume cc.STP.	Sample Tube Volume cc.STP.	Adsorbed Volume cc.STP.	Nitrogen P_o mm.Hg.	Bulb Pressure mm.Hg.	$\frac{P}{P_o}$	$\frac{P}{(P_o-P)v} \times 10^3$
			Baddeleyite					
1	10.482	4.833	0.236	5.413	778	14.8	0.019	3.582
2	10.482	4.454	0.352	5.676	778	22	0.028	5.127
3	10.482	3.993	0.448	6.041	778	28	0.036	6.180
4	10.482	3.318	0.654	6.510	780	41	0.0526	8.522
5	10.482	1.650	1.341	7.491	780	84	0.1077	16.111
			Fine Hematite					
1	36.218	14.453	0.712	21.053	778	57.6	0.074	3.801
2	36.218	11.649	1.251	23.318	778	101	0.130	6.407
3	36.218	8.814	1.850	25.554	780	150	0.192	9.302
4	36.218	4.701	2.688	28.849	782	216	0.276	13.210

FIGURE 56

B.E.T. PLOTS FOR NITROGEN GAS ADSORPTION

○ - Hematite

□ - Baddeleyite

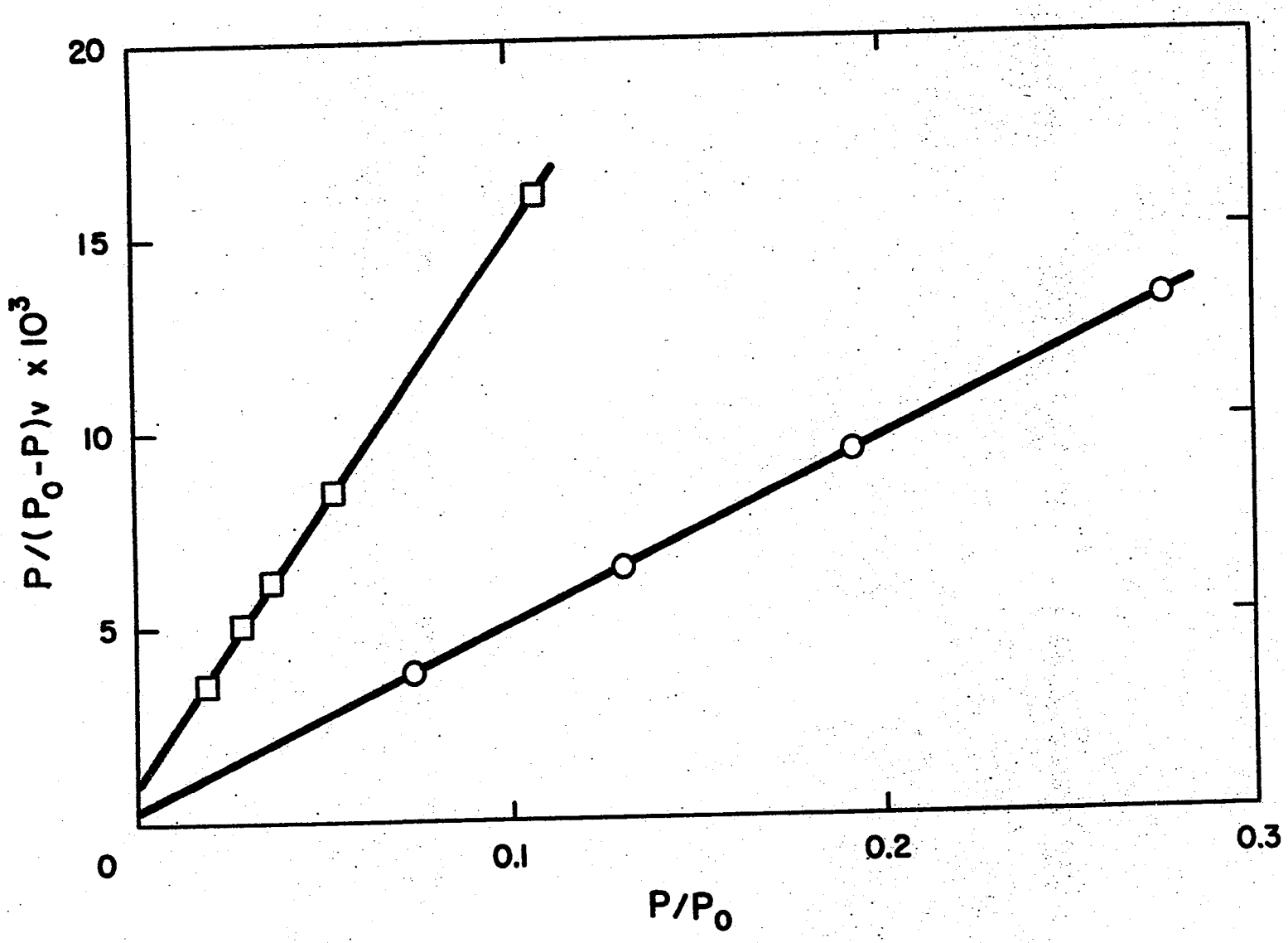
20
15
10
5
0
0.1
0.2
0.3
P/(P0-P)v x 10^3
P/P0

TABLE XXV

DETERMINATION OF SPECIFIC SURFACES

Sample	Weight gm.	B.E.T. Slope	B.E.T. Inter-cept	v_m cc.STP.	c	Specific Surface $cm^2/gm.$
C. Hematite (A)	1.5447	23.536	0.69	0.04128	35.1	1383
C. Hematite (B)	1.8810	20.000	0.51	0.04885	40.6	1361
Average					37.7	1372
Silica (A)	0.8561	44.975	2.05	0.02127	22.9	1302
Silica (B)	1.0171	33.933	1.43	0.02828	24.7	1457
Silica (C)	1.4301	27.090	0.92	0.03871	28.1	1420
Average					25.2	1407
Rutile (A)	1.9228	7.125	0.23	0.1360	32.2	3700
Rutile (B)	2.3561	6.130	0.21	0.1580	30.2	3520
Average					31.2	3610
Baddeleyite	1.8763	0.1416	9.5	7.011×10^{-4}	150	162,900
Hematite	4.2134	0.0465	3.3	21.354×10^{-4}	142	264,400

APPENDIX IV

X-RAY DIFFRACTION ANALYSIS

FIGURE 57

X-RAY DIFFRACTION PATTERN FOR α-QUARTZ

Copper Radiation

40 kV, 19 mA, 1 hour.

Magnification 2.1 X

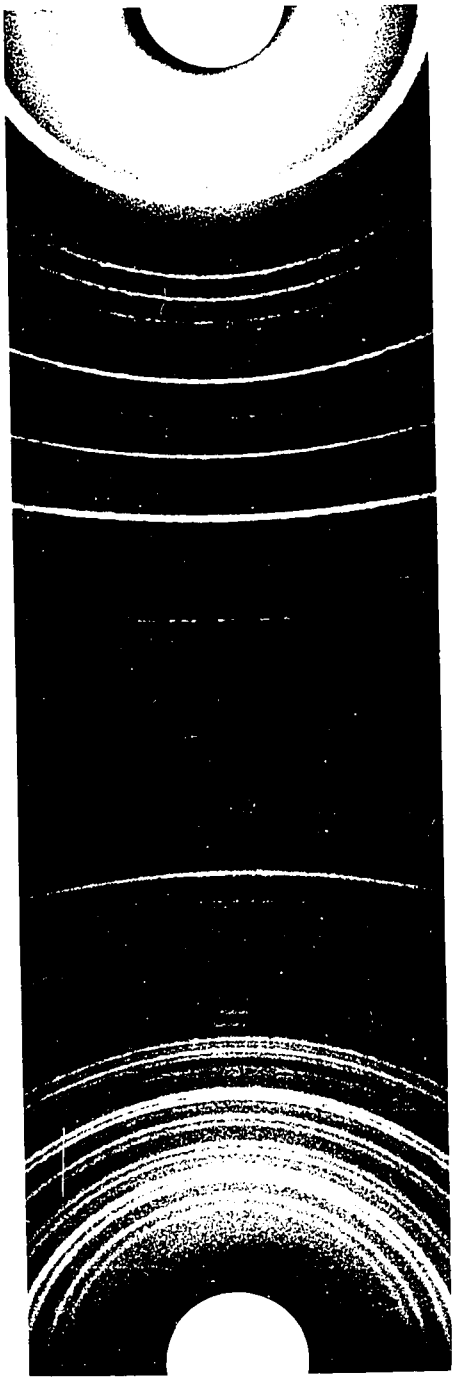

TABLE XXVI

X-RAY IDENTIFICATION OF

α-QUARTZ

2θ	I/I_1 (est.)	d	d Card5-0494	Error	I/I_1
20.16, 21.26 } 20.71	50	4.29	4.26	+0.03	35
25.96, 27.36 } 26.66	100	3.34	3.343	-0.003	100
36.96	15	2.43	2.458	-0.028	12
39.76	10	2.27	2.282	-0.012	12
40.56	5	2.22	2.237	-0.017	6
42.76	15	2.12	2.128	-0.008	9
46.26	10	1.96	1.980	-0.020	6
50.26	40	1.82	1.817	-0.003	17
55.36	20	1.66	1.672 1.659	-0.012 +0.001	7 3
60.36	30	1.53	1.541	-0.011	15
64.36	10	1.44	1.453	-0.013	3
66.06	2	1.41	1.418	-0.008	<1
68.36	50	1.37	1.382 1.375 1.372	-0.012 -0.005 -0.002	7 11 9
73.66	10	1.28	1.288	-0.008	3
75.76	15	1.25	1.256	-0.006	4
77.96	8	1.22	1.228	-0.008	2
80.06	25	1.20	1.1997 1.1973	+0.0003 +0.00027	5 2
81.46	25	1.18	1.1838 1.1802	-0.0038 -0.0002	4 4
83.96	10	1.15	1.1530	-0.0030	2
84.96	1	1.14	1.1408	-0.0008	<1
87.56	1	1.11	1.1144	-0.0044	<1
91.06	20	1.08	1.0816	-0.0016	4
92.76	5	1.06	1.0636	-0.0036	1
94.96	10	1.04	1.0477 1.0437	-0.0077 -0.0037	2 2
96.36	10	1.03	1.0346	-0.0046	2
98.86	10	1.015	1.0149	+0.0001	2
102.46	15	0.989	0.9896	-0.0006	<1
104.26	10	0.976	0.9762	-0.0002	1
106.66	10	0.961	0.9607	+0.0003	2

continued...

TABLE XXVI (cont'd)

α-QUARTZ

2θ	I/I_1 (est.)	d
114.56	25	.916
115.76	2	.910
118.16	8	.898
120.16	8	.889
122.56	8	.879
126.96	1	.861
131.06	1	.847
132.86	1	.841
134.36	1	.836
136.16	10	.830
136.86	5	
137.56	10	.826
138.36	5	
140.06	2	.820
140.66	2	
142.86	10	.812
143.76	10	.810
144.66	1	
146.26	5	.805
147.06	5	
149.66	5	.798
150.66	5	
151.86	1	
152.96	15	.792
154.36	10	
156.66	8	.786
158.06	5	

* There is no comparison for these lines. They are assumed to belong to the α-quartz pattern.

FIGURE 58

X-RAY DIFFRACTION PATTERN FOR HEMATITE

Iron Radiation

25 kV, 11 mA, 1 hour

Magnification 2,1 X

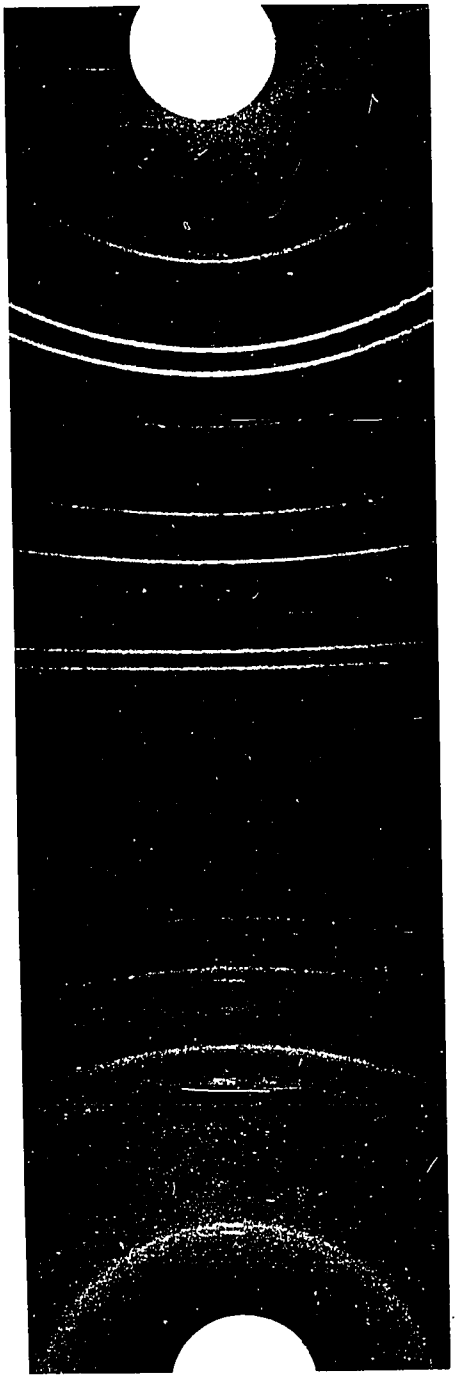

TABLE XXVII

X-RAY IDENTIFICATION OF

HEMATITE (α-Fe_2O_3)

2θ	I/I_1 (est.)	d	d Card No.2-0942	Error	I/I_1
30.72	30	3.66	3.67	-0.01	50
38.12	4	2.97	-		
42.02	100	2.70	2.69	+0.01	100
45.12	90	2.52	2.51	+0.01	80
51.92	40	2.21	2.20	+0.01	60
63.12	50	1.85	1.84	+0.01	80
69.22	60	1.70	1.69	+0.01	90
74.02	10	1.61	1.60	+0.01	50
80.72	50	1.50	1.48	+0.02	70
83.02	50	1.46	1.45	+0.01	70
90.82	2	1.36	1.35	+0.01	20
94.52	10	1.32	1.31	+0.01	60
99.72	5	1.27	1.26	+0.01	40
103.12	1	1.24	1.23	+0.01	10
107.92	5	1.20	1.21	-0.01	10
111.52	5	1.17	1.16	+0.01	40
115.12	8	1.15	1.14	+0.01	40
121.52	10	1.11	1.10	+0.01	60
123.12	1	1.10	1.10	0.00	60
131.62	15	1.06	1.05	+0.01	60
136.12	4	1.04	1.04	0.00	20
154.52	10	0.992	0.99	+0.002	50
155.62	6	0.992			

FIGURE 59

X-RAY DIFFRACTION PATTERN FOR

SYNTHETIC RUTILE

Copper Radiation

40 kV, 19 mA, 0.5 hour.

Magnification 2.1 X

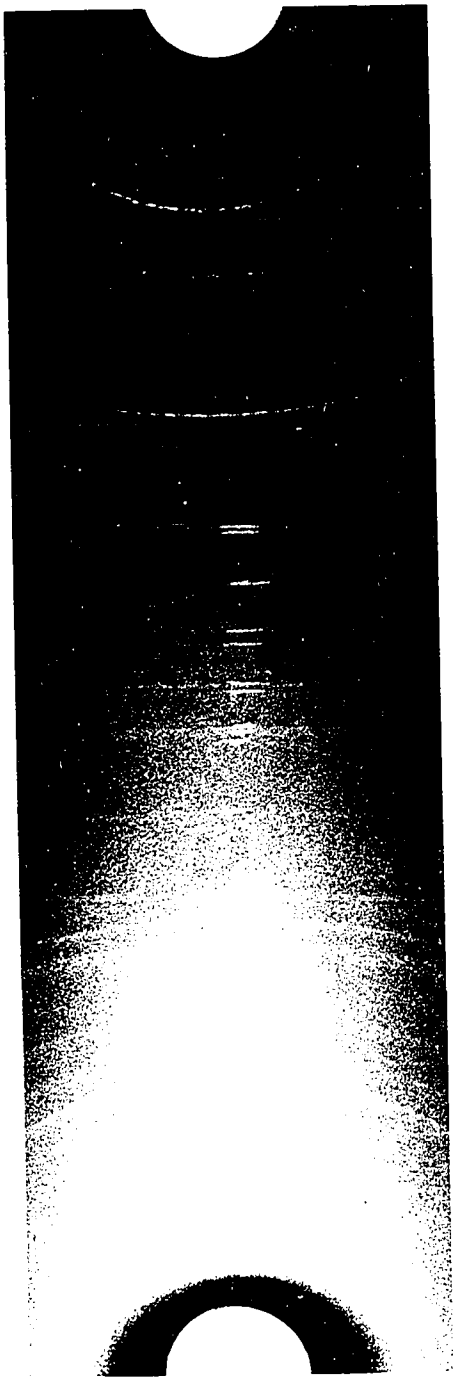

TABLE XXVIII

X-RAY IDENTIFICATION OF

SYNTHETIC RUTILE

2θ	I/I_1 (est.)	d	d Card 4-0551	Error	I/I_1
27.64	100	3.23	3.245	-0.015	100
36.24	60	2.48	2.489	-0.009	41
38.74	2	2.32	2.297	+0.023	7
41.14	40	2.19	2.188	+0.002	22
43.94	5	2.06	2.054	+0.006	9
54.14	80	1.694	1.687	+0.007	50
56.54	40	1.627	1.624	+0.003	16
62.54	10	1.485	1.480	+0.005	8
63.84	10	1.457	1.453	+0.004	6
68.54	40	1.369	1.360	+0.009	16
69.44	40	1.353	1.347	+0.006	7
			1.305		1
76.24	2	1.249	1.243	+0.006	3
			1.200		1
82.24	2	1.172	1.1700	+0.002	4
83.94	2	1.153	1.1485	+0.0045	4
			1.1140		1
89.24	4	1.097	1.0933	+0.0036	4
90.14	2	1.089	1.0827	0.0063	4
94.74	5	1.048	1.0424	+0.0056	5
95.14	5	1.044	1.0424	+0.0016	4
96.44	1	1.034	1.0361	+0.0021	4
			1.0273		3
105.54	2	0.9686	0.9642	+0.0042	2
115.84	1	0.9098	0.9071	+0.0027	3
117.24	1	0.9030	0.9007	+0.0023	3
119.74	4	0.8913	0.8892	+0.0021	5
122.24	4	{0.8795			
123.14	4	0.8780}	0.8773	+0.0014	6
130.84	2	{0.8469			
131.54	2	0.8467}	0.8437	+0.0031	5
135.94	4	{0.8309			
136.74	4	0.8306}	0.8290	+0.0017	5
139.44	10	{0.8210			
140.64	8	0.8200}	0.8196	+0.0009	8

FIGURE 60

X-RAY DIFFRACTION PATTERN FOR

PRECIPITATED ZIRCONIA (BADDELEYITE).

Copper Radiation

40 kV, 19 mA, 1 hour.

Magnification 2.1 X

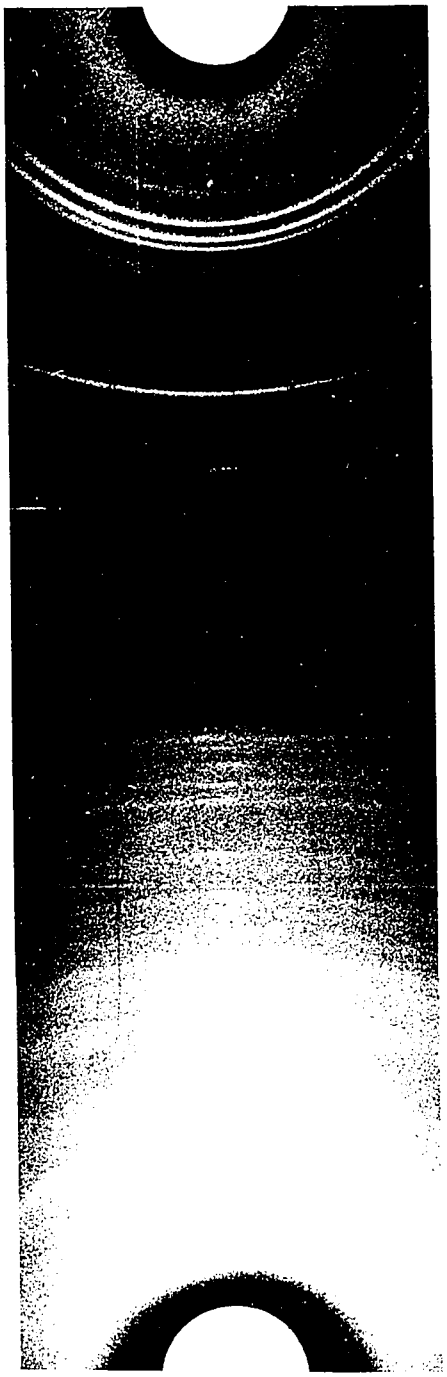

TABLE XXIX

X-RAY IDENTIFICATION OF PRECIPITATED ZIRCONIA (BADDELEYITE)

2θ	I/I_1 (est.)	d	d Card 7-343	Error	I/I_1
			5.05		5
24.18	70	3.681	3.69	-0.009	15
28.48	100	3.134	3.16	-0.026	100
			{2.95	*-0.008	*70
30.38	100	2.942	2.92	+0.022	100
31.58	60	2.833	2.84	-0.007	65
			{2.62	{-0.026	20
34.58	10	2.594	2.60	-0.006	12
35.18	10	2.541	2.54	+0.001	15
38.58	1	2.334	2.33	+0.004	5
40.78	5	2.213	2.21	+0.003	10
			{2.02	{-0.017	7
45.28	5	2.003	1.99	+0.013	7
49.38	5	1.845	1.846	-0.001	15
50.38	90	1.811	1.877	-0.006	20
53.88	5	1.701	1.693	+0.008	10
55.38	7	1.659	1.655	+0.004	12
57.28	1	1.608	1.609	-0.001	5
58.28	1	1.583	1.581	+0.002	5
60.08	10	1.540	1.542	-0.002	10
61.28	1	1.513	1.508	+0.005	5
62.78	5	1.480	1.477	+0.003	10
64.08	1	1.453	1.449	+0.004	3
65.78	2	1.420	1.420	0.000	7
71.18	1	1.325	1.322	+0.003	5
74.58	1	1.272	1.262	+0.010	5
81.48	2	1.181			
85.18	1	1.139			
88.28	1	1.107			
93.78	1	1.056			
95.18	2	1.044			
96.38	1	1.034			
96.38	1	1.034			
98.68	1	1.016			
101.28	1	0.9971			
103.38	1	0.9824			
110.48	1	0.9383			
115.38	1	0.9121			
120.28	1	0.8889			
123.68	2	0.8744			
125.88	1	0.8657			

*2.92 100% line of ZrO_2(cubic) Card 7-337

2.95 70% line of Baddeleyite Card 2-0464 .

The exposure of these films was difficult in two cases. First, the exposure of rutile to X-ray radiation caused considerable fluorescene of the titanium atom, due to its low atomic weight. Iron radiation caused complete fogging of the film and copper radiation was better but not perfect. The forward reflection region was clear but the back reflection was fogged. The use of a molybdenum target would compress the diffraction lines in the forward region. The best solution would be the use of a chromium target which was not available. The best compromise was the use of the copper radiation as reported in Table XXVIII.

Second, the zirconia (baddeleyite) was so fine that it caused line broading and a diffuse pattern in the back reflection region. However, it was found to be clear enough for this work.

APPENDIX V

CALCULATION OF SURFACE CHARGE DENSITY AND DIFFERENTIAL CAPACITY

The surface charge density may be calculated from the adsorption density by using the following conversion factors:-

$$1 \text{ mole} = 6.023 \times 10^{23} \text{ molecules}$$
$$1 \text{ electronic charge} = 4.803 \times 10^{-10} \text{ e.s.u.}$$
$$1 \text{ coulomb.} = 10^{6} \ \mu\text{coulombs.}$$
$$1 \ \mu\text{mole} = 10^{-6} \text{ moles .}$$

One must assume that there is one electronic charge on each hydrogen and hydroxyl ion and that a mole of each contains 6.023×10^{23} electronic charges. Hence, the surface charge density is determined as follows:-

$$\text{Surface Charge Density, } \sigma = \text{Adsorption Density } (\Gamma_{H^+} - \Gamma_{OH^-})\left(\frac{\mu\text{moles}}{\text{gm.}}\right)$$
$$\times 10^{-6}\left(\frac{\text{moles}}{\mu\text{mole}}\right) \times 6.023 \times 10^{23} \left(\frac{\text{molecules}}{\text{mole}}\right)$$
$$\times 4.803 \times 10^{-10} \left(\frac{\text{e.s.u.}}{\text{molecule}}\right)$$
$$\times 3.336 \times 10^{-10} \left(\frac{\text{coulomb}}{\text{e.s.u.}}\right) \times 10^{6} \ \frac{\mu\text{coul.}}{\text{coul.}}$$
$$= (\Gamma_{H^+} - \Gamma_{OH^-}) \times 4.803 \times 6.023 \times 3.36 \times 10^{3} \ \frac{\mu\text{coul.}}{\text{gm.}}$$
$$= (\Gamma_{H^+} - \Gamma_{OH^-}) \times 9.64 \times 10^{4} \ \frac{\mu\text{coul.}}{\text{gm.}}$$

If one assumes the B.E.T. surface area to be the same area as that exposed to the solution and available for hydrogen and hydroxyl ion adsorption, then the surface charge density for the hematite sample, expressed in terms of area available, becomes

$$\sigma_{Hem.} = (\Gamma_{H^+} - \Gamma_{OH^-})_{Hem.} \times 9.64 \times 10^4 \frac{\mu coul.}{gm.} \times \frac{1}{26.4} \frac{gm.}{M.^2} \times \frac{1}{10^4} \frac{M.^2}{cm.^2}$$

$$= 0.364 \, (\Gamma_{H^+} - \Gamma_{OH^-})_{Hem.} \frac{\mu coul.}{cm.^2}$$

The differential capacity may be calculated from the differention of the adsorption density with respect to pH or, more simply, from the slope of the adsorption density vs. pH curve. The conversion factors involved in addition to those in the previous section are:-

1 pH unit = - 0.05915 volts

1 volt = 3.3356×10^{-3} e.s.u.(pot'l)

1 e.s.u.(capacity) = $\frac{1 \text{ e.s.u.(charge)}}{1 \text{ e.s.u.(pot'l.)}}$

1 e.s.u.(capacity) = 1.11263×10^{-12} farads

1 farad = 10^6 μfarads .

Using the same conditions as for the surface charge density, the differential capacity, C_i, becomes:-

$$C_i = \frac{d(\Gamma_{H^+} - \Gamma_{OH^-})}{d(pH)} \left(\frac{\mu mole}{gm\text{-}pH \text{ unit}}\right) \times 10^{-6} \left(\frac{mole}{\mu mole}\right) \times 6.023 \times 10^{23} \left(\frac{molecules}{mole}\right)$$

$$\times 4.803 \times 10^{-10} \left(\frac{e.s.u.(charge)}{molecule}\right) \times \frac{-1}{0.05915} \left(\frac{pH \text{ unit}}{volt}\right)$$

$$\times \frac{1}{3.3356 \times 10^{-3}} \left(\frac{volt}{e.s.u(pot'l)}\right) \times 1 \left(\frac{e.s.u.(cap) \; e.s.u.(pot'l)}{e.s.u.(charge)}\right)$$

$$\times 1.11263 \times 10^{-12} \left(\frac{fd.}{e.s.u.charge}\right) \times 10^6 \left(\frac{\mu fd.}{fd.}\right)$$

$$= -\frac{d(\Gamma_{H^+} - \Gamma_{OH^-})}{d(pH)} \times \frac{6.023 \times 4.803 \times 1.11263}{0.05915 \times 3.3356} \times 10^4 \frac{\mu fd.}{gm.}$$

$$= -\frac{d(\Gamma_{H^+} - \Gamma_{OH^-})}{d(pH)} \times 1.632 \times 10^6 \frac{\mu fd.}{gm.}$$

Using the B.E.T. surface area, with the reservations expressed above, the differential capacity per unit area for hematite becomes:-

$$C_{i(Hem.)} = -\left(\frac{d(\Gamma_{H^+} - \Gamma_{OH^-})}{d(pH)}\right)_{Hem.} \times 1.632 \times 10^6 \frac{\mu fd.}{gm.} \times \frac{1}{26.4} \frac{gm.}{M.^2} \times \frac{1}{10^4} \frac{M.^2}{cm.^2}$$

$$= -\left(\frac{d(\Gamma_{H^+} - \Gamma_{OH^-})}{d(pH)}\right)_{Hem.} \times 6.19 \frac{\mu fd.}{cm^2.}$$

The constants for each oxide are listed below

Constant	Hematite	Zirconia	Rutile
Specific Surface($M.^2$/gm.)	26.4	16.3	0.37
Surface Charge Density Conversion $\left(\frac{\mu coul.}{cm.^2}\right)$	0.364	0.590	25.9
Differential Capacity Conversion $\left(\frac{\mu fd.}{gm.^2}\right)$	6.19	10.03	440

Sample Calculation

From Figure 29 at a pH 9.50, the acid additions were as follows:-

No Hematite - 1.085 mℓ. of 1.000 N HCl
4 gm. " - 0.995 " " " " "

The change in volume = Volume with hematite
- volume with no hematite
= 0.995 - 1.085 mℓ.
= -0.090 mℓ.

$$\text{Adsorption per grams, } (\Gamma_{H^+} - \Gamma_{OH^-}) = \frac{\text{Change in Vol.(m}\ell\text{) X Molality}\left(\frac{\mu\text{moles}}{\text{m}\ell.}\right)}{\text{Weight of Hematite (gm.)}}$$

$$= - \frac{0.090\ \text{m}\ell. \text{X } 1000\ \mu\text{mole/m}\ell.}{4\ \text{gm.}}$$

$$= -\ 22.5\ \mu\text{moles/gm.}$$

$$\frac{d(\Gamma_{H^+} - \Gamma_{OH^-})}{d(pH)} \text{ (measured from Figure 32)} = -\ 22.9\ \mu\text{mole/gm/pH unit.}$$

$$\text{Surface Charge Density, } \sigma = (\Gamma_{H^+} - \Gamma_{OH^-}) \text{ X } 9.64 \text{ X } 10^4$$
$$= -\ 22.5 \text{ X } 9.64 \text{ X } 10^4$$
$$= -\ 21.6 \text{ X } 10^5\ \mu\text{coul./gm.}$$

$$\text{Surface Charge Density, } \sigma = (\Gamma_{H^+} - \Gamma_{OH^-}) \text{ X } 0.364$$
$$= -\ 22.5 \text{ X } 0.364$$
$$= -\ 8.2\ \mu\text{coul./cm}^2$$

$$\text{Differential Capacity, } C_i = -\ \frac{d(\Gamma_{H^+} - \Gamma_{OH^-})}{d(pH)} \text{ X } 1.632 \text{ X } 10^6$$
$$= -\ (-\ 22.9) \text{ X } 1.632 \text{ X } 10^6$$
$$= 37.5 \text{ X } 10^6\ \mu\text{fd./gm.}$$

$$\text{Differential Capacity}, C_i = - \frac{d(\Gamma_{H^+} - \Gamma_{OH^-})}{d(pH)} \times 6.19$$

$$= - (- 22.9) \times 6.19$$

$$= 141 \ \mu fd./cm.^2$$

TABLE XXX

CALCULATION OF SURFACE CHARGE DENSITY AND DIFFERENTIAL CAPACITY

HEMATITE IN 0.1 N KCl SOLUTION

TESTS No.23 AND No.24.

pH	Acid Volume		Change In Acid Volume	Adsorption $\Gamma_{H^+} - \Gamma_{OH^-}$	$-\left[\frac{d(\Gamma_{H^+} - \Gamma_{OH^-})}{d(pH)}\right]$	Surface Charge Density		Differential Capacity	
	Solids	No Solids							
	mℓ.	mℓ.	mℓ.	μmoles/gm.	μmoles/gm.	μcoul/gm. x 10^{-5}	μcoul/cm.^{2}	μfd./gm. x 10^{-6}	μfd./cm.^{2}
11.12	0.000	0.470	-0.470	-117.5	192.5	-113.0	-42.8	314	1190
11.00	0.210	0.585	-0.375	- 93.8	130.0	-90.3	-34.2	212	805
10.75	0.500	0.765	-0.265	-66.3	62.1	-63.9	-24.2	101	385
10.50	0.665	0.885	-0.220	-55.0	42.5	-53.0	-20.0	69.5	263
10.25	0.810	0.980	-0.170	-42.5	34.4	-40.9	-15.5	56.2	213
10.00	0.900	1.040	-0.140	-35.0	27.5	-33.7	-12.8	44.9	170
9.75	0.955	1.065	-0.110	-27.5	25.0	-26.4	-10.0	40.9	154
9.50	0.995	1.085	-0.090	-22.5	22.9	-21.6	-8.2	37.5	141
9.25	1.032	1.102	-0.070	-17.5	22.9	-16.8	-6.4	37.5	141
9.00	1.072	1.115	-0.043	-10.8	26.2	-10.4	-3.9	43.0	162
8.75	1.113	1.128	-0.015	-3.8	31.0	-3.7	-1.4	50.6	192
8.50	1.153	1.140	0.013	3.3	38.6	3.2	1.2	63.3	238
8.25	1.225	1.143	0.082	20.5	59.0	19.7	7.5	96.6	365
8.00	1.350	1.147	0.203	50.8	64.6	49.0	18.5	105	400
7.75	1.495	1.151	0.344	86.0	92.6	82.8	31.4	151	572
7.50	1.640	1.155	0.485	121.3	156.0	117.0	44.2	255	750
8.63	1.133	1.133	0.000	0.0	35.0	0.0	0.0	57.0	216

TABLE XXXI

CALCULATION OF SURFACE CHARGE DENSITY AND DIFFERENTIAL CAPACITY

HEMATITE IN 0.01 N KCl SOLUTION

TESTS No. 20 AND No. 21.

pH	Acid Volume		Change In Acid Volume	Adsorption $\Gamma_{H^+} - \Gamma_{OH^-}$	$-\left[\frac{d(\Gamma_{H^+} - \Gamma_{OH^-})}{d(pH)}\right]$	Surface Charge Density		Differential Capacity	
	Solids	No Solids							
	mℓ.	mℓ.	mℓ.	μmoles/gm.	μmoles/gm.	μcoul/gm. x 10^{-5}	μcoul/cm.^{2}	μfd/gm. x 10^{-6}	μfd./cm.^{2}
11.20	0.000	0.380	-0.380	-95.0	119.00	-91.5	-34.6	194	735
11.00	0.340	0.610	-0.270	-67.5	90.1	-65.0	-24.6	147	558
10.75	0.620	0.820	-0.200	-50.0	50.9	-48.1	-18.2	83.0	315
10.50	0.790	0.940	-0.150	-37.5	34.0	-36.1	-13.7	55.5	210
10.25	0.900	1.025	-0.125	-31.3	24.8	-30.1	-11.4	40.4	153
10.00	0.978	1.075	-0.097	-24.3	20.9	-23.4	-8.8	34.0	129
9.75	1.033	1.108	-0.075	-18.8	18.4	-18.1	-6.9	30.0	112
9.50	1.070	1.135	-0.065	-16.3	23.5	-15.7	-5.9	38.3	145
9.25	1.115	1.155	-0.040	-10.0	23.5	-9.6	-3.6	38.3	145
9.00	1.145	1.160	-0.015	-3.8	23.5	-3.7	-1.4	38.3	145
8.75	1.125	1.165	0.020	5.0	33.9	4.8	1.8	55.3	209
8.50	1.225	1.170	0.055	13.8	41.6	13.3	5.0	62.9	257
8.25	1.270	1.172	0.098	24.5	41.6	23.6	8.9	62.9	257
8.00	1.315	1.175	0.140	35.0	41.6	33.7	12.7	62.9	257
7.75	1.360	1.177	0.183	45.8	41.6	44.0	16.7	62.9	257
7.50	1.400	1.178	0.218	54.5	41.6	52.5	19.9	62.9	257
7.25	1.455	1.180	0.275	68.8	55.0	66.3	25.1	89.8	340
7.00	1.515	1.182	0.333	83.3	65.7	80.2	30.3	107	406
6.75	1.600	1.184	0.416	104.0	125.0	100.0	37.8	204	772
6.64	1.700	1.186	0.514	128.5	133.2	123.9	46.8	217	825
8.90	1.162	1.162	0.000	0.0	30.2	0.0	0.0	49.2	187

TABLE XXXII

CALCULATION OF SURFACE CHARGE DENSITY AND DIFFERENTIAL CAPACITY

HEMATITE IN 0.001 N KCl SOLUTION

TESTS No. 17 AND No. 18.

pH	Acid Volume		Change In Acid Volume	Adsorption $\Gamma_{H^+} - \Gamma_{OH^-}$	$\left[\frac{d(\Gamma_{H^+} - \Gamma_{OH^-})}{d(pH)}\right]$	Surface Charge Density		Differential Capacity	
	Solids	No Solids							
	mℓ.	mℓ.	mℓ.	μmoles/gm.	μcoul/gm.	μcoul/gm. x10^{-5}	μcoul/cm.^{2}	μfd./gm. x10^{-6}	μfd./cm.^{2}
11.00	0.355	0.645	-0.290	-72.5	78.5	-69.9	-26.4	128	486
10.75	0.600	0.820	-0.220	-55.0	40.8	-53.0	-20.1	66.5	253
10.50	0.765	0.955	-0.190	-47.5	33.9	-45.7	-17.3	55.3	210
10.25	0.875	1.030	-0.155	-38.8	30.8	-37.3	-14.1	50.2	191
10.00	0.942	1.070	-0.128	-32.0	28.5	-30.8	-11.7	46.5	176
9.50	1.015	1.115	-0.100	-25.0	23.6	-24.0	-9.1	38.5	146
9.00	1.080	1.125	-0.045	-11.3	23.1	-10.9	-4.1	37.7	143
8.50	1.148	1.140	0.008	2.0	23.1	1.9	0.7	37.7	143
8.00	1.202	1.150	0.052	13.0	23.1	12.5	4.7	37.7	143
7.50	1.240	1.151	0.091	22.8	18.2	21.9	8.3	29.7	113
7.00	1.277	1.152	0.125	31.3	14.3	30.1	11.4	23.3	89
6.50	1.302	1.153	0.149	37.3	14.3	35.9	13.6	23.3	89
6.00	1.335	1.157	0.178	44.5	14.3	42.8	16.2	23.3	89
5.50	1.365	1.160	0.195	48.8	15.0	47.0	17.8	24.5	93
5.00	1.415	1.163	0.252	63.0	20.6	60.6	23.0	33.7	128
4.50	1.465	1.172	0.293	73.3	28.2	70.6	26.7	46.0	175
4.00	1.565	1.205	0.360	90.0	41.7	86.7	32.8	68.0	258
3.90	1.605	1.220	0.385	96.3	58.1	92.8	35.1	95.0	360
3.82	1.640	1.230	0.410	102.5	65.8	98.8	37.3	108	417
3.75	1.665	1.240	0.245	106.3	73.0	102.6	38.8	119	453
8.55	1.139	1.139	0.000	0.0	23.1	0.0	0.0	37.7	143

TABLE XXXIII

CALCULATION OF SURFACE CHARGE DENSITY AND DIFFERENTIAL CAPACITY

HEMATITE IN 0.0001 N KCl SOLUTION

TESTS No.14 AND No.16..

pH	Acid Volume		Change In Acid Volume	Adsorption $\Gamma_{H^+} - \Gamma_{OH^-}$	$\left[\frac{d(\Gamma_{H^+}-\Gamma_{OH^-})}{d(pH)}\right]$	Surface Charge Density		Differential Capacity	
	Solids	No Solids							
	mℓ.	mℓ.	mℓ.	μmoles/gm.	μmoles/gm.	μcoul/gm. x10^{-5}	μcoul/cm.^{2}	μfd. /gm. x10^{-6}	μfd. /cm.^{2}
11.15	0.080	0.360	-0.280	-70.0	132	-67.5	-25.5	215	816
11.00	0.340	0.580	-0.240	-60.0	44.7	-57.8	-21.9	73.0	276
10.75	0.635	0.810	-0.175	-43.8	32.2	-42.2	-16.0	52.5	199
10.50	0.785	0.945	-0.160	-40.0	23.4	-38.5	-14.6	38.2	145
10.25	0.890	1.027	-0.137	-34.3	22.0	-33.0	-12.5	35.9	136
10.00	0.960	1.070	-0.110	-27.5	21.7	-26.4	-10.0	35.4	134
9.50	1.043	1.120	-0.073	-18.3	21.7	-17.6	-6.7	35.4	134
9.00	1.110	1.145	-0.035	-8.8	21.7	-8.5	-3.2	35.4	134
8.50	1.163	1.158	0.005	1.3	20.5	1.3	0.5	33.4	126
8.00	1.230	1.160	0.070	17.5	19.8	16.9	6.4	32.3	122
7.50	1.262	1.165	0.097	24.3	17.5	23.4	8.9	28.6	108
7.00	1.295	1.170	0.125	31.3	15.1	30.1	11.4	24.7	93
6.50	1.322	1.175	0.147	36.8	15.1	35.4	13.4	24.7	93
6.00	1.360	1.180	0.180	45.0	15.1	43.3	16.4	24.7	93
5.50	1.397	1.187	0.210	52.5	16.0	50.5	19.1	26.1	99
5.00	1.430	1.195	0.235	58.8	18.1	56.6	21.4	29.5	112
4.50	1.483	1.200	0.283	70.8	26.1	68.2	25.8	42.6	161
4.00	1.600	1.242	0.358	89.5	42.5	86.1	32.6	69.5	263
3.75	1.680	1.300	0.380	95.0	53.6	91.5	34.6	87.6	332
3.50	1.800	1.400	0.400	100.0	-	96.4	36.4	-	-
8.60	1.156	1.156	0.000	0.0	20.7	0.0	0.0	33.8	127

TABLE XXXIV

CALCULATION OF SURFACE CHARGE DENSITY AND DIFFERENTIAL CAPACITY

BADDELEYITE IN 0.1 N KCl SOLUTION

TESTS No.31a AND No.31b

pH	Base Volume		Change In Base Volume	Adsorption $\Gamma_{H^+} - \Gamma_{OH^-}$	$\left[\frac{d(\Gamma_{H^+}-\Gamma_{OH^-})}{d(pH)}\right]$	Surface Charge Density		Differential Capacity	
	Solids	No Solids							
	mℓ.	mℓ.	mℓ.	μmole/gm.	μmole/gm.	μcoul/gm. x10^{-5}	μcoul/cm.^{2}	μfd/gm x10^{-6}	μfd/cm.^{2}
9.50	1.055	0.874	0.181	-53.4	14.0	-51.4	-31.5	22.9	141
9.00	1.015	0.855	0.160	-47.2	13.8	-45.5	-27.8	22.5	139
8.50	0.984	0.851	0.133	-39.3	17.5	-37.8	-23.2	28.5	176
8.00	0.950	0.850	0.100	-29.5	17.5	-28.4	-17.4	28.5	176
7.50	0.919	0.849	0.070	-20.7	13.5	-19.9	-12.2	22.0	136
7.00	0.890	0.848	0.042	-12.4	12.2	-12.0	-7.3	19.9	123
6.50	0.868	0.847	0.021	-6.5	12.2	-6.3	-3.8	19.9	123
6.00	0.842	0.846	-0.004	1.2	11.9	1.2	0.7	19.6	120
5.50	0.819	0.845	-0.026	1.7	12.4	7.4	4.6	20.2	125
5.00	0.795	0.844	-0.049	14.5	12.4	14.0	8.6	20.2	125
4.50	0.768	0.843	-0.075	22.2	12.4	21.4	13.1	20.2	125
4.00	0.720	0.818	-0.098	28.9	12.4	27.8	17.1	20.2	125
3.75	0.676	0.782	-0.106	31.3	18.4	30.1	18.5	30.0	185
3.50	0.607	0.733	-0.126	37.2	34.1	36.0	22.0	55.6	243
3.25	0.460	0.638	-0.178	52.5	39.6	50.5	31.0	64.6	298
3.00	0.265	0.48	-0.215	63.5	39.6	61.2	37.5	64.6	398
6.08	0.846	0.846	0.000	0.0	11.9	0.0	0.0	19.6	120

TABLE XXXV

CALCULATION OF SURFACE CHARGE DENSITY AND DIFFERENTIAL CAPACITY

BADDELEYITE IN 0.01 N KCl SOLUTION

TESTS No.31a AND No.32.

pH	Base Volume		Change In Base Volume	Adsorption $\Gamma_{H^+} - \Gamma_{OH^-}$	$-\left[\frac{d(\Gamma_{H^+}-\Gamma_{OH^-})}{d(pH)}\right]$	Surface Charge Density		Differential Capacity	
	Solids	No Solids							
	mℓ.	mℓ.	mℓ.	μmoles/gm.	μmoles/gm.	μcoul/gm. x10^{-5}	μcoul/cm.^{2}	μfd/gm. x10^{-6}	μfd/cm.^{2}
9.50	1.012	0.874	0.138	-40.7	4.6	-39.2	-24.0	7.5	46
9.00	0.986	0.855	0.131	-38.7	8.3	-37.2	-22.8	13.6	83
8.50	0.462	0.851	0.111	-32.8	12.7	-31.5	-19.4	20.7	128
8.00	0.938	0.850	0.088	-26.0	12.7	-25.0	-15.3	20.7	128
7.50	0.910	0.849	0.061	-18.1	12.7	-17.4	-10.7	20.7	128
7.00	0.885	0.848	0.037	-10.9	12.1	-10.5	-6.4	19.8	122
6.50	0.864	0.847	0.017	-5.0	10.7	-4.8	-3.0	17.5	107
6.00	0.842	0.846	-0.004	1.2	10.1	1.2	0.7	16.5	101
5.50	0.825	0.845	-0.020	5.9	9.9	5.7	3.5	16.2	99
5.00	0.805	0.844	-0.039	11.5	8.9	11.1	6.8	14.5	89
4.50	0.782	0.843	-0.061	18.1	8.9	17.4	10.7	14.5	89
4.00	0.746	0.818	-0.072	21.3	8.9	20.4	12.6	14.5	89
3.75	0.703	0.782	-0.079	23.4	12.2	22.5	13.8	19.9	123
3.50	0.640	0.733	-0.093	27.5	23.6	26.5	16.2	38.4	237
3.25	0.520	0.638	-0.118	34.9	26.1	33.6	20.6	42.5	262
3.00	0.339	0.480	-0.141	41.7	26.1	40.2	24.6	42.5	262
6.09	0.846	0.846	0.000	0.0	10.2	0.0	0.0	16.6	102

TABLE XXXVI

CALCULATION OF SURFACE CHARGE DENSITY AND DIFFERENTIAL CAPACITY

BADDELEYITE IN 0.001 N KCl SOLUTION

TESTS No.31a AND No.33.

pH	Base Volume		Change In Base Volume	Adsorption $\Gamma_{H^+} - \Gamma_{OH^-}$	$-\left[\frac{d(\Gamma_{H^+}-\Gamma_{OH^-})}{d(pH)}\right]$	Surface Charge Density		Differential Capacity	
	Solids	No Solids							
	mℓ.	mℓ.	mℓ.	μmoles/gm.	μmoles/gm.	μcoul./gm. x10^{-5}	μcoul./cm.^{2}	μfd./gm. x10^{-6}	μfd./cm.^{2}
9.00	0.982	0.855	0.127	-37.5	11.4	-36.1	-22.2	18.6	115
8.50	0.956	0.851	0.105	-31.0	11.8	-29.8	-17.6	19.3	119
8.00	0.933	0.850	0.083	-24.5	11.8	-23.6	-14.5	19.3	119
7.50	0.908	0.849	0.059	-17.9	11.8	-16.8	-10.5	19.3	119
7.00	0.883	0.848	0.035	-10.8	9.4	-10.2	-6.6	15.4	94
6.50	0.863	0.847	0.016	-4.7	8.8	-4.5	-2.8	14.4	88
6.00	0.843	0.846	-0.003	0.9	8.8	0.9	0.5	14.3	88
5.50	0.828	0.845	-0.017	5.0	8.8	4.8	2.8	14.3	88
5.00	0.809	0.844	-0.035	10.6	8.8	10.2	6.6	14.3	88
4.50	0.784	0.843	-0.059	17.4	8.8	16.8	10.5	14.4	88
4.00	0.750	0.818	-0.068	20.1	8.8	19.3	11.9	14.4	88
3.75	0.709	0.782	-0.073	21.6	10.3	20.8	12.8	16.8	104
3.50	0.647	0.733	-0.086	25.4	15.7	24.4	15.0	25.6	158
3.25	0.528	0.638	-0.110	32.5	22.4	31.2	19.2	36.5	225
3.00	0.360	0.480	-0.120	35.4	22.5	34.0	20.9	36.7	226
6.07	0.846	0.846	0.000	0.0	8.8	0.0	0.0	14.3	88

TABLE XXXVII

CALCULATION OF SURFACE CHARGE DENSITY AND DIFFERENTIAL CAPACITY

RUTILE IN 0.1 N KCl SOLUTION

TESTS No.34 AND No.35.

pH	Base Volume		Change In Base Volume	Adsorption $\Gamma_{H^+} - \Gamma_{OH^-}$	$-\left[\frac{d(\Gamma_{H^+}-\Gamma_{OH^-})}{d(pH)}\right]$	Surface Charge Density		Differential Capacity	
	Solids	No Solids							
	mℓ.	mℓ.	mℓ.	μmoles/gm.	μmoles/gm.	μcoul/gm. $x10^{-5}$	μcoul/cm.^{2}	μfd/gm. $x10^{-6}$	μfd/cm.^{2} $x10^{-3}$
10.75	1.200	1.055	0.145	-42.8	31.7	-41.2	-1113	51.6	13.9
10.50	1.084	0.967	0.117	-34.5	22.5	-33.2	-897	36.6	9.91
10.25	1.020	0.917	0.103	-30.5	18.9	-29.3	-793	30.8	8.31
10.00	0.973	0.887	0.086	-25.5	22.8	-24.6	-663	37.2	10.1
9.50	0.893	0.855	0.038	-11.3	27.9	-10.9	-294	45.5	12.3
9.00	0.865	0.850	0.015	-4.5	19.1	-4.3	-117	31.2	8.42
8.50	0.860	0.849	0.011	-3.3	6.0	-3.2	-85.8	9.8	2.64
8.00	0.855	0.848	0.007	-2.0	2.4	-1.9	-52.0	3.9	1.08
7.50	0.850	0.847	0.003	-1.0	2.4	-1.0	-26.0	3.9	1.08
7.00	0.845	0.846	-0.001	0.3	2.4	0.3	7.8	3.9	1.08
6.50	0.839	0.845	-0.006	1.8	2.4	1.7	46.8	3.9	1.08
6.00	0.834	0.844	-0.010	3.0	2.4	2.9	78.0	3.9	1.08
5.50	0.829	0.843	-0.014	4.3	2.4	4.1	112	3.9	1.08
5.00	0.824	0.841	-0.017	5.0	3.6	4.8	130	5.9	1.56
4.50	0.810	0.835	-0.025	7.5	6.7	7.2	195	10.9	2.96
4.00	0.766	0.810	-0.044	13.0	12.7	12.5	338	20.7	5.59
3.75	0.725	0.782	-0.057	16.7	17.2	16.1	434	28.0	7.58
3.50	0.661	0.739	-0.078	23.0	37.5	22.2	598	61.1	16.5
3.25	0.538	0.662	-0.124	36.5	67.1	35.2	949	110	29.5
3.00	0.333	0.518	-0.185	54.5	78.7	52.5	1418	129	34.6
7.10	0.846	0.846	0.000	0.0	2.4	0.0	0.0	3.9	1.08

TABLE XXXVIII

CALCULATION OF SURFACE CHARGE DENSITY AND DIFFERENTIAL CAPACITY

RUTILE IN 0.01 N KCl SOLUTION

TESTS No.33 AND No.34.

pH	Base Volume		Change In	Adsorption	$-\left[\frac{d(\Gamma_{H^+}-\Gamma_{OH^-})}{d(pH)}\right]$	Surface Charge Density		Differential Capacity	
	Solid	No Solids	Base Volume	$\Gamma_{H^+} - \Gamma_{OH^-}$					
	mℓ.	mℓ.	mℓ.	μmoles/gm.	μmoles/gm.	μcoul./gm. x10^{-5}	μcoul./cm.^{2}	μfd./gm. x10^{-6}	μfd./cm.^{2} x10^{-3}
10.75	1.152	1.055	0.097	-28.8	11.7	-27.7	-749	19.1	5.13
10.50	1.057	0.967	0.090	-26.5	14.6	-25.5	-689	23.8	6.40
10.25	0.990	0.917	0.073	-21.5	22.4	-20.7	-559	36.6	9.86
10.00	0.942	0.887	0.055	-16.3	18.3	-15.7	-424	29.8	8.04
9.50	0.884	0.855	0.029	-8.5	12.7	-8.2	-221	20.7	5.57
9.00	0.861	0.850	0.011	-3.3	5.3	-3.2	-85.8	8.7	2.35
8.50	0.857	0.849	0.008	-2.3	1.4	-2.2	-59.8	2.3	0.64
8.00	0.853	0.848	0.005	-1.5	1.4	-1.4	-39.0	2.3	0.64
7.50	0.849	0.847	0.002	-0.5	1.4	-0.5	-13.0	2.3	0.69
7.00	0.845	0.846	-0.001	0.3	1.4	0.3	7.8	2.3	0.64
6.50	0.842	0.845	-0.003	1.0	1.4	1.0	26.0	2.3	0.64
6.00	0.838	0.844	-0.006	1.8	1.4	1.7	46.8	2.3	0.64
5.50	0.833	0.843	-0.010	3.0	1.4	2.9	78.0	2.3	0.64
5.00	0.829	0.841	-0.012	3.5	2.0	3.4	91.0	3.3	0.88
4.50	0.820	0.835	-0.015	4.5	4.2	4.3	117	6.9	1.83
4.00	0.784	0.810	-0.026	7.8	8.1	7.5	203	13.2	3.57
3.75	0.747	0.782	-0.035	10.3	14.2	9.9	268	23.2	6.25
3.50	0.689	0.739	-0.050	14.8	24.7	14.3	385	40.3	10.8
3.25	0.585	0.662	-0.077	22.8	41.6	22.0	593	68.0	18.3
3.00	0.395	0.518	-0.123	36.3	51.4	35.0	944	83.8	22.6
7.13	0.846	0.846	0.000	0.0	1.4	0.0	0.0	2.3	0.64

TABLE XXXIX

CALCULATION OF SURFACE CHARGE DENSITY AND DIFFERENTIAL CAPACITY

RUTILE IN 0.001 N KCl SOLUTION

TESTS No.34 AND No.36.

pH	Base Volume		Change In Base Volume	Adsorption $\Gamma_{H^+} - \Gamma_{OH^-}$	$-\left[\frac{d(\Gamma_{H^+}-\Gamma_{OH^-})}{d(pH)}\right]$	Surface Charge Density		Differential Capacity	
	Solids	No Solids							
	mℓ.	mℓ.	mℓ.	μmoles/gm.	μmoles/gm.	μcoul/gm. x10^{-5}	μcoul/cm^2	μfd/gm. x10^{-6}	μfd/cm^2 x10^{-3}
10.75	1.119	1.055	0.064	-19.0	8.9	-18.3	-494	14.5	3.91
10.50	1.028	0.967	0.061	-18.0	11.0	-17.3	-468	17.1	4.84
10.25	0.963	0.917	0.046	-13.5	16.1	-13.0	-351	26.3	7.09
10.00	0.920	0.887	0.033	-9.8	12.8	-9.4	-255	20.7	5.62
9.50	0.873	0.855	0.018	-5.3	8.4	-5.1	-138	13.7	3.69
9.00	0.855	0.850	0.005	-1.5	2.6	-1.4	-39.0	4.2	1.16
8.50	0.853	0.849	0.004	-1.2	0.8	-1.2	-31.2	1.3	0.35
8.00	0.850	0.848	0.002	-0.5	0.8	-0.6	-15.6	1.3	0.35
7.50	0.848	0.847	0.001	-0.3	0.8	-0.3	-7.8	1.3	0.35
7.00	0.845	0.846	-0.001	0.3	0.8	0.3	7.8	1.3	0.35
6.50	0.843	0.845	-0.002	0.6	0.8	0.6	15.6	1.3	0.35
6.00	0.840	0.844	-0.004	1.2	0.8	1.2	31.2	1.3	0.35
5.50	0.838	0.843	-0.005	1.5	0.8	1.4	39.0	1.3	0.35
5.00	0.835	0.841	-0.006	1.8	1.3	1.7	46.8	2.1	0.56
4.50	0.827	0.835	-0.008	2.3	2.1	2.2	59.8	3.4	0.94
4.00	0.796	0.810	-0.014	4.3	3.4	4.1	112	5.5	1.52
3.75	0.765	0.782	-0.017	5.0	4.3	4.8	130	7.0	1.91
3.50	0.717	0.739	-0.022	6.5	8.0	6.3	169	13.1	3.52
3.25	0.630	0.662	-0.032	9.5	14.5	9.1	247	23.7	6.37
3.00	0.470	0.518	-0.048	14.3	25.6	13.8	372	41.7	11.3
7.17	0.846	0.846	0.000	0.0	0.8	0.0	0.0	1.3	0.35

APPENDIX VI

SURFACE TENSION, CONDUCTANCE AND ABSORPTION SPECTRUM DATA

In order to use the equation relating surface tension to the capillary rise in two tubes, the radii of the tubes must be accurately calibrated. Using the following data, the radii have been calculated.

Density of mercury, ρ_{Hg}, at 23°C = 13.5389 gm./cm^3.

Weight of mercury in Tube 1 = 2.6671 gm.

Weight of mercury in Tube 2 = 0.1000 gm.

Test No.	Length of Mercury (cm.)	
	Tube 1	Tube 2
1	5.621	4.103
2	5.617	4.111
3	5.628	4.108
Av.	5.622	4.107

$$\text{Radius of Tube 1} = W/(\rho_{Hg}\ \ell\ \pi)$$

$$= 2.6671/(13.5389 \times 5.622 \times \pi)$$

$$= 1.0561 \times 10^{-1}\ \text{cm.}$$

$$\text{Radius of Tube 2} = 0.1000/(13.5389 \times 4.107 \times \pi)$$

$$= 2.393 \times 10^{-2}\text{cm.}$$

Assuming the density of the solutions is approximately 1.00, then

$$\gamma = [\rho \frac{g}{2} (\frac{r_1 r_2}{r_1 - r_2})] \Delta h$$

$$= [\frac{1.00 \times 980.6}{2} (\frac{1.0561 \times 10^{-1} \times 2.393 \times 10^{-2}}{1.0561 \times 10^{-1} - 2.393 \times 10^{-2}})] \Delta h$$

$$= 15.175 \Delta h$$

The surface tension was determined by measuring the height of liquid in the capillaries three times for each solution. The average is used to calculate the surface tension listed in Table XL.

TABLE XL

SURFACE TENSION OF DEHYDROABIETYLAMINE

ACETATE IN NEUTRAL SOLUTIONS

Concentration (mg./ℓ.)	pH	Δh (cm.)	γ (dynes/cm.)
0.0	5.40	4.702 4.707 4.705	71.40
0.0	5.47	4.740 4.735 4.740	71.90
0.2	5.55	4.724 4.732 4.735	71.78
0.5	5.48	4.744 4.749 4.755	72.07
0.5	5.50	4.713 4.717 4.707	71.50
1.0	5.62	4.689 4.676 4.689	71.09
2.0	5.60	4.691 4.690 4.690	71.17
5.0	5.90	4.492 4.557 4.528	68.77

TABLE XL (continued)

Concentration (mg./ℓ.)	pH	Δh (cm.)	γ (dynes/cm.)
10	6.25	4.454 4.452 4.458	67.61
10	6.28	4.562 4.560 4.570	69.25
20	6.45	4.530 4.525 4.528	68.70
20	6.42	4.352 4.358 4.361	66.12
50	6.05	4.048 4.060 4.051	61.50
50	6.20	4.319 4.317 4.314	65.50
100	6.20	3.740 3.741 3.745	56.78
100	6.15	3.841 3.848 3.838	58.31

TABLE XL (continued)

Concentration (mg./ℓ.)	pH	Δh (cm.)	γ (dynes/cm.)
200	6.25	3.549 3.548 3.545	53.83
300	6.30	3.152 3.135 3.146	47.71
500	6.40	3.062 3.062 3.068	46.50
700	6.48	2.808 2.813 2.758	42.38
900	6.41	2.747 2.755 2.739	41.69
2000	6.60	2.373 2.473 2.420	36.75

TABLE XLI

SPECIFIC CONDUCTANCE OF DEHYDROABIETYLAMINE

ACETATE SOLUTIONS.

Concentration	Resistance	Specific Conductance
(mg./ℓ.)	ohms	mhos/cm.x10^4
2000	322	3.12
1712	373	2.69
1471	431	2.33
1233	507	1.98
1053	594	1.69
867	713	1.41
698	880	1.14
522	1,165	0.862
407	1,490	0.675
315	1,910	0.527
222	2,720	0.370
149	3,990	0.252
100	5,900	0.170
63	10,030	0.100
23	31,400	0.032

TABLE XLII

EQUIVALENT CONDUCTANCE OF DEHYDROABIETYLAMINE ACETATE SOLUTIONS

Concentration		$(\text{Concentration})^{1/2}$	Specific Conductance	Equivalent Conductance
mg./ℓ.	equiv./ℓ.	$(\text{equiv./ℓ})^{1/2}$	mho/cm.	$(\text{mho-cm}^2\text{./equiv.})$
2000	5.79×10^{-3}	0.0760	31.2×10^{-5}	5[illegible].0
1200	3.47×10^{-3}	0.0589	19.2×10^{-5}	55.3
1000	2.89×10^{-3}	0.0538	16.0×10^{-5}	55.4
800	2.32×10^{-3}	0.0482	13.1×10^{-5}	56.5
600	1.74×10^{-3}	0.0417	9.85×10^{-5}	56.6
400	1.16×10^{-3}	0.0341	6.60×10^{-5}	56.9
300	8.68×10^{-4}	0.0295	4.98×10^{-5}	57.4
200	5.79×10^{-4}	0.0241	3.37×10^{-5}	58.3
100	2.89×10^{-4}	0.0170	1.70×10^{-5}	58.9
50	1.45×10^{-4}	0.0120	0.85×10^{-5}	59.2
30	8.68×10^{-5}	0.0093	0.52×10^{-5}	59.5

TABLE XLIII

ABSORPTION SPECTRUM OF

DEHYDROABIETYLAMINE ACETATE SOLUTIONS

Wavelength (mμ)	Concentration ($\frac{mg.}{\ell.}$)	Slit Width (mm)	%Trans.	Absorb'n.
215	2000	1.20	0.25	2.60
220	"	1.10	0.25	2.60
225	"	0.90	0.22	2.65
230	"	0.80	0.32	2.49
232	"	0.70	0.22	2.65
234	"	"	3.1	1.51
236	"	"	13.5	0.875
238	"	"	25.0	0.603
240	"	"	28.7	0.547
242	"	0.68	26.5	0.578
244	"	"	21.7	0.667
246	"	"	15.9	0.800
248	"	"	11.3	0.947
250	"	"	7.4	1.14
252	"	"	4.4	1.32
254	"	0.55	2.6	1.60
256	"	"	1.82	1.74
258	"	"	0.80	2.10
260	"	"	0.36	2.45
262	"	"	0.30	2.54
264	"	"	0.13	2.90
266	"	"	0.18	2.80
268	"	"	0.14	2.87
270	"	"	0.33	2.48
272	"	0.48	0.37	2.40
274	"	"	0.59	2.23
278	"	"	1.20	1.93
279	"	"	4.9	1.31
280	"	"	13.9	0.860
281	"	"	27.9	0.559
282	"	"	40.9	0.389
283	"	"	53.9	0.269

continued...

TABLE XLIII(continued)

Wavelength(mμ)	Concentration($\frac{mg.}{\ell}$)	Slit Width (mm)	%Trans.	Absorb'n.
284	2000	0.48	64.8	0.190
286	"	"	76.4	0.117
288	"	"	82.2	0.085
290	"	"	84.4	0.074
295	"	"	86.0	0.065
300	"	0.40	86.0	0.065
325	"	"	89.3	0.049
254	2000	0.55	2.6	1.60
"	1000	"	15.1	0.820
"	500	"	37.7	0.424
"	200	"	65.9	0.182
"	100	"	79.3	0.101
264	500	0.55	14.8	0.830
"	200	"	45.2	0.344
"	100	"	65.7	0.182
"	50	"	80.2	0.095
"	20	"	89.6	0.048
254	0	0.55	95.6	0.020
264	0	0.55	96.7	0.015

APPENDIX VII

TABULATED ADSORPTION, WORK OF ADHESION AND FLOTATION RESULTS

TABLE XLIV

ADSORPTION OF DEHYDROABIETYLAMINE ACETATE ON QUARTZ
IN NEUTRAL SOLUTIONS (spec. surf. = 1407 $cm^2./gm.$)

Test No.	Solution Concentration			pH of Solution	Weight of Amine Adsorbed	Specific Adsorption			Surface Coverage
	Before Adsorption	After Adsorption							
	mg./ℓ.	mg./ℓ.	μ mole/ℓ.		μgm.	μgm./gm.	μgm./cm^2.	μ mole/M^2.	%
1	2000	1900	5,500	6.00	4750	2375	1.690	49.0	1470
2	1000	940	2,720	5.95	2845	1423	1.005	29.1	874
3	500	455	1,318	5.70	2140	1070	0.760	22.0	660
4	200	160	463	5.45	1900	950	0.675	19.5	587
5	100	77	223	5.40	1191	596	0.424	12.3	368
6	50	34	98.5	5.40	760	380	0.270	7.82	235
7	20	11.4	33.0	5.05	408	204	0.145	4.20	126
8	10	2.6	7.51	5.00	351	176	0.125	3.62	108
9	5	0.6	1.74	5.00	209	105	0.0743	2.15	64.6
10	2	0.1	0.29	5.03	90.2	45.1	0.0321	0.93	27.9

TABLE XLV

ADSORPTION OF DEHYDROABIETYLAMINE ACETATE ON HEMATITE

IN NEUTRAL SOLUTIONS (spec. surf. = 1372 $cm^2./gm.$)

Test No.	Solution Concentration			pH of Solution	Weight of Amine Adsorbed	Specific Adsorption			Surface Coverage
	Before Adsorption	After Adsorption							
	mg./ℓ.	mg./ℓ.	μmole/ℓ.		μgm.	μgm./gm.	μgm./cm^2.	μmole/M^2.	%
1	2000	1960	5675	6.08	1900	950	0.692	20.0	601
2	1000	955	2765	6.06	2138	1069	0.779	22.5	676
3	500	465	1347	5.84	1663	832	0.606	17.5	527
4	200	177	513	5.68	1093	547	0.398	11.5	346
5	100	78	226	5.40	1045	523	0.381	11.0	331
6	50	34.5	100	5.36	736	368	0.268	7.76	233
7	20	11.0	31.9	5.38	428	214	0.156	4.52	136
8	10	5.5	16.0	5.45	214	107	0.0780	2.26	67.8
9	5	1.5	4.35	5.35	166	83	0.0605	1.75	52.5
10	2	0.8	2.32	5.38	57	28	0.0209	0.604	18.2
11	1	0.2	0.58	5.42	37	19	0.0136	0.396	11.8

TABLE XLVI

ADSORPTION OF DEHYDROABIETYLAMINE ACETATE ON RUTITE

IN NEUTRAL SOLUTIONS (spec. surf. = 3,610 $cm^2/gm.$)

Test No.	Solution Concentration			pH of Solution	Weight of Amine Adsorbed	Specific Adsorption			Surface Coverage
	Before Adsorption	After Adsorption							
	mg./ℓ.	mg./ℓ.	μmole/ℓ.		μgm.	μgm/gm.	μgm./cm^2	μmole/M^2	%
1	2000	1.908	5520	6.35	4370	2185	0.6000	17.3	520
2	1000	932	2700	6.40	3230	1615	0.442	12.8	385
3	500	424	1225	6.40	3610	1805	0.495	14.3	430
4	500	430	1243	6.00	3320	1660	0.455	13.2	397
5	200	148	428	6.40	2470	1235	0.338	9.80	295
6	200	150	434	5.62	2375	1188	0.326	9.40	283
7	100	63.6	184	6.45	1730	865	0.237	6.85	206
8	100	65.9	191	5.42	1620	810	0.222	6.41	193
9	50	28.1	81.5	6.50	1040	520	0.142	4.12	124
10	50	30.0	86.7	5.80	950	475	0.130	3.76	113
11	25.4	12.6	36.5	6.55	608	304	0.0832	2.41	72.5
12	20	7.5	21.7	5.60	594	297	0.0814	2.35	70.6
13	10	4.0	11.6	5.47	285	143	0.0390	1.13	36.0
14	5	0.9	2.61	5.60	195	97.5	0.0264	0.77	24.6
15	2	0.2	0.58	5.80	85.5	42.7	0.0117	0.338	10.8

TABLE XLVII

ADSORPTION OF DEHYDROABIETYLAMINE ACETATE ON BADDELEYITE IN NEUTRAL SOLUTIONS (spec. surf. = 16.3 M^2/gm.)

Test No.	Solution Concentration			pH of Solution	Weight of Amine Adsorbed	Specific Adsorption			Surface Coverage
	Before Adsorption	After Adsorption							
	mg./ℓ.	mg./ℓ.	μmole/ℓ.		μgm.	μgm./gm.	μgm./cm^2	μmole/M^2	%
1	2000	942	2740	6.35	50,150	25,080	0.1540	4.46	134
2	2000	928	2690	6.05	51,000	25,500	0.1565	4.53	137
3	2000	894	2600	6.25	52,500	26,250	0.1610	4.67	141
4	1000	338	980	5.90	31,450	15,730	0.0965	2.80	84.3
5	1000	380	1104	5.75	29,450	14,720	0.0905	2.62	79.0
6	1000	306	890	5.85	32,900	16,450	0.1010	2.92	88.0
7	500	130	378	6.05	17,600	8,800	0.0540	1.56	47.0
8	500	145	420	6.00	16,900	8,450	0.0519	1.50	45.1
9	500	125	363	5.80	17,800	8,900	0.0546	1.58	47.6
10	200	30.0	87.1	5.75	8,070	4,040	0.0248	0.720	21.7
11	200	27.0	78.5	5.95	8,210	4,100	0.0252	0.730	22.0
12	100	5.0	14.5	6.10	4,500	2,250	0.0138	0.400	12.1
13	100	5.4	15.7	6.20	4,480	2,240	0.0137	0.40	12.0
14	50	1.5	4.35	6.10	2,300	1,150	0.0071	0.20	6.1

TABLE XLVIII

DETERMINATION OF "$(\Gamma_R)_o$" AND "b" FOR HEMATITE AND RUTILE

Concentration	Specific Adsorption	C_R/Γ_R	Remarks
μmole/ℓ.	Gibbs	μmole/ℓ. Gibbs	
Hematite			
10,000	22.4	446	
5,675	20.0	284	$(\Gamma_R)_o$ = 23.2 Gibbs
5,000	21.8	229	
2,765	22.5	123	b = 2.87×10^{-3}
2,000	19.4	103	(μmole/ℓ.)$^{-1}$
1,347	17.5	77	
1,000	16.3	61.4	
573	11.5	44.6	
500	13.3	37.6	
226	11.0	20.5	
200	9.4	21.3	
Rutile			
10,000	18.0	555	
5,520	17.4	317	$(\Gamma_R)_o$ = 18.6 Gibbs
5,000	17.3	291	
2,700	12.5	216	b = 2.83×10^{-3}
2,000	15.5	129	(μmole/ℓ.)$^{-1}$
1,225	14.3	86	
1,000	13.3	75.7	
500	10.2	49.0	
429	9.8	44.0	
200	6.4	31.0	
184	6.8	27.0	

TABLE XLIX

ADSORPTION OF DEHYDROABIETYLAMINE ACETATE ON RUTILE

AS A FUNCTION OF CONCENTRATION AND pH (spec. surf. = 3,610 $cm.^2/gm.$)

Test No.	Solution Concentration			pH of Solution	Weight of Amine Adsorbed	Specific Adsorption			Surface Coverage
	Before Adsorption	After Adsorption							
	mg./ℓ	mg./ℓ	μmole/ℓ		μgm.	μgm./gm.	$\mu gm./cm^2$	$\mu mole/M^2$	%
A-1	87.3	87.0	252	2.50	19.5	7.2	0.00135	0.04	1.2
A-2	155	150	435	2.50	242	121	0.0323	0.87	28.4
A-3	282	276	816	2.50	300	150	0.0405	1.17	35.2
A-4	541	530	1570	2.50	500	250	0.0675	1.95	87.9
A-5	515	505	1490	2.50	500	250	0.0675	1.95	87.9
A-6	2050	2040	5900	2.50	500	250	0.0675	1.95	87.9
B-1	25	19.9	57.6	3.90	244	122	0.0329	0.95	28.6
B-2	50	42.8	124	3.90	344	172	0.0465	1.35	40.4
B-3	100	90.2	261	3.90	469	235	0.0632	1.83	55.0
B-4	200	184	533	3.80	759	380	0.102	2.95	88.9
B-5	500	480	1390	3.90	950	475	0.128	3.70	111.2
B-6	1000	980	2840	3.80	959	480	0.129	3.73	112.2
B-7	2000	1976	5720	3.83	1156	578	0.155	4.49	134.7
C-1	25.2	14.5	42.0	5.00	512	256	0.0692	2.00	60.2
C-2	150	34.5	100	5.00	742	371	0.100	2.90	87.0
C-3	100	70.4	204	5.98	1410	705	0.190	5.50	165
C-4	200	162	470	5.00	1815	908	0.245	7.10	213
C-5	500	454	1313	5.98	2195	1098	0.296	8.57	245
C-6	1000	958	2770	4.98	2000	1000	0.270	7.82	235
C-7	2000	1952	5660	5.02	2300	1150	0.310	8.97	270

continued....

TABLE XLIX (continued)

Test No.	Solution Concentration			pH of Solution	Weight of Amine Adsorbed	Specific Adsorption			Surface Coverage
	Before Adsorption	After Adsorption							
	mg./ℓ.	mg./ℓ.	μmole/ℓ.		μgm.	μgm./gm.	μgm./cm.^{2}	μmole/M.^{2}	%
D-1 to D-7	See Table XLVI								
E-1	25	2.5	7.2	9.65	1083	542	0.146	4.23	127
E-2	30	2.0	5.8	9.70	1350	675	0.182	5.27	158
E-3	50	21.9	63.5	8.65	1342	671	0.181	5.24	158
E-4	50	23.0	66.6	8.70	1300	650	0.175	5.07	152
E-5	100	63.2	183	8.05	1760	880	0.237	6.86	206
E-6	100	66.0	191	8.28	1645	823	0.222	6.43	193
E-7	200	140	405	7.85	2860	1430	0.386	11.2	346
E-8	200	145	420	7.98	2645	1323	0.357	10.3	310
E-9	500	431	1250	7.25	3300	1650	0.445	12.9	387
E-10	1000	917	2660	7.23	3920	1960	0.529	15.3	460
E-11	2000	1894	5490	6.92	5730	2565	0.691	20.0	602

TABLE L

ADSORPTION OF DEHYDROABIETYLAMINE ACETATE ON QUARTZ
AS A FUNCTION OF pH(spec. surf. = 1407 $cm.^2/gm.$)

Test No.	Solution Concentration			pH of Solution	Weight of Amine Adsorbed	Specific Adsorption			Surface Coverage
	Before Adsorption	After Adsorption							
	mg./ℓ	mg./ℓ	μmole/ℓ		μgm.	μgm./gm.	$\mu gm/cm^2$	$\mu mole/M.^2$	%
1	47.9	2.7	7.8	10.68	2130	1065	0.757	21.92	657
2	48.9	2.3	6.7	10.05	2200	1100	0.782	22.62	680
3	49.1	2.1	6.1	9.82	2220	1110	0.790	22.85	687
4	49.3	2.8	8.1	9.70	2195	1098	0.780	22.60	677
5	49.5	5.0	14.5	8.80	2100	1050	0.747	21.60	650
6	49.6	6.5	18.8	8.04	2035	1017	0.723	20.93	629
7	49.7	10.5	30.4	6.80	1850	925	0.658	19.05	571
8	49.8	17.2	49.8	6.48	1540	770	0.547	15.82	475
9	49.9	29.0	84.0	6.30	1460	730	0.520	15.04	451
10	50.0	39.5	114	6.00	495	248	0.176	5.09	153
11	50.0	49.8	144	4.25	9.5	4.7	0.0033	0.10	2.9
12	50.0	49.7	144	3.90	14.2	7.1	0.0050	0.15	4.3
13	50.0	49.9	144	3.80	4.7	2.3	0.0016	0.05	1.4
14	49.8	49.7	144	3.58	4.7	2.3	0.0016	0.05	1.4
15	49.7	49.5	143	3.38	9.5	4.7	0.0033	0.10	2.9
16	50.0	48.0	139	5.00	9.5	47.5	0.033	0.95	28.6
17	50.0	45.0	130	5.55	238	119	0.084	2.45	73.8

TABLE L (continued)

ADSORPTION OF DEHYDROABIETYLAMINE ACETATE ON QUARTZ

AS A FUNCTION OF pH

Test No.	pH of Solution	Solution Concentration After Adsorption	Specific Adsorption	Specific Adsorption Corrected to Solution Concentration of 100μ mole/ℓ.	Surface Coverage
		μmole/ℓ	μmole/M^2	μmole/M^2	%
1	10.68	7.8	21.92	62.6	1880
2	10.05	6.7	22.62	68.5	2060
3	9.82	6.1	22.85	71.8	2160
4	9.70	8.1	22.60	63.3	1900
5	8.80	14.5	21.60	47.7	1430
6	8.04	18.8	20.93	41.5	1250
7	6.80	30.4	19.05	31.0	932
8	6.48	49.8	15.82	21.1	634
9	6.30	84.0	15.04	16.2	487
10	6.00	114	5.09	4.82	145
11	4.25	144	0.10	.082	2.5
12	3.90	144	0.15	.125	3.7
13	3.80	144	0.05	.040	1.2
14	3.58	144	0.5	.040	1.2
15	3.38	143	0.10	.082	2.5
16	5.00	139	0.95	.081	24.2
17	5.55	130	2.45	2.15	64.8

TABLE LI

ADSORPTION OF DEHYDROABIETYLAMINE ACETATE ON HEMATITE AS A FUNCTION OF pH (spec.surf. = 1372 $cm^2./gm.$)

Test No.	Solution Concentration			pH of Solution	Weight of Amine Adsorbed	Specific Adsorption			Surface Coverage
	Before Adsorption	After Adsorption							
	mg./ℓ	mg./ℓ	μmole/ℓ		μgm.	μgm./gm.	μgm./cm^2	μmole/M^2	%
1	49.5	49.4	143	2.85	4.8	2.4	0.0018	0.05	1.6
2	59.8	49.7	144	3.58	4.8	2.4	0.0018	0.05	1.6
3	50.0	49.7	144	3.70	14.4	7.2	0.0053	0.15	4.6
4	50.0	34.5	100	5.50	736	368	0.268	7.75	233
5	50.0	34.0	98.5	5.62	760	380	0.277	8.01	241
6	50.0	34.0	98.5	5.72	760	380	0.277	8.01	241
7	49.8	31.0	89.9	6.10	896	448	0.326	9.44	283
8	49.5	11.2	32.4	6.60	1820	910	0.662	19.17	575
9	48.9	1.5	4.34	9.67	2250	1125	0.820	23.75	713
10	47.9	3.4	9.85	10.35	2120	1060	0.773	22.40	675
11	49.2	3.5	10.13	9.00	2165	1083	0.789	22.80	687
12	49.3	4.5	13.03	8.25	2083	1042	0.760	22.00	664
13	49.6	18.5	53.6	7.00	1480	740	0.540	15.63	471
14	49.7	24.0	69.5	6.70	1222	611	0.446	12.92	390
15	49.8	36.0	104	6.52	655	328	0.239	6.92	208
16	49.9	35.5	103	6.43	685	342	0.249	7.21	213
17	50.0	47.5	137	4.40	119	60	0.0437	1.27	38.3
18	49.9	49.7	144	3.80	9.5	4.7	0.0034	0.098	3.0
19	50.0	49.0	142	4.10	47.5	23.8	0.0173	0.50	15.0
20	50.0	45.0	130	5.00	214	107	0.0780	2.26	68.0

TABLE LI (continued)

ADSORPTION OF DEHYDROABIETYLAMINE ACETATE ON HEMATITE

AS A FUNCTION OF pH.

Test No.	pH of Solution	Solution Concentration After Adsorption	Specific Adsorption	Specific Adsorption Corrected to Solution concentration of 100 μmole/ℓ.	Surface coverage
		μmole/ℓ.	μmole/M^2.	μmole/M^2	%
1	2.85	143	0.05	0.04	1.3
2	3.58	144	0.05	0.04	1.3
3	3.70	144	0.15	0.13	3.8
4	5.50	100	7.75	7.75	233
5	5.62	98.5	8.01	8.08	242
6	5.72	98.5	8.01	8.08	242
7	6.10	89.9	9.44	9.95	298
8	6.60	32.4	19.17	21.7	654
9	9.67	4.3	23.75	23.7	715
10	10.35	9.9	22.40	23.1	695
11	9.00	10.1	22.80	23.1	695
12	8.25	13.0	22.00	23.0	693
13	7.00	53.6	15.63	18.4	554
14	6.70	69.5	12.92	15.5	467
15	6.52	104	6.92	6.79	204
16	6.43	103	7.21	7.10	214
17	4.40	137	1.27	1.09	32.8
18	3.80	144	0.10	0.08	2.5
19	4.10	142	0.50	0.42	12.7

TABLE LII

ADSORPTION OF DEHYDROABIETYLAMINE ACETATE ON RUTILE
AS A FUNCTION OF pH (spec. surf. = 3,610 cm^2./gm.)

Test No.	Solution Concentration			pH of Solution	Weight of Amine Adsorbed	Specific Adsorption			Surface Coverage
	Before Adsorption	After Adsorption							
	mg./ℓ.	mg./ℓ.	μmole/ℓ.		μgm.	μgm./gm.	μgm./cm^2	μmole/M^2	%
1	50	48.5	140	3.65	71	36	0.0096	0.283	8.5
2	50	42.5	123	4.70	356	178	0.0480	1.43	42.9
3	50	36.2	105	4.90	655	328	0.0884	2.63	78.8
4	50	34.2	99.0	5.00	750	375	0.101	3.00	90.0
5	50	30.5	88.4	5.10	925	463	0.125	3.71	111
6	50	27.0	78.1	5.25	1091	545	0.147	4.37	131
7	50	17.5	50.6	5.35	831	416	0.112	6.20	186
8	50	7.5	21.7	5.55	2020	1010	0.272	8.09	242
9	50	0.7	2.0	6.30	2340	1170	0.316	9.38	281
10	50	1.0	2.9	8.00	2330	1165	0.315	9.34	280
11	50	0.6	1.7	8.90	2343	1172	0.317	9.40	282
A-1	50	49.8	144	2.50	9.5	4.8	0.0013	0.038	1.1
B-2	50	42.8	124	3.90	344	172	0.0465	1.35	40.4
C-2	50	34.5	100	4.98	742	371	0.100	2.90	87.0
D-2	50	28.1	81.5	5.50	1040	520	0.140	4.12	124
E-3	50	21.9	63.5	8.65	1342	671	0.181	5.24	158

TABLE LII (continued)

ADSORPTION OF DEHYDROABIETYLAMINE ACETATE ON RUTILE

AS A FUNCTION pH

Test No.	pH of Solution	Solution Concentration After Adsorption	Specific Adsorption	Specific Adsorption Corrected to Solution Concentration of 100 μmole/ℓ.	Surface Coverage
		μmole/ℓ.	μmole/M.^{2}	μmole/M.^{2}	%
1	3.65	140	0.283	0.242	7.3
2	4.70	123	1.43	1.29	38.8
3	4.90	105	2.63	2.56	77.1
4	5.00	99.0	3.00	3.02	91.0
5	5.10	88.4	3.71	3.95	119
6	5.25	78.1	4.37	4.94	149
7	5.35	50.6	6.20	8.70	262
8	5.55	21.7	8.09	16.4	494
9	6.30	2.0	9.38	17.0	512
10	8.00	2.9	9.34	17.0	512
11	8.90	1.7	9.40	17.1	515
A-1	2.50	144	0.038	0.032	1.0
B-2	3.90	124	1.35	1.21	36.4
C-2	4.98	100	2.90	2.90	87.4
D-2	5.50	81.5	4.12	4.53	136
E-3	8.65	63.5	5.24	6.59	198

TABLE LIII

ADSORPTION OF DEHYDROABIETYLAMINE ACETATE ON BADDELEYITE AS A FUNCTION OF pH (spec. surf. = 16.3 $M.^2/gm.$)

Test No.	Solution Concentration			pH of Solution	Weight of Amine Adsorbed	Specific Adsorption			Surface Coverage
	Before Adsorption	After Adsorption							
	mg./ℓ.	mg./ℓ.	μmole/ℓ.		μgm.	μgm./gm.	μgm./$cm.^2$	μmole/$M.^2$	%
1	50.0	1.5	10.15	10.15	2300	1150	0.00705	0.205	6.18
2	50.0	2.2	7.15	7.15	2270	1135	0.00696	0.202	6.08
3	50.0	3.5	10.1	6.35	2210	1105	0.00678	0.196	5.90
4	50.0	2.9	8.40	6.25	2240	1120	0.00687	0.199	6.00
5	50.0	3.3	9.6	6.15	2220	1110	0.00681	0.197	5.93
6	50.0	4.7	13.6	5.90	2150	1075	0.00660	0.191	5.75
7	50.0	34.5	100	5.35	735	368	0.00226	0.146	4.40
8	50.0	31.7	91.7	5.15	870	435	0.00267	0.077	2.32
9	50.0	34.3	99.2	5.10	745	372	0.00228	0.066	1.99
10	50.0	44.5	129	4.65	265	133	0.00082	0.023	0.69
11	50.0	45.5	132	3.80	214	107	0.00066	0.019	0.57
12	50.0	46.7	135	3.30	157	79	0.00048	0.014	0.42
13	50.0	46.9	136	3.05	147	74	0.00045	0.013	0.39
14	50.0	47.2	137	2.10	133	67	0.00041	0.012	0.36

TABLE LIII (continued)

ADSORPTION OF DEHYDROABIETYLAMINE ACETATE ON BADDELEYITE

AS A FUNCTION OF pH

Test No.	pH of Solution	Solution Concentration After Adsorption	Specific Adsorption	Specific Adsorption Corrected to Solution Concentration of 100μ moles/ℓ.	Surface Coverage
		μmole/ℓ.	μmole/M^2	μmole/M^2	%
1	10.15	4.34	0.205	0.980	29.5
2	7.15	6.36	0.202	0.794	23.9
3	6.35	10.1	0.196	0.615	18.5
4	6.25	8.40	0.199	0.686	20.7
5	6.15	9.6	0.197	0.636	19.2
6	5.90	13.6	0.191	0.517	15.6
7	5.35	100	0.146	0.146	4.40
8	5.15	91.7	0.077	0.080	2.41
9	5.10	99.2	0.066	0.066	1.99
10	4.65	129	0.023	0.022	0.66
11	3.80	132	0.019	0.017	0.57
12	3.30	135	0.014	0.012	0.36
13	3.05	136	0.013	0.011	0.33
14	2.10	137	0.012	0.010	0.30

TABLE LIV

WORK OF ADHESION OF AN AIR BUBBLE ON QUARTZ

Concentration of DHAA	Surface Tension, γ	Contact Angle, θ			Cos θ_E	1 - cos θ_E	Work of Adhesion
		Advancing	Equilibrium	Receding			
mg./ℓ.	dynes/cm.	degrees	degrees	degrees			ergs/cm^2.
0	71.65	0	0	0	1.000	0.000	0.00
0.2	71.78	0	0	0	1.000	0.000	0.00
0.5	71.79	3	13	22	0.975	0.025	1.79
1	71.09	21	31	43	0.856	0.144	10.25
2	71.17	27	37	49	0.799	0.201	14.30
5	68.77	26	38	49	0.788	0.212	14.58
10	68.43	27	38	47	0.788	0.212	14.50
20	67.41	31	42	53	0.743	0.258	17.36
50	63.50	35	46	59	0.695	0.305	19.38
100	57.55	35	48	53	0.670	0.330	19.00
200	53.83	35	47	59	0.681	0.319	17.15
500	46.50	42	53	65	0.601	0.399	18.55
1000	41.50	41	51	65	0.630	0.370	15.35
2000	36.75	35	48	58	0.670	0.330	12.12

TABLE LV

WORK OF ADHESION OF AN AIR BUBBLE ON HEMATITE

Concentration of DHAA	Surface Tension, γ	Contact Angle, θ			Cos θ_E	1 - cos θ_E	Work of Adhesion
		Advancing	Equilibrium	Receding			
mg./ℓ.	dynes/cm.	degrees	degrees	degrees			ergs/cm^2.
0	71.65	0	0	0	1.000	0.000	0.00
0.2	71.78	0	0	0	1.000	0.000	0.00
0.5	71.79	0	0	0	1.000	0.000	0.00
1	71.09	8	10	20	0.985	0.015	1.07
2	71.17	14	18	27	0.950	0.050	3.56
5	68.77	14	21	40	0.934	0.066	4.53
10	68.43	24	31	48	0.856	0.144	9.84
20	67.41	27	35	51	0.820	0.180	12.11
50	63.50	38	45	63	0.707	0.293	18.60
100	57.55	36	49	65	0.655	0.345	19.85
200	53.83	33	49	67	0.655	0.345	18.60
500	46.50	35	51	71	0.630	0.370	17.20
1000	41.50	29	48	67	0.670	0.330	13.70
2000	36.75	33	44	54	0.720	0.280	10.30

TABLE LVI

WORK OF ADHESION OF AN AIR BUBBLE ON RUTILE

Concentration of DHAA	Surface Tension, γ	Contact Angle, θ			Cos θ_E	1-cos θ_E	Work of Adhesion
		Advancing	Equilibrium	Receding			
mg./ℓ.	dynes/cm.	degrees	degrees	degrees			ergs/cm^2.
0	71.65	0	0	0	1.000	0.000	0.00
0.2	71.78	0	0	0	1.000	0.000	0.00
0.5	71.79	10	20	30	0.940	0.060	4.30
1	71.09	40	54	89	0.588	0.412	29.30
2	71.17	45	66	90	0.407	0.593	42.20
5	68.77	48	64	90	0.438	0.562	38.60
10	68.43	53	58	90	0.530	0.470	32.10
20	67.41	49	64	90	0.438	0.562	37.80
50	63.50	45	65	92	0.422	0.578	36.70
100	57.55	41	62	81	0.470	0.530	30.50
200	53.83	25	50	72	0.643	0.357	19.20
500	46.50	30	47	70	0.682	0.318	14.80
1000	41.00	19	35	68	0.820	0.180	7.47
2000	36.75	8	30	61	0.866	0.134	4.92

TABLE LVII

WORK OF ADHESION OF AN AIR BUBBLE ON BADDELEYITE

Concentration of DHAA	Surface Tension, γ	Contact Angle θ			Cos θ_E	1 - cos θ_E	Work of Adhesion
		Advancing	Equilibrium	Receding			
mg./ℓ.	dynes/cm.	degrees	degrees	degrees			ergs/cm^2.
0	71.65	-	-	-	1.000	0.000	0.00
0.2	71.78	-	-	-	"	"	"
0.5	71.79	-	-	-	"	"	"
1	71.09	-	-	-	"	"	"
2	71.17	-	-	-	"	"	"
5	68.77	-	-	-	"	"	"
10	68.43	-	-	-	"	"	"
20	67.41	-	20	-	0.940	0.060	4.04
50	63.50	-	35	-	0.820	0.180	11.42
100	57.55	-	41	-	0.755	0.245	14.10
200	53.83	-	55	-	0.574	0.426	22.90
500	46.50	-	57	-	0.545	0.455	21.10
1000	41.00	-	56	-	0.560	0.440	18.05
2000	36.75	-	58	-	0.530	0.470	17.25

TABLE LVIII

HALLIMOND TUBE

FLOTATION RESULTS

Total Amine Concentration (initial)	Percent Recovery			
	Quartz	Hematite	Rutile	Baddeleyite
mg./l.				
0	2.8	2.7	7.4	2.3
2	44.5	42.7	28.5	-
5	78.4	48.5	52.0	-
10	87.2	63.9	63.0	-
20	89.5	80.0	67.7	-
50	93.2	76.5	72.6	7.5
100	96.5	79.5	76.0	22.5
200	92.4	84.5	73.2	24.0
500	88.2	80.6	66.4	30.4
1000	80.3	76.1	63.5	30.5
2000	45.9	71.0	21.5	34.4
50 (pH)=	49.7 (3.70)	40.0 (3.75)	44.8 (3.70)	-
50 (pH)=	93.6 (9.10)	83.9 (8.88)	75.8 (8.31)	-
500 (pH)=	-	-	-	4.3 (3.70)
500 (pH)=	-	-	-	32.9 (5.70)

TABLE LIX

HALLIMOND TUBE FLOTATION OF SILICA AND HEMATITE
(USING 50% SiO_2 - 50% Fe_2O_3 SAMPLES)

Sample No.	Weight %	Analysis		Distribution		pH	Amine Conc'n mg./ℓ	Starch Conc'n mg./ℓ
		%Fe_2O_3	%SiO_2	%Fe_2O_3	%SiO_2			
A Froth	66.1	49.6	50.4	64.5	67.9	5.2	2	0
Conc.	33.9	53.5	46.5	35.5	32.1			
B Froth	71.5	48.5	51.5	69.3	74.0	5.3	5	0
Conc.	28.5	53.8	46.2	30.7	26.0			
C Froth	76.0	48.3	51.7	72.6	79.0	5.3	10	0
Conc.	24.0	57.5	42.5	27.4	21.0			
D Froth	79.5	47.2	52.8	74.3	84.5	5.3	20	0
Conc.	20.5	62.7	37.3	25.7	15.5			
E Froth	31.0	60.5	39.5	38.0	24.2	9.7	2	25
Conc.	69.0	44.5	55.5	62.0	75.8			
F Froth	33.6	46.8	53.2	31.6	35.1	9.6	5	25
Conc.	66.4	50.8	49.2	68.4	64.9			
G Froth	48.0	33.7	66.3	32.6	63.0	9.9	10	25
Conc.	52.0	64.3	35.7	67.4	37.0			
H Froth	50.0	24.3	75.7	24.4	75.3	9.9	20	25
Conc.	50.0	75.3	24.7	75.6	24.7			
I Froth	17.7	27.1	72.9	9.7	25.7	9.9	2	25*
Conc.	82.3	54.6	45.4	90.3	74.3			
J Froth	22.6	29.7	70.3	13.6	31.2	9.8	5	25*
Conc.	77.4	55.0	45.0	86.4	68.8			
K Froth	27.7	15.1	84.9	11.6	64.3	9.6	10	25*
Conc.	72.3	71.2	28.8	88.4	35.7			
L Froth	51.3	15.7	84.3	16.0	86.5	9.9	20	25*
Conc.	48.7	86.5	13.5	84.0	13.5			

* Starch and KOH added 5 hours prior to amine addition.

APPENDIX VIII

CALCULATION OF

SURFACE FREE ENERGY DECREASE

TABLE LX

CHANGE IN SURFACE FREE ENERGY (in ergs/cm.^{2}) AS A FUNCTION OF pH

Mineral	Hematite				Rutile			Baddeleyite		
N.of KCl. / pH	10^{-4}	10^{-3}	10^{-2}	10^{-1}	10^{-3}	10^{-2}	10^{-1}	10^{-3}	10^{-2}	10^{-1}
3	-	-	-	-	-194	-385	-599	-16.2	-18.2	-24.5
3.5	-	-	-	-	-100	-212	-332	-11.0	-12.2	-15.7
4	-40.3	-43.4	-	-	-65.6	-128	-213	-7.23	-7.57	-10.1
4.5	-31.9	-34.6	-	-	-40.9	-83.1	-139	-4.01	-4.40	-4.65
5	-24.5	-26.5	-	-	-26.0	-53.4	-89.1	-1.81	-2.15	-2.77
5.5	-18.6	-20.6	-	-	-16.1	-33.6	-54.6	-0.51	-0.57	-0.79
6	-13.6	-15.0	-	-	- 6.2	-13.8	-24.8	-	-	-
6.07	-	-	-	-	-	-	-	0.00	0.00	0.00
6.5	-9.15	-9.89	-	-	-3.1	-6.9	-12.3	-0.38	-0.40	-0.49
6.75	-	-	-15.7	-	-	-	-	-	-	-
7	-5.47	-6.05	-11.6	-	-	-	-	-1.53	-1.70	-2.27
7.13	-	-	-	-	0.0	0.0	0.0	-	-	-
7.25	-	-	-8.07	-	-	-	-	-	-	-
7.5	-2.71	-3.06	-5.36	-	-3.0	-6.1	-9.1	-3.96	-4.30	-5.08
7.75	-	-	-3.20	-7.35	-	-	-	-	-	-
8	-0.89	-1.05	-1.53	-3.00	-5.2	-12.2	-18.3	-7.57	-8.13	-9.65
8.25	-	-	-0.63	-0.90	-	-	-	-	-	-
8.5	-0.05	-0.07	-0.10	-0.12	-7.2	-18.3	-29.7	-12.2	-13.2	-15.7
8.68	0.00	0.00	0.00	0.00	-	-	-	-	-	-
9	-0.26	-0.28	-0.31	-0.32	-13.5	-27.2	-59.5	-18.4	-19.6	-23.3
9.5	-1.56	-1.60	-1.95	-1.97	-44.5	-74.2	-124	-	-26.2	-32.2
10	-3.97	-4.04	-4.60	-4.82	-94.0	-156	-243	-	-	-
10.25	-	-	-6.34	-9.19	-	-	-	-	-	-
10.5	-7.50	-7.59	-8.42	-12.5	-202	-336	-475	-	-	-
10.75	-	-	-11.3	-16.2	-	-	-	-	-	-
11	-12.7	-13.4	-	-	-	-	-	-	-	-

The results tabled below are obtained either by use of the integrated form of equation(72) where possible or by graphical integration of adsorption density vs. logarithm of concentration diagrams.

TABLE LXI

CHANGE IN SURFACE FREE ENERGY AS A FUNCTION OF DEHYDROABIETYLAMINE ACETATE CONCENTRATION

Concentration	Change in Surface Free Energy			
	Quartz	Hematite	Rutile	Baddeleyite
μmoles/ℓ.	ergs/cm.^{2}	ergs/cm.^{2}	ergs/cm.^{2}	ergs/cm.^{2}
0.3	-5.15	-1.73	-1.19	-0.25
1	-8.45	-3.16	-2.17	-0.46
3	-13.3	-5.48	-3.66	-0.80
10	-21.7	-10.00	-5.85	-1.45
30	-34.1	-17.3	-11.9	-2.51
100	-55.9	-31.6	-21.7	-4.58
200	-	-45.6	-	-
300	-87.9	-56.0	-36.6	-7.93
400	-	-64.2	-	-
500	-	-70.8	-48.3	-
700	-	-82.9	-57.3	-
1000	-143.8	-96.5	-68.6	-14.5
2000	-	-126.6	-91.6	-
3000	-226	-147.4	-108.3	-5.0
4000	-	-163.3	-	-
5000	-	-173.9	-129.8	-
7000	-320	-192.6	-144.3	-38.3

The decrease in surface free energy as a function of pH is reported in Table LX for hematite, rutile, and baddeleyite. There are no results for quartz since a different method was used to determine the zero-point-of-charge.

BIBLIOGRAPHY

(1) Cofield, G.E. and MacKnight, D.F.; Mining Review, 52, No.10, March 1963.

(2) Bureau of Mines, U. S. Dept. of the Int., Minerals Year-book, 1963.

(3) Wittur, G.E.; "Iron Ore Survey", Cdn. Min. Journal, Feb. 1965.

(4) Gauvin, G.E.; Mineral's Year-book, 1965 (Preliminary), Dept. of Mines and Technical Surveys.

(5) De Vaney, F.D.; The Int. Min. Proc. Cong., The Inst. of Min. and Metal, London, 1960.

(6) Roe, L.A.; "Iron Ore Beneficiation", Minerals Publ. Co. Box 85, Lake Bluff, Ill.

(7) Steep Rock Iron Mines, Ltd.; private communication from an unpublished paper. "Cationic Flotation of Silica from Earthy Iron Ores".

(8) Maltby, P.D.R., and Pickett, D.E.; "Low-Silica Hematite Concentrates", Tech. Bull. TB41, Dept. of Mines and Technical Surveys, Ottawa.

(9) Major-Marothy, G.; "Research on Cationic Silica Flotation of Lean, Earthy Iron Ores", 27th Annual Mining Symposium, Duluth, Minn. (1966) p. 189-192.

(10) Joy, A.S. and Robinson, A.J.; "Flotation-Recent Progress in Surface Science", Vol. 2, Academic Press, p. 172.

(11) DeBoer, J.H.; "The Dynamic Character of Adsorption". Clarendon Press, Oxford, p. 45 ff.

(12) Langmuir, I.; J. Am. Chem. Soc., 40, 1361, (1918).

(13) Freundlich, H.; "Colloid and Capillary Chemistry" Methuen and Co., London, 1926.

(14) Zeldowitch, J.; Acta Physiochim, U.S.S.R. 1, 961 (1934) and R. Sipps; J. Chem. Phys., 16, 490, (1948)

(15) Brunauer, S.; Emmett, P.H.; and Teller, E.; "Adsorption of Gases in Multimolecular Layers", J. Am. Chem. Soc., 60, 309, (1938).

(16) Adamson, A.W.; "Physical Chemistry of Surfaces", Inter-Science Publ., Inc. New York (1960) p. 481.

(17) Hansen, R.S.; Fu, Y.; and Bartell, F.F.; J. Phys. and Coll. Chem., 53, 769, (1949).

(18) Hansen, R.S.; and Craig, R.P.; J. Phy.Chem., 58, 211,(1954).

(19) Bartell, F.E.; and Scheffer, G.N.; J. Am. Chem. Soc., 53, 2507,(1931).

(20) Kipling, J.J.; Ouart. Revs. (London), 5, 60,(1951).

(21) Helmholtz, H. von "Studies of the Electrical Limiting Layer"; Ann. Physik., 7, 337, (1879).

(22) Gouy, G.; "Electric Charge at the Surface of an Electrolyte", J. Phys., 9, 457, (1910).

(23) Chapman, D.L.; "A Contribution to the Theory of Electro-capillarity", Phil. Mag., 25, 475, (1913).

(24) Stern, O.; "The Theory of the Electrolyte Double Layer", Z. Electrochem.; 30, 508, (1924).

(25) Grahame, D.C.; "The Electrical Double Layer and the Theory of Electro-capillarity", Chem. Revs., 41, 441, (1947).

(26) Mysells, K.J.; "Introduction to Colloid Chemistry", London, Interscience Publ. Ltd., 1959, p. 315-333.

(27) Purcell, G.; Sc.D.Thesis, "The Effect of 18 - Carbon Unsaturated Fatty Acids on the Electrokinetic and Flotation Properties of Rutile", Penn. State Univ., 1961.

(28) Adamson, A.W.; "Physical Chemistry of Surfaces", London, Interscience Publ. Ltd. 1960, p.179-190, 207-214.

(29) Osipow , L.I., "Surface Chemistry, Theory and Industrial Application", Reinhold Publ. Corp'n., New York, p.70-2.

(30) Gaudin, A.M.; "Flotation", McGraw Hill, 1957, p.101.

(31) DeBruyn, P.L.; "The Electrical Double Layer", The Structure and Properties of Interfaces Conference, July 1963, at M.I.T.,p.30.

(32) Smith, G.W.; and Salman T.; "Zero-Point-of-Charge of Hematite and Zirconia", Cdn. Met. Quart., 5, No.2, 93, (1966).

(33) Parks, G.A., and deBruyn, P.L.; "The Zero-Point-of-Charge of Oxides", J. Phy. Chem., 66, 967, (1962).

(34) Yopps, J.A.; and Fuerstenau, D.W.; "The Zero-Point-of-Charge of Alpha Alumina," J. Coll. Sci., 19,61, (1964).

(35) Glemser, O.; and Rieck, G.; Z. anorg. U. All. gem. Chem., 297, 175, (1958).

(36) Glasstone, S.; "Introduction to Electrochemistry", Van Nostrand, New York.

(37) Parks, G.A.,:"The Isoelectric Points of Solid Oxides, Solid Hydroxides and Aqueous Hydroxo Complex Systems", Chem. Rev., 65, 177, (1965).

(38) Dupre, A.; "Theorie Mecanique de la Chaleur", Paris 1869,369.

(39) Young, T.; "Works of (G. Peacock ed.)" Vol. 1, p.432,(Murray, London)

(40) Osipow, L.I.; "Surface Chemistry", Monograph No. 153, Reinhold Publ., p.235.

(41) Danielli, J.F.; Pankhurst, K.G.A.; and Riddiford, A.C.; "Recent Progress in Surface Science", Vol.2, p.112, (1964) Academic Press.

(42) Bikerman, J.J.; "Proc. 2nd Intern. Congr. Surface Activity", London, 3, 125, (1957).

(43) Pethica, B.A., and Pethica T.J.P.; "Proc. 2nd Intern. Congr. Surface Activity", London,3, 131,(1957).

(44) Gray, V.R.; "Proc. 2nd Intern. Congr. Surface Activity", London, 3, 191, (1957).

(45) Collins, R.E.; and Cooke, C.E.; Jr.; Trans. Faraday Soc., 55, 1602, (1959).

(46) McNutt, J.E.; and Andes, G.M.; J. Chem. Phys., 30, 1300, (1959).

(47) Lester, G.R.; J. Colloid Sci., 16, 315, (1961).

(48) Paterson, J.G.; "The Effect of Sodium Cyanide on the Adsorption of Sodium Isopropyl Xanthate on Synthetic Chalcocite", M. Eng. Thesis, McGill University, (1966).

(49) Adamson, A.W.; "Physical Chemistry of Surfaces", Interscience Publ., New York, p.272.

(50) Foukes, F.M.; and Harkins, W.D.; J. Am. Chem. Soc., 62,3377,(1940).

(51) Adam, N.K.; "The Physics and Chemistry of Surfaces", 3rd Ed., Oxford Univ. Press, London. 1941.

(52) Adam, N.K.; and Jessop, G.; J. Chem. Soc., 127, 1863, (1925).

(53) Gaudin, A.M.;"Flotation", 2nd Ed., McGraw-Hill, 1957, p.173-6.

(54) Gaudin, A.M.; "Flotation", 2nd.Ed., McGraw-Hill, 1957, p.217-270.

(55) Gaudin, A.M.; Haynes, C.B.; and Haas, E.C.; "Flotation Fundamentals IV", Utah Eng. Expt. Stat., Tech. Paper 7, (1920).

(56) Gaudin, A.M.; and Sorensen P.M.; "Flotation Fundamentals II", Utah Eng. Expt. Stat., Tech. Paper 4, (1928).

(57) Kellogg, H.H.; and Vasquez-Rosas, H.; "Amine Flotation of Sphalerite-galena Ores", Trans. AIMME, 169, 476, (1946).

(58) Brown, D.J.; "Potentriometric Titrations", M.I.T., (1953).

(59) Rogers, J.; and Sutherland K.L.; "Principles of Flotation-Activation of Minerals and Adsorption of Collectors", Trans. AIMME, 169, 317,(1946).

(60) Smith, R.W.; "Contact Angles in a Quartz-Dodecylammonium Acetate Solution - Nitrogen System ", Proc. S.D. Acad. Sci., 41, 150, (1962).

(61) Broome, F.K.; Ralston, A.W.; and Thornton, M.H.; "Complex-Formation with High Molecular Weight Amines I", J.Am.Chem.Soc.,68, 67,(1946).

(62) DeBruyn,P.L.; "Adsorption of Dodecylammonium Acetate on Quartz", Ph.D. Thesis, M.I.T. (1952).

(63) Morrow, J.G.; "Adsorption of Dodecylammonium Acetate on Hematite and Spalerite", Ph.D. Thesis, M.I.T., (1952).

(64) Gaudin, A.M.; and Morrow, J.G.; "Adsorption of Dodecylammonium Acetate on Hematite and its Flotation Effect", Trans. AIMME, 199, 1196, (1954).

(65) Bloecher, F.W.; Jr.; "Concerning the Adsorption of Dodecylamine", M.Sc. Thesis, M.I.T.,(1949).

(66) Elsevier's Encyclopedia of Organic Chemistry, Vol. 13, p.964-69, Elsevier Publ. Co., N.Y. and Amsterdam.

(67) Hercules Rosin Amines, Technical Bulletin No. PC-132A.

(68) Hercules Rosin Amine D and Acetate, Product Information No.N5-283.

(69) Bishop, W.T.; and Nemeth, N.; Private Communications.

(70) Richards, R.H.; and Locke, C.E.; Textbook of Ore Dressing, McGraw-Hill, N.Y., 1940.

(71) Oko, M.U.; "Adsorption of Fatty Acid Soaps on Hematite", M.Eng. Thesis, McGill University, 1965.

(72) Iwasaki, I.; Strathmore, R.B.; and Kim, Y.S.; "Surface Properties and Flotation Characteristics of Magnetite", Trans. AIME, 223, 113, (1962).

(73) Beals, M.D.; National Lead Co., Private Communications.

(74) Baldwin, W.J.; National Lead Co., Private Communications.

(75) Meites, L.; and Meites, T.; "Removal of Oxygen from Gas Streams", Anal. Chem, 20, 984, (1948).

(76) Lapointe, C.M.; "Competitive Adsorption of Oleic Acid by Quartz and Hematite", Dept. of Mines and Technical Surveys, Research Report R108.

(77) Nemeth, N.; "Adsorption of Dehydroabietylamine Acetate on Quartz and Hematite", M. Eng. Thesis, McGill University, (1964).

(78) Gaudin, A.M.; and Bloecher, K.W.; "Concerning the Adsorption of Dodecylamine on Quartz", Trans. AIME, 187, 499, (1950).

(79) Taggart, A.F.; Taylor, T.C.; and Rice, C.R.; "Experiments with Flotation Reagents", Trans. AIME, 87, 285, (1930).

(80) Harkins, W.D.; and Brown, F.E.; "Surface Tension of Water and Benzene", J.Am.Chem.Soc., 41, 499, (1919).

(81) Wilson, J.M.; Newcombe, R.J.; Denaro, A.R.; and Rickett, R.M.; "Experiments in Physical Chemistry",p.77, Pergamon Press, 1962.

(82) Fuerstenau, D.W.; Metzger, P.H.; and Steel, G.D.; "How to use this Modified Hallimond Tube for Better Flotation Testing", Eng. and Min. Journal,158, March, 69,(1957).

(83) Hallimond, A.F.; "Laboratory Apparatus for Flotation Tests", Mining Magazine, 70, 87, (1944).

(84) Fuerstenau, D.W.;"Streaming Potential Studies on Quartz in Solutions of Aminium Acetates in Relation to the Formation of Hemi-Micelles at the Quartz-Solution Interface", J.Phy. Chem., 60, 981, (1956).

(85) Buchanan, A.S.; and Johansen, P.G.; "An Application of the Microelectrophoresis Method to the Study of the Surface Properties of Insoluble Oxides", Australian J. Chem., 10, 398, (1957).

(86) Plaksin, E.; "Interaction of Minerals with Gases and Reagents in Flotation", Trans.AIME, 214, 319, (1959).

(87) Adamson, A.W.;"Physical Chemistry of Surfaces", New York,p.70.

(88) Ralston, A.W.; Hoerr, G.W.; and Hoffman, E.T., "Studies on High Molecular Weight Aliphatic Amines and their Salts. IV. Electrical Conductivities of Aqueous Solutions of the Hydrochlorides and Acetates of Dodecyl-and Octadecyl-amines", J.Am.Chem.Soc., 64, 97, (1942).

(89) Daniels, F.; and Alberty, R.A.; "Physical Chemistry", John Wiley and Sons, New York, p.400.

(90) Choi, H.S., and Whang, K.U.; "Surface Properties and Floatability of Zircon", Trans. CIMM., 66, 242, (1963).

(91) Danilova, E.V., "Flotation of Feldspar by Laurylamine", Concentration of Valuable Minerals (papers), Mekhanobr Inst. 1, (1952).

(92) Zagirova, E.K.; "Investigations of the Principal Factors Affecting the Action of Cationic Reagents", Mintsevetmet,(1954).

(93) Joy, A.S.; and Watson, D.; "Adsorption of Collector and Potential-Determining Ions in Flotation of Hematite with Dodecylamine", Trans. I.M.M., 73, 333, (1963-64).

(94) Sutherland, K.L.; and Wark, I.W.; "Principles of Flotation", Aust. Inst. of Min. and Met. (Inc), 310, 280, (1955).

(95) Parks, G.A.; unpublished data in Ref.(37) attributed to Holmes and Feeney.

(96) Amphlett, C.B.; MacDonald, L.A.; and Redman, M.J.; "Synthetic Inorganic Ion-Exchange Materials, Part II", J. Inorg. Nucl. Chem., 6, 236 , (1958).

(97) Mattson, S.; and Pugh, A.J.; Soil Sci., 38, 229, (1934).

(98) Verwey, E.J.W., "The Electrical Double Layer of Oxidic Substances Especially in Non-Aqueous Media", Rec. Trav. Chim., 60, 625, (1941).

(99) Parks, G.A.; "A Study of the Surface of Ferric Oxide in Aqueous Systems", Ph.D. Thesis, M.I.T. (1960).

(100) Thomas, A.W.; Colloid Chemistry, McGraw-Hill, New York, (1934).

(101) Rollinson, C.L.; "Olation and Related Chemical Processes", Chapt.13 in Bailar, "Chemistry of the Co-ordination Compounds", Reinhold Publ.Co., N.Y. (1956).

(102) Purcell, G.; and Sun, S.C.; "Significance of Double Bonds in Fatty Acid Flotation - An Electrokinetic Study", Trans. AIME, 226, 6, (1963).

(103) Buchanan, A.S.; and Johansen P.G.; "An Application of the Microelectrophoresis Method to the Study of the Surface Properties of Insoluble Oxides", Australian J. Chem., 10, 392, (1957).

(104) Graham, K.; and Madeley, J.D.; "Relation Between the Zeta-Potential of Rutile and its Flotation with Sodium Dodecyl Sulphate", J. Appl'd. Chem. (London), 12, 485, (1962).

(105) Fuerstenau, D.W.; "Correlation of Contact Angles, Adsorption Density, Zeta-Potentials, and Flotation Rate", Trans. AIME, 208, 1365, (1957).

(106) Sen, K.C.; and Ghosh, B.N.; "Studies on the Gelation of Silicic Acid Sols, Part 3", J. Ind. Chem. Soc., 33, 209, (1956).

(107) Hückel, W.; "Structural Chemistry of Inorganic Compounds", Vol.1, Elesevier Publ.Co., New York, 1950, p.226.

(108) Bhappu, R.B.; State Bureau of Mines and Mineral Resources, N.M. Inst. of Min. and Tech., Socorro, personal communication through Parks, G.A. (1964).

(109) Ahmed, S.M.; "Studies of the Dissociation of Oxide Surfaces at the Liquid-Solid Interface", Cdn. J. Chem., 44, 1663, (1966).

(110) Devanathan, M.A.V.; and Tilak, B.V.K.; "The Structure of the Electrical Double Layer at the Metal-Solution Interface", Chem. Rev. 65, 635, (1965).

(111) MacKor, E.L.; "The Properties of the Electrical Double Layer I, II, and III ", Rec. Trav. Chim., 70, 663, 747 and 763, (1951).

(112) Hammett, L.P.; "Solution of Electrolytes", McGraw-Hill, New York, 1936.

(113) Beck, M.T.; Acta Chim. Acad. Sci. Hung., 4, 227, (1954).

(114) Johnston, H.L.; Cuta, F; and Garrett, A.B.; "The Solubility of Silver Oxide in Water in Alkali and in Alkaline Salt Solutions", J. Am.Chem. Soc., 55, 2311, (1933).

(115) Liberti, A.; Chiantella, V.; and Corigliano, F.; "Mononuclear Hydrolysis of Titanium (IV) From Partition Equilibria", J. Inorg. Nucl. Chem., 25, 415, (1963).

(116) Schmets, J.; and Pourbaix, M.; "Equilibrium Potential -pH diagram for the System Ti - H_2O ", CITCE, 6th Conf., 167, (1954).

(117) Brown, J.; Jaap, W.J., and Ritchie, P.D.; "Physico-Chemical Studies X* - A Comparative Study of the Solubility and Adsorptive Properties of Finely Divided Silica and Titania", J. Appl'd.Chem. (London), 9, 153, (1959).

(118) Solovkin, A.S.; Zhur.neorg.Khim, 2, 611, (1957). (Russian) from Bjerrum, J.; Schwarzenbach, G.;and Sillen, L.G.; "Stability Constants Part II - Inorganic Ligands", London, The Chem. Soc. 1958.

(119) Sheka, I.A.; and Pevzner, Ts. V.; "Solubility of Zirconium and Hafnium Hydroxides in Sodium Hydroxide Solutions", Russ. J. Inorg. Chem., 5, 1119, (1960).

(120) Latimer, W.M.; "Oxidation Potentials", London, 1952.

(121) Wicks, C.E.; and Block, F.E.; "Thermodynamic Properties of 65 Elements-Their Oxides, Halides Carbides and Nitrides, USBM Bull. 605, (1963).

(122) Gayer, K.H.; and Woontner, L.; "The Solubility of Ferrous Hydroxide and Ferric Hydroxide in Acidic and Basic Media at 25°C.", J. Phy. Chem., 60, 1569, (1956).

(123) Hedstrom, B.O.A., "Studies of the Hydrolysis of Metal Ions VII- The Hydrolysis of Iron (III) Ion, Fe^{+3} ", Arkiv, Kemi.,6, 1, (1954).

(124) Biederman, G.; and Schlindler, P.; "On the Solubility Product of Precipitated Iron (III) Hydroxide", Acta Chem. Scand. 11, 731, (1952).

(125) Milburn, R.M.; "A Spectrophotometric Study of the Hydrolysis of Iron (III) Ion", J. Am. Chem. Soc., 79, 537,(1957).

(126) Lamb, A.B.; and Jacques, A.G.; J. Am. Chem. Soc., 60, 1212, (1938).

(127) Lengweiler, H.; Buser, W.; and Feitnecht, W.; "Die Ermittlung der Löslichkeit von Eisen (III)-hydroxiden mit ^{59}Fe I". Helv. Chim. Acta.,44, 796, (1961).

(128) Flint, E.P.; and Wells, L.S.; J. Res.Nat. Bur. Stand., 12, 751, (1934).

(129) Alexander, G.B.; Heston, W.M.; and Iler, R.K.; "The Solubility of Amorphous Silica in Water", J. Phy. Chem., 58, 453, (1954).

(130) Arbiter, N.; Kellogg, H.H.; and Taggart, A.F.; "The Mechanisms of Collection of Metals and Metallic Sulphides by Amines and Amine Salts", Trans. AIME, 153, 517, (1943).

(131) Cook, M.A.; and Nixon, J.C.; "Theory of Water-Repellant Films on Solids Formed by Adsorption from Aqueous Solutions of Heteropolar Compounds", J. Phys. and Coll. Chem., 54, 445, (1950).

(132) Salman, T.; and Robertson, R.F.; "Adsorption of Hexyl Mercaptans on Sphalerite", Trans. CIMM, 59, 508, (1966).

(133) Iwasaki, I.; "Electrochemical Studies of Adsorption on Silver Sulphide Surfaces", Sc.D. Thesis, M.I.T., (1957).

(134) Iwasaki, I.; and deBruyn, P.L.; "The Electrochemical Double Layer on Silver Sulphide at pH 4.7 I. In the Absence of Specific Adsorption", J. Phy. Chem., 62, 594, (1958).